OBESITY AND ENDOTHELIAL DYSFUNCTION: MECHANISMS, METHOD DEVELOPMENT AND INTERVENTIONS

Erika M. Cerri

A thesis submitted to
The University of Birmingham
for the degree of
DOCTOR OF PHILOSOSPHY

School of Sport & Exercise Sciences
The University of Birmingham
September 2009

Abstract

The principle aims of this thesis were to determine the effect of lowering plasma fatty acids (FA) on muscle microvascular blood volume (MBV) at rest and during exercise, investigate whether near-infrared spectroscopy (NIRS) can be used to measure muscle MBV in the obese, develop the contrast enhanced ultrasound (CEU) method in our laboratory for measuring muscle MBV of the human forearm, and use CEU to measure the MBV response to an oral glucose tolerance test (OGTT). No differences were observed in exercise-induced increases in MBV or resting MBV between control and low FA conditions created by niacin ingestion in lean and obese individuals. NIRS was not suited to measure muscle MBV in participants with a thick subcutaneous adipose tissue layer. The CEU method was successfully developed to measure MBV in the human forearm. CEU revealed a significant increase in MBV in response to an OGTT in lean trained individuals. This technique will be used in future studies to generate novel information on the suspected impaired MBV response after meal ingestion in obese individuals and to assess the effectiveness of interventions aimed at improving the MBV response and glycemic control to avoid the development of type II diabetes and cardiovascular disease.

Acknowledgements

I would like to thank the many people who have helped me complete this thesis.

My supervisor Prof. Anton Wagenmakers for giving me the opportunity to continue pursuing my curiosity in this research area and for all his patience, support, encouragement and advice in helping me grow as an academic and researcher. My second supervisor Prof. Michael Frenneaux for his encouragement and advice over the course of the PhD.

The staff members in the school: Dr. Maggie Brown, Steve Allen, Dave McIntyre, Rob Wheeler, and the office staff for all their help and advice. A special thank you to Dr. George Balanos for all his time, support and encouragement in piloting and conducting the final experimental study, to Dr. Steve Rattigan for his generous help and advice in developing the contrast enhanced ultrasound method, and to Dr. Chris Shaw for all his time and help in the pilot testing of the CEU technique. A special thank you also to Thomas Barker and Dr. Girish Dwivedi for carrying clinical responsibility and for their generous time, advice, and assistance in my final experimental study. The staff at the Wellcome Trust Clinical Research Facility for all their support and reliability which helped keep me positive and motivated while conducting my final experimental study in their clinic.

All the postgrads, ex-postgrads, and friends, in particular Manj, Michelle, Carl, Eric, Ali, Sarah, Joannis, Antonis, Andrea, Sophie, Anne, Derek, Jane and Tony, for all their help, company, and support.

A special thank you Prof. René Verheijen and the medical team at the VU medisch centrum for having put me back together in one functional piece after the cancer and instilled in me the curiosity and motivation which lead me to this PhD and my career path.

A very big thank you to my Ali for his constant support and enthusiasm during the ups and downs of the PhD, and to my family, especially mum, who patiently listened to my enthusiastic ramblings on biochemical pathways for the past four years and even read my chapters.

Table of Contents

LIST OF FIGURES

LIST OF TABLES

Chapter 1

INTRODUCTION

1.1 The global obesity problem

1.1.1 Perspectives

Obesity is a significant global health problem greatly affecting mortality and quality of life. It is a popular topic of conversation for governments, doctors, and the general public, and there is great emphasis on the need to stop this global epidemic, especially in children. But what is obesity? And why exactly is it a health threat?

Obesity is the accumulation of adipose tissue to excess and to an extent which presents a health risk to the individual (World Health Organisation 2009[1]). It is crudely defined using the body mass index (BMI) which is calculated from height and weight using the formula: [BMI = (weight in kg) / (height in m^2)]. A BMI of 30 or greater defines the individual as being obese. The development of obesity involves the interaction of many variables including environmental, hormonal, genetic predisposition, adipokine receptor defects and many more (Stapleton et al. 2008[2]). Despite the complex nature, the principal contributing factor appears to be an imbalance between energy intake and expenditure (Stapleton et al. 2008[2]). The indisputable change in lifestyle over the last 30 years, involving reductions in physical activity and increases in consumption of calories and fat, has resulted in a dramatic worldwide rise in the prevalence of obesity.

Previously, in many cultures, being overweight was a sign of wealth; a sign that the individual did not have to do physical labour and had enough money to purchase ample amounts of food. However, in these modern times, it has become glaringly evident that

being obese is a serious health risk associated with the development of numerous pathologies which, simplistically, will cost (a) the individual: reduced life expectancy and quality of life, and (b) the economy: billions of pounds in health care and medical costs. As stated by Professor Philip James, chairman of the International Obesity Taskforce: obesity truly does constitute "one of the most important medical and public health problems of our time".

1.1.2 Global and UK increases in obesity rates

Although the US has led the world in its staggering increases in the prevalence of obesity, the rest of the world is flagrantly following suit. Globally, an estimated 400 million adults were classed as obese in 2005, with the expectation of an increase to 700 million by 2015 (World Health Organisation 2006[3]). In the UK, nearly a quarter of the population was classed as obese in 2007 and it is predicted that by 2025 almost half of men and over a third of women will be obese (NHS Information Centre 2009[4]). The epidemic scale of the UK obesity problem was confirmed in the statistics from the government report of the Health Profile of England 2008: with 23 % of the adult population classed as obese, the UK has the highest obesity prevalence in Europe.

Mirroring the adult obesity epidemic is the dramatic global rise in the number of overweight and obese children (Figure 1.1). Although the highest absolute rates are seen in children from the USA, the rise in overweight children in the UK between 1995 and 2000 is alarming. In the UK, the obesity rates for 4-5 year old children has nearly

doubled since 1990, while that for 10-11 year olds has more than tripled since then (Figure 1.2; Dinsdale and Rutter 2008[5]).

This increase in overweight and obesity in children is of particular concern as it is related to the subsequent overweight or obesity in adulthood, as well as increased risk of adult morbidity and mortality (Guo et al. 2002[6]; World Health Organisation 2006[3]). Indeed, the negative health consequences arising from the obese condition, such as type II diabetes, will appear at an earlier age, causing the individuals to face subsequent ill health for much of their adult life.

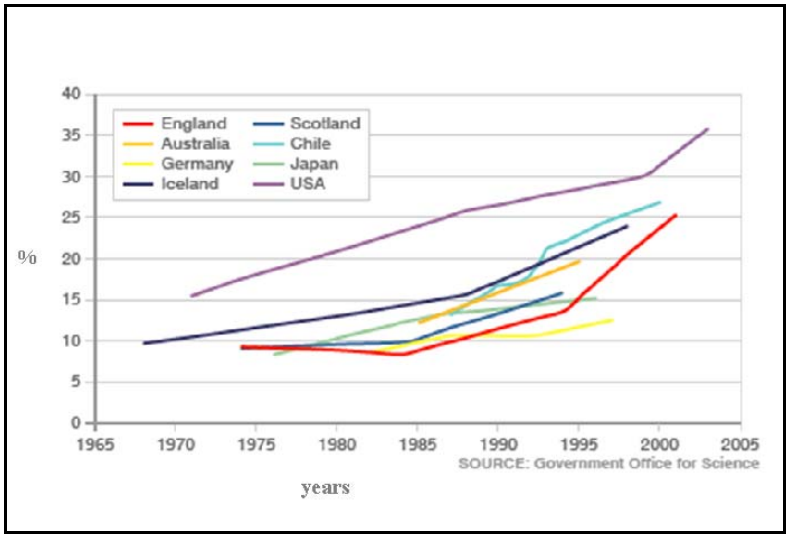

Figure 1.1 Worldwide increase in the number of overweight children over the past 40 years. Data shown as percentage overweight.

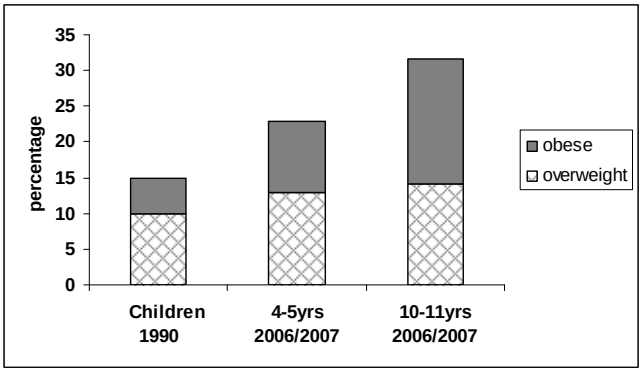

Figure 1.2 Childhood overweight and obesity rates of 2006/2007 for 4-5 and 10-11 year olds as compared to the averages recorded for children in 1990 in England. Data from the National Child Measurement Programme in the National Obesity Observatory report of June 2008.

1.1.3 Obesity-associated pathologies

According to the World Health Organisation (1998)[7] "obesity is becoming one of the most important contributors to ill-health in adults". In the UK alone, the number of deaths attributable to obesity per year has reached 30,000, while in the USA the figure is 10 times higher and in 2005 obesity overtook smoking as the leading preventable cause of illness and premature death (Marinou et al. 2009[8]). Indeed, as BMI increases, so does the risk of certain chronic diseases including cardiovascular disease, type II diabetes, hypertension, the metabolic syndrome, peripheral vascular disease, gall bladder disease, some cancers, obstructive sleep apnea, arthritic disorders, and non-alcoholic fatty liver disease (World Health Organisation 2006[3]; Byrne et al. 2009[9]; Stapleton et al. 2008[2]; Shoelson et al. 2007[10]).

Amongst the obesity-related diseases, the rise in the worldwide prevalence of type II diabetes in adults is particularly striking. For every unit increment in BMI, the risk of type II diabetes increases by 18 % (Helmrich et al. 1991[11]) and now more than 180 million adults worldwide are estimated to have diabetes, with this number predicted to double by 2030 (World Health Organisation 2006[12]). In 2005, the annual death rate from diabetes was estimated at 1.1 million, with the prediction of a greater than 50 % increase in the following 10 years if urgent action is not taken (World Health Organisation 2006[12]).

The early metabolic defects that lead to the development of type II diabetes are common to several other obesity-related pathologies, namely: hypertension, the metabolic syndrome, peripheral vascular disease, and cardiovascular disease. The principal defects are vascular endothelial dysfunction and insulin resistance in liver, adipose tissue, and skeletal muscle. Thus in addressing these common defects the development of the network of pathologies stemming from the endothelial dysfunction and insulin resistance may be limited.

It is of great importance to immediately take measures to prevent further increases in obesity and the obesity-related pathologies. Although life expectancy is still on the increase in the UK, *healthy* life expectancy appeared to be levelling off already in 2001 (Figure 1.3; Science and technology committee 2005[13]). With the dramatic increase in childhood obesity in the last decade, one can speculate that as these individuals approach middle age, there will be a massive increase in the prevalence of obesity-related

pathologies prompting a dramatic fall in healthy life expectancy. Thus despite the favourable appearance of an increasing life expectancy, the population will spend an increasing number of years in ill health unless immediate measures are taken.

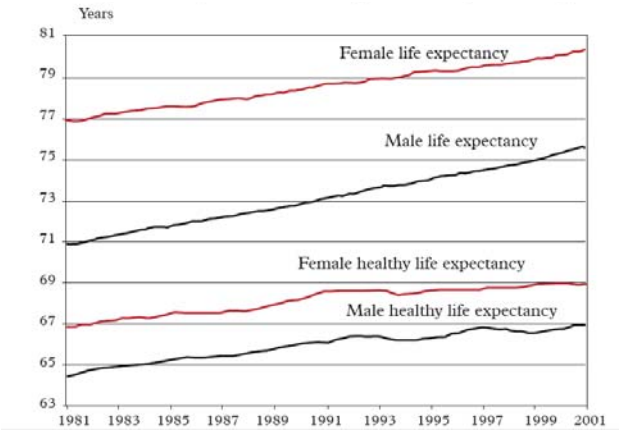

Figure 1.3 Life expectancy and healthy life expectancy for males and females in the UK population.

1.2 Functional, metabolic, and structural impairments in the obese

It was originally assumed that overweight and obese individuals combined an increased subcutaneous and visceral adipose tissue mass with maintenance of relatively normal physiological functions, metabolic rates and regulation mechanisms, and organ/tissue structure. However, in recent years it has become apparent that, even in the early stages of obesity, abnormalities are present in the function, metabolism, and structure of most organs and tissues. The presence of such abnormalities can be regarded as the early steps in the mechanisms that eventually lead to pathology and early mortality in chronically

overweight, obese and morbidly obese individuals. In this section, an overview will be given of the most important functional, metabolic, and structural impairments that have been described in obese patients in the recent literature. The focus will be on the abnormalities which contribute to impairment of vascular function and promote the loss of glycemic control, thus contributing to the development of type II diabetes and cardiovascular disease.

1.2.1 Adipose tissue: source of fatty acids and inflammatory cytokines

Although initially viewed as simply a store for excess fats, the adipose tissue plays a crucial role in the regulation of plasma lipid levels, especially in the postprandial periods when dynamic changes in plasma lipid concentration occur. In healthy individuals, the adipose tissue will limit the postprandial excursions in circulating fatty acids (FA) and lipids by suppressing the release of FA and promoting the uptake of triacylglycerol (TG; Frayn 2002[14]) via lipolysis of lipoproteins (especially chylomicrons and very low density lipoproteins). In the obese state however, the adipose tissue is unable to quickly respond to the changes in lipid concentration after a meal and, therefore, plasma FA and TG excursions are much higher (Frayn 2002[14]).

The impaired ability to regulate postprandial lipid excursions arises from metabolic impairments within the adipocytes. The release of FA from the adipocytes is under the control of hormone sensitive lipase (HSL), an enzyme present in the adipocytes. The hydrolysis of TG, leading to the clearance of TG from the blood, and the uptake of FA in the adipocytes is under the control of lipoprotein lipase (LPL), an enzyme present on the

endothelial cells of adipose tissue capillaries. Insulin normally inhibits HSL and activates LPL (Frayn 2002[14]). Thus in the postprandial state, when insulin levels are elevated, the release of FA is normally suppressed while the clearance of TG from the blood will be increased. This leads to low plasma FA and TG concentrations. In obesity however, the adipocytes develop resistance to insulin, and thus the normal coordination between adipose tissue lipolysis and TG clearance is lost and leads to increased postprandial lipid excursions (Frayn 2002[14]). Even the hyperinsulinaemia often present in obesity is not able to reduce adipose tissue lipolysis in the postprandial period (Frayn 2002[14]), therefore, there is a continued net release of FA from the abdominal and visceral adipose tissue compartments.

A very important recent observation is that low-grade inflammation always occurs within the adipose tissue of obese individuals with substantial increases in the levels of macrophage infiltration (Stapleton et al. 2008[2]; Berg and Scherer 2005[15]; Bakker et al. 2009[16]; Meyers and Gokce 2007[17]). In obese mice, 50 % of the cells in adipose tissue were found to consist of macrophages, compared to 5-10 % in lean mice (Bakker et al. 2009[16]). The macrophages lead to a substantial local production of inflammatory cytokines (TNFα, IL-1 and IL-6). These inflammatory cytokines are assumed to be the main cause of the insulin resistance of the adipose tissue cells and, therefore, the cause of the mentioned loss of coordination between FA release and TG clearance in the postprandial state in obese subjects. Some of these inflammatory cytokines are released into the systemic circulation and will, therefore, also be the cause of metabolic impairments in the liver, skeletal muscle, and potentially many other tissues (Berg and

Scherer 2005[15]; Bakker et al. 2009[16]; Bastard et al. 2006[18]; Shoelson et al. 2006[19]; Goossens 2008[20]).

Adipose tissue in obese individuals has also been observed to contain larger adipocytes as opposed to more small cells (Frayn 2002[14]; Goossens 2008[20]). It has been suggested that the larger adipocytes are generally less sensitive to insulin (Frayn 2002[14]; Roberts et al. 2009[21]; Goossens 2008[20]), and would therefore reduce the ability of the adipose tissue to respond appropriately to the lipid excursions in the postprandial state. Furthermore, it has been suggested that there are alterations in the structure of the adipose tissue microvasculature in obesity, as the normal postprandial increase in adipose tissue blood flow is blunted (Frayn 2002[14]; Karpe and Tan 2005[22]; Goossens 2008[20]). This could also reduce the delivery of TG to the adipose tissue for storage, and explain the reduced lipid buffering capacity of the adipose tissue in the obese in the postprandial state (Frayn 2002[14]).

In addition to the mentioned structural changes, the location of the adipose tissue stores seems to play a role in the severity of the resulting metabolic impairments. Visceral adipose tissue, which is stored between the intestines in upper/abdominal obesity, is commonly regarded as the most active fat deposit promoting systemic inflammation in the obese state (Stapleton et al. 2008[2]; Berg and Scherer 2005[15]; Jensen 2008[23]; Shoelson et al. 2006[19]). Visceral fat has been suggested to contain a greater number of macrophages and monocytes than subcutaneous adipose tissue stores (Bakker et al 2009[16]). Fatty acids and inflammatory cytokines released by the visceral adipose tissue

compartment enter the systematic circulation via the portal vein and the liver. Most of the fatty acids released by visceral adipose tissue are taken up by the liver and used for the synthesis of very low density triglycerides (VLDL-TG) thus explaining the high plasma TG and VLDL-TG concentrations in individuals with visceral adiposity. A continuous exposure of the liver to high concentrations of fatty acids and inflammatory cytokines released by adipose tissue and channelled to the liver via the portal vein has been suggested to be the primary cause of non-alcoholic fatty liver disease, the hepatic expression of the metabolic syndrome (see section 1.2.2).

1.2.2 Liver and non-alcoholic fatty liver disease: source of VLDL-TG and glucose

The liver has a multitude of functions, but the central metabolic role is the regulation of plasma glucose and fat concentrations in order to maintain homeostasis despite varied glucose and fat ingestion with every meal (Fritsche et al. 2008[24]). In obesity, however, the increased visceral and subcutaneous adiposity exposes the liver to increased concentrations of FA and inflammatory cytokines. Chronic delivery of FA in excess of its capacity to oxidize FA and synthesize VLDL-TG will lead to the accumulation of TG in the liver. The build up of TG in the liver, in combination with the constant exposure to high levels of inflammatory cytokines, eventually results in the development of non-alcoholic fatty liver disease (NAFLD; Byrne et al. 2009[9]). NAFLD refers to a wide-spectrum of liver damage ranging from simple steatosis (fatty liver; that is liver with fat content > 5 %) to steatohepatitis (fatty liver with inflammation and apoptotic hepatocytes), advanced fibrosis (liver tissue with excessive extracellular matrix and increased collagen content) and cirrhosis (liver failure due to the fact that liver tissue is

extensively replaced by scar tissue with a poor blood supply). Advanced liver fibrosis and cirrhosis are nearly always attended by inflammation and infiltration with monocytes and macrophages (Byrne et al. 2009[9]). NAFLD is the most common form of abnormal liver function among adults in Western countries (Targher et al. 2007[25]). NAFLD has a high prevalence amongst obese individuals (estimates 70-100%), especially in those with morbid obesity (Bellentani et al. 2000[26]; Byrne et al. 2009[9]; Marchesini et al. 2008[27]).

A normal healthy liver has a high capacity to produce VLDL-TG from the FA released by the visceral and subcutaneous adipose tissue stores and will be able to prevent substantial increases in plasma FA concentrations. A normal healthy liver also plays an important role in the clearance of interleukin 6 (IL-6) and potentially other inflammatory cytokines released by the visceral and subcutaneous adipose tissue stores (Garibotto et al. 2007[28]). However, in the various forms of NAFLD, the capacity of the liver to oxidize fatty acids and to synthesize VLDL-TG is reduced, principally due to tissue and mitochondrial damage caused by reactive oxygen species (ROS) and leading to a reduced capacity to oxidize FA (Byrne et al. 2009[9]). As NAFLD is often combined with inflammation, the liver itself will also become a source of inflammatory cytokines in obese individuals with NAFLD. This implies that obese individuals with NAFLD are likely to have higher systemic concentrations of FA and inflammatory cytokines and may explain why NAFLD is an independent risk factor for cardiovascular disease (Byrne et al. 2009[9]).

NAFLD is often regarded as the hepatic expression of the metabolic syndrome as the

liver, consequently to the fat accumulation, develops insulin resistance (Byrne et al. 2009[9]). The insulin resistance also implies that increased rates of gluconeogenesis are seen in obese individuals with NAFLD, and that gluconeogenesis continues in the postprandial period. This increased hepatic glucose production contributes to the hyperglycemia in obese individuals with NAFLD (Byrne et al. 2009[9]).

Collectively, the continuous release of FA and inflammatory cytokines from visceral and subcutaneous adipose tissue, and the release of FA, VLDL-TG, inflammatory cytokines and glucose from the liver in obese individuals with NAFLD, will lead to a high exposure of the skeletal muscle and vascular endothelium to these compounds. This will promote the development of functional, metabolic, and structural impairments in these tissues, which will result in the loss of glycemic control and over time lead to the development of type II diabetes and cardiovascular disease. The nature of these impairments and their consequences are described in sections 1.2.3 – 1.2.5.

1.2.3 Skeletal muscle: key role in glycemic control and energy balance

The skeletal muscle plays a key role in glycemic control and energy balance. The importance of skeletal muscle in glycemic control stems from the fact that it is the largest tissue for glucose uptake in the body, responsible for 80 % of the glucose disposal (Ferrannini et al. 1985[29]; Defronzo et al. 1985[30]; Nuutila et al. 1994[31]). With regards to energy balance, skeletal muscle not only allows for energy to be expended via exercise, but also through the energy-requiring processes of nutrient storage occurring within the muscle fibres.

Glucose transport into skeletal muscle fibres primarily occurs through the process of facilitated diffusion utilising glucose transporter proteins (GLUTs). GLUT4 is primarily responsible for insulin-mediated glucose uptake in skeletal muscle (Watson and Pessin 2001[32]). GLUT4 continually cycles between the cell plasma membrane and intracellular compartments and under basal fasting conditions the majority of GLUT4 is located within interior membrane vesicles of the muscle fibre (microsomes). Upon insulin-stimulation, GLUT4 exocytosis increases dramatically resulting in a large proportion of GLUT4 becoming incorporated into the cell surface, allowing entry of glucose into the muscle cell (Chang et al. 2004[33]; Thong et al. 2005[34]; Wojtaszewski and Richter 2006[35]). In the obese population, however, the elevated circulating FA, TG, and inflammatory cytokines originating from the adipose tissue and liver promote the accumulation of FA metabolites and activate inflammation within the muscle fibre (Schenk et al. 2008[36]). Both the accumulation of FA metabolites and inflammatory cytokines have been shown to promote impaired insulin signalling in the muscle fibre. The mechanisms leading to insulin resistance in the muscle fibre are very similar to those operating in the microvascular endothelium (described in detail in section 1.3) and involve IRS-1 serine phosphorylation and activation of the proinflammatory signalling pathways. Figure 1.4 presents a summary of the key muscle fibre functions which are controlled, at least in part, by the insulin signalling cascade, and which would thus be affected by insulin resistance.

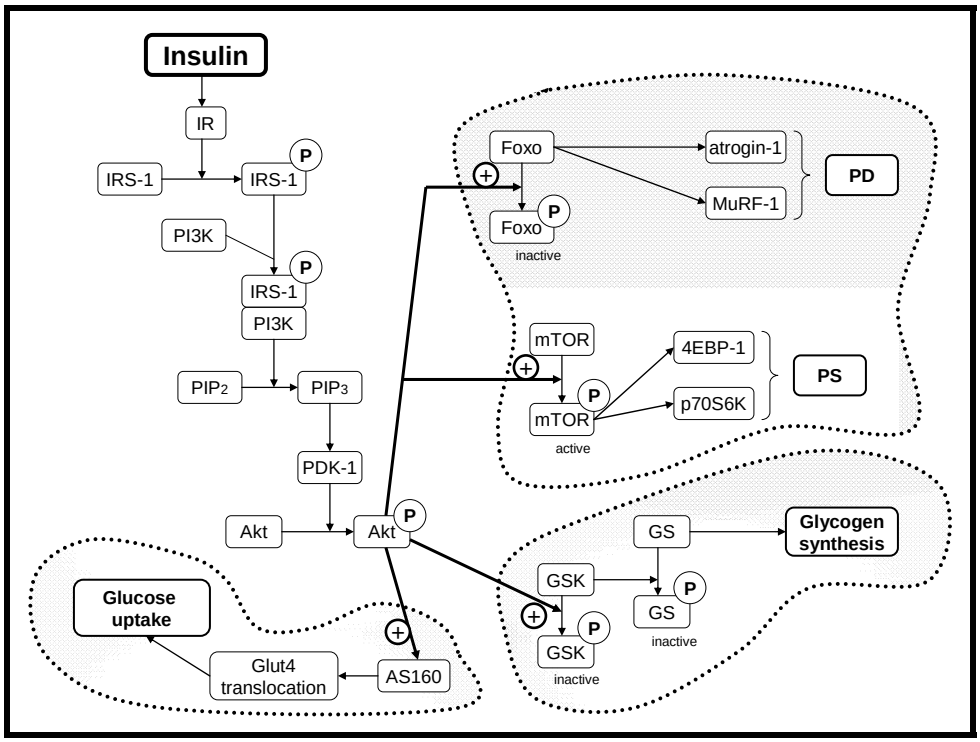

Figure 1.4 Skeletal muscle fibre insulin signalling cascade and the key muscle functions controlled, at least in part, by insulin signalling. Insulin resistance in the skeletal muscle fibre will result in impaired insulin signalling and bear consequences for glucose uptake, glycogen synthesis, and protein synthesis and degradation. Impaired insulin signalling will reduce glucose uptake by impairing GLUT 4 translocation (Wojtaszewski and Richter 2006[35]). Impaired insulin signalling will reduce glycogen synthesis by limiting the phosphorylation and thus inactivation of GSK which will result in active GSK phosphorylating and inactivating GS, thereby reducing glycogen synthesis (Wojtaszewski and Richter 2006[35]). Impaired insulin signalling will reduce protein synthesis by limiting the activation of mTOR and thus the activation of initiation (4EBP-1) and elongation (p70S6K) factors involved in PS (Jackman and Kandarian 2004[37]; Kandarian and Jackman 2006[38]). Impaired insulin signalling will increase protein degradation as the Foxo class of transcription factors will remain unphosphorylated and thus not restricted to the cytoplasm, allowing it to travel to the nucleus and promote the expression of the ubiquitin ligases (atrogin-1 and MuRF-1) which would induce PD via the ubiquitin proteasome system (Sandri et al. 2004[39]). Abbreviations: IR, insulin receptor; IRS-1, insulin receptor substrate 1; PI3K, phosphatidylinositol-3-kinase; PIP_2, phosphatidylinositol-4,5-biphosphate; PIP_3, phosphatidylinositol-3,4,5-triphosphate; PDK-1, phosphoinositide-dependent kinase 1; AS160, Akt substrate of 160 kDa; 4EBP-1, 4E binding protein 1;

p70S6K, p70S6 kinase; GSK, glycogen synthase kinase; GS, glycogen synthase; PS, protein synthesis; PD, protein degradation; mTOR, mammalian target of rapamycin; Foxo, forkhead box O; MuRF-1, muscle ring-finger-1;

In the muscle fibre, elevated FA metabolites and inflammatory cytokines will impair insulin signalling and subsequently reduce GLUT4 translocation and glucose uptake (Pan et al. 1997[40]; Ellis et al. 2000[41]; Itani et al. 2001[42]; Itani et al. 2002[43]; Turinsky et al. 1990[44]; Straczkowski et al. 2004[45]; Yu et al. 2002[46]; Schenk et al. 2008[36]; Belfort et al. 2005[47]; Dresner et al. 1999[48]; Griffin et al. 1999[49]; Plomgaard et al. 2005[50]). In addition to reducing GLUT4 translocation, insulin resistance can decrease the glucose uptake capacity of the muscle fibre, as the capacity for glucose storage is dependent on muscle mass. Under normal conditions, rises in plasma insulin following meal ingestion stimulate the transport of amino acids into skeletal muscle (Hundal et al. 1989[51]) and lead to increases in protein synthesis rates and decreases in protein degradation rates (Wagenmakers 1999[52]), thereby promoting the maintenance and growth of skeletal muscle mass. In obesity, however, the insulin resistance results in impaired amino acid uptake into the muscle fibre, reduced meal-induced increases of protein synthesis, and reduced meal-induced suppression of protein degradation and therefore a progressive loss of muscle mass (Pereira et al. 2008[53]; Chevalier et al. 2005[54]; Kandarian and Jackman 2006[38]; Sandri et al. 2004[39]; Wang et al. 2006[55]). In addition, inactivity will also lead to muscle mass loss via reductions in protein synthesis and increases in protein degradation (Kandarian 2006[38]; Jackman 2004[37]). As obese individuals often lead a sedentary lifestyle, this may accelerate their loss of muscle mass and lead to a vicious cycle. The

net result is a loss of muscle mass and thus a reduction in glucose storage capacity, jeopardizing glycemic control.

Skeletal muscle plays a key role in determining total energy expenditure, which is clearly of central importance to energy balance and weight management. There are three components of total energy expenditure: basal metabolic rate, diet-induced thermogenesis (DIT), and the energy cost of physical activity (Westerterp 2004[56]). DIT is related to the stimulation of energy-requiring processes in the postprandial period, including intestinal digestion and absorption, the initial steps of nutrient metabolism, and the storage of the absorbed but not yet oxidized nutrients (Tappy 1996[57]). In skeletal muscle, DIT and exercise-induced energy expenditure are of particular importance. In skeletal muscle, insulin stimulates mitochondrial respiration (Petersen et al. 2005[58]), increases the uptake of glucose and amino acids, and stimulates glycogen and protein synthesis. All these processes require energy (ATP) and, therefore, make substantial contributions to DIT in lean individuals (Petersen et al. 2005[58]; Wagenmakers 2005[59]). The insulin resistance in the muscle of obese individuals, therefore, seems to make a substantial contribution to the well-known reduction in DIT in obese individuals (de Jonge and Bray 1997[60]; Tappy 1996[57]). Failure of skeletal muscle to increase its metabolic rate in insulin resistant individuals in the postprandial state (Petersen et al. 2005[58]) is clinically highly relevant, as it may at least partially contribute to the weight maintenance problems that people with insulin resistance experience. When there is a gradual reduction in basal and insulin-induced energy expenditure at the muscle level during the development of type II diabetes, food intake should be reduced in proportion to the lower ATP need of the

muscles. Failure to correct for the lower muscle energy requirement will lead to a positive energy balance and to further weight gain.

The insulin resistance present in the muscle fibres of the obese also promotes a reduction in total daily energy expenditure. The loss of muscle mass in obesity resulting from the insulin resistance will reduce muscle force (Jones and Round 1996[61]) and this will have a negative impact on mobility and stability in day to day life and promote the adoption of a more sedentary lifestyle.

The combination of a low muscle mass with a high fat mass will also lead to premature fatigue during exercise as the workload per kilogram muscle will be substantially higher than in the lean. Inflammation of skeletal muscle tissue in obese individuals leads to a further reduction in exercise capacity. Inflammatory cytokines, especially high levels as occur in obese individuals with NAFLD and liver inflammation, have also been associated with strong feelings of fatigue (Byrne et al. 2009[9]). The cause of the fatigue may both involve muscle and central fatigue mechanisms. In the muscle fibres of dogs, inflammatory cytokines have been shown to lead to reductions in the resting membrane potential (Tracey et al. 1986[62]), which not only reduces contractility but also leads to premature fatigue in endurance exercise (Sejersted and Sjøgaard 2000[63]). Reductions in resting membrane potential of 10-50% (Cunningham et al. 1971[64]) and severe reductions in intramuscular potassium concentrations (Gamrin et al. 1997[65]) have also been observed in critically-ill intensive care unit patients with high systemic concentration of inflammatory cytokines. Smaller decreases in resting membrane potential and

intramuscular potassium will also lead to premature fatigue during exercise (Sejersted and Sjøgaard 2000[63]) and cannot be excluded to occur in patients with obesity and NAFLD with liver inflammation. Systemic levels of inflammatory cytokines also have strong associations with a poor self-rated health and subjective feelings of a low fitness level and little energy (Unden et al. 2007[66]). The fatigue experienced by obese patients with NAFLD, therefore, may also involve central components. Independent of whether the fatigue involves muscle or central mechanisms, the likely consequence are the promotion of the adoption of a sedentary lifestyle which will increase the likelihood of further weight gain in obese individuals.

These impairments in skeletal muscles of obese individuals jeopardize glycemic control and weight maintenance, and are also exacerbated by the impairments in macrovascular and microvascular function (described in section 1.2.4) as rarefaction and reduced perfusion will limit the delivery of glucose, amino acids, and insulin to the muscle fibres.

1.2.4 The vasculature: key role in glycemic control and obesity-induced pathology

The entire vasculature is covered with an endothelial cell layer on the luminal side, separating the blood from the vessel wall. The endothelium is a dynamic tissue that plays a central role in vascular function and the maintenance of vascular health. Its main functions include maintenance of blood circulation and fluidity, controlling the coagulation and inflammatory responses, and regulating vascular tone (Gonzalez and Selwyn 2003[67]). In obesity, the elevated FA and inflammatory cytokines lead to endothelial dysfunction. Initially, endothelial dysfunction leads to loss of glycemic

control and an imbalance between vasodilation and vasoconstriction in the fasted resting state, after meal ingestion and potentially during exercise, while in the longer term it leads to micro- and macrovascular pathology and the development of type II diabetes and CVD (Caballero 2003[68]; Jonk et al. 2007[69]; Meyers and Gokce 2007[17]; Muniyappa et al. 2007[70]; Rask-Madsen and King 2007[71]; Stapleton et al. 2008[2]; Bakker et al. 2009[16]).

1.2.4.1 Macrovasculature: supports microvascular function and glycemic control

The macrovasculature serves to deliver blood to the organs of the body and distribute the cardiac output between the organs (Orasanu and Plutzky 2009[72]; Safar et al. 2008[73]). In this way, the macrovasculature supports microvascular function and plays a role in the delivery of glucose to the skeletal muscle for adequate disposal after a carbohydrate-containing meal. The function of the macrovasculature in distributing blood, oxygen and fuels between different organs and tissues is controlled through the selective, timely activation of endothelial vasodilation and vasoconstriction mechanisms in response to the metabolic needs of these organs and tissues.

In the macrovasculature, shear stress arising from the interaction between a high blood flow and the glycocalyx (glycoproteins attached to the luminal side of endothelial cells) that covers the endothelium will stimulate nitric oxide (NO) production and lead to vasodilation (Gouverneur et al. 2006[74]; Chatzizisisi et al. 2007[75]). Similarly, increases in insulin that result from meal ingestion or insulin infusion will induce NO production and lead to vasodilation (Vincent et al. 2006[76]; Clark et al. 2003[77]; Laakso et al. 1990[78]). However, in obese individuals endothelial dysfunction will lead to an imbalance between

vasodilation and vasoconstriction leading to net vasoconstriction. In obese individuals there are impairments in both shear stress-induced (Brook et al. 2001[79]; Hamdy et al. 2003[80]; Meyers and Gokce 2007[17]; Arcaro et al. 1999[81]) and insulin-induced (Laakso et al. 1990[78]) NO-dependent vasodilation. Furthermore, in obese individuals, endothelial dysfunction activates several mechanisms that lead to vasoconstriction (Bakker et al. 2009[16]; Meyers and Gokce 2007[17])

The endothelial dysfunction observed in the macrovasculature of obese individuals is induced by the elevated circulating levels of FA, TG, and inflammatory cytokines originating from the adipose tissue and the liver (Bakker et al. 2009[16]; Byrne et al. 2009[9]; Sulistio et al. 2008[82]). Chronic hyperglycemia and hyperinsulinemia, as occurs in more severe obesity with impaired glucose tolerance, also contribute to the endothelial dysfunction (Bakker et al. 2009[16]). Furthermore, chronic exposure of endothelial cells to high levels of FA, TG, glucose and inflammatory cytokines enhances the production of ROS, which further exacerbate endothelial dysfunction and increase the imbalance between vasodilation (reduced) and vasoconstriction (enhanced) through a number of mechanisms (Orasanu and Plutzky 2009[72]; Bakker et al. 2009[16]; Pacher et al. 2007[83]). The imbalance between vasodilation and vasoconstriction is an important cause of hypertension.

Long term exposure of the endothelium of the macrovasculature to high systemic levels of inflammatory cytokines eventually leads to the expression of adhesion molecules and the attachment of leukocytes and macrophages to the endothelium. This will result in

local production of inflammatory cytokines followed by the loss of integrity of the endothelial lining, macrophage infiltration, atherosclerosis and vascular smooth muscle cell proliferation (Wagenmakers et al. 2006[84]; Meyers and Gokce 2007[17]; Bakker et al. 2009[16]; Gimbrone et al. 2000[85]).

The presence of atherosclerotic plaques will induce oscillatory blood flow and shear stress patterns, which have been shown to further activate vasoconstrictor and atherogenic pathways (Chatzizisisi et al. 2007[75]). Atherosclerosis also leads to an increase in arterial stiffness, as well as further increasing hypertension and the development of obesity-related pathology (Kurukulasuriya et al. 2008[86]).

Thus the elevated circulating levels of FA, TG, and inflammatory cytokines occurring in obesity will induce endothelial dysfunction in the macrovasculature which will impair its ability to support microvascular function and oxygen and substrate delivery to skeletal muscle, an effect which will worsen over time with the development of atherosclerosis and macrovascular pathology.

1.2.4.2 Microvasculature of skeletal muscle: key role in glycemic control

The microvasculature controls the delivery of oxygen and nutrients to match the metabolic needs of skeletal muscle fibres and support normal tissue function over a wide range of energy expenditures (Segal 2005[87]; Orasanu and Plutzky 2009[72]). It is the endothelium of the microvasculature that plays a central role in regulating the recruitment or opening of previously under-perfused or non-perfused capillaries that surround the

skeletal muscle fibres, particularly during exercise and in the postprandial state (Segal 2005[87]). During exercise, adenosine and potassium released from the contracting muscle fibres are the major players dilating terminal arterioles (Hudlicka 1985[88]; van Teefelen 2006[89]; Clifford and Hellsten 2004[90]). Opening of the muscle capillary bed together with the increase in cardiac output will lead to an increase in blood flow and shear stress and, therefore, lead to shear stress induced NO-dependent vasodilation of feeding and resistance arteries and potentially the larger arterioles (Clifford and Hellsten 2004[90]; Kooijman 2008[91]). A careful interplay between these mechanisms ensures that perfusion of the capillaries surrounding skeletal muscle fibres exactly matches the fuel and oxygen demands of each skeletal muscle fibre. After meal ingestion, insulin stimulates NO-mediated vasodilation of terminal arterioles to increase skeletal muscle perfusion and allow the delivery of insulin, glucose, and amino acids to the muscle fibres for clearance (Rattigan et al. 2006[92]; Vincent et al. 2006[76]; Muniyappa and Gokce 2007[70]).

In obesity, however, there appears to be a general impairment in endothelial function of both the macrovasculature and the microvasculature (Jonk et al. 2007[69]). The elevated levels of circulating FA and inflammatory cytokines have been shown to impair activation of endothelial nitric oxide synthase (eNOS) and thus reduce NO production and NO-dependent vasodilation (Kim et al. 2005[93]; Rattigan et al. 2006[92]; Muniyappa and Gokce 2007[70]). Indeed, in response to increases in insulin, resulting from insulin infusion and meal ingestion, a marked impairment has been observed in muscle microvascular recruitment in obese individuals (Clerk et al. 2006[94]; de Jongh et al. 2004[95]; Laakso et al. 1990[78]; Keske et al. 2009[96]). The high concentration of insulin that prevails in obese

humans has also been shown to activate a vasoconstriction pathway, thereby potentially leading to net postprandial vasoconstriction and reduced perfusion of the microvasculature in skeletal muscle (Eringa et al. 2004[97]). Whether a significant limitation exists in the exercise-induced dilation and increase in blood flow of the muscle microvasculature is currently not known, but such limitations do exist in the muscle of patients with type II diabetes (Womack et al. 2009[98]).

Microvascular perfusion relies on the balance between vasodilation and vasoconstriction, and their response to various stimuli. In obesity, it appears that this balance is lost, with a net shift towards vasoconstriction (Bakker et al. 2009[16]) and a reduction in microvascular perfusion under basal and/or stimulated conditions. Reduced skeletal muscle perfusion has been observed in the fasted resting state in obese mice and obese Zucker rats (Wallis et al. 2002[99]; Frisbee 2007[100]), and has been proposed to occur in humans with hypertension and the metabolic syndrome (Lind and Lithell 1993[101]). A multitude of mechanisms are involved in creating this shift in vasoregulation and will be described in detail in section 1.3. Also contributing to impaired skeletal muscle microvascular function are structural impairments of the microvasculature. Reduced capillary density (rarefaction) has been observed in the skeletal muscle of obese rats (Frisbee 2007[100]) and human individuals (Gavin et al. 2005[102]), and are likely to contribute to reductions in perfusion. In addition, the early imbalance between vasodilation and vasoconstriction can lead to functional rarefaction and may limit skeletal muscle perfusion.

Thus the metabolic and structural impairments in the obese skeletal muscle microvasculature will hinder its normal function, thereby reducing the delivery of fuel and oxygen during exercise, and of insulin and glucose in the postprandial state. This will exacerbate the impairments of the obese skeletal muscle fibre and accelerate the loss of glycemic control, promoting the development of type II diabetes and CVD.

1.2.5 Loss of glycemic control

The increased adiposity of the obese causes functional impairments in various tissues with an array of consequences, but a key consequence is the loss of glycemic control. Although the subsequent hyperglycemia bathes all cells of every tissue, it is the tissues which are unable to reduce glucose uptake in the face of elevated glucose levels which incur damage from the excessive glucose concentrations within the cells (Brownlee 2005[103]). The endothelium is one such tissue, and the loss of glycemic control in obese but otherwise healthy individuals is of particular importance because the hyperglycemia can exacerbate the vascular dysfunction which is conducive to a state of chronic hyperglycemia. Chronic hyperglycemia is also seen as a cause of local inflammation and enhances the progression of obesity-related pathology, in particular type II diabetes and CVD.

The loss of glycemic control impairs both the function of skeletal muscle fibres and their microvasculature (Muniyappa et al. 2007[70]). This then leads to a vicious cycle as chronic hyperglycemia and hyperinsulinemia further exacerbate the insulin resistance of skeletal muscle fibres, and the endothelial dysfunction and insulin resistance of the vasculature,

thereby further jeopardizing glycemic control. Endothelial dysfunction is considered to be the earliest marker of impaired vascular health (Meyers and Gokce 2007[17], Potenza and Montagnani 2008[104]; Kim et al. 2008[105]), yet it is reciprocally interconnected to vascular insulin resistance in the promotion of impaired vascular function and hyperglycemia (Figure 1.5; Muniyappa et al. 2007[70]).

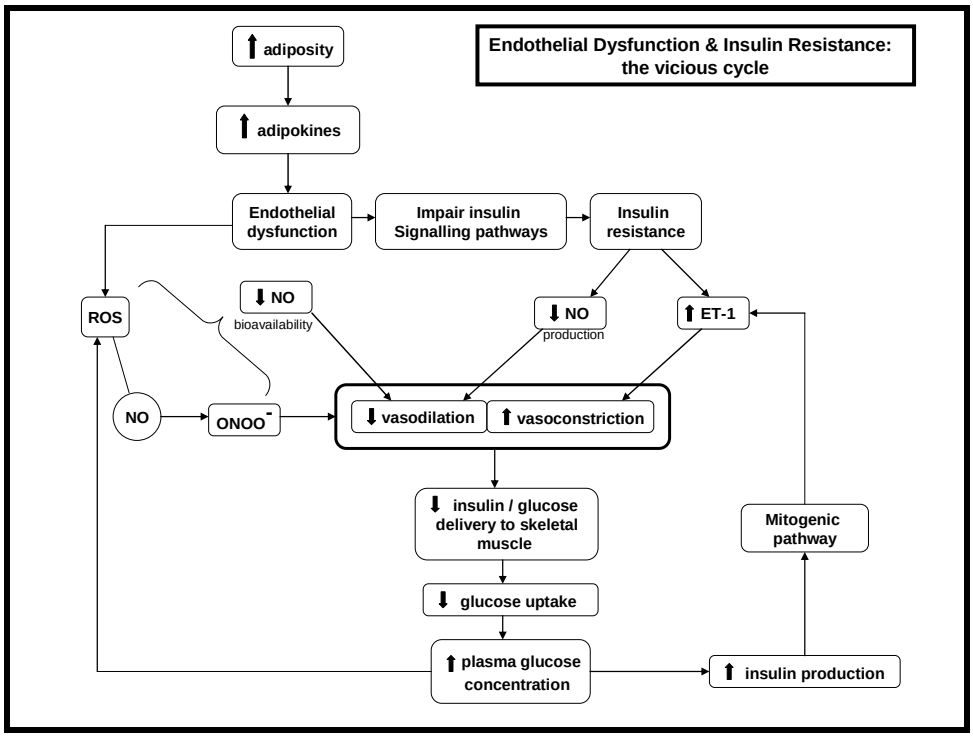

Figure 1.5 The vicious cycle between hyperglycemia and endothelial dysfunction. Abbreviations: NO, nitric oxide; ROS, reactive oxygen species; $ONOO^-$, peroxynitrite; ET-1, endothelin-1.

Glycemic control is commonly assessed by an oral glucose tolerance test (OGTT). Despite obesity, some individuals display normal glycemic control during an OGTT, which would seem incongruous with the evident excess adiposity. There are, however,

various explanations for this observation in some obese individuals. Firstly, compensatory mechanisms, such as increased pancreatic insulin production (Muniyappa et al. 2007[70]) may still be present and sufficient to overcome the insulin resistance and promote glucose clearance. Secondly, in individuals who have only recently gained the excess adiposity, the impairments may still be developing and compensatory mechanisms may still effectively promote glucose clearance. Thirdly, lower body adiposity tends to involve less macrophage infiltration and less adipokine production than upper body / visceral adiposity (Jensen 2008[23]; Shoelson et al. 2006[19]), and would therefore induce a less severe glucose intolerance.

Thus the *rate* of development of chronic hyperglycemia and the related pathologies will depend on various factors, however unless action is taken to address the underlying vascular and skeletal muscle fibre impairments, the development will continue and type II diabetes and CVD will eventually follow. It is of particular importance to correct glucose intolerance before the development of chronic hyperglycemia, because reducing elevated glucose levels appears to only limit but not prevent microvascular disease progression, while having little effect on improving macrovascular disease progression (Johansen et al. 2005[106]; Orasanu and Plutzky 2009[72]).

1.3 The mechanisms that lead to functional, metabolic, and structural impairments in the skeletal muscle microvasculature

Impairments in skeletal muscle microvascular perfusion have been identified in obese individuals and contribute significantly to reduced glucose clearance (Muniyappa et al. 2007[70]; Clerk et al. 2006[94]; Keske at al. 2009[96]). The impaired perfusion appears to stem from rarefaction as well as an imbalance between vasodilation and vasoconstriction mechanisms. The biochemical mechanisms leading to decreased vasodilation and increased vasoconstriction involve the normal and MAPK-dependant insulin signalling cascade in the microvascular endothelium, activation of enzymes producing superoxide anions and scavenging NO, increased peroxynitrite production, and increased sympathetic nerve activity leading to contraction of the vascular smooth muscle cells that surround the arterioles.

1.3.1 Insulin signalling cascades

Within the vasculature, insulin can activate two distinct signalling pathways, namely the PI3K-dependent pathway and MAPK-dependent pathway. The PI3K-dependent pathway in the vasculature shares striking similarities with that in the skeletal muscle fibre (Jansson 2007[107]; Muniyappa et al. 2007[70]) and is responsible for endothelial nitric oxide synthase (eNOS) activation and NO production, inducing vasodilation. The binding of insulin to the insulin receptor on the endothelium leads to tyrosine phosphorylation of the insulin receptor substrate-1 (IRS-1) which then binds to and activates phosphatidylinositol-3-kinase (PI3K). This induces the conversion of phosphatidylinositol-4,5-biphosphate (PIP_2) to phosphatidylinositol-3,4,5-triphosphate (PIP_3) which subsequently activates phosphoinositide-dependent kinase 1 (PDK-1). PDK-1 phosphorylates and activates Akt which directly phosphorylates and activates

eNOS for NO production (Muniyappa et al. 2007[70]; Figure 1.6). On the other hand, the MAPK-dependent pathway is responsible for endothelin-1 (ET-1) production, inducing vasoconstriction (Muniyappa et al. 2007[70]; Jansson 2007[107]; Bakker et al. 2009[16]). Insulin activates this pathway also via the insulin receptor substrate but possibly via IRS-2 rather than IRS-1, which then activates Ras, subsequently inducing a phosphorylation cascade involving Raf, the kinases of mitogen activated protein kinase/extracellular signal-regulated kinase (MAPKK/ERKK), and MAPK/ERK, ending with ET-1 production (Muniyappa et al. 2007[70]; Bakker et al. 2009[16]; Eringa et al. 2004[97]; Figure 1.6). Furthermore, in addition to activating ET-1 production, insulin activation of the MAPK-dependent signalling pathway also stimulates vascular cell adhesion molecule (VCAM-1) and E-selectin expression (Muniyappa et al. 2007[70]; Jansson 2007[107]), both of which contribute to the development of a pro-atherogenic environment and thus promote vascular dysfunction.

These two vascular insulin signalling pathways have been shown to interact, with the phosphorylated active form of Akt in the PI3K-dependent pathway appearing to suppress the MAPK-dependent pathway (Reusch et al. 2001[108]; Muniyappa et al. 2007[70]). Thus under healthy conditions, insulin will stimulate the PI3K-dependent pathway resulting in NO production and, in the process, the activation of Akt will suppress the MAPK-dependent pathway and prevent ET-1 production. In this way, insulin would promote a vasodilation response. Indeed, insulin has been shown to recruit and rapidly increase blood flow in human skeletal muscle capillaries (Rattigan et al. 2006[92]; Jansson 2007[107]; Barrett et al. 2009[109]).

In obesity, however, the insulin resistance is characterized by a pathway specific impairment: only the PI3K-dependent pathway is impaired while the MAPK-dependent pathway remains intact (Muniyappa et al. 2007[70]; Eringa et al. 2004[97]; Jansson 2007[107]; Bakker et al. 2009[16]; Jiang et al. 1999[110]). As hyperinsulinemia is commonly associated with insulin resistance, it will lead to excessive activation of the MAPK-dependent signalling pathway, and lead to a shift in balance from the vasodilator actions of insulin towards the vasoconstrictor actions of insulin (Muniyappa et al. 2007[70]; Jansson 2007[107]). This has been demonstrated in obese humans (Mather et al. 2002[111]) and in the skeletal muscle arterioles of obese rats (Eringa et al. 2007[112]).

Thus, an imbalance between insulin-mediated vasodilation and vasoconstriction is created through impairments of the PI3K-dependent insulin signalling pathway to reduce NO and promote ET-1 production. Fatty acids have been found to play a central role in impairing the endothelial PI3K-dependent pathway and promoting endothelial dysfunction, while hyperglycemia, TNFα, and angiotensin II have also been found to contribute (Muniyappa et al. 2007[70]). As the microvascular effects of insulin have been suggested to account for 50 % of insulin-mediated glucose clearance (Muniyappa et al. 2007[70]), understanding the biochemical basis of this impaired vascular function and identifying ways in which perfusion may be increased to improve glucose clearance, are of clear importance to halt the escalation of impaired glycemic control.

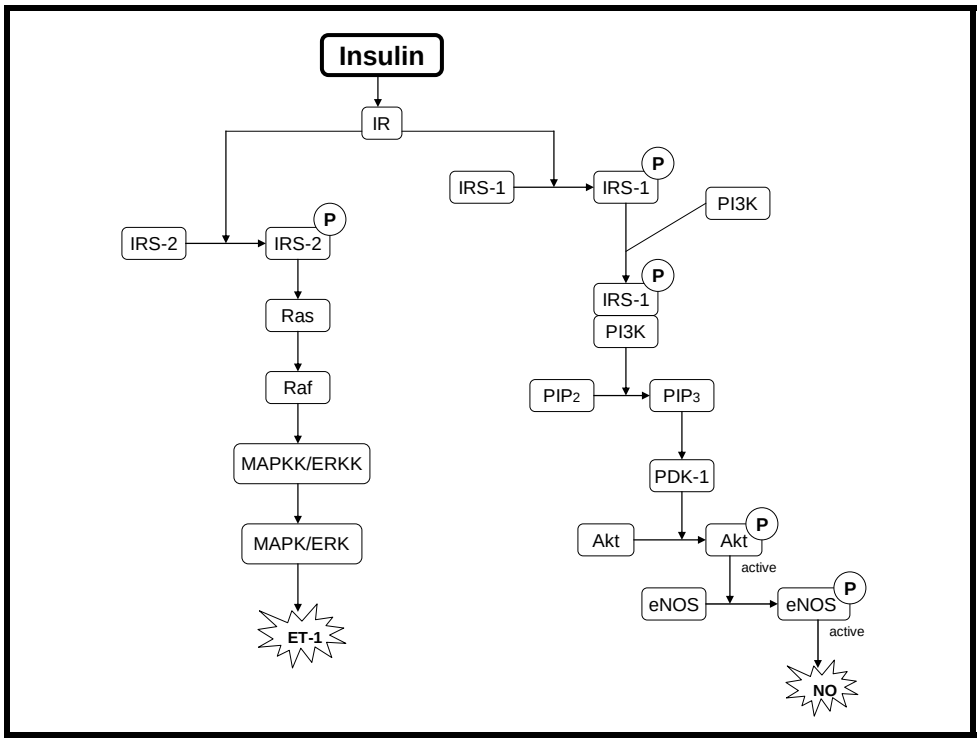

Figure 1.6 Vascular insulin signalling. Abbreviations: IR, insulin receptor; IRS, insulin receptor substrate; MAPKK, mitogen-activated protein kinase kinase; ERKK, extracellular signal-regulated kinase kinase; MAPK, mitogen-activated protein kinase; ERK, extracellular signal-regulated kinase; ET-1, endothelin-1; PI3K, phosphatidylinositol-3-kinase; PIP_2, phosphatidylinositol-4,5-biphosphate; PIP_3, phosphatidylinositol-3,4,5-triphosphate; PDK-1, phosphoinositide-dependent kinase 1; eNOS, endothelial nitric oxide synthase; NO, nitric oxide.

1.3.2 The fatty acid effect

Infusion of intralipid-heparin mixtures leading to substantial increases in plasma FA concentrations impairs insulin-mediated capillary recruitment and glucose uptake in humans and rats (Clerk et al. 2002[113]; de Jongh et al. 2004[114]; Liu et al. 2009[115]). The important role of high plasma FA concentrations in impairing microvascular function is

also supported by the improvement in capillary recruitment observed in obese women after overnight lowering of plasma FA with Acipimox ingestion (de Jongh et al. 2004[114]).

FAs play a central role in impairing skeletal muscle microvascular function principally through the impairment of the PI3K-dependent insulin signalling cascade. In addition, FA can also increase the production of ROS, which can decrease NO bioavailability via NO quenching, thereby further impairing the vasodilatory effect of insulin. Furthermore the peroxynitrite produced in the reaction of NO with superoxide anions (O_2^-), will promote an array of effects which will induce an imbalance between vasodilation and vasoconstriction and thus jeopardise skeletal muscle perfusion and glycemic control. The loss of NO not only impairs vascular function through reduced vasodilation, but also through the loss of its vasoprotective effects including anti-atherogenic and anti-proliferative properties and inhibition of leukocyte and platelet adhesion to the vascular wall (Johansen et al. 2005[106]). Therefore NO production and bioavailability is of central importance to vascular function.

1.3.2.1 FA in obesity

FAs are stored in adipose tissue as TG and can be released into the circulation via lipolysis of the TG by the enzyme HSL (Arner 1999[116]). In healthy individuals, insulin will inhibit HSL activity thereby reducing the efflux of FA from the adipose tissue stores in the postprandial period (Arner 1999[116]; Kamagate and Dong 2008[117]). Obesity, however, is characterised by increased adiposity and insulin resistance. The ability of insulin to suppress lipolysis in adipose tissue is reduced in insulin resistance (Jansson

2007[107]; Yesilova et al. 2005[118]; Baldeweg et al. 2000[119]). Thus it would seem logical that in obese insulin resistant states, a greater efflux of FA from the adipose tissue would occur, resulting in elevated blood FA concentrations. Indeed, there is evidence depicting that increased FA is released into the circulation because regulation of lipolysis becomes resistant to insulin (Baldeweg et al. 2000[119]), and numerous studies show elevated FA levels in obesity (Bickerton et al. 2008[120]; Jensen et al. 1989[121]; Hennes et al. 1996[122]; de Jongh et al. 2004[95]; Coppack et al. 1992[123]; Hickner et al. 1999[124]). Nevertheless, this finding is not universal.

For example, Reeds et al. (2006)[125] found that even extremely obese people had normal circulating FA concentrations. This could potentially be explained by the very high fasting insulin concentrations observed in these participants, sufficient in normalizing the plasma FA levels. It has also been observed that the elevations in plasma FA are not directly proportional to the excess fat mass (Bickerton et al. 2008[120]) which may result from variations of lipolysis in different fat depots. Thus the lack of universality of plasma FA concentrations in obesity may be partly explained by the apparent influence of fat distribution on FA release. Subcutaneous abdominal fat appears to be the major depot contributing to systemic FA concentrations (Bickerton et al. 2008[120]). Indeed, individuals with abdominal obesity tend to have higher circulating levels of FA than individuals with lower body fat distribution despite a comparable BMI (Guo et al. 1999[126]). In hyperinsulinaemia, adipose tissue lipolysis is greater in upper body obesity compared with lower body obesity or lean controls (Jensen 2008[23]) such that plasma FA concentrations are three fold higher in upper body obese than in lower body obese

(Jensen 2008[23]). This would imply a resistance to the antilipolytic effects of insulin on adipocytes in upper body obesity (Jensen 2008[23]).

It is also worth noting that FA concentrations would be affected not only by the release of FA from adipose, but also by the uptake of FA in various tissues. Impaired FA uptake by skeletal muscle has been demonstrated in obesity (Colberg et al. 1995[127]) and may contribute to elevated FA concentrations.

While FA concentrations in obesity appear equivocal, elevated triacylglycerol (TG) levels are often associated with visceral obesity as well as insulin resistance (Kamagate and Dong 2008[117]). Bickerton et al. (2008)[120] found FA concentrations did not differ between obese and control groups, while levels of TG were significantly higher in the obese group. Indeed, hypertriglyceridaemia has been shown to result from an increase in hepatic TG release in insulin resistant states (Baldeweg et al. 2000[119]; Kamagate and Dong 2008[117]) with possible contributions from reduced TG clearance via impaired LPL (Baldeweg et al. 2000[119]).

FAs are substrates for TG synthesis in the liver (Arner 1999[116]). Increased FA delivery to the liver will, in conjunction with the hepatic production of apolipoprotein B100 (ApoB100; Kamagate and Dong 2008[117]), stimulate the production of TG (Arner 1999[116]), resulting in elevated VLDL-TG secretion from the liver into the circulation (Arner 1999[116]; Bradbury 2006[128]; Yesilova et al. 2005[118]). The secretion of VLDL-TG from the liver is tightly controlled by insulin in both a direct and indirect fashion

(Kamagate and Dong 2008[117]). The direct mechanism has yet to be fully elucidated, however it seems to involve insulin directly inhibiting ApoB production and secretion in the liver (Lewis et al. 1995[129]; Alexander et al. 1976[130]; Taghibiglou et al. 2000[131]). Indirectly, insulin dictates liver VLDL-TG production via controlling the release of its substrate, FA, through HSL inhibition in adipose tissue (den Boer et al. 2006[132]). Although, originally, the latter mechanism was thought to be the only way in which insulin influenced VLDL-TG production, the inhibition of VLDL-TG production by insulin was only partly accounted for by the suppression of FA release from the adipose tissue (den Boer et al. 2006[132]; Baldeweg et al. 2000[119]), revealing the presence of additional ways by which insulin controls liver VLDL-TG production. Thus, for normal healthy individuals, in the fasting state when insulin concentrations are low, VLDL-TG release from the liver is increased, while the release is suppressed in the postprandial state when insulin concentrations are high (Kamagate and Dong 2008[117]).

In obese and insulin resistant individuals however, a reduced ability of insulin to suppress the release of VLDL-TG from the liver has been observed (Kamagate and Dong 2008[117]; Yesilova et al. 2005[118]). More specifically, Lewis et al. (1996)[133] found that chronically insulin resistant hyperinsulinaemic obese individuals were resistant to the suppressive effect of insulin on VLDL ApoB, thereby allowing for VLDL-TG synthesis and increased efflux from the liver despite the presence of insulin.

Furthermore, in the obese states where FA levels are elevated, the increased delivery of FA to the liver would provide extra substrate for TG synthesis thereby contributing to the

VLDL-TG production and release (Lewis et al. 1995[129]). It is also possible that despite reports of normal plasma FA concentrations in obesity, individuals with visceral obesity still supply the liver with excess FA. This is because visceral fat is the only deposit directly connected to the liver by the portal vein (Arner 1999[116]; Jensen 2008[23]). Thus it is possible that in visceral obesity, a high efflux of FA from this adipose tissue store directly supplies the liver with excess FA for increased VLDL-TG synthesis and release while the systemic circulation displays normal FA concentrations.

In addition to increased liver VLDL-TG production in obesity, impairments of TG clearance into adipose tissue may contribute to the hypertriglyceridaemia as adipose tissue is the major site for TG-rich lipoprotein clearance (Jensen 2008[23]). There is some evidence indicating a reduction in VLDL-TG clearance across the abdominal subcutaneous adipose tissue in obese humans due to impaired LPL activity despite hyperinsulinaemia (Coppack et al. 1992[123]; Knudsen et al. 1995[134]).

The clearance of TG from the circulation involves hydrolysis of the TG from the lipoproteins and subsequent uptake of the resulting FA into the surrounding tissue. LPL is the rate-limiting enzyme in the hydrolysis of TG lipoproteins and it is expressed in the capillaries of adipose tissue, skeletal and cardiac muscle, and the mammary gland (Fielding 1998[135]). LPL is located on the luminal side of the endothelium in the vascular space bound to the endothelium (Fielding 1998[135]). In this way, the TG from the lipoprotein particles passing through the capillaries with endothelium-bound LPL will be hydrolysed and the resulting FA taken up and either stored or oxidized, depending on the tissue and nutritional state (Fielding 1998[135]; Oram and Bornfeldt 2004[136]).

Although LPL is encoded by the same gene, it is expressed to different extents in different tissues and its activity too is regulated in a tissue-specific manner. LPL is an insulin-sensitive enzyme. In normal conditions, LPL is active in the adipose tissue during the fed state when insulin levels are elevated and suppressed during fasting when insulin levels are low, whereas the reverse is true in muscle (Fielding 1998[135]). In insulin resistance, however, elevated insulin levels would not stimulate the hydrolysis and uptake of the TG into adipose tissue, contributing to elevated circulating TG levels. Furthermore, in the skeletal muscle microcirculation, insulin would not effectively suppress the hydrolysis of TG into FA for uptake. Therefore, in hyperinsulinaemia, the elevated circulating TG could theoretically result in elevated local FA concentrations with in skeletal and cardiac muscle microvasculature despite potentially normal systemic FA concentrations. Such local elevations in FA can affect the microvascular perfusion of the skeletal muscle in the obese through manipulation of vasodilation and vasoconstriction.

Elevated plasma FA can directly affect vasodilation and vasoconstriction mechanisms of the skeletal muscle microcirculation in three ways: i) promote serine phosphorylation of IRS-1, ii) activate nuclear factor κB (NFκB), and iii) promote O_2^- production. The latter will increase peroxynitrite formation which can affect vasodilation and vasoconstriction via several mechanisms which are described below.

1.3.2.2 IRS-1 serine phosphorylation

FAs have been shown to reduce insulin-stimulated eNOS activity and NO production via impairments in the activation of PI3K, PDK-1, Akt, and eNOS (Muniyappa et al. 2007[70]). The impaired activation of these signalling intermediates originates from the serine phosphorylation of IRS-1. Under normal healthy conditions, IRS-1 is phosphorylated on the tyrosine residue, allowing it to subsequently bind to and activate PI3K. The phosphorylation of IRS-1 on the serine residue impairs tyrosine phosphorylation (Shoelson et al. 2006[19]) and the subsequent binding of IRS-1 to PI3K, thereby halting downstream activation of the signalling pathway.

Elevated FA concentrations result in elevated cellular concentrations of lipid metabolites, namely diacylglycerol (DAG), ceramide, and long-chain fatty acyl coenzyme A (LCFA-CoA; Muniyappa et al. 2007[70]). These metabolites have been found to activate serine kinases such as protein kinase C (PKC; Bruce et al. 2006[137]; Itani et al. 2002[43]; Muniyappa et al. 2007[70]), c-Jun NH_2-terminal kinase (JNK; Hirosumi et al. 2002[138]; Rizzo et al. 1999[139]; Shoelson et al. 2006[19]; Shoelson et al. 2007[10]; Muniyappa et al. 2007[70]), and inhibitory κB kinase (IKKB; Sriwijitkamol et al. 2006[140]; Kim et al. 2005[93]; Shoelson et al. 2007[10]; Evans et al. 2002[141]; Kuroki et al. 1998[142]; Muniyappa et al. 2007[70]). Activation of PKC has been implicated in promoting the serine phosphorylation of IRS-1 and reduced insulin-mediated activation of Akt and eNOS (Muniyappa et al. 2007[70]; Bakker et al. 2009[16]; Serne et al. 2006[143]; Kim et al. 2006[144]). Likewise, activation of JNK has been found to increase IRS-1 serine phosphorylation and subsequently decrease insulin-mediated NO production in endothelial cells (Kim et al. 2005[145]; Shoelson et al. 2006[19]; Shoelson et al. 2007[10]; Aguirre et al. 2000[146]; Bakker et

al. 2009[16]). IKKB has also been implicated in promoting serine phosphorylation of IRS-1 both directly and via NFκB activation (Kim et al. 2001[147]; Itani et al. 2002[43]; Gao et al. 2002[148]; Kim et al. 2005[145]; Shoelson et al. 2006[19]). PKC appears to be involved in the activation of IKK and JNK (Shoelson et al. 2007[10]; Shoelson et al. 2006[19]) and may therefore exert its phosphorylation effects on IRS-1 via IKK and JNK rather than directly, however this has yet to be fully elucidated.

Serine phosphorylation of IRS-1 will inactivate IRS-1 and prevent downstream activation of the insulin signalling cascade and thus insulin-stimulated NO production. The impaired Akt activation will relieve the suppression of the MAPK-dependent pathway, enhancing ET-1 production and promoting an imbalance between vasodilation and vasoconstriction, leading to net vasconstriction (Figure 1.7).

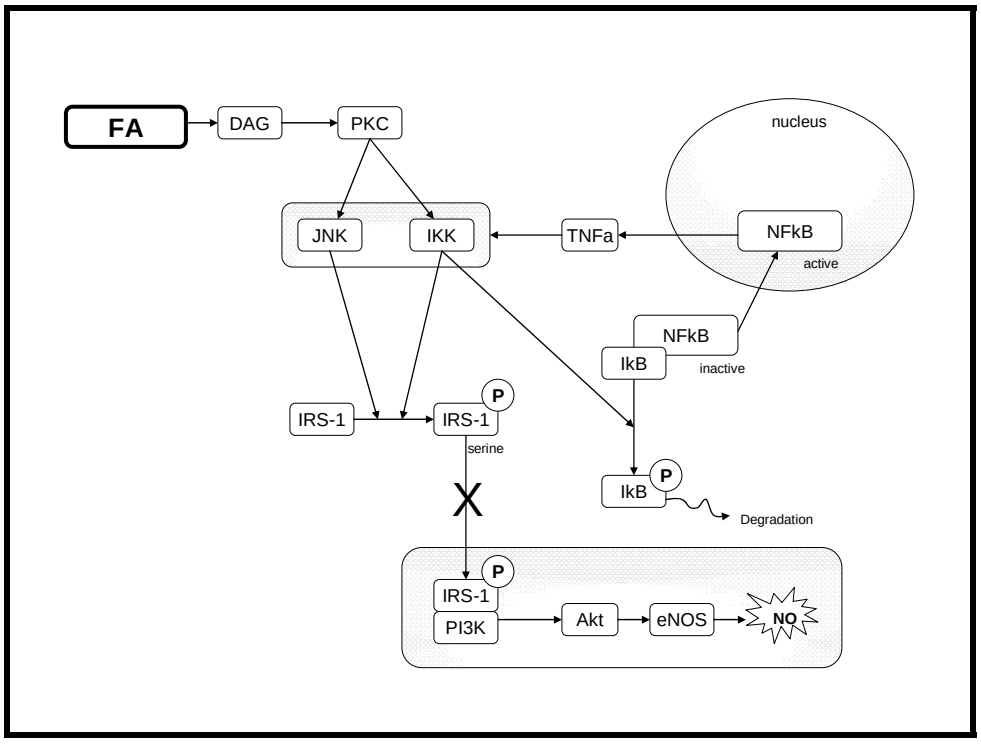

Figure 1.7 Effect of an increased fatty acid (FA) load on the skeletal muscle microvascular endothelium. Abbreviations: DAG, diacylglycerol; PKC, protein kinase C; JNK, c-Jun NH_2-terminal kinase; IKK, inhibitor κB kinase; TNFα, tumor necrosis factor alpha; IRS-1, insulin receptor substrate 1; PI3K, phosphatidylinositol-3-kinase; eNOS, endothelial nitric oxide synthase; NO, nitric oxide; NFκB, nuclear factor κB; IκB, inhibitor κB.

1.3.2.3 NFκB activation

NFκB is a crucial transcription factor involved in inflammation and antiapoptopic signalling. It has been found to play a role in the development of lipid-induced insulin resistance (Staiger et al. 2006[149]; Artwohl et al. 2004[150]; Evans et al. 2002[141]; Schenk et al. 2008[36]). NFκB is normally found in its inactive form, bound to inhibitor κB (IκB), in the cytoplasm. Its activation requires the phosphorylation and subsequent degradation of IκB so that NFκB is free to move into the nucleus to exert its effects (Pacher et al. 2007[83]; Shoelson et al. 2006[19]). FAs activate NFκB via activation of IKK, probably via PKC (Sriwijitkamol et al. 2006[140]; Staiger et al. 2006[149]; Evans et al. 2002[141]; Muniyappa et al. 2007[70]). The activated IKK will phosphorylate IκB, thereby releasing NFκB (Pacher et al. 2007[83]; Sriwijitkamol et al. 2006[140]).

NFκB can indirectly contribute to impaired insulin-mediated vasodilation by increasing the expression and synthesis of TNFα (Sriwijitkamol et al. 2006[140]; Shoelson et al. 2007[10]; Barnes and Karin 1997[151]). TNFα can stimulate IKK and JNK activation (de Alvaro et al. 2004[152]; Bakker et al. 2009[16]; Muniyappa et al. 2007[70]), thereby inducing IRS-1 serine phosphorylation and impeding the progression of the signalling pathway for

NO production, as well as further promoting NFκB activation in a self-sustaining cycle (Luberto et al. 2000[153]; Shoelson et al. 2006[19]; Figure 1.7).

Furthermore, activation of NFκB can impair microvascular function via the promotion of vascular inflammation and atherosclerosis. NFκB can activate numerous genes involved in inflammation, including vascular cell adhesion molecule (VCAM), inter-cellular adhesion molecule-1 (ICAM-1), and E-selectin, which promote the influx of macrophages and monocytes to the arterial wall, inducing ROS production and atherosclerosis (Bakker et al. 2009[16]; Shoelson et al. 2006[19]; Shoelson et al. 2007[10]; Jansson 2007[107]).

1.3.2.4 FA-induced elevations in ROS

FAs have been shown to induce ROS production in the vasculature via mitochondrial uncoupling (Du et al. 2006[154]; Evans et al. 2002[141]; Muniyappa et al. 2007[70]) and by increasing the expression and protein content of nicotinamide adenine dinucleotide phosphate (NADPH) oxidase (Brandes and Kreuzer 2005[155]; Inoguchi et al. 2000[156]; Wagenmakers et al. 2006[84]; Muniyappa et al. 2007[70]; Bakker et al. 2009[16]). FAs induce mitochondrial ROS production by providing electron donors to the mitochondrial electron transport chain (Du et al. 2006[154]). PKC activation by FAs can activate NADPH oxidase leading to the production of superoxide anions (O_2^-; the most reactive form of ROS) in endothelial cells (Muniyappa et al. 2007[70]). The increased generation of ROS, in turn, decreases the concentration of intracellular glutathione, an important endogenous antioxidant (Evans et al. 2002[141]), and makes the vasculature more prone to suffer from oxidative damage and develop pathology.

Elevated ROS levels impair microvascular function in a number of ways. FA-induced ROS production activates NFκB, which further stimulates pro-inflammatory cytokine production (Muniyappa et al. 2007[70]; Itani et al. 2002[43]; Bakker et al. 2009[16]) and impairs microvascular function as discussed above. FA-induced ROS production can also activate the hexosamine biosynthetic pathway and increase the formation of advanced glycation end-products (AGEs; Muniyappa et al. 2007[70]), both of which may contribute to impaired PI3K-dependent signalling pathway (Muniyappa et al. 2007[70]). This will be discussed in section 1.3.3.1. Furthermore, superoxide anions can impair insulin's vasoactive effects by reducing NO bioavailability. Superoxide anions have a high affinity for NO and in the reaction between the two, peroxynitrite is produced (Pacher et al. 2007[83]). Peroxynitrite can impair microvascular function via several mechanisms as explained in the next section.

1.3.2.5 Peroxynitrite formation

The reaction of NO with O_2^- leads to peroxynitrite formation (Pacher et al. 2007[83]), and despite its short half-life (10 – 20 ms), peroxynitrite ($ONOO^-$) has been suggested to be able to cross biological membranes, diffuse one or two cell diameters, and react with several reactive biomolecules to exert its effects (Pacher et al. 2007[83]). Elevated levels of $ONOO^-$ have been suggested to impair microvascular function via (i) reduced activation of guanylate cyclase, (ii) antagonism of calcium-activated and voltage-gated potassium channels, (iii) prostaglandin I_2 synthase inhibition, (iv) eNOS uncoupling, and (v) Akt inhibition (Figure 1.8).

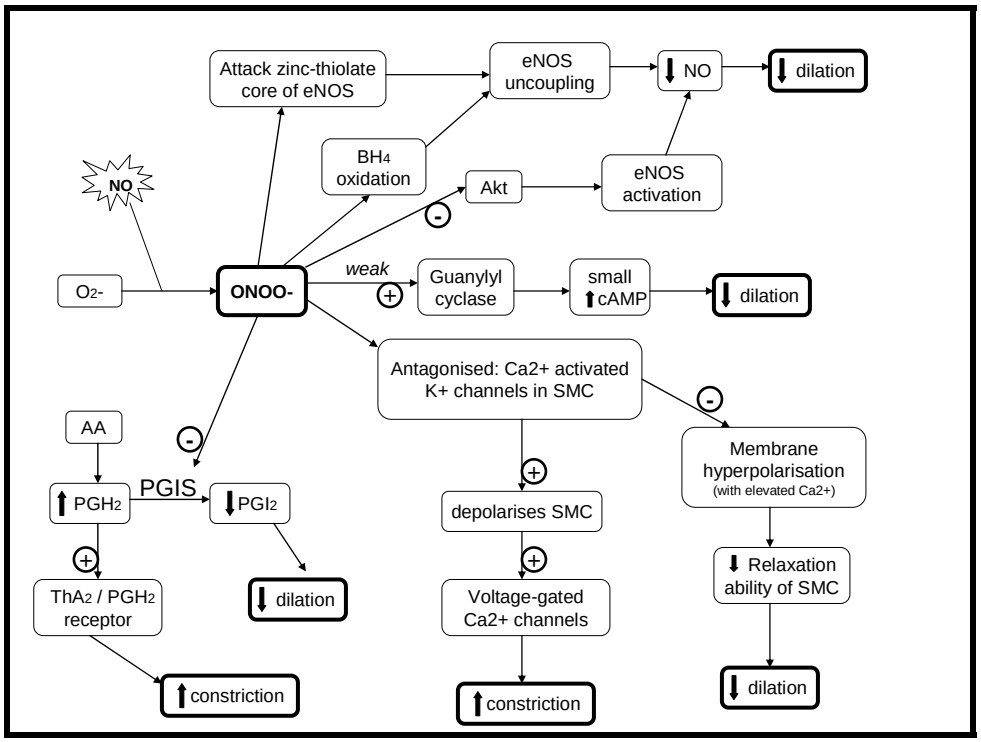

Figure 1.8 The effect of peroxynitrite ($ONOO^-$) on mechanisms controlling vasodilation and vasoconstriction. Abbreviations: eNOS, endothelial nitric oxide synthase; NO, nitric oxide; O_2^-, superoxide anion; AA, arachidonic acid; PGH_2, prostaglandin H_2; PGIS, prostaglandin I_2 synthase; PGI_2, prostaglandin I_2; ThA_2, thromboxane A_2; BH_4, tetrahydrobiopterin; cAMP, cyclic adenosine monophosphate; Ca^{2+}, calcium ion; K^+, potassium ion; SMC, smooth muscle cell.

Reduced activation of guanylate cyclase

In the vasculature, most of the bioavailable NO is generated in the endothelium (Muniyappa et al. 2007[70]). Under normal conditions, NO diffuses into the vascular smooth muscle cells (VSMC) where it activates guanylate cyclase to increase cyclic adenosine monophosphate (cAMP) levels and evoke vasorelaxation (Pacher et al. 2007[83]). However, in insulin resistance, the reduced NO bioavailability will limit

guanylate cyclase activation. Although $ONOO^-$ can activate guanylate cyclase in vitro, it is only a weak activator, thus reducing the vasodilation response in comparison to that of NO (Zou et al. 2002[157]; Liu et al. 2002[158]).

Antagonism of calcium-activated and voltage-gated potassium channels

In the VSMC of coronary arterioles, peroxynitrite has been shown to antagonise calcium-activated potassium channels partly through nitration of tyrosine residues in channel proteins (Bubolz et al. 2007[159]). This would inhibit membrane hyperpolarisation in the presence of calcium, reducing the relaxation ability of VSMCs, and thereby reducing the vasodilation potential (Liu and Gutterman 2002[160]; Brzezinska et al. 2000[161]; Benham et al. 1986[162]). It seems $ONOO^-$ may also inhibit voltage-gated potassium channels in VSMC (Bubolz et al. 2007[159]; Li et al. 2004[163]) which will decrease potassium efflux, resulting in the depolarization of the VSMC. This in turn opens the voltage-sensitive calcium channels causing an increase in intracellular calcium and subsequent vasoconstriction (Michelakis 2002[164]). Whether this impaired vasodilation and increased vasoconstriction effect occurs in skeletal muscle arterioles is yet to be determined, but it may be one of the ways in which $ONOO^-$ impairs vasoregulation in the skeletal muscle microvasculature.

Prostaglandin I_2 synthase inhibition

Peroxynitrite has been found to inhibit prostaglandin I_2 synthase (PGIS) through tyrosine nitration (Pacher et al. 2007[83]; Zou et al. 2004[165]; Cai et al. 2004[166]). This will reduce the production of PGI_2 (also known as prostacyclin), a potent vasodilator, resulting in

reduced vasodilation (Zou et al. 2002[157]; Pacher et al. 2007[83]). Furthermore, inhibition of PGIS will result in the accumulation of prostaglandin H_2 (PGH_2), the precursor of PGI_2. This will increase thromboxane (Th) A_2/PGH_2 receptor activation causing the mobilisation of cytoplasmic calcium and subsequent vasoconstriction (Zou et al. 2002[157]; Zou et al. 2004[165]; Kent et al. 1993[167]; Romero and Reckelhoff 1999[168]).

eNOS uncoupling

NO is produced by the eNOS dimer via a sequence of tightly coupled reactions requiring several cofactors (Bakker et al. 2009[16]). During NO production, the eNOS dimer is stabilised by tetrahydrobiopterin (BH_4) (Bakker et al. 2009[16]). The term 'eNOS uncoupling' describes the loss of structural interaction between BH_4 and eNOS, resulting in the production of O_2^- instead of NO as eNOS will transfer its electrons to molecular oxygen rather than to L-arginine (Jasson 2007[107]; Nickenig and Harrison 2002[169]). When cofactor or substrate concentrations are low, eNOS may become uncoupled (Jansson 2007[107]). There appear to be two ways in which $ONOO^-$ may evoke eNOS uncoupling. Firstly, $ONOO^-$ is a potent oxidiser of BH_4 (Landmesser et al. 2003[170]; Pacher et al. 2007[83]; Muniyappa et al. 2007[70]), thus the formation of $ONOO^-$ will deplete the cofactor (Paravicini and Touyz 2006[171]; Pacher et al. 2007[83]). Secondly, it seems $ONOO^-$ may attack the zinc-thiolate core of eNOS directly to cause enzymatic uncoupling of eNOS, thereby reducing NO production and thus decreasing dilation (Zou et al. 2002A[172]; Zou et al. 2004[165]; Pacher et al. 2007[83]).

Akt inhibition

Akt is involved in the activation of eNOS leading to NO production. $ONOO^-$ has been found to inhibit Akt (Pacher et al. 2007[83]) which would reduce NO production thereby decreasing the vasodilation potential. Inhibition of Akt will also relieve the suppression of the MAPK-dependent pathway of insulin, thereby allowing for ET-1 production and subsequent constriction (Reusch et al. 2001[108]; Gratton et al. 2001[173]; Federici et al. 2002[174]).

1.3.3 Other factors playing a role in impairing vasoregulation

1.3.3.1 Hyperglycemia

Hyperglycemia can lead to both a decrease in vasodilation and an increase in vasoconstriction, which it accomplishes via several mechanisms. The most important mechanisms are summarised below and appear to stem from the same primary source of increased mitochondrial superoxide anion production in endothelial cells (Brownlee 2001[175]; Brownlee 2005[103]; Nishikawa et al. 2000[176]; Du et al. 2000[177]).

Increased mitochondrial O_2^- production leads to reduced vasodilation and increased vasoconstriction as it has been show to act as a primer for other sources of O_2^- production. There are several ways in which this might occur, including (i) activation of NADPH oxidase, (ii) eNOS uncoupling, (iii) increased flux through the hexosamine pathway, and (iv) increased production of advanced glycation end-products (AGE; Figure 1.9; Brownlee 2005[103]; Johansen et al. 2005[106]; Maritim et al. 2003[178]; Ceriello 2003[179]; Pacher et al. 2007[83]; Bakker et al. 2009[16]; Muniyappa et al. 2007[70]; Orasanu and Plutzky 2009[72]). Additionally, mitochondrial O_2^- production stimulates increased glucose

metabolism through the polyol pathway. This indirectly contributes to increased O_2^- by promoting AGE formation and by decreasing the intracellular concentrations of reduced glutathione, an antioxidant (Brownlee 2005[103], Lorenzi 2007[180]; Pacher et al. 2007[83]). In this way, the excessive O_2^- produced is met by reduced antioxidant defences which would increase the susceptibility of the endothelial cell to oxidative stress.

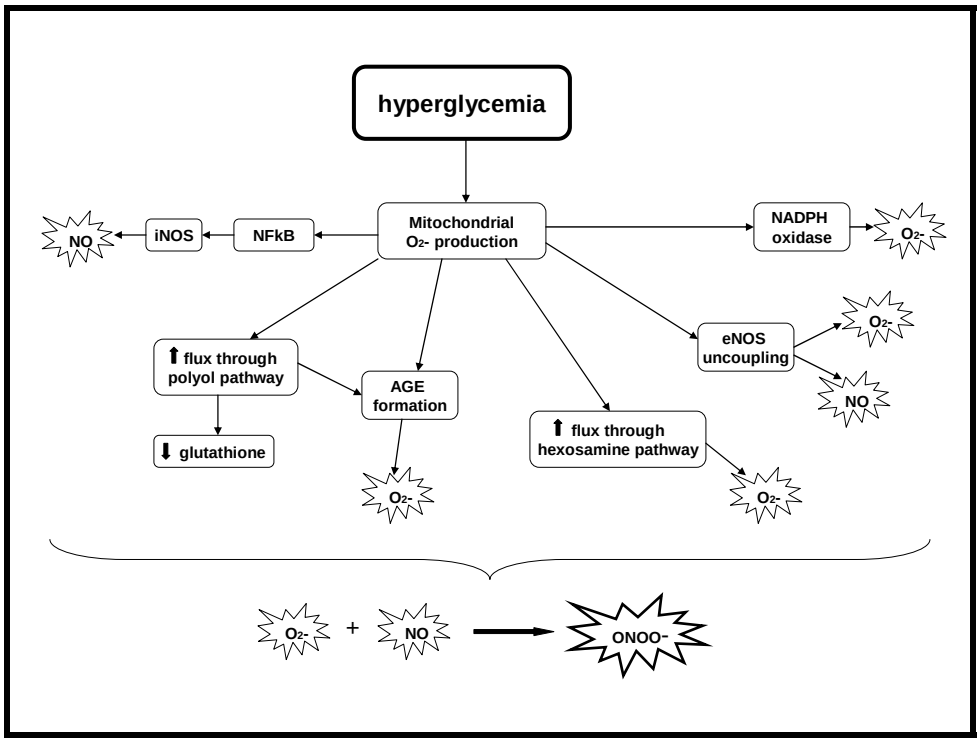

Figure 1.9 Mechanisms by which hyperglycemia increases peroxynitrite formation. Abbreviations: O_2^-, superoxide anion; NFκB, nuclear factor κB; iNOS, inducible nitric oxide synthase; NO, nitric oxide; NADPH oxidase, nicotinamide adenine dinucleotide phosphate oxidase; AGE, advanced glycation end-product; $ONOO^-$, peroxynitrite.

The second step in the impairment of normal vasoregulatory function in hyperglycemia involves the subsequent formation of $ONOO^-$. Increased $ONOO^-$ formation is due to the

elevations of O_2^- as well as the activation of an alternative source of NO. Hyperglycemia, through mitochondrial O_2^- generation, can activate NFκB which in turn has been shown to increase inducible NOS (iNOS) expression and NO production (Ceriello 2003[179]; Pacher et al. 2007[83]). In this way elevated levels of O_2^- and NO are simultaneously produced and they will spontaneously combine to form $ONOO^-$ (Pacher et al. 2007[83]). $ONOO^-$ can reduce vasodilation and promote vasoconstriction as discussed in section 1.3.2.5 above.

Thirdly, hyperglycemia can impair vasoregulation by inducing a shift in glucose metabolism towards the hexosamine pathway. This not only results in O_2^- production, but also in the formation of O-linked glycoproteins. O-linked glycosylation of serine/threonine residues of the insulin signalling proteins affects eNOS activation, thus reducing NO production (Brownlee 2001[175]; Federici et al. 2002[174]; Evans et al. 2002[141]; Bakker et al. 2009[16]; Muniyappa et al. 2007[70]; Figure 1.10). The result is a decreased vasodilation effect as well as increased vasoconstriction due to the reduced Akt suppression of the MAPK-dependent pathway leading to ET-1 production.

The fourth mechanism by which hyperglycemia can impair vasoregulation is via activation of the IKK and NFκB signaling pathway (Brownlee 2001[175]; Maritim et al. 2003[178]; Pacher et al. 2007[83], Kim et al. 2005[145]; Bakker et al. 2009[16]). Activation of the IKK and NFκB signalling pathway may impair Akt activation via IRS-1 serine phosphorylation either by IKK directly or indirectly via TNFα production and JNK activation as discussed in section 1.3.2.2 (Figure 1.10). Hyperglycemia-induced NFκB activation also appears to increase ET-1 production in endothelial cells and thus lead to

vasoconstriction (Muniyappa et al. 2007[70]). Furthermore, activation of NFκB by hyperglycemia can induce endothelial inflammation as it regulates pro-inflammatory and pro-atherosclerotic target genes and would thus impair vascular function (Orasanu and Plutzky 2009[72]).

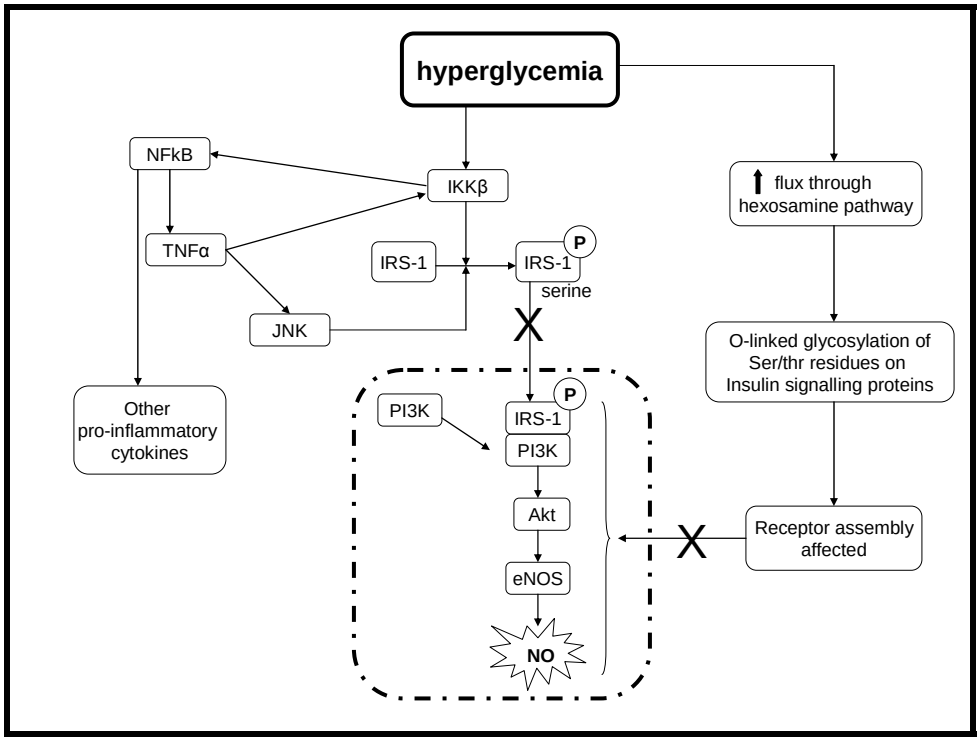

Figure 1.10 Mechanisms by which hyperglycemia impairs the metabolic insulin signalling cascade. Abbrevations: IKKβ, inhibitor κB kinase β; NFκB, nuclear factor κB; TNFα, tumor necrosis factor alpha; JNK, c-Jun NH_2-terminal kinase; IRS-1, insulin receptor substrate 1; PI3K, phosphatidylinositol-3-kinase; eNOS, endothelial nitric oxide synthase; NO, nitric oxide.

1.3.3.2 TNFα

The most extensively studied pro-inflammatory cytokine implicated in insulin resistance is TNFα (Muniyappa et al. 2007[70]). Adipose tissue is a main source of TNFα, and its release from adipose tissue is increased in obesity (Berg and Scherer 2005[15]; Bakker et

al. 2009[16]). The mRNA and protein levels of TNFα are elevated in adipose tissue of obese humans (Shoelson et al. 2007[10]) and this overproduction of TNFα appears to be associated with adipocyte size (Kahn and Flier 2000[181]). The adipocytes are not solely responsible for the increased TNFα secretion from the adipose tissue. In obesity, it seems the enlarged adipocytes initiate inflammation by secreting low amounts of TNFα which stimulate the production of monocyte chemoattractant protein-1 (MCP-1; Bakker et al. 2009[16]). In turn, MCP-1 attracts macrophages to the adipose tissue and these infiltrated macrophages contribute significantly to the TNFα production (Bakker et al. 2009[16]). The elevated production of adipokines by adipose tissue also leads to increased circulating levels of adipokines and induces endothelial inflammation. This involves activation of NFκB and subsequent TNFα production within the endothelial cell.

Within the endothelial cell, TNFα can activate JNK and IKK (Shoelson et al. 2006[19]; Muniyappa et al. 2007[70]). Subsequently, JNK and IKK, will directly impair the PI3K-dependent insulin signalling pathway at the level of the IRS-1, reducing NO production while alleviating the suppression of ET-1 production (Muniyappa et al. 2007[70]). TNFα activation of IKK will also induce NFκB activation, thus creating an amplification cycle for TNFα and its insulin resistance promoting effects (Barnes and Karin1997[151]; Evans et al. 2002[141]), thus inducing a self-sustaining state of inflammation (Shoelson et al. 2006[19]; Shoelson et al. 2007[10]; Jansson 2007[107]). Furthermore, TNFα has been implicated in the activation of NADPH oxidase (Frey et al. 2002[182]; Li et al. 2002[183]; de Keulenaer et al. 1998[184]) and the subsequent production of O_2^- will also contribute to impaired vasoregulation, as previously discussed (in section 1.3.2.4).

1.3.3.3 Angiotensin II

Angiotensin II (Ang II) is an established factor in the pathogenesis of most cardiovascular disorders and a natural regulator of blood pressure. It is the central effector of the renin-angiotensin system (RAS; Nickenig and Harrison 2002[169]) and mediates its effects via the Ang II type 1 receptor (AT1R; van Linthout et al. 2009[185]). Ang II is a potent vasoconstrictor, but at low levels, the constriction effect is mild and mainly in the larger arteries (Stapleton et al. 2008[2]). Adipose tissue plays a primary role in the production of angiotensinogen, the precursor of Ang II (Cassis et al. 2008[186]), with visceral adipose tissue showing greater expression of angiotensinogen than subcutaneous fat (Stapleton et al. 2008[2]). Indeed, in obesity, Ang II levels are usually elevated (Hall 2003[187])

Elevated levels of Ang II have been implicated in a strong vasoconstrictor response which can lead to inflammation, vascular remodelling, thrombosis, and plaque rupture (Stapleton et al. 2008[2]). Ang II, therefore, plays a key role in endothelial dysfunction. The most important mechanism by which Ang II operates is the promotion of ROS production via increased expression and production of NADPH oxidase (Jansson 2007[107]; van Linthout et al. 2009[188]; Nickenig and Harrison 2002[169]). Ang II also leads to endothelial dysfunction via increased expression of ICAM-1 and via increased ET-1 production by the endothelium (Jansson 2007[107]). The mechanism by which Ang II increases ICAM-1 expression most likely involves NFκB activation (Stapleton et al. 2008[2]), while the mechanisms by which Ang II increases ET-1 release most likely

involves its ability to activate JNK and MAPK pathways (Jansson 2007[107]). Activation of the JNK pathway would impair the PI3K-dependent pathway and thus reduce NO production as well as relieve the suppression of the MAPK-dependent pathway for ET-1 production.

Taken together, the vascular effects of elevated Ang II levels likely play a role in obesity-related skeletal muscle microvascular impairments leading to endothelial dysfunction and reduced tissue perfusion.

1.3.3.4 Sympathetic Nerve Activity

Sympathetic nerve activity (SNA) is primarily regulated within the areas of the brainstem that control cardiovascular function. SNA is involved in the regulation of vascular tone in the microvasculature of skeletal muscle by promoting α-adrenergic vasoconstriction of the VSMC (Fisher et al. 2009[189]). In obese individuals, skeletal muscle appears to be an important peripheral target of increases in SNA (Seals and Bell 2004[190]). Substantial elevations in muscle SNA (MSNA) are seen in obesity (Alvarez et al. 2002[191]; Straznicky et al. 2009[192]), especially in visceral obesity (Alvarez et al. 2002[191]; Kurukulasuriya et al. 2008[86]) and have a negative impact on the balance between vasodilation and vasoconstriction in the muscle microvasculature. Weight loss leads to a reduction in MSNA in obese individuals and this seems to indicate that there is a direct relationship between adiposity and MSNA (Seals and Bell 2004[190]). Increased MSNA activity has been suggested to lead to elevations in blood pressure and induce vascular remodelling which would promote endothelial dysfunction and reduce microvascular perfusion. Nevertheless, despite demonstrating an elevated MSNA in the postabsorptive state, obese

individuals display a blunted SNA response to meal ingestion (Straznicky et al. 2009[192] and 2009[193]). After meal ingestion, increases in MSNA are seen in healthy individuals and are important for inducing energy expenditure via DIT (Lowell and Bachman 2003[194]; Straznicky et al. 2009[193]; Schwartz 1987[195]; de Jonge and Bray 1997[60]; Tappy 1996[57]). Indeed, approximately a third of the thermogenic effect of food can be accounted for by meal-induced increments in SNA (Lowell and Bachman 2003[194]; Straznicky et al. 2009[193]). Failure to increase MSNA in the obese after meal ingestion seems to explain a substantial proportion of the reduction in DIT that is observed in obese individuals (Lowell and Bachman 2003[194]; de Jonge and Bray 1997[60]; Tappy 1996[57]). Thus not only basal increases in MSNA potentially jeopardize microvascular perfusion through increased α-adrenergic vasoconstriction, but the blunted SNA increase to meal ingestion will contribute to reduced energy expenditure, making it more difficult to tackle and reduce the excess adiposity so central to the impaired microvascular perfusion of the skeletal muscle.

1.4. Long-term obesity and the development of diabetes type II and cardiovascular disease

Over time, the elevated levels of FA, TG, inflammatory cytokines, insulin, glucose, Ang II and SNA will damage the microvasculature and lead to the development of atherosclerosis. This will reduce the flow of blood through the vessels and eventually lead to an irregular and at times oscillatory rather than constant laminar flow (Chatzizisisi

et al. 2007[75]). The shear stress arising from oscillatory and irregular flow has been shown to activate pathways in the endothelium that promote a pro-atherogenic environment (Pacher et al. 2007[83]; Thijssen et al. 2009[196]; Shaaban and Duerinckx 2000[197]; Chatzizisis et al. 2007[75]), further exacerbating vascular health and the impaired glycemic control. The long term result is the development of pathology, in particular type II diabetes and CVD, both of which impose serious health consequences. They are considered preventable diseases, yet type II diabetes is estimated to kill in excess of 26,000 people in England yearly (Yorkshire & Humber Public Health Observatory 2008[198]), while CVD kills more than 110,000 people in England every year (Department of Health 2008[199]).

Type II diabetes is a metabolic disorder diagnosed, and thus largely defined by, chronic hyperglycemia (Orasanu and Plutzky 2009[72]). It is diagnosed by a fasting plasma glucose concentration of $\geq$ 7.0 mmol and a 2 h post OGTT plasma glucose concentration of $\geq$ 11.1 mmol (World Health Organisation 1999[200]). It is the most common form of diabetes, comprising 90 % of the cases (World Health Organisation 2006[12]). Type II diabetic patients are typically resistant to the action of insulin (World Health Organisation 2006[12]) though upon clinical diagnosis, disorders in both insulin action and insulin secretion are usually present (World Health Organisation 1999[200]). Patients are typically obese or display increased abdominal fat deposition despite a BMI below the obese range (World Health Organisation 1999[200]). Over time, the high glucose levels will severely damage the microvasculature leading to irreversible damage to kidneys, eyes, and nerves (Bakker et al. 2009[16]). Indeed, the long-term effects of type II diabetes

include progressive development of nephropathy, which may lead to renal failure, retinopathy, which may lead to blindness, and neuropathy, which may lead to foot ulcers, gangrene, and amputations. Furthermore, hyperglycemia can also damage the macrovasculature, hence the increased risk of cardiovascular, peripheral vascular, and cerebrovascular disease (World Health Organisation 1999[200]) in diabetic patients.

Cardiovascular disease encompasses all diseases that involve the heart and circulatory system, including coronary heart disease, angina, heart attack and stroke, and is the most common cause of death in the UK (British Heart Foundation 2009[201]). The low-grade inflammation and insulin resistance characteristic of obesity promotes the development of CVD (Gonzalez and Selwyn 2003[67]). Of particular importance is the loss of the vaso-protective effects of NO as its bioavailability is reduced (Wagenmakers et al. 2006[84]; Johansen et al. 2005[106]). Without the protective effects of NO, the systemic inflammation will activate NFκB and induce local inflammation in the vasculature which will induce the development of vascular pathology through increased monocyte adhesion, enhanced platelet aggregation and thrombosis, increased inflammation, and the development of foam cell formation for atherosclerosis (Wagenmakers et al. 2006[84]; Marinou et al. 2009[8]; Insull 2009[202]).

Taken together, the serious health consequences of long-term obesity and the principle role of the vasculature in the development of obesity-related pathology, delineate the urgent need to identify ways to improve vascular function particularly for glycemic control in the obese population before the onset of overt type II diabetes and CVD.

1.5 Outline of the thesis

1.5.1 General outline

Chapter 1 gives an introduction of obesity and the functional, metabolic and structural impairments occurring in the adipose tissue, liver, skeletal muscle and vasculature of obese individuals. This chapter also delineates the importance of glycemic control in the prevention of pathology, primarily type II diabetes and CVD, and provides an overview of the biochemical mechanisms that lead to impairments in glucose delivery and uptake in the skeletal muscle of obese individuals, thereby jeopardising glycemic control after meal ingestion.

Chapters 2 and 3 are experimental studies aiming to determine the role that increased FA plays in reducing vasodilation and increasing vasoconstriction during exercise (**chapter 2**) and under resting conditions (**chapter 3**) using near infrared spectroscopy (NIRS) for the measurement of total haemoglobin content (THC) as a measure muscle microvascular blood volume (MBV) in lean and obese individuals. Attempts to measure muscle MBV with NIRS in obese subjects in **chapters 2 and 3** were not successful. Therefore the ability of NIRS to penetrate through different thickness of the adipose tissue layer to give skeletal muscle specific THC information was investigated in **chapter 4**. Results showed an inability of NIRS to measure the expected changes in THC, oxygenated haemoglobin, and oxygen saturation in the skeletal muscle of the participants

with the thickest subcutaneous adipose tissue layer, despite the use of a probe with a larger interoptode distance and thus having a greater penetration depth. Therefore, despite previous studies indicating the theoretical ability of NIRS to penetrate even a large adipose tissue thickness, we found that in practice this theory did not hold.

Consequently, we decided to undertake a more direct method to measure MBV, namely contrast enhanced ultrasound (CEU). The CEU measurement techniques and analysis procedures routinely used in earlier publications lacked detailed descriptions and also had limitations, thus we made a number of modifications to generate the optimal CEU testing and analysis procedures for measurement of skeletal muscle MBV, microvascular flow velocity (MFV), and microvascular blood flow (MBF) in the human forearm (**chapter 5**). This newly developed CEU method was then used to investigate the skeletal muscle MBV, MFV, and MBF response to an oral glucose tolerance test (OGTT) in healthy lean trained individuals (**chapter 6**). This enabled us to see significant increases in MBV and MBF during the OGTT.

In **chapter 7** (general discussion) the main findings and conclusions of the experimental studies are summarized. This is followed by suggestions for future experiments by combining the new information generated in the experimental chapters and that extracted from the most recent literature. These future studies aim to generate new important information defining the extent of the impaired MBV response and glucose disposal after meal ingestion in obese individuals, as well as developing optimal interventions aimed at ameliorating this impairment.

1.5.2 Aims and hypotheses of the experimental chapters

Section 1.3.2.1 of the introduction depicts the central role of increased adipose tissue lipolysis, leading to high plasma FA concentrations and FA uptake in skeletal muscle, and in impairing vasodilation and promoting vasoconstriction through numerous mechanisms. This prompted us to investigate the effect of inhibiting adipose tissue lipolysis on muscle total haemoglobin content (THC) measured at rest and during exercise in obese and lean subjects. Oral ingestion of niacin, a specific inhibitor of adipose tissue lipolysis, was used to create a time window of 90 min with a low plasma FA concentration followed by a time window with an increased plasma FA concentration. This approach was used during exercise in **chapter 2** and at rest in **chapter 3**. The hypothesis of **chapter 2** was that a decrease in plasma FA in obese individuals would increase the exercise-induced vasodilation as reflected by an increased THC measured by NIRS, while a reduction in the exercise-induced vasodilation would occur in lean and obese participants during the period with elevated plasma FA concentrations. In **chapter 3** the net balance between vasodilation and vasoconstriction was measured at rest during low and high plasma FA levels in lean and obese participants. Here the hypothesis was that in the obese, vasoconstriction mechanisms would be active and by lowering plasma FA levels there would be a reduction in vasoconstriction and this would be reflected by an increase in THC as measured by NIRS. For the lean participants, we hypothesized that an increase in vasoconstriction, and thus a decrease in THC, would be seen in the high FA condition.

The results of the experiments in **chapters 2 and 3** suggested that the NIRS method did not generate the expected muscle specific THC results in obese participants with a large adipose tissue thickness (ATT). We therefore investigated the ability of NIRS to penetrate three different ranges of subcutaneous adipose tissue thickness (ATT) (**chapter 4**) with two NIRS probes with a different interoptode distance (ID) and therefore different theoretical measurement depth. The hypothesis was that the 'superficial' probe (probe A) would only be able to generate muscle specific information in the subjects with a thin or moderate ATT, while the 'deep' probe (probe B), manufactured specifically for us with a greater ID, would allow us to make muscle specific NIRS measurements at all ATTs.

The investigations described in **chapter 4** led to the conclusion that NIRS is not able to generate muscle specific THC measurements in obese subjects even with the 'deep' probe. This prompted us to look for another technique to measure skeletal muscle MBV in obese individuals. We chose to introduce the CEU method to our laboratory. Once the method was developed and modified for our experimental interests (**chapter 5**) it was used to investigate the skeletal muscle MBV, MFV, and MBF response to an OGTT in healthy lean trained participants (**chapter 6**). Our hypothesis was that the OGTT would produce a measureable increase in MBV and this would be reflected by (i) increased glucose disposal, (ii) increased energy expenditure, (iii) decreased fat oxidation rates, and (iv) increased glucose oxidation rates. We also measured brachial artery diameter to test the hypothesis that increased vasodilation would also be seen higher up the arterial tree and not just the microvasculature.

1.6 REFERENCE LIST

1. World Health Organisation. Obesity. 2009.

2. Stapleton PA, James ME, Goodwill AG, Frisbee JC. Obesity and vascular dysfunction. Pathophysiology 2008;15:79-89.

3. World Health Organisation. Obesity and overweight. Fact Sheet No. 311, 2006.

4. The NHS Information Center. Statistics on obesity, physical activity, and diet. 2009:1-214.

5. Dinsdale H, Rutter H. National Child Measurement Programme: Detailed analysis of the 2006/07 national dataset. National Obesity Observatory. 2008:1-79.

6. Guo SS, Wu W, Chumlea WC, Roche AF. Predicting overweight and obesity in adulthood from body mass index values in childhood and adolescence. Am J Clin Nutr 2002;76:653-658.

7. World Health Organisation. Life in the 21st century: A vision for all. The World Health Report. 1998:1-226.

8. Marinou K, Tousoulis D, Antonopoulos AS, Stefanadi E, Stefanadis C. Obesity and cardiovascular disease: From pathophysiology to risk stratification. Int J Cardiol 2009.

9. Byrne CD, Olufadi R, Bruce KD, Cagampang FR, Ahmed MH. Metabolic disturbances in non-alcoholic fatty liver disease. Clin Sci (Lond) 2009;116:539-564.

10. Shoelson SE, Herrero L, Naaz A. Obesity, inflammation, and insulin resistance. Gastroenterology 2007;132:2169-2180.

11. Helmrich SP, Ragland DR, Leung RW, Paffenbarger RS, Jr. Physical activity and reduced occurrence of non-insulin-dependent diabetes mellitus. N Engl J Med 1991;325:147-152.

12. World Health Organisation. Diabetes. fact sheet 312 ed. 2006.

13. Science and Technology Committee. Aging: Scientific aspects. House of Lords. 2005:1-133.

14. Frayn KN. Adipose tissue as a buffer for daily lipid flux. Diabetologia 2002;45:1201-1210.

15. Berg AH, Scherer PE. Adipose tissue, inflammation, and cardiovascular disease. Circ Res 2005;96:939-949.

16. Bakker W, Eringa EC, Sipkema P, van H, V. Endothelial dysfunction and diabetes: roles of hyperglycemia, impaired insulin signaling and obesity. Cell Tissue Res 2009;335:165-189.

17. Meyers MR, Gokce N. Endothelial dysfunction in obesity: etiological role in atherosclerosis. Curr Opin Endocrinol Diabetes Obes 2007;14:365-369.

18. Bastard JP, Maachi M, Lagathu C, Kim MJ, Caron M, Vidal H, Capeau J, Feve B. Recent advances in the relationship between obesity, inflammation, and insulin resistance. Eur Cytokine Netw 2006;17:4-12.

19. Shoelson SE, Lee J, Goldfine AB. Inflammation and insulin resistance. J Clin Invest 2006;116:1793-1801.

20. Goossens GH. The role of adipose tissue dysfunction in the pathogenesis of obesity-related insulin resistance. Physiol Behav 2008;94:206-218.

21. Roberts R, Hodson L, Dennis AL, Neville MJ, Humphreys SM, Harnden KE, Micklem KJ, Frayn KN. Markers of de novo lipogenesis in adipose tissue: associations with small adipocytes and insulin sensitivity in humans. Diabetologia 2009;52:882-890.

22. Karpe F, Tan GD. Adipose tissue function in the insulin-resistance syndrome. Biochem Soc Trans 2005;33:1045-1048.

23. Jensen MD. Role of body fat distribution and the metabolic complications of obesity. J Clin Endocrinol Metab 2008;93:S57-S63.

24. Fritsche L, Weigert C, Haring HU, Lehmann R. How insulin receptor substrate proteins regulate the metabolic capacity of the liver--implications for health and disease. Curr Med Chem 2008;15:1316-1329.

25. Targher G, Bertolini L, Padovani R, Rodella S, Tessari R, Zenari L, Day C, Arcaro G. Prevalence of nonalcoholic fatty liver disease and its association with

cardiovascular disease among type 2 diabetic patients. Diabetes Care 2007;30:1212-1218.

26. Bellentani S, Saccoccio G, Masutti F, Croce LS, Brandi G, Sasso F, Cristanini G, Tiribelli C. Prevalence of and risk factors for hepatic steatosis in Northern Italy. Ann Intern Med 2000;132:112-117.

27. Marchesini G, Moscatiello S, Di DS, Forlani G. Obesity-associated liver disease. J Clin Endocrinol Metab 2008;93:S74-S80.

28. Garibotto G, Sofia A, Balbi M, Procopio V, Villaggio B, Tarroni A, Di MM, Cappelli V, Gandolfo MT, Valli A, Verzola D. Kidney and splanchnic handling of interleukin-6 in humans. Cytokine 2007;37:51-54.

29. Ferrannini E, Bjorkman O, Reichard GA, Jr., Pilo A, Olsson M, Wahren J, Defronzo RA. The disposal of an oral glucose load in healthy subjects. A quantitative study. Diabetes 1985;34:580-588.

30. Defronzo RA, Gunnarsson R, Bjorkman O, Olsson M, Wahren J. Effects of insulin on peripheral and splanchnic glucose metabolism in noninsulin-dependent (type II) diabetes mellitus. J Clin Invest 1985;76:149-155.

31. Nuutila P, Knuuti MJ, Heinonen OJ, Ruotsalainen U, Teras M, Bergman J, Solin O, Yki-Jarvinen H, Voipio-Pulkki LM, Wegelius U, . Different alterations in the insulin-stimulated glucose uptake in the athlete's heart and skeletal muscle. J Clin Invest 1994;93:2267-2274.

32. Watson RT, Pessin JE. Subcellular compartmentalization and trafficking of the insulin-responsive glucose transporter, GLUT4. Exp Cell Res 2001;271:75-83.

33. Chang L, Chiang S.H., Saltiel AR. Insulin signaling and the regulation of glucose transport. 10 ed. 2004:65-71.

34. Thong FSL, Dugani CB, Klip A. Turning signals on and off: GLUT4 traffic in the insulin-signaling highway. 20 ed. 2005:271-284.

35. Wojtaszewski JF, Richter EA. Effects of acute exercise and training on insulin action and sensitivity: focus on molecular mechanisms in muscle. Essays Biochem 2006;42:31-46.

36. Schenk S, Saberi M, Olefsky JM. Insulin sensitivity: modulation by nutrients and inflammation. J Clin Invest 2008;118:2992-3002.

37. Jackman RW, Kandarian SC. The molecular basis of skeletal muscle atrophy. Am J Physiol Cell Physiol 2004;287:C834-C843.

38. Kandarian SC, Jackman RW. Intracellular signaling during skeletal muscle atrophy. Muscle Nerve 2006;33:155-165.

39. Sandri M, Sandri C, Gilbert A, Skurk C, Calabria E, Picard A, Walsh K, Schiaffino S, Lecker SH, Goldberg AL. Foxo transcription factors induce the atrophy-related ubiquitin ligase atrogin-1 and cause skeletal muscle atrophy. Cell 2004;117:399-412.

40. Pan DA, Lillioja S, Kriketos AD, Milner MR, Baur LA, Bogardus C, Jenkins AB, Storlien LH. Skeletal muscle triglyceride levels are inversely related to insulin action. Diabetes 1997;46:983-988.

41. Ellis BA, Poynten A, Lowy AJ, Furler SM, Chisholm DJ, Kraegen EW, Cooney GJ. Long-chain acyl-CoA esters as indicators of lipid metabolism and insulin sensitivity in rat and human muscle. Am J Physiol Endocrinol Metab 2000;279:E554-E560.

42. Itani SI, Pories WJ, MacDonald KG, Dohm GL. Increased protein kinase C theta in skeletal muscle of diabetic patients. Metabolism 2001;50:553-557.

43. Itani SI, Ruderman NB, Schmieder F, Boden G. Lipid-induced insulin resistance in human muscle is associated with changes in diacylglycerol, protein kinase C, and IkappaB-alpha. Diabetes 2002;51:2005-2011.

44. Turinsky J, O'Sullivan DM, Bayly BP. 1,2-Diacylglycerol and ceramide levels in insulin-resistant tissues of the rat in vivo. J Biol Chem 1990;265:16880-16885.

45. Straczkowski M, Kowalska I, Nikolajuk A, Dzienis-Straczkowska S, Kinalska I, Baranowski M, Zendzian-Piotrowska M, Brzezinska Z, Gorski J. Relationship between insulin sensitivity and sphingomyelin signaling pathway in human skeletal muscle. Diabetes 2004;53:1215-1221.

46. Yu C, Chen Y, Cline GW, Zhang D, Zong H, Wang Y, Bergeron R, Kim JK, Cushman SW, Cooney GJ, Atcheson B, White MF, Kraegen EW, Shulman GI. Mechanism by which fatty acids inhibit insulin activation of insulin receptor

substrate-1 (IRS-1)-associated phosphatidylinositol 3-kinase activity in muscle. J Biol Chem 2002;277:50230-50236.

47. Belfort R, Mandarino L, Kashyap S, Wirfel K, Pratipanawatr T, Berria R, Defronzo RA, Cusi K. Dose-response effect of elevated plasma free fatty acid on insulin signaling. Diabetes 2005;54:1640-1648.

48. Dresner A, Laurent D, Marcucci M, Griffin ME, Dufour S, Cline GW, Slezak LA, Andersen DK, Hundal RS, Rothman DL, Petersen KF, Shulman GI. Effects of free fatty acids on glucose transport and IRS-1-associated phosphatidylinositol 3-kinase activity. J Clin Invest 1999;103:253-259.

49. Griffin ME, Marcucci MJ, Cline GW, Bell K, Barucci N, Lee D, Goodyear LJ, Kraegen EW, White MF, Shulman GI. Free fatty acid-induced insulin resistance is associated with activation of protein kinase C theta and alterations in the insulin signaling cascade. Diabetes 1999;48:1270-1274.

50. Plomgaard P, Bouzakri K, Krogh-Madsen R, Mittendorfer B, Zierath JR, Pedersen BK. Tumor necrosis factor-alpha induces skeletal muscle insulin resistance in healthy human subjects via inhibition of Akt substrate 160 phosphorylation. Diabetes 2005;54:2939-2945.

51. Hundal HS, Rennie MJ, Watt PW. Characteristics of acidic, basic and neutral amino acid transport in the perfused rat hindlimb. J Physiol 1989;408:93-114.

52. Wagenmakers AJ. Tracers to investigate protein and amino acid metabolism in human subjects. Proc Nutr Soc 1999;58:987-1000.

53. Pereira S, Marliss EB, Morais JA, Chevalier S, Gougeon R. Insulin resistance of protein metabolism in type 2 diabetes. Diabetes 2008;57:56-63.

54. Chevalier S, Marliss EB, Morais JA, Lamarche M, Gougeon R. Whole-body protein anabolic response is resistant to the action of insulin in obese women. Am J Clin Nutr 2005;82:355-365.

55. Wang X, Hu Z, Hu J, Du J, Mitch WE. Insulin resistance accelerates muscle protein degradation: Activation of the ubiquitin-proteasome pathway by defects in muscle cell signaling. Endocrinology 2006;147:4160-4168.

56. Westerterp KR. Diet induced thermogenesis. Nutr Metab (Lond) 2004;1:5.

57. Tappy L. Thermic effect of food and sympathetic nervous system activity in humans. Reprod Nutr Dev 1996;36:391-397.

58. Petersen KF, Dufour S, Shulman GI. Decreased insulin-stimulated ATP synthesis and phosphate transport in muscle of insulin-resistant offspring of type 2 diabetic parents. PLoS Med 2005;2:e233.

59. Wagenmakers AJ. Insulin resistance in the offspring of parents with type 2 diabetes. PLoS Med 2005;2:e289.

60. de Jonge L, Bray GA. The thermic effect of food and obesity: a critical review. 5(6):622-31 ed. 1997:622-631.

61. Jones D, Round J. Skeletal mucle in health and disease. A textbook of muscle physiology. Manchester: Manchester University Press, 1996.

62. Tracey KJ, Lowry SF, Beutler B, Cerami A, Albert JD, Shires GT. Cachectin/tumor necrosis factor mediates changes of skeletal muscle plasma membrane potential. J Exp Med 1986;164:1368-1373.

63. Sejersted OM, Sjogaard G. Dynamics and consequences of potassium shifts in skeletal muscle and heart during exercise. 80 ed. 2000:1411-1481.

64. Cunningham JN, Jr., Carter NW, Rector FC, Jr., Seldin DW. Resting transmembrane potential difference of skeletal muscle in normal subjects and severely ill patients. J Clin Invest 1971;50:49-59.

65. Gamrin L, Andersson K, Hultman E, Nilsson E, Essen P, Wernerman J. Longitudinal changes of biochemical parameters in muscle during critical illness. Metabolism 1997;46:756-762.

66. Unden AL, Andreasson A, Elofsson S, Brismar K, Mathsson L, Ronnelid J, Lekander M. Inflammatory cytokines, behaviour and age as determinants of self-rated health in women. Clin Sci (Lond) 2007;112:363-373.

67. Gonzalez MA, Selwyn AP. Endothelial function, inflammation, and prognosis in cardiovascular disease. Am J Med 2003;115 Suppl 8A:99S-106S.

68. Caballero AE. Endothelial dysfunction in obesity and insulin resistance: a road to diabetes and heart disease. Obes Res 2003;11:1278-1289.

69. Jonk AM, Houben AJ, de Jongh RT, Serne EH, Schaper NC, Stehouwer CD. Microvascular dysfunction in obesity: a potential mechanism in the pathogenesis

of obesity-associated insulin resistance and hypertension. Physiology (Bethesda) 2007;22:252-260.

70. Muniyappa R, Montagnani M, Koh KK, Quon MJ. Cardiovascular actions of insulin. Endocr Rev 2007;28:463-491.

71. Rask-Madsen C, King GL. Mechanisms of Disease: endothelial dysfunction in insulin resistance and diabetes. Nat Clin Pract Endocrinol Metab 2007;3:46-56.

72. Orasanu G, Plutzky J. The pathologic continuum of diabetic vascular disease. J Am Coll Cardiol 2009;53:S35-S42.

73. Safar ME, Rizzoni D, Blacher J, Muiesan ML, gabiti-Rosei E. Macro and microvasculature in hypertension: therapeutic aspects. J Hum Hypertens 2008;22:590-595.

74. Gouverneur M, Berg B, Nieuwdorp M, Stroes E, Vink H. Vasculoprotective properties of the endothelial glycocalyx: effects of gluid shear stress. 259 ed. 2006:393-400.

75. Chatzizisis YS, Coskun AU, Jonas M, Edelman ER, Feldman CL, Stone PH. Role of endothelial shear stress in the natural history of coronary atherosclerosis and vascular remodeling: molecular, cellular, and vascular behavior. J Am Coll Cardiol 2007;49:2379-2393.

76. Vincent MA, Clerk LH, Lindner JR, Price WJ, Jahn LA, Leong-Poi H, Barrett EJ. Mixed meal and light exercise each recruit muscle capillaries in healthy humans. Am J Physiol Endocrinol Metab 2006;290:E1191-E1197.

77. Clark MG, Wallis MG, Barrett EJ, Vincent MA, Richards SM, Clerk LH, Rattigan S. Blood flow and muscle metabolism: a focus on insulin action. Am J Physiol Endocrinol Metab 2003;284:E241-E258.

78. Laakso M, Edelman SV, Brechtel G, Baron AD. Decreased effect of insulin to stimulate skeletal muscle blood flow in obese man. A novel mechanism for insulin resistance. J Clin Invest 1990;85:1844-1852.

79. Brook RD, Bard RL, Rubenfire M, Ridker PM, Rajagopalan S. Usefulness of visceral obesity (waist/hip ratio) in predicting vascular endothelial function in healthy overweight adults. Am J Cardiol 2001;88:1264-1269.

80. Hamdy O, Ledbury S, Mullooly C, Jarema C, Porter S, Ovalle K, Moussa A, Caselli A, Caballero AE, Economides PA, Veves A, Horton ES. Lifestyle modification improves endothelial function in obese subjects with the insulin resistance syndrome. Diabetes Care 2003;26:2119-2125.

81. Arcaro G, Zamboni M, Rossi L, Turcato E, Covi G, Armellini F, Bosello O, Lechi A. Body fat distribution predicts the degree of endothelial dysfunction in uncomplicated obesity. Int J Obes Relat Metab Disord 1999;23:936-942.

82. Sulistio MS, Zion A, Thukral N, Chilton R. PPARgamma agonists and coronary atherosclerosis. Curr Atheroscler Rep 2008;10:134-141.

83. Pacher P, Beckman JS, Liaudet L. Nitric oxide and peroxynitrite in health and disease. Physiol Rev 2007;87:315-424.

84. Wagenmakers AJ, van Riel NA, Frenneaux MP, Stewart PM. Integration of the metabolic and cardiovascular effects of exercise. Essays Biochem 2006;42:193-210.

85. Gimbrone MA, Jr., Topper JN, Nagel T, Anderson KR, Garcia-Cardena G. Endothelial dysfunction, hemodynamic forces, and atherogenesis. Ann N Y Acad Sci 2000;902:230-239.

86. Kurukulasuriya LR, Stas S, Lastra G, Manrique C, Sowers JR. Hypertension in obesity. Endocrinol Metab Clin North Am 2008;37:647-62, ix.

87. Segal SS. Regulation of blood flow in the microcirculation. Microcirculation 2005;12:33-45.

88. Hudlicka O. Regulation of muscle blood flow. Clin Physiol 1985;5:201-229.

89. van Teeffelen. Rapid dilation of arterioles with single contraction of hamster skeletal muscle. 290 ed. 2006:H119-H127.

90. Clifford PS, Hellsten Y. Vasodilatory mechanisms in contracting skeletal muscle. J Appl Physiol 2004;97:393-403.

91. Kooijman M. Flow-mediated dilatation in the superficial femoral artery is nitric oxide mediated in humans. 586 ed. 2008:1137-1145.

92. Rattigan S, Bradley EA, Richards SM, Clark MG. Muscle metabolism and control of capillary blood flow: insulin and exercise. Essays Biochem 2006;42:133-144.

93. Kim F, Tysseling KA, Rice J, Pham M, Haji L, Gallis BM, Baas AS, Paramsothy P, Giachelli CM, Corson MA, Raines EW. Free fatty acid impairment of nitric oxide production in endothelial cells is mediated by IKKbeta. Arterioscler Thromb Vasc Biol 2005;25:989-994.

94. Clerk LH, Vincent MA, Jahn LA, Liu Z, Lindner JR, Barrett EJ. Obesity blunts insulin-mediated microvascular recruitment in human forearm muscle. Diabetes 2006;55:1436-1442.

95. de Jongh RT, Serne EH, Ijzerman RG, de Vries G, Stehouwer CD. Impaired microvascular function in obesity: implications for obesity-associated microangiopathy, hypertension, and insulin resistance. Circulation 2004;109:2529-2535.

96. Keske MA, Clerk LH, Price WJ, Jahn LA, Barrett EJ. Obesity Blunts Microvascular Recruitment in Human Forearm Muscle Following a Mixed Meal. Diabetes Care 2009.

97. Eringa EC, Stehouwer CD, van Nieuw Amerongen GP, Ouwehand L, Westerhof N, Sipkema P. Vasoconstrictor effects of insulin in skeletal muscle arterioles are mediated by ERK1/2 activation in endothelium. Am J Physiol Heart Circ Physiol 2004;287:H2043-H2048.

98. Womack L, Peters D, Barrett EJ, Kaul S, Price W, Lindner JR. Abnormal skeletal muscle capillary recruitment during exercise in patients with type 2 diabetes mellitus and microvascular complications. J Am Coll Cardiol 2009;53:2175-2183.

99. Wallis MG, Wheatley CM, Rattigan S, Barrett EJ, Clark AD, Clark MG. Insulin-mediated hemodynamic changes are impaired in muscle of Zucker obese rats. Diabetes 2002;51:3492-3498.

100. Frisbee JC. Obesity, insulin resistance, and microvessel density. Microcirculation 2007;14:289-298.

101. Lind L, Lithell H. Decreased peripheral blood flow in the pathogenesis of the metabolic syndrome comprising hypertension, hyperlipidemia, and hyperinsulinemia. Am Heart J 1993;125:1494-1497.

102. Gavin TP, Stalling H.W., Zwetsloot KA, Westerkamp LM, Ryan NS, Moore RA, Pofahl WE, Hickner RC. Lower capillary density but no difference in VEGF expression in obese vs. lean young skeletal muscle in humans. J Appl Physiol 2005;98:315-321.

103. Brownlee M. The pathobiology of diabetic complications: a unifying mechanism. Diabetes 2005;54:1615-1625.

104. Potenza MA, Montagnani M. Abnormal insulin signaling: early detection of silent coronary artery disease-erectile dysfunction? Curr Pharm Des 2008;14:3737-3748.

105. Kim F, Pham M, Maloney E, Rizzo NO, Morton GJ, Wisse BE, Kirk EA, Chait A, Schwartz MW. Vascular inflammation, insulin resistance, and reduced nitric oxide production precede the onset of peripheral insulin resistance. Arterioscler Thromb Vasc Biol 2008;28:1982-1988.

106. Johansen JS, Harris AK, Rychly DJ, Ergul A. Oxidative stress and the use of antioxidants in diabetes: linking basic science to clinical practice. Cardiovasc Diabetol 2005;4:5.

107. Jansson PA. Endothelial dysfunction in insulin resistance and type 2 diabetes. J Intern Med 2007;262:173-183.

108. Reusch HP, Zimmermann S, Schaefer M, Paul M, Moelling K. Regulation of Raf by Akt controls growth and differentiation in vascular smooth muscle cells. J Biol Chem 2001;276:33630-33637.

109. Barrett EJ, Eggleston EM, Inyard AC, Wang H, Li G, Chai W, Liu Z. The vascular actions of insulin control its delivery to muscle and regulate the rate-limiting step in skeletal muscle insulin action. Diabetologia 2009;52:752-764.

110. Jiang ZY, Lin YW, Clemont A, Feener EP, Hein KD, Igarashi M, Yamauchi T, White MF, King GL. Characterization of selective resistance to insulin signaling in the vasculature of obese Zucker (fa/fa) rats. J Clin Invest 1999;104:447-457.

111. Mather KJ, Mirzamohammadi B, Lteif A, Steinberg HO, Baron AD. Endothelin contributes to basal vascular tone and endothelial dysfunction in human obesity and type 2 diabetes. Diabetes 2002;51:3517-3523.

112. Eringa EC, Stehouwer CD, Roos MH, Westerhof N, Sipkema P. Selective resistance to vasoactive effects of insulin in muscle resistance arteries of obese Zucker (fa/fa) rats. Am J Physiol Endocrinol Metab 2007;293:E1134-E1139.

113. Clerk LH, Rattigan S, Clark MG. Lipid infusion impairs physiologic insulin-mediated capillary recruitment and muscle glucose uptake in vivo. Diabetes 2002;51:1138-1145.

114. de Jongh RT, Serne EH, Ijzerman RG, de VG, Stehouwer CD. Free fatty acid levels modulate microvascular function: relevance for obesity-associated insulin resistance, hypertension, and microangiopathy. Diabetes 2004;53:2873-2882.

115. Liu Z, Liu J, Jahn LA, Fowler DE, Barrett E. Infusing lipid raises plasma FFA and induces insulin resistance in muscle microvasculature. x ed. 2009:x.

116. Arner P. The role of adipose tissue in lipoprotein metabolism. 146 ed. 1999:S11-S12.

117. Kamagate A, Dong HH. FoxO1 integrates insulin signaling to VLDL production. Cell Cycle 2008;7:3162-3170.

118. Yesilova Z, Ozata M, Oktenli C, Bagci S, Ozcan A, Sanisoglu SY, Uygun A, Yaman H, Karaeren N, Dagalp K. Increased acylation stimulating protein concentrations in nonalcoholic fatty liver disease are associated with insulin resistance. Am J Gastroenterol 2005;100:842-849.

119. Baldeweg SE, Golay A, Natali A, Balkau B, Del PS, Coppack SW. Insulin resistance, lipid and fatty acid concentrations in 867 healthy Europeans. European Group for the Study of Insulin Resistance (EGIR). Eur J Clin Invest 2000;30:45-52.

120. Bickerton AS, Roberts R, Fielding BA, Tornqvist H, Blaak EE, Wagenmakers AJ, Gilbert M, Humphreys SM, Karpe F, Frayn KN. Adipose tissue fatty acid metabolism in insulin-resistant men. Diabetologia 2008;51:1466-1474.

121. Jensen MD, Haymond MW, Rizza RA, Cryer PE, Miles JM. Influence of body fat distribution on free fatty acid metabolism in obesity. J Clin Invest 1989;83:1168-1173.

122. Hennes MM, O'Shaughnessy IM, Kelly TM, LaBelle P, Egan BM, Kissebah AH. Insulin-resistant lipolysis in abdominally obese hypertensive individuals. Role of the renin-angiotensin system. Hypertension 1996;28:120-126.

123. Coppack SW, Evans RD, Fisher RM, Frayn KN, Gibbons GF, Humphreys SM, Kirk ML, Potts JL, Hockaday TD. Adipose tissue metabolism in obesity: lipase action in vivo before and after a mixed meal. Metabolism 1992;41:264-272.

124. Hickner RC, Racette SB, Binder EF, Fisher JS, Kohrt WM. Suppression of whole body and regional lipolysis by insulin: effects of obesity and exercise. J Clin Endocrinol Metab 1999;84:3886-3895.

125. Reeds DN, Stuart CA, Perez O, Klein S. Adipose tissue, hepatic, and skeletal muscle insulin sensitivity in extremely obese subjects with acanthosis nigricans. Metabolism 2006;55:1658-1663.

126. Guo Z, Hensrud DD, Johnson CM, Jensen MD. Regional postprandial fatty acid metabolism in different obesity phenotypes. Diabetes 1999;48:1586-1592.

127. Colberg SR, Simoneau JA, Thaete FL, Kelley DE. Skeletal muscle utilization of free fatty acids in women with visceral obesity. J Clin Invest 1995;95:1846-1853.

128. Bradbury MW. Lipid metabolism and liver inflammation. I. Hepatic fatty acid uptake: possible role in steatosis. Am J Physiol Gastrointest Liver Physiol 2006;290:G194-G198.

129. Lewis GF, Uffelman KD, Szeto LW, Weller B, Steiner G. Interaction between free fatty acids and insulin in the acute control of very low density lipoprotein production in humans. J Clin Invest 1995;95:158-166.

130. Alexander CA, Hamilton RL, Havel RJ. Subcellular localization of B apoprotein of plasma lipoproteins in rat liver. J Cell Biol 1976;69:241-263.

131. Taghibiglou C, Carpentier A, Van Iderstine SC, Chen B, Rudy D, Aiton A, Lewis GF, Adeli K. Mechanisms of hepatic very low density lipoprotein overproduction in insulin resistance. Evidence for enhanced lipoprotein assembly, reduced intracellular ApoB degradation, and increased microsomal triglyceride transfer protein in a fructose-fed hamster model. J Biol Chem 2000;275:8416-8425.

132. den Boer MA, Voshol PJ, Kuipers F, Romijn JA, Havekes LM. Hepatic glucose production is more sensitive to insulin-mediated inhibition than hepatic VLDL-triglyceride production. Am J Physiol Endocrinol Metab 2006;291:E1360-E1364.

133. Lewis GF, Steiner G. Acute effects of insulin in the control of VLDL production in humans. Implications for the insulin-resistant state. Diabetes Care 1996;19:390-393.

134. Knudsen P, Eriksson J, Lahdenpera S, Kahri J, Groop L, Taskinen MR. Changes of lipolytic enzymes cluster with insulin resistance syndrome. Botnia Study Group. Diabetologia 1995;38:344-350.

135. Fielding F. Lipoprotein lipase and the disposition of dietary fatty acids. 80 ed. 1998:495-502.

136. Oram JF, Bornfeldt KE. Direct effects of long-chain non-esterified fatty acids on vascular cells and their relevance to macrovascular complications of diabetes. Front Biosci 2004;9:1240-1253.

137. Bruce CR, Thrush AB, Mertz VA, Bezaire V, Chabowski A, Heigenhauser GJ, Dyck DJ. Endurance training in obese humans improves glucose tolerance and mitochondrial fatty acid oxidation and alters muscle lipid content. Am J Physiol Endocrinol Metab 2006;291:E99-E107.

138. Hirosumi J, Tuncman G, Chang L, Gorgun CZ, Uysal KT, Maeda K, Karin M, Hotamisligil GS. A central role for JNK in obesity and insulin resistance. Nature 2002;420:333-336.

139. Rizzo MT, Leaver AH, Yu WM, Kovacs RJ. Arachidonic acid induces mobilization of calcium stores and c-jun gene expression: evidence that intracellular calcium release is associated with c-jun activation. Prostaglandins Leukot Essent Fatty Acids 1999;60:187-198.

140. Sriwijitkamol A, Christ-Roberts C, Berria R, Eagan P, Pratipanawatr T, Defronzo RA, Mandarino LJ, Musi N. Reduced skeletal muscle inhibitor of kappaB beta content is associated with insulin resistance in subjects with type 2 diabetes: reversal by exercise training. Diabetes 2006;55:760-767.

141. Evans JL, Goldfine ID, Maddux BA, Grodsky GM. Oxidative stress and stress-activated signaling pathways: a unifying hypothesis of type 2 diabetes. Endocr Rev 2002;23:599-622.

142. Kuroki T, Inoguchi T, Umeda F, Nawata H. Effect of eicosapentaenoic acid on glucose-induced diacylglycerol synthesis in cultured bovine aortic endothelial cells. Biochem Biophys Res Commun 1998;247:473-477.

143. Serne EH, de Jongh RT, Eringa EC, Ijzerman RG, de Boer MP, Stehouwer CD. Microvascular dysfunction: causative role in the association between hypertension, insulin resistance and the metabolic syndrome? Essays Biochem 2006;42:163-176.

144. Kim JA, Montagnani M, Koh KK, Quon MJ. Reciprocal relationships between insulin resistance and endothelial dysfunction: molecular and pathophysiological mechanisms. Circulation 2006;113:1888-1904.

145. Kim F, Tysseling KA, Rice J, Gallis B, Haji L, Giachelli CM, Raines EW, Corson MA, Schwartz MW. Activation of IKKbeta by glucose is necessary and sufficient to impair insulin signaling and nitric oxide production in endothelial cells. J Mol Cell Cardiol 2005;39:327-334.

146. Aguirre V, Uchida T, Yenush L, Davis R, White MF. The c-Jun NH(2)-terminal kinase promotes insulin resistance during association with insulin receptor substrate-1 and phosphorylation of Ser(307). J Biol Chem 2000;275:9047-9054.

147. Kim JK, Kim YJ, Fillmore JJ, Chen Y, Moore I, Lee J, Yuan M, Li ZW, Karin M, Perret P, Shoelson SE, Shulman GI. Prevention of fat-induced insulin resistance by salicylate. J Clin Invest 2001;108:437-446.

148. Gao Z, Hwang D, Bataille F, Lefevre M, York D, Quon MJ, Ye J. Serine phosphorylation of insulin receptor substrate 1 by inhibitor kappa B kinase complex. J Biol Chem 2002;277:48115-48121.

149. Staiger K, Staiger H, Weigert C, Haas C, Haring HU, Kellerer M. Saturated, but not unsaturated, fatty acids induce apoptosis of human coronary artery endothelial cells via nuclear factor-kappaB activation. Diabetes 2006;55:3121-3126.

150. Artwohl M, Roden M, Waldhausl W, Freudenthaler A, Baumgartner-Parzer SM. Free fatty acids trigger apoptosis and inhibit cell cycle progression in human vascular endothelial cells. FASEB J 2004;18:146-148.

151. Barnes PJ, Karin M. Nuclear factor-kappaB: a pivotal transcription factor in chronic inflammatory diseases. N Engl J Med 1997;336:1066-1071.

152. deAlvaro C., Teruel T, Hernandez R, Lorenzo M. Tumor necrosis factor alpha produces insulin resistance in skeletal muscle by activation of inhibitor kappaB kinase in a p38 MAPK-dependent manner. J Biol Chem 2004;279:17070-17078.

153. Luberto C, Yoo DS, Suidan HS, Bartoli GM, Hannun YA. Differential effects of sphingomyelin hydrolysis and resynthesis on the activation of NF-kappa B in normal and SV40-transformed human fibroblasts. J Biol Chem 2000;275:14760-14766.

154. Du X, Edelstein D, Obici S, Higham N, Zou MH, Brownlee M. Insulin resistance reduces arterial prostacyclin synthase and eNOS activities by increasing endothelial fatty acid oxidation. J Clin Invest 2006;116:1071-1080.

155. Brandes RP, Kreuzer J. Vascular NADPH oxidases: molecular mechanisms of activation. Cardio Res 2005;65:16-27.

156. Inoguchi T, Li P, Umeda F, Yu HY, Kakimoto M, Imamura M, Aoki T, Etoh T, Hashimoto T, Naruse M, Sano H, Utsumi H, Nawata H. High glucose level and free fatty acid stimulate reactive oxygen species production through protein kinase C--dependent activation of NAD(P)H oxidase in cultured vascular cells. Diabetes 2000;49:1939-1945.

157. Zou MH, Shi C, Cohen RA. High glucose via peroxynitrite causes tyrosine nitration and inactivation of prostacyclin synthase that is associated with thromboxane/prostaglandin H(2) receptor-mediated apoptosis and adhesion

molecule expression in cultured human aortic endothelial cells. Diabetes 2002;51:198-203.

158. Liu Y, Terata K, Chai Q, Li H, Kleinman LH, Gutterman DD. Peroxynitrite inhibits Ca2+-activated K+ channel activity in smooth muscle of human coronary arterioles. Circ Res 2002;91:1070-1076.

159. Bubolz AH, Wu Q, Larsen BT, Gutterman DD, Liu Y. Ebselen reduces nitration and restores voltage-gated potassium channel function in small coronary arteries of diabetic rats. Am J Physiol Heart Circ Physiol 2007;293:H2231-H2237.

160. Liu Y, Gutterman DD. Oxidative stress and potassium channel function. Clin Exp Pharmacol Physiol 2002;29:305-311.

161. Brzezinska AK, Gebremedhin D, Chilian WM, Kalyanaraman B, Elliott SJ. Peroxynitrite reversibly inhibits Ca(2+)-activated K(+) channels in rat cerebral artery smooth muscle cells. Am J Physiol Heart Circ Physiol 2000;278:H1883-H1890.

162. Benham CD, Bolton TB, Lang RJ, Takewaki T. Calcium-activated potassium channels in single smooth muscle cells of rabbit jejunum and guinea-pig mesenteric artery. J Physiol 1986;371:45-67.

163. Li H, Gutterman DD, Rusch NJ, Bubolz A, Liu Y. Nitration and functional loss of voltage-gated K+ channels in rat coronary microvessels exposed to high glucose. Diabetes 2004;53:2436-2442.

164. Michelakis E. Anorectic drugs and vascular disease: the role of voltage-gated K+ channels. Vascul Pharmacol 2002;38:51-59.

165. Zou MH, Cohen R, Ullrich V. Peroxynitrite and vascular endothelial dysfunction in diabetes mellitus. Endothelium 2004;11:89-97.

166. Cai H, McNally JS, Weber M, Harrison DG. Oscillatory shear stress upregulation of endothelial nitric oxide synthase requires intracellular hydrogen peroxide and CaMKII. J Mol Cell Cardiol 2004;37:121-125.

167. Kent KC, Collins LJ, Schwerin FT, Raychowdhury MK, Ware JA. Identification of functional PGH2/TxA2 receptors on human endothelial cells. Circ Res 1993;72:958-965.

168. Romero JC, Reckelhoff JF. State-of-the-Art lecture. Role of angiotensin and oxidative stress in essential hypertension. Hypertension 1999;34:943-949.

169. Nickenig G, Harrison DG. The AT(1)-type angiotensin receptor in oxidative stress and atherogenesis: part I: oxidative stress and atherogenesis. Circulation 2002;105:393-396.

170. Landmesser U, Dikalov S, Price SR, McCann L, Fukai T, Holland SM, Mitch WE, Harrison DG. Oxidation of tetrahydrobiopterin leads to uncoupling of endothelial cell nitric oxide synthase in hypertension. J Clin Invest 2003;111:1201-1209.

171. Paravicini TM, Touyz RM. Redox signaling in hypertension. Cardiovasc Res 2006;71:247-258.

172. Zou MH, Shi C, Cohen RA. Oxidation of the zinc-thiolate complex and uncoupling of endothelial nitric oxide synthase by peroxynitrite. J Clin Invest 2002;109:817-826.

173. Gratton JP, Morales-Ruiz M, Kureishi Y, Fulton D, Walsh K, Sessa WC. Akt down-regulation of p38 signaling provides a novel mechanism of vascular endothelial growth factor-mediated cytoprotection in endothelial cells. J Biol Chem 2001;276:30359-30365.

174. Federici M, Menghini R, Mauriello A, Hribal ML, Ferrelli F, Lauro D, Sbraccia P, Spagnoli LG, Sesti G, Lauro R. Insulin-dependent activation of endothelial nitric oxide synthase is impaired by O-linked glycosylation modification of signaling proteins in human coronary endothelial cells. Circulation 2002;106:466-472.

175. Brownlee M. Biochemistry and molecular cell biology of diabetic complications. Nature 2001;414:813-820.

176. Nishikawa T, Edelstein D, Du XL, Yamagishi S, Matsumura T, Kaneda Y, Yorek MA, Beebe D, Oates PJ, Hammes HP, Giardino I, Brownlee M. Normalizing mitochondrial superoxide production blocks three pathways of hyperglycaemic damage. Nature 2000;404:787-790.

177. Du XL, Edelstein D, Rossetti L, Fantus IG, Goldberg H, Ziyadeh F, Wu J, Brownlee M. Hyperglycemia-induced mitochondrial superoxide overproduction activates the hexosamine pathway and induces plasminogen activator inhibitor-1 expression by increasing Sp1 glycosylation. Proc Natl Acad Sci U S A 2000;97:12222-12226.

178. Maritim AC, Sanders RA, Watkins JB, III. Diabetes, oxidative stress, and antioxidants: a review. J Biochem Mol Toxicol 2003;17:24-38.

179. Ceriello A. New insights on oxidative stress and diabetic complications may lead to a "causal" antioxidant therapy. Diabetes Care 2003;26:1589-1596.

180. Lorenzi M. The polyol pathway as a mechanism ofr diabetic retinopathy: attractive, elusive, and resilient. 2007 ed. 2007:1-10.

181. Kahn BB, Flier JS. Obesity and insulin resistance. J Clin Invest 2000;106:473-481.

182. Frey RS, Rahman A, Kefer JC, Minshall RD, Malik AB. PKCzeta regulates TNF-alpha-induced activation of NADPH oxidase in endothelial cells. Circ Res 2002;90:1012-1019.

183. Li JM, Mullen AM, Yun S, Wientjes F, Brouns GY, Thrasher AJ, Shah AM. Essential role of the NADPH oxidase subunit p47(phox) in endothelial cell superoxide production in response to phorbol ester and tumor necrosis factor-alpha. Circ Res 2002;90:143-150.

184. De Keulenaer GW, Alexander RW, Ushio-Fukai M, Ishizaka N, Griendling KK. Tumour necrosis factor alpha activates a p22phox-based NADH oxidase in vascular smooth muscle. Biochem J 1998;329 (Pt 3):653-657.

185. Van LS, Spillmann F, Lorenz M, Meloni M, Jacobs F, Egorova M, Stangl V, De GB, Schultheiss HP, Tschope C. Vascular-Protective Effects of High-Density Lipoprotein Include the Downregulation of the Angiotensin II Type 1 Receptor. Hypertension 2009.

186. Cassis LA, Police SB, Yiannikouris F, Thatcher SE. Local adipose tissue renin-angiotensin system. Curr Hypertens Rep 2008;10:93-98.

187. Hall JE. The kidney, hypertension, and obesity. Hypertension 2003;41:625-633.

188. Van LS, Spillmann F, Lorenz M, Meloni M, Jacobs F, Egorova M, Stangl V, De GB, Schultheiss HP, Tschope C. Vascular-Protective Effects of High-Density Lipoprotein Include the Downregulation of the Angiotensin II Type 1 Receptor. Hypertension 2009.

189. Fisher JP, Young CN, Fadel PJ. Central sympathetic overactivity: maladies and mechanisms. Auton Neurosci 2009;148:5-15.

190. Seals DR, Bell C. Chronic sympathetic activation: consequence and cause of age-associated obesity? Diabetes 2004;53:276-284.

191. Alvarez GE, Beske SD, Ballard TP, Davy KP. Sympathetic neural activation in visceral obesity. Circulation 2002;106:2533-2536.

192. Straznicky NE, Lambert GW, Masuo K, Dawood T, Eikelis N, Nestel PJ, McGrane MT, Mariani JA, Socratous F, Chopra R, Esler MD, Schlaich MP, Lambert EA. Blunted sympathetic neural response to oral glucose in obese subjects with the insulin-resistant metabolic syndrome. Am J Clin Nutr 2009;89:27-36.

193. Straznicky NE, Lambert GW, McGrane MT, Masuo K, Dawood T, Nestel PJ, Eikelis N, Schlaich MP, Esler MD, Socratous F, Chopra R, Lambert EA. Weight loss may reverse blunted sympathetic neural responsiveness to glucose ingestion in obese subjects with metabolic syndrome. Diabetes 2009;58:1126-1132.

194. Lowell BB, Bachman ES. Beta-Adrenergic receptors, diet-induced thermogenesis, and obesity. J Biol Chem 2003;278:29385-29388.

195. Schwartz RS, Jaeger LF, Silberstein S, Veith RC. Sympathetic nervous system activity and the thermic effect of feeding in man. Int J Obes 1987;11:141-149.

196. Thijssen DH, Dawson EA, Tinken TM, Cable NT, Green DJ. Retrograde flow and shear rate acutely impair endothelial function in humans. Hypertension 2009;53:986-992.

197. Shaaban AM, Duerinckx AJ. Wall shear stress and early atherosclerosis: a review. AJR Am J Roentgenol 2000;174:1657-1665.

198. Yorkshire & Humber Public Health Observatory. Diabetes attributable deaths: Estimating the excess deaths among people with diabtes. 2008.

199. Department of Health. Coronary heart disease. 2008.

200. World Health Organisation. Definition, diagnosis and classification of diabetes mellitus and its complications. 1999:1-65.

201. British Heart Foundation. Cardiovascular disease. 2009.

202. Insull W, Jr. The pathology of atherosclerosis: plaque development and plaque responses to medical treatment. Am J Med 2009;122:S3-S14.

Chapter 2

THE EFFECT OF ACUTE CHANGES IN PLASMA FATTY ACID CONCENTRATIONS ON MUSCLE MICROVASCULAR BLOOD VOLUME IN SEDENTARY LEAN AND OBESE HUMANS DURING ACUTE EXERCISE BOUTS

2.1 INTRODUCTION

A dramatic rise in obesity is occurring worldwide and with it comes the increased risk for development of obesity-related pathologies including hypertension, vascular and coronary artery disease, atherosclerosis, insulin resistance, and type II diabetes (World Health Organisation 2006[1]). The obese population suffers from a generalized impairment in endothelial function (Jonk et al. 2007[2]). This involves increased basal vasoconstriction caused by endothelin-1, angiotensin II, tumor necrosis factor α (TNFα), peroxynitrite and elevated sympathetic neural activity (Cohen 2007[3]; Pacher et al. 2007[4]; Bakker et al. 2009[5]; Stapleton et al. 2008[6]; Fisher et al. 2009[7]), and reduced NO-dependent vasodilation in response to a variety of physiological stimuli, including decreased NO-dependent vasodilation of feeding and resistance arteries in response to shear stress (humans: Arcaro et al. 1999[8], Brook et al. 2001[9]; Hamdy et al. 2003[10], Meyers and Gokce 2007[11]; rats: Frisbee and Stepp 2001[12]; Frisbee 2004[13]). Whether the decreased vasodilator response and increased vasoconstriction at the level of feeding and resistance vessels also operates at the level of the terminal arterioles, limiting capillary perfusion and increases in microvascular blood volume (MBV) during exercise, is currently not known.

During exercise, increases in muscle MBV are the result of two vasodilatior processes, namely NO-dependent vasodilation of feeding and resistance arteries and potentially arterioles (Clifford and Hellsten 2004[14]; Kooijman 2008[15]), and contraction-induced vasodilation of terminal arterioles via mechanisms involving, among others, adenosine

and potassium release from the contracting muscle fibres (Hudlicka 1985[16]; van Teefelen 2006[17]; Clifford and Hellsten 2004[14]). Elevated levels of plasma fatty acids (FA) have been found to impair the activation of endothelial nitric oxide synthase (eNOS; Kim et al. 2005[18]) and vasodilation in response to shear stress (Vogel et al. 1997[19]). Furthermore, elevated FA levels also induce vasoconstriction through a variety of mechanisms in the fasted, resting state (Pacher et al. 2007[4]; Eringa et al. 2004[20]; Serne et al. 2006[21]; Brandes and Kreuzer 2005[22]; Bedard and Krause 2007[23]; Chinen et al. 2007[24]). Although the contraction-induced vasodilation of terminal arterioles via adenosine and potassium is not expected to be affected by high plasma FA concentrations, a limitation in the net vasodilation response, due to mechanistic impairments for NO-dependent vasodilation, in conjunction with increased activation of vasoconstriction mechanisms, could mean that maximal skeletal muscle perfusion is not achieved by the obese during exercise. Consequently, the delivery of oxygen and blood-borne fuels, and the clearance of metabolic waste products would be restricted, thus reducing exercise tolerance in the obese population.

Obesity is commonly associated with increased circulating levels of plasma FA (Bickerton et al. 2008[25]; Jensen et al. 1989[26]; Hennes et al. 1996[27]; de Jongh et al. 2004[28]; Coppack et al. 1992[29]; Hickner et al. 1999[30]) and triglycerides (TG; Kamagate and Dong 2008[31]; Bickerton et al. 2008[25]; Lewis et al. 2002[32]; Frayn 2002[33]). Hydrolysis of plasma TG by lipoprotein lipase in the muscle capillary bed may further increase the local FA concentration (Oram and Bornfeldt 2004[34]; Fielding 1998[35]). A large body of recent literature suggests that acute and chronic exposure of the microvasculature to high plasma

FA play a role both in impairing the mechanisms that determine fasted and insulin-mediated NO-dependent vasodilation and in activating several of the mechanisms leading to vasoconstriction (summarised in Figure 2.1; detailed overview given in Discussion section).

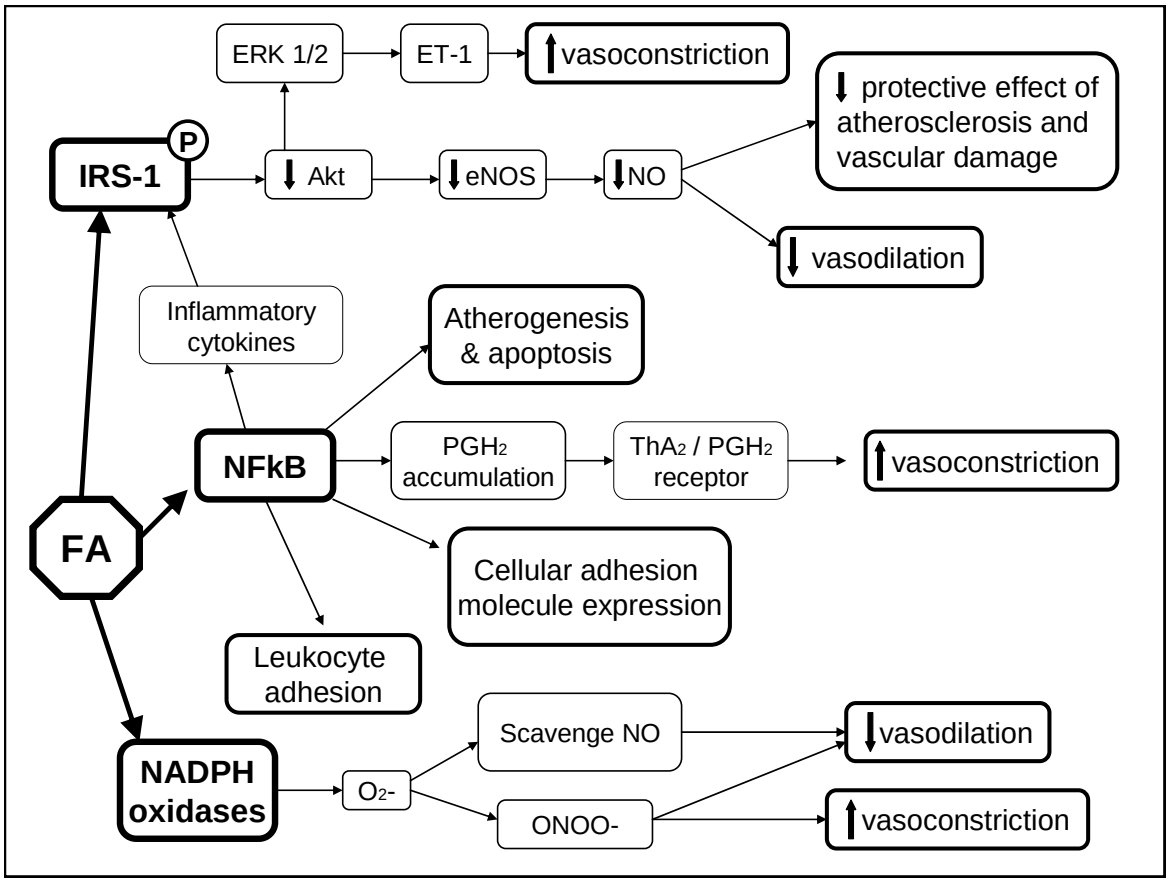

Figure 2.1 Schematic presentation of the main endothelial mechanisms by which a high concentration of plasma fatty acids (FA) reduce vasodilation and increase vasoconstriction of terminal arterioles leading to a net increase in vascular tone of the microvasculature and a potential for underperfusion of skeletal muscle in the fasted resting state, and potentially during acute exercise. Abbreviations: IRS-1, insulin receptor substrate-1; eNOS, endothelial nitric oxide synthase; NO, nitric oxide; ERK 1/2, extracellular signal-regulated kinase 1/2; ET-1, endothelin 1; NFκB, nuclear factor κB; PGH_2, prostaglandin H_2; ThA_2, thromboxane A_2; O_2^-, superoxide anion; $ONOO^-$, peroxynitrite. Figure compiled with information taken from several references (Kim et al. 2005[18]; Gao et al. 2002[36]; McAllister and Laughlin 2006[37]; Landmesser

and Drexler 2007[38]; Federici et al. 2002[39]; Reusch et al. 2001[40]; Gratton et al. 2001[41]; Thijssen et al. 2008[42]; Eringa et al. 2004[20]; Serne et al. 2006[21]; Cardillo et al. 1999[43]; Artwohl et al. 2004[44]; Chinen et al. 2007[24]; Sriwijitkamol et al. 2006[45]; Barnes and Karin 1997[46]; Evans et al. 2002[47]; de Alvaro et al. 2004[48]; Shoelson et al. 2007[49]; Hotamisligil et al. 1996[50]; Gao et al. 2003[51]; Yamamoto et al. 1995[52]; Wagenmakers et al. 2006[53]; Bedard and Krause 2007[23]; Pacher et al. 2007[4]; Zou et al. 2002[54]; Bubolz et al. 2007[55]). A detailed explanation of the mechanisms is given in the Discussion (section 2.4).

The aims of the present study, therefore, were to (i) determine if the decreased vasodilation response to shear stress seen in obese individuals also leads to reduced increases in MBV during exercise, and (ii) investigate whether acute changes in the plasma FA concentration induced by niacin can influence skeletal muscle MBV in the exercising muscle of obese subjects. Total hemoglobin content (THC) of the biceps brachii muscle, an indirect measure of MBV, was monitored using near-infrared spectroscopy (NIRS). Niacin was used to create an initial low, and subsequent high plasma FA concentration (Carlson et al. 1968[56], Wang et al. 2000[57]). Exercise was introduced to examine the effects of low and high FA levels on net increases in MBV in sedentary lean and obese humans. The experimental protocol involved two trials, niacin and placebo, each of which consisted of performing two bouts of incremental arm cranking exercise until self-perceived exhaustion. The first exercise bout (ex 1) commenced 1 hour post niacin ingestion during the low FA phase of the niacin trial, while the second bout of exercise (ex 2) commenced 3 hours post niacin ingestion during the high FA phase of the niacin trial. The hypothesis was that, during the placebo trial, the increase in THC during the exercise bouts would be greater in the lean subjects, as the

obese are expected to have elevated FA levels and impaired increases in MBV in response to exercise. Due to normal fasting plasma FA levels, vasodilation mechanisms should not be impaired and vasoconstriction mechanisms should not be active in lean participants. During the niacin trial, the initial decrease in FA was expected to reduce the microvascular impairments in the obese, allowing for a greater increase in THC during exercise as compared to placebo. The lean participants would show a distinctly smaller THC increase during the exercise bout in the high FA phase of the niacin trial compared to placebo as, according to the hypothesis, the elevated FA would create microvascular impairments, reducing the vasodilation response to exercise and potentially activating the mentioned vasoconstriction mechanisms.

Blood samples were taken throughout the trials for analysis of plasma lactate and FA. The expectation was that lactate levels would rise when muscle perfusion was low due to an increase in anaerobic respiration resulting from reduced oxygen delivery to the working muscle. We thus hypothesized that the greatest increase in plasma lactate concentrations would occur during the second exercise bout in the high FA phase of the niacin trial for the lean group, while obese participants would show the smallest increase in lactate production during exercise in the low FA phase of the niacin trial as compared to placebo.

2.2 MATERIALS AND METHODS

2.2.1 Subjects

A total of 8 lean and 8 obese, sedentary, healthy volunteers were recruited by word of mouth in The University of Birmingham to participate in this study. Their physical characteristics are displayed in Table 2.1. Volunteers met individually with the researcher to discuss the study, provide written informed consent, and complete preliminary measurements including a general health questionnaire, a physical activity questionnaire, measurement of height and weight, and determination of NIRS optimal probe positioning (see below). The research has been carried out in accordance with the Declaration of Helsinki (2000) of the World Medical Association and has been approved by the Ethics Committee of the School of Sport and Exercise Sciences at The University of Birmingham.

Table 2.1 Characteristics of the two participant groups.

	Lean	**Obese**
Age (years)	20.4 *(± 2.3)*	24.6 *(± 5.1)*
Gender (m/f)	5/3	3/5
Skin thickness (mm)	3.1 *(± 0.5)*	11.4 *(± 2.8)*
Height (m)	1.73 *(± 0.11)*	1.70 *(± 0.12)*
Weight (kg)	65.6 *(± 8.7)*	102 *(± 25.2)*
BMI (kg/m^2)	21.8 *(± 1.6)*	34.6 *(± 3.5)*

Skin thickness was measured over the biceps brachii with skin fold callipers and represents an average of three measurements. Values given are the mean of 8 participants with standard deviations given in brackets.

2.2.2 NIRS measurements

NIRS is a non-invasive optical technique based on the oxygen-dependent absorption changes of haemoglobin and myoglobin. While differentiation between oxygenated and deoxygenated states of the chromophores can be made, it is not possible to distinguish between haemoglobin and myoglobin as their absorption spectra overlap (van Beekvelt et al. 2001[58]). We used a continuous-wave NIR spectrometer (ISS OxyplexTS 95306, Champaign IL, USA), which measures the absorbance of the NIRS light at wavelengths of 692 nm and 834 nm and uses calibrated software routines to calculate absolute concentrations from the measured NIR absorbance. Deoxygenated haemoglobin and myoglobin (Hb/Mb) absorbance was measured at wavelength 692 nm, while the sum of deoxygenated and oxygenated Hb/Mb was measured at wavelength 834 nm as they exhibit similar absorption coefficients at this higher wavelength (Wilson et al. 1989[59]). Since myoglobin concentrations were unlikely to change over the testing period, the sum of the absorbance signals at 834 nm was taken to reflect the relative change in THC (assuming a constant hematocrit –Kell et al. 2004[60]). We assumed that the changes in THC would reflect changes in capillary blood volume as NIRS measurements primarily reflect the microcirculation in skeletal muscle (Mancini et al. 1994[61]). NIRS measurements were carried out on the biceps brachii with a probe having an interoptode distance (ID) of 3-4.4 cm. This ID would allow a measurement depth of up to 2.2 cm based on the assumption that the measurement depth is half the ID (van Beekvelt et al. 2001[58]; Cui et al. 1991[62]; Homma et al. 1996[63]). The NIRS measurement unit was given at least a 2 h warm up time as this minimised the signal drift in time and was calibrated before each trial. Data was sampled at 2000 Hz, displayed in real time, and stored on disk for off-line analysis.

2.2.3 Determination of optimal probe position

The optimum probe position for the individual was identified by systematically drawing five marks on the belly of the bicep of their dominant arm and making measurements with the NIRS probe for 2 min on each mark. The mark with the highest THC value was noted as the optimum probe position for the individual. The positioning marks were made with a black ballpoint pen and their placement was identified for each participant in the following way: (a) half distance between elbow (olcranon process) and shoulder (coracoid process) = mark 0; (b) circumference of arm at point 0 divided by 4; (c) value (0.25 of circumference) from point 0 across biceps towards inner arm = mark 1; (d) marks 2-5 are 1.5cm from mark 1, as shown in Figure 2.2.

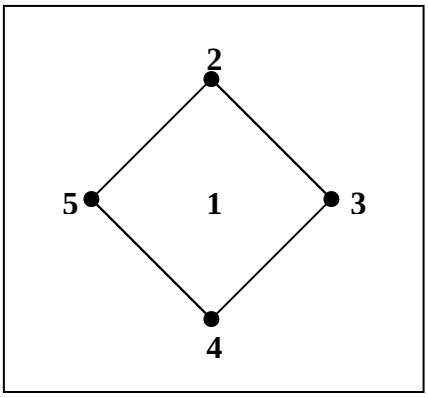

Figure 2.2 Position codes for determination of optimal NIRS probe position on biceps brachii of each participant. The positions were determined by (a) measuring half the distance between the elbow (olcranon process) and shoulder (coracoid process) = point 0; (b) measuring the circumference of the arm from point 0 and dividing it by 4; (c) the value (0.25 of circumference) from point 0 across biceps towards inner arm = mark 1; (d) marks 2-5 are 1.5 cm from mark 1. NIRS measurements were made for 2 min on each point and the point with the highest THC value was noted as the optimum probe position for the individual.

2.2.4 Niacin

Niacin (vitamin B3) is a nicotinic acid analogue which inhibits the release of FA from the adipose tissue, thereby decreasing blood FA concentrations. This mechanism involves niacin binding to the HM74 receptor on the adipocyte (Tunaru et al. 2003[64]), leading to a suppression of intracellular cAMP levels, which in turn decrease cAMP-dependent protein kinase activity. The result is a reduced association of hormone sensitive lipase and the lipid droplets within the adipocyte, thereby decreasing lipolysis and the subsequent release of FA into the blood stream (Christie et al. 1996[65]). As skeletal muscle does not express the HM74 receptor, this effect of niacin remains specific to adipose tissue (Tunaru et al. 2003[64]). A particular characteristic of niacin is its biphasic effect on plasma FA concentrations as after the low FA phase a rebound phase follows, elevating FA levels above basal concentrations. Pilot studies from our laboratory showed 500 mg of niacin to cause a decrease in FA commencing 10 min post capsule ingestion and reaching the lowest point at 60 min before beginning to rise again, surpassing baseline values 3 h post capsule ingestion, peaking at about 4 h and slowly returning towards baseline levels at about 5-6 h. For this reason measurements were made over a 6 h period post niacin ingestion and two exercise bouts were conducted, one being placed during the low FA condition and the second in the rebound high FA condition created by the niacin. Side-effects of niacin ingestion include flushing, itching, nausea, gastrointestinal complaints, headaches, and skin rashes. In the present study, 30-50 min after capsule ingestion, 15 out of 16 participants showed flushing characterised by redness of the face, neck, and arms. Shortly after capsule ingestion, 3 out of 16 participants reported a feeling of nausea which lasted approximately 15 min.

2.2.5 Experimental Protocol

Volunteers visited the laboratory on two occasions, arriving between 6 and 8 am in the overnight fasted state. The day before testing, participants were instructed to refrain from exercise and ingestion of caffeine, and to consume a low-fat evening meal at 7 pm, followed by only low-fat snacks if they could not resist additional food intake. They were instructed to refrain from food and calorie intake from 10 pm, drinking only water until completion of the trial the following day. Visits were at least two days apart and were identical except for the contents of the capsules ingested. Two capsules were given together, each containing 250 mg of either niacin or placebo (microcrystalline cellulose) and administration was double-blinded.

Upon arrival at the laboratory, participants were asked to lie down on the bed while a flexible 20-gauge Teflon catheter (Quickcath, Becton Dickinson, Plymouth United Kingdom) was inserted in the antecubital vein and fitted with a 3-way stopcock (PVB Medizintechnik, Kirchseean, Germany) to allow for repeated blood sampling. The NIRS probe was randomly assigned to the left or right arm for each participant and secured over the predetermined optimal position on the biceps brachii of the same arm for both visits. After a 10 min NIRS baseline measurement, a baseline blood sample was taken and the participant was asked to ingest two 250 mg capsules both containing either placebo or niacin. NIRS measurements continued for the entire duration of the trial. A blood sample was taken 1 h after capsule ingestion and the first arm cranking exercise commenced. Participants cycled with their arms at 50 revolutions per minute while the

workload was increased every 5 min until self-perceived exhaustion, as determined by a Borg Scale (1979). Blood samples were taken at the start of exercise, after every other exercise stage increment, and at the end of exercise (Figure 2.3). Participants were then asked to sit or lie down quietly again until the second exercise session, occurring 3 hrs post capsule ingestion. A blood sample was also taken 2 h post capsule ingestion between exercise sessions. The second exercise was identical to the first in terms of increasing workload and blood sampling. Upon completion of the exercise, NIRS measurements were terminated, the final blood sample was taken, and once the catheter and NIRS probe were removed participants could leave the laboratory.

The experiment was performed in a double blind manner with neither participant nor experimenter aware which trial was niacin or placebo. Females were tested in the luteal phase of the menstrual cycle to exclude hormonal variations with a potential impact on fat metabolism.

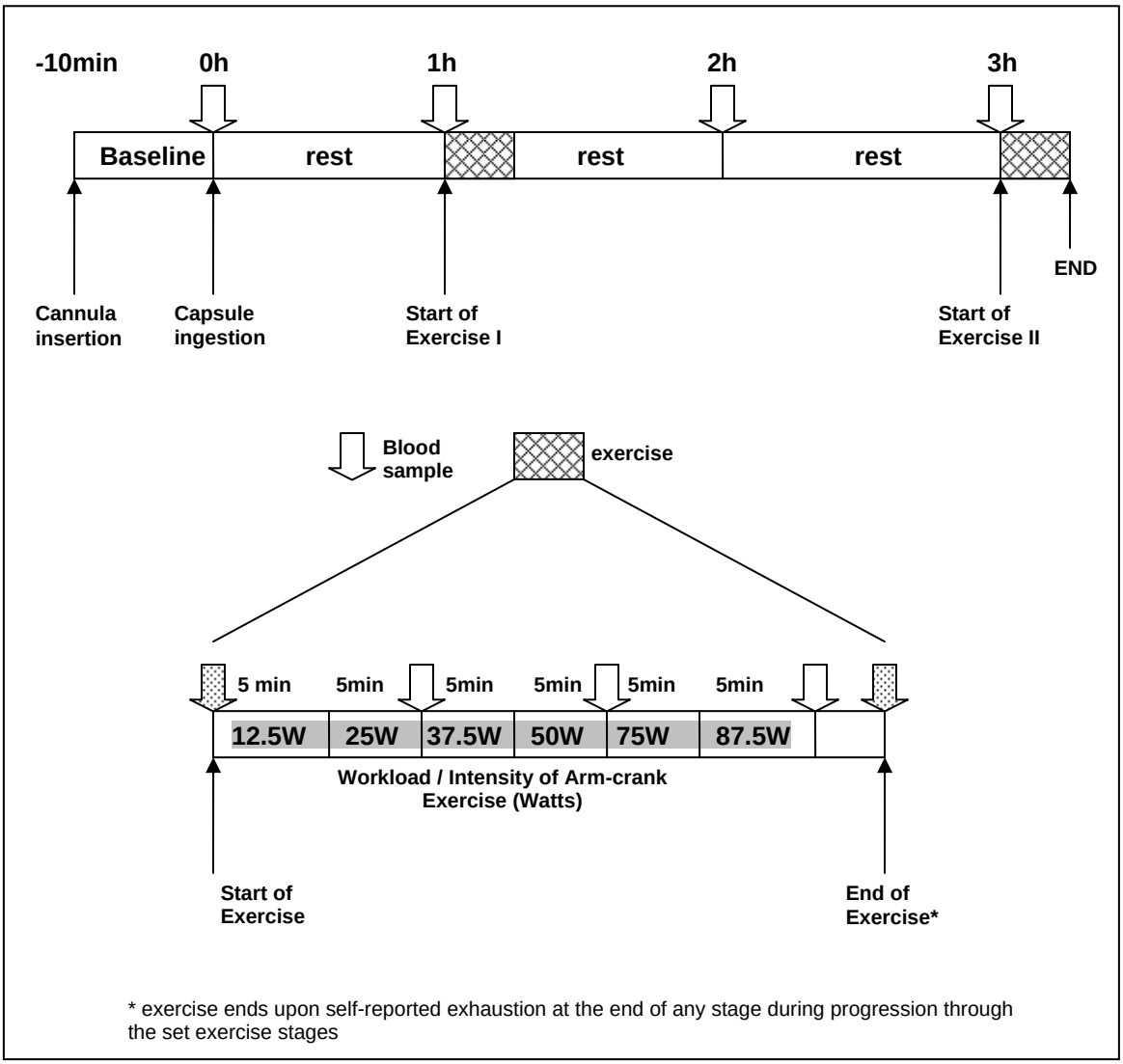

Figure 2.3 Exercise protocol completed by participants at 1 h and 3 h post niacin ingestion. Participants cycled with their arms at 50 revolutions per minute while the workload was increased every 5 min until self-perceived exhaustion, as determined by a Borg Scale (1979). Blood samples were taken at the start of exercise, after every other exercise stage increment, and at the end of exercise. If participants reached exhaustion at the end of a stage after which a sample was taken, then no additional blood sample was necessary.

2.2.6 Blood Samples

Blood samples (7 ml) were collected in EDTA-containing tubes and centrifuged at 1000 g for 10 min at 4 °C. Aliquots of plasma were frozen immediately in liquid nitrogen and stored at -80 °C. Plasma FA concentrations were analysed (NEFA-C; Wako Chemicals, Neuss, Germany), with a COBAS Mira Plus semiautomatic analyzer (ABX Diagnostics). Plasma lactate concentrations were analysed (lactic acid; Horiba ABX, Monpellier, France) with a COBAS Mira Plus semiautomatic analyzer (ABX Diagnostics).

2.2.7 Statistical Analysis

Two-tailed independent samples t-tests were carried out between lean and obese groups for THC increase values from start to end of exercise 1 and 2 in the placebo trial to investigate whether there are differences between groups in the ability to increase THC in response to exercise.

Two-tailed paired samples t-tests were carried out between trials for the THC increase values from start to end exercise 1 and 2 in both lean and obese groups to investigate whether there was a difference in perfusion with different plasma FA conditions for each participant group.

Two-tailed paired samples t-tests were carried bout between exercise 1 and 2 for the niacin trials in both participant groups to investigate whether the different FA conditions affected the lactate increase in each exercise bout for both participant groups. Two-tailed paired samples t-tests were also carried out between trials for the lactate increase values from start to end exercise 1 in the obese group and exercise 2 in the lean group to

investigate whether there was a difference in perfusion with different plasma FA conditions for each participant group.

Two way ANOVAs for repeated measures were carried out on plasma FA data for trial and time between the two exercise bouts and participant groups to investigate whether there were significant changes in FA during exercise bouts between trials for both participant groups.

If significance was found the Bonferroni post hoc test was applied.

All statistical tests were carried out using SPSS for Windows version 16.0 software package (Chicago, IL, USA). All data are reported as means ± SD and statistical significance was set at $P < 0.05$.

2.3 RESULTS

2.3.1 Total Haemoglobin Content

For both groups there was an increase in THC over time during each of the exercise bouts, though the increase is more distinguishable in the lean groups. Figure 2.4 shows the mean data of the groups in both trial conditions. The THC increase from start to end exercise in the placebo trials was not found to be significantly different between lean and obese groups for exercise 1 and 2 ($P = 0.078$ and $P = 0.420$, respectively). The THC increase from start to end exercise was not significantly different between trials for

exercise 1 or 2 in the lean group (P = 0.878 and P = 0.897, respectively) nor the obese group (P = 0.377 and P = 0.721, respectively). Table 2.2 shows the mean THC values at the key time points for both groups and trial conditions.

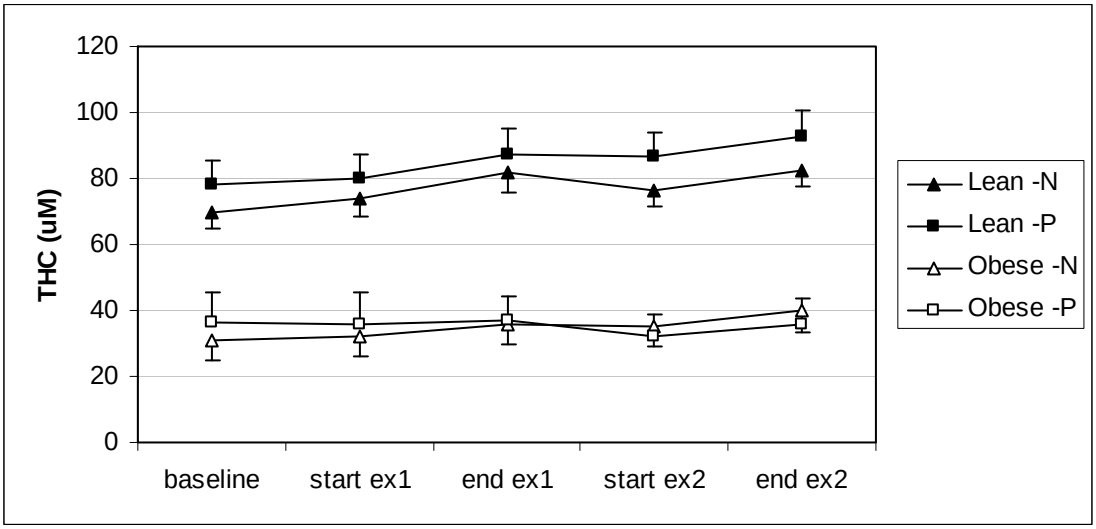

Figure 2.4 Total haemoglobin content (µM) for lean and obese groups during niacin (N) and placebo (P) trials. As there was individual variation in exercise duration, data has been expressed as start and end exercise values for each group and trial condition. Values given are the mean of 8 subjects per group.

Table 2.2 Total haemoglobin content (µM) for lean and obese groups during niacin (N) and placebo (P) trials.

	Lean –N	**Lean –P**	**Obese –N**	**Obese –P**
Baseline	70.0 *(±14.3)*	78.3 *(±19.5)*	31.1 *(±17.6)*	36.3 *(±25.7)*
Start ex1	73.9 *(±15.2)*	79.8 *(±21.2)*	31.9 *(±17.2)*	35.6 *(±27.8)*
End ex1	81.9 *(±17.3)*	87.3 *(±22.9)*	36.0 *(±18.3)*	36.7 *(±21.1)*
Start ex2	73.9 *(±14.5)*	86.5 *(±21.3)*	35.4 *(±18.4)*	32.1 *(±19.2)*

End ex2	82.7 *(±14.6)*	92.7 *(±22.9)*	39.9 *(±18.9)*	35.8 *(±23.0)*

Values are given as the means ± standard deviations (SD) of 8 subjects in each group.

2.3.2 Plasma fatty acids

The blood samples confirmed that the ingestion of 500 mg niacin led to an initial decrease in plasma FA concentrations followed by a rebound phase in which the plasma FA concentrations increased above baseline (Figure 2.5). In exercise 1, plasma FA was significantly different between trials for lean and obese groups ($P = 0.017$ and $P = 0.001$, respectively). In exercise 2, plasma FA was not significantly different between trials for lean and obese groups ($P = 0.253$ and $P = 0.207$, respectively) though plasma FA was higher in the niacin trial in both groups as compared to placebo. Table 2.3 presents the exact mean plasma FA values and their standard deviations.

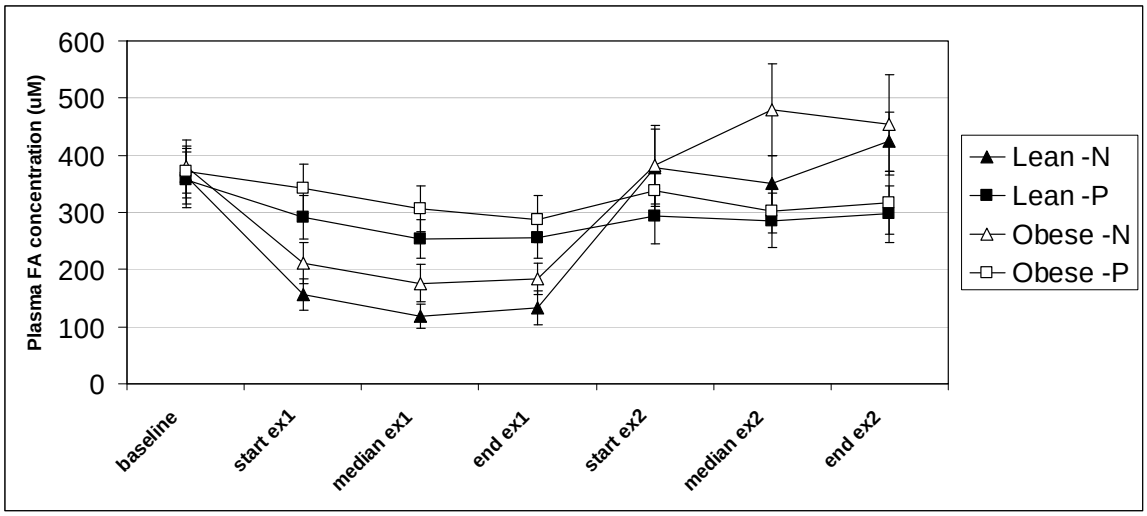

Figure 2.5 Plasma fatty acid values (μM) for lean and obese groups during niacin (N) and placebo (P) trials. Due to individual variation in exercise duration, data has been expressed as start and end exercise values for each group and trial condition. Values given are the mean of 8 subjects per group.

Table 2.3 Plasma fatty acid values (μM) for lean and obese groups during niacin (N) and placebo (P) trials

	Lean –N	**Lean –P**	**Obese –N**	**Obese –P**
Baseline	363.5 *(±135.0)*	356.6 *(±138.2)*	379.6 *(±132.2)*	370.9 *(±126.9)*
Start ex1	155.8 *(±76.5)*	292.1 *(±108.3)*	211.0 *(±100.9)*	341.5 *(±122.8)*
Median ex1	118.0 *(±58.6)*	253.3 *(±94.9)*	176.4 *(±90.4)*	306.6 *(±114.1)*
End ex1	133.3 *(±82.9)*	256.1 *(±105.1)*	183.5 *(±77.4)*	288.4 *(±117.9)*
Start ex2	378.0 *(±192.0)*	293.4 *(±138.4)*	382.5 *(±194.2)*	338.9 *(±101.8)*
Median ex2	350.3 *(±137.1)*	286.0 *(±132.4)*	479.9 *(±225.4)*	302.4 *(±101.9)*
End Ex2	424.1 *(±146.0)*	297.0 *(±139.2)*	453.6 *(±230.4)*	317.3 *(±153.9)*

Values given as means ± standard deviations (SD) of 8 subjects in each group

2.3.3 Plasma lactate

A distinct rise in lactate levels can be seen at the end of both exercise bouts for all groups and trials. The lactate increase over exercise in the niacin trial between exercise bouts 1 and 2 is not significantly different for the obese group (P = 0.074). Higher lactate concentrations were observed after the first exercise bout than after the second exercise bout (5.6 mM and 3.7 mM, respectively). In the lean group the lactate increase over exercise in the niacin trial between exercise bouts 1 and 2 does reach significance (P = 0.050) with greater lactate concentrations at the end of the first exercise bout than after

the second exercise bout (5.4 mM and 4.5 mM, respectively). The lactate increase over exercise 1 is not significantly different between trials for the obese group (P = 0.672) nor is it significant between trials in exercise 2 for the lean group (P = 0.356). Figure 2.6 shows the change in lactate concentrations for niacin and placebo trials in lean and obese groups, while Table 2.4 presents the exact mean lactate values and their standard deviations.

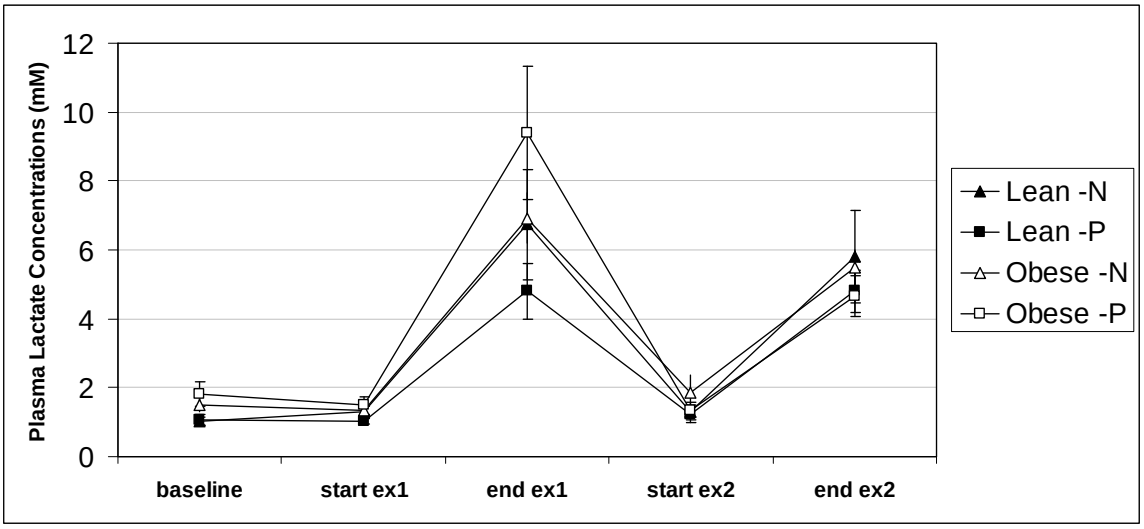

Figure 2.6 Mean lactate values (mM) for lean and obese groups during niacin (N) and placebo (P) trials. Due to individual variation in exercise duration, data has been expressed as start and end exercise values for each group and trial condition. Values given are the mean of 8 subjects per group.

Table 2.4 Lactate values (mM) for lean and obese groups during niacin (N) and placebo (P) trials

	Lean –N	**Lean –P**	**Obese –N**	**Obese –P**
Baseline	1.0 *(±0.3)*	1.1 *(±0.4)*	1.5 *(±0.5)*	1.8 *(±1.0)*
Start ex1	1.3 *(±0.4)*	1.0 *(±0.2)*	1.3 *(±0.6)*	1.5 *(±0.8)*

End ex1	6.7 *(±4.5)*	4.8 *(±2.1)*	6.9 *(±1.9)*	9.4 *(±5.5)*
Start ex2	1.3 *(±0.6)*	1.2 *(±0.6)*	1.8 *(±1.4)*	1.4 *(±0.6)*
End ex2	5.8 *(±3.8)*	4.8 *(±1.5)*	5.5 *(±1.3)*	4.6 *(±1.7)*

Values given as means ± standard deviations (SD) of 8 subjects in each group

2.4 DISCUSSION

Obese individuals have been reported to have impairments in insulin-induced NO-dependent vasodilation and insulin-induced increases in microvascular perfusion (Jonk et al. 2007[2]; Clerk et al. 2006[66]; de Jongh et al. 2004[28]; Laasko et al. 1990[67]). As obese individuals also show a reduction in NO-dependent vasodilation in response to shear stress (Arcaro et al. 1999[8]; Brook et al. 2001[9]; Hamdy et al. 2003[10]; Meyers and Gokce 2007[11]), this may reduce microvascular perfusion during exercise. It has been suggested that the elevated levels of circulating FA contribute significantly to the reduced net vasodilation response by both impairing vasodilation mechanisms and activating vasoconstriction mechanisms. This provided the rational to reduce plasma FA concentration in this study with niacin, a vitamin naturally occurring in our food, to investigate the potential for increasing exercise-mediated vasodilation and MBV in obese individuals.

The mechanisms through which FA impair vasodilation include (i) increased insulin receptor substrate-1 (IRS-1) serine phosphorylation, (ii) activation of nuclear factor κB

(NFκB) network, and (iii) production of superoxide anions (O_2^-) and are summarized in Figure 2.1. IRS-1 serine phosphorylation will prevent downstream activation of the insulin-signaling cascade, resulting in reduced Akt activation, eNOS activation and the subsequent NO production (Kim et al. 2005[18]; Gao et al. 2002[36]). A reduction in NO production will decrease the vasodilation response, but will also reduce the protective effect of NO on atherosclerosis and vascular damage (McAllister and Laughlin 2006[37]; Landmesser and Drexler 2007[38]). Furthermore, the decreased Akt activation will relieve the inhibition of the mitogenic insulin signaling pathway, thus explaining the high plasma levels of endothelin-1 (ET-1), which is a potent local vasoconstrictor produced by the endothelial cells (Federici et al. 2002[39]; Reusch et al. 2001[40]; Gratton et al. 2001[41]; Thijssen et al. 2008[42]; Eringa et al. 2004[20]; Serne et al. 2006[21]; Cardillo et al. 1999[43]). Activation of the NFκB network by elevated FA has been shown in cultured endothelial cells (Kim et al. 2005[18]; Artwohl et al. 2004[44]; Staiger et al. 2006[68]), skeletal muscle of healthy (Itani et al. 2002[69]) and type II diabetic humans (Sriwijitkamol et al. 2006[45]), and in obese Zucker rats (Chinen et al. 2007[24]). NFκB can indirectly lead to increased IRS-1 serine phosphorylation through stimulation of inflammatory cytokine production (Barnes and Karin 1997[46]; Evans et al. 2002[47]; de Alvaro et al. 2004[48]; Sriwijitkamol et al. 2006[45]; Shoelson et al. 2007[49]) which will activate IKK and promote IRS-1 serine phosphorylation (Hotamisligil et al. 1996[50]; de Alvaro et al. 2004[48]; Gao et al. 2002[36]; Gao et al. 2003[51]). NFκB pathway activation also leads to vasoconstriction via accumulation of prostaglandin H_2 (PGH_2) leading to thromboxane A_2 (ThA_2)/PGH_2 receptor activation (Barnes and Karin 1997[46]; Yamamoto et al. 1995[52]). Furthermore, activation of NFκB will increase the expression of cellular adhesion molecules and

leukocyte adhesion (vascular inflammation) and, therefore, will increase local exposure to inflammatory cytokines (Wagenmakers et al. 2006[53]). Lastly, high circulating levels of FA have been proposed to activate NADPH oxidase in the endothelium and vascular smooth muscle (VSM), leading to excess production of superoxide anions (O_2^-; Brandes and Kreuzer 2005[22]; Bedard and Krause 2007[23]; Chinen et al. 2007[24]). Superoxide anions scavenge NO thereby reducing basal vasodilation, while peroxynitrite, the end product of this reaction, has been shown to increase vasoconstriction and reduce vasodilation through a variety of mechanisms (Pacher et al. 2007[4]; Zou et al. 2002[54]; Bubolz et al. 2007[55]). Silver et al. (2007)[70] recently provided evidence that the above mechanisms not only operate in obese subjects with the metabolic syndrome and cardiovascular disease, but also in overweight and obese individuals without obvious pathology, by showing increased protein expression of ET-1, NADPH oxidase and NFκB, and evidence of protein nitrosylation by peroxynitrite in vascular endothelial cells harvested from these individuals.

Ingestion of niacin produced a biphasic response in plasma FA concentrations in line with previous studies (Wang et al. 2000[57]). Initially FA decreased maximally 53 % and 43 % from placebo in lean and obese groups, respectively, and this was found to be significantly different from placebo. This decrease was followed by a maximal FA increase of 43 % and 59 % from placebo in lean and obese groups, respectively, though this did not reach statistical significance. In this way, niacin created two experimental conditions, allowing testing of the hypotheses that low FA concentrations would increase MBV and high FA concentrations would decrease MBV during exercise.

Despite the biphasic manipulation of plasma FA, the THC and lactate responses to exercise in the two participant groups were not in line with our hypothesis. There was no significant difference in the exercise-induced THC increase between trials during exercise-1 or -2 in the obese or lean group. Nor was there a significant difference in the exercise-induced THC increase between groups during the placebo trial. In the obese group, lactate concentrations were expected to be reduced during exercise-1 in the niacin trial (low FA phase), however no significant difference between trials was found during exercise-1, nor was there a significant difference between exercise bouts for the niacin trial. In the lean group, a significant difference in lactate levels was seen between exercise bouts for the niacin trial; however, the lactate levels were higher during exercise in the low FA phase as opposed to the high FA phase.

One of the potential explanations as to why the THC and lactate data was not in line with our hypotheses could be the short duration of the low and high FA phase created by niacin. Alterations in gene expression and protein content of NADPH oxidase and NFκB which would be required to modify the balance between vasoconstriction and vasodilation (Silver et al. 2007[70]) are likely to take longer than the periods with high and low FA concentrations induced by niacin ingestion (Figure 2.5). Furthermore, acute changes in plasma FA concentrations do not necessarily lead to acute decreases in endothelial concentrations of fatty acid metabolites (long-chain fatty acyl-CoA and diacylglycerol) that activate protein kinase C and increase serine phosphorylation of IRS-1 and thus reduce NO production and vasodilation in the resting fasted state (Serne et al.

2006[21]; Naruse et al. 2006[71]). Thus it is possible that the FA manipulation effects were too transient to alter NADPH oxidase and NFκB gene expression, and IRS-1 serine phosphorylation.

In conclusion, the manipulation of plasma FA concentrations with niacin did not have a clear effect on THC and lactate levels during exercise. This may be explained by the FA manipulation effects being too transient to alter NADPH oxidase and NFκB gene expression, and IRS-1 serine phosphorylation. Future studies should use alternative ways to induce prolonged alterations in FA concentrations.

2.5 REFERENCE LIST

1. World Health Organisation. Obesity and overweight. Fact Sheet No. 311, 2006.

2. Jonk AM, Houben AJ, de Jongh RT, Serne EH, Schaper NC, Stehouwer CD. Microvascular dysfunction in obesity: a potential mechanism in the pathogenesis of obesity-associated insulin resistance and hypertension. Physiology (Bethesda) 2007;22:252-260.

3. Cohen JD. Overview of physiology, vascular biology, and mechanisms of hypertension. J Manag Care Pharm 2007;13:S6-S8.

4. Pacher P, Beckman JS, Liaudet L. Nitric oxide and peroxynitrite in health and disease. Physiol Rev 2007;87:315-424.

5. Bakker W, Eringa EC, Sipkema P, van H, V. Endothelial dysfunction and diabetes: roles of hyperglycemia, impaired insulin signaling and obesity. Cell Tissue Res 2009;335:165-189.

6. Stapleton PA, James ME, Goodwill AG, Frisbee JC. Obesity and vascular dysfunction. Pathophysiology 2008;15:79-89.

7. Fisher JP, Young CN, Fadel PJ. Central sympathetic overactivity: maladies and mechanisms. Auton Neurosci 2009;148:5-15.

8. Arcaro G, Zamboni M, Rossi L, Turcato E, Covi G, Armellini F, Bosello O, Lechi A. Body fat distribution predicts the degree of endothelial dysfunction in uncomplicated obesity. Int J Obes Relat Metab Disord 1999;23:936-942.

9. Brook RD, Bard RL, Rubenfire M, Ridker PM, Rajagopalan S. Usefulness of visceral obesity (waist/hip ratio) in predicting vascular endothelial function in healthy overweight adults. Am J Cardiol 2001;88:1264-1269.

10. Hamdy O, Ledbury S, Mullooly C, Jarema C, Porter S, Ovalle K, Moussa A, Caselli A, Caballero AE, Economides PA, Veves A, Horton ES. Lifestyle modification improves endothelial function in obese subjects with the insulin resistance syndrome. Diabetes Care 2003;26:2119-2125.

11. Meyers MR, Gokce N. Endothelial dysfunction in obesity: etiological role in atherosclerosis. Curr Opin Endocrinol Diabetes Obes 2007;14:365-369.

12. Frisbee JC, Stepp DW. Impaired NO-dependent dilation of skeletal muscle arterioles in hypertensive diabetic obese Zucker rats. Am J Physiol Heart Circ Physiol 2001;281:H1304-H1311.

13. Frisbee JC. Enhanced arteriolar alpha-adrenergic constriction impairs dilator responses and skeletal muscle perfusion in obese Zucker rats. J Appl Physiol 2004;97:764-772.

14. Clifford PS, Hellsten Y. Vasodilatory mechanisms in contracting skeletal muscle. J Appl Physiol 2004;97:393-403.

15. Kooijman M. Flow-mediated dilatation in the superficial femoral artery is nitric oxide mediated in humans. 586 ed. 2008:1137-1145.

16. Hudlicka O. Regulation of muscle blood flow. Clin Physiol 1985;5:201-229.

17. van Teeffelen. Rapid dilation of arterioles with single contraction of hamster skeletal muscle. 290 ed. 2006:H119-H127.

18. Kim F, Tysseling KA, Rice J, Pham M, Haji L, Gallis BM, Baas AS, Paramsothy P, Giachelli CM, Corson MA, Raines EW. Free fatty acid impairment of nitric oxide production in endothelial cells is mediated by IKKbeta. Arterioscler Thromb Vasc Biol 2005;25:989-994.

19. Vogel RA, Corretti MC, Plotnick GD. Effect of a single high-fat meal on endothelial function in healthy subjects. Am J Cardiol 1997;79:350-354.

20. Eringa EC, Stehouwer CD, van Nieuw Amerongen GP, Ouwehand L, Westerhof N, Sipkema P. Vasoconstrictor effects of insulin in skeletal muscle arterioles are mediated by ERK1/2 activation in endothelium. Am J Physiol Heart Circ Physiol 2004;287:H2043-H2048.

21. Serne EH, de Jongh RT, Eringa EC, Ijzerman RG, de Boer MP, Stehouwer CD. Microvascular dysfunction: causative role in the association between hypertension, insulin resistance and the metabolic syndrome? Essays Biochem 2006;42:163-176.

22. Brandes RP, Kreuzer J. Vascular NADPH oxidases: molecular mechanisms of activation. Cardio Res 2005;65:16-27.

23. Bedard K, Krause KH. The NOX family of ROS-generating NADPH oxidases: physiology and pathophysiology. Physiol Rev 2007;87:245-313.

24. Chinen I, Shimabukuro M, Yamakawa K, Higa N, Matsuzaki T, Noguchi K, Ueda S, Sakanashi M, Takasu N. Vascular lipotoxicity: endothelial dysfunction via fatty-acid-induced reactive oxygen species overproduction in obese Zucker diabetic fatty rats. Endocrinology 2007;148:160-165.

25. Bickerton AS, Roberts R, Fielding BA, Tornqvist H, Blaak EE, Wagenmakers AJ, Gilbert M, Humphreys SM, Karpe F, Frayn KN. Adipose tissue fatty acid metabolism in insulin-resistant men. Diabetologia 2008;51:1466-1474.

26. Jensen MD, Haymond MW, Rizza RA, Cryer PE, Miles JM. Influence of body fat distribution on free fatty acid metabolism in obesity. J Clin Invest 1989;83:1168-1173.

27. Hennes MM, O'Shaughnessy IM, Kelly TM, LaBelle P, Egan BM, Kissebah AH. Insulin-resistant lipolysis in abdominally obese hypertensive individuals. Role of the renin-angiotensin system. Hypertension 1996;28:120-126.

28. de Jongh RT, Serne EH, Ijzerman RG, de Vries G, Stehouwer CD. Impaired microvascular function in obesity: implications for obesity-associated microangiopathy, hypertension, and insulin resistance. Circulation 2004;109:2529-2535.

29. Coppack SW, Evans RD, Fisher RM, Frayn KN, Gibbons GF, Humphreys SM, Kirk ML, Potts JL, Hockaday TD. Adipose tissue metabolism in obesity: lipase action in vivo before and after a mixed meal. Metabolism 1992;41:264-272.

30. Hickner RC, Racette SB, Binder EF, Fisher JS, Kohrt WM. Suppression of whole body and regional lipolysis by insulin: effects of obesity and exercise. J Clin Endocrinol Metab 1999;84:3886-3895.

31. Kamagate A, Dong HH. FoxO1 integrates insulin signaling to VLDL production. Cell Cycle 2008;7:3162-3170.

32. Lewis GF, Carpentier A, Adeli K, Giacca A. Disordered fat storage and mobilization in the pathogenesis of insulin resistance and type 2 diabetes. Endocr Rev 2002;23:201-229.

33. Frayn KN. Adipose tissue as a buffer for daily lipid flux. Diabetologia 2002;45:1201-1210.

34. Oram JF, Bornfeldt KE. Direct effects of long-chain non-esterified fatty acids on vascular cells and their relevance to macrovascular complications of diabetes. Front Biosci 2004;9:1240-1253.

35. Fielding F. Lipoprotein lipase and the disposition of dietary fatty acids. 80 ed. 1998:495-502.

36. Gao Z, Hwang D, Bataille F, Lefevre M, York D, Quon MJ, Ye J. Serine phosphorylation of insulin receptor substrate 1 by inhibitor kappa B kinase complex. J Biol Chem 2002;277:48115-48121.

37. McAllister RM, Laughlin MH. Vascular nitric oxide: effects of physical activity, importance for health. Essays Biochem 2006;42:119-131.

38. Landmesser U, Drexler H. Endothelial function and hypertension. Curr Opin Cardiol 2007;22:316-320.

39. Federici M, Menghini R, Mauriello A, Hribal ML, Ferrelli F, Lauro D, Sbraccia P, Spagnoli LG, Sesti G, Lauro R. Insulin-dependent activation of endothelial nitric oxide synthase is impaired by O-linked glycosylation modification of signaling proteins in human coronary endothelial cells. Circulation 2002;106:466-472.

40. Reusch HP, Zimmermann S, Schaefer M, Paul M, Moelling K. Regulation of Raf by Akt controls growth and differentiation in vascular smooth muscle cells. J Biol Chem 2001;276:33630-33637.

41. Gratton JP, Morales-Ruiz M, Kureishi Y, Fulton D, Walsh K, Sessa WC. Akt down-regulation of p38 signaling provides a novel mechanism of vascular endothelial growth factor-mediated cytoprotection in endothelial cells. J Biol Chem 2001;276:30359-30365.

42. Thijssen DH, Rongen GA, Smits P, Hopman MT. Physical (in)activity and endothelium-derived constricting factors: overlooked adaptations. J Physiol 2008;586:319-324.

43. Cardillo C, Nambi SS, Kilcoyne CM, Choucair WK, Katz A, Quon MJ, Panza JA. Insulin stimulates both endothelin and nitric oxide activity in the human forearm. Circulation 1999;100:820-825.

44. Artwohl M, Roden M, Waldhausl W, Freudenthaler A, Baumgartner-Parzer SM. Free fatty acids trigger apoptosis and inhibit cell cycle progression in human vascular endothelial cells. FASEB J 2004;18:146-148.

45. Sriwijitkamol A, Christ-Roberts C, Berria R, Eagan P, Pratipanawatr T, Defronzo RA, Mandarino LJ, Musi N. Reduced skeletal muscle inhibitor of kappaB beta content is associated with insulin resistance in subjects with type 2 diabetes: reversal by exercise training. Diabetes 2006;55:760-767.

46. Barnes PJ, Karin M. Nuclear factor-kappaB: a pivotal transcription factor in chronic inflammatory diseases. N Engl J Med 1997;336:1066-1071.

47. Evans JL, Goldfine ID, Maddux BA, Grodsky GM. Oxidative stress and stress-activated signaling pathways: a unifying hypothesis of type 2 diabetes. Endocr Rev 2002;23:599-622.

48. deAlvaro C., Teruel T, Hernandez R, Lorenzo M. Tumor necrosis factor alpha produces insulin resistance in skeletal muscle by activation of inhibitor kappaB kinase in a p38 MAPK-dependent manner. J Biol Chem 2004;279:17070-17078.

49. Shoelson SE, Herrero L, Naaz A. Obesity, inflammation, and insulin resistance. Gastroenterology 2007;132:2169-2180.

50. Hotamisligil GS, Peraldi P, Budavari A, Ellis R, White MF, Spiegelman BM. IRS-1-mediated inhibition of insulin receptor tyrosine kinase activity in TNF-alpha- and obesity-induced insulin resistance. Science 1996;271:665-668.

51. Gao Z, Zuberi A, Quon MJ, Dong Z, Ye J. Aspirin inhibits serine phosphorylation of insulin receptor substrate 1 in tumor necrosis factor-treated cells through targeting multiple serine kinases. J Biol Chem 2003;278:24944-24950.

52. Yamamoto K, Arakawa T, Ueda N, Yamamoto S. Transcriptional roles of nuclear factor kappa B and nuclear factor-interleukin-6 in the tumor necrosis factor alpha-dependent induction of cyclooxygenase-2 in MC3T3-E1 cells. J Biol Chem 1995;270:31315-31320.

53. Wagenmakers AJ, van Riel NA, Frenneaux MP, Stewart PM. Integration of the metabolic and cardiovascular effects of exercise. Essays Biochem 2006;42:193-210.

54. Zou MH, Shi C, Cohen RA. Oxidation of the zinc-thiolate complex and uncoupling of endothelial nitric oxide synthase by peroxynitrite. J Clin Invest 2002;109:817-826.

55. Bubolz AH, Wu Q, Larsen BT, Gutterman DD, Liu Y. Ebselen reduces nitration and restores voltage-gated potassium channel function in small coronary arteries of diabetic rats. Am J Physiol Heart Circ Physiol 2007;293:H2231-H2237.

56. Carlson LA, Oro L, Ostman J. Effect of a single dose of nicotinic acid on plasma lipids in patients with hyperlipoproteinemia. Acta Med Scand 1968;183:457-465.

57. Wang W, Basinger A, Neese RA, Christiansen M, Hellerstein MK. Effects of nicotinic acid on fatty acid kinetics, fuel selection, and pathways of glucose production in women. Am J Physiol Endocrinol Metab 2000;279:E50-E59.

58. van Beekvelt MC, Borghuis MS, van Engelen BG, Wevers RA, Colier WN. Adipose tissue thickness affects in vivo quantitative near-IR spectroscopy in human skeletal muscle. Clin Sci (Lond) 2001;101:21-28.

59. Wilson JR, Mancini DM, McCully K, Ferraro N, Lanoce V, Chance B. Noninvasive detection of skeletal muscle underperfusion with near-infrared spectroscopy in patients with heart failure. Circulation 1989;80:1668-1674.

60. Kell RT, Farag M, Bhambhani Y. Reliability of erector spinae oxygenation and blood volume responses using near-infrared spectroscopy in healthy males. Eur J Appl Physiol 2004;91:499-507.

61. Mancini DM, Bolinger L, Li H, Kendrick K, Chance B, Wilson JR. Validation of near-infrared spectroscopy in humans. J Appl Physiol 1994;77:2740-2747.

62. Cui W, Kumar C, Chance B. Experimental study of migration depth for the photons measured at sample surface. I. Time resolved spectroscopy and imaging. Proc SPIE Int Soc Opt Eng 1991;1431:180-191.

63. Homma S, Fukunaga T, Kagaya A. The influence of adipose tissue thickness on Near Infrared Spectoscopic signals in the measurement of human muscle. J Biomed Opt 1996;1:418-424.

64. Tunaru S, Kero J, Schaub A, Wufka C, Blaukat A, Pfeffer K, Offermanns S. PUMA-G and HM74 are receptors for nicotinic acid and mediate its anti-lipolytic effect. Nat Med 2003;9:352-355.

65. Christie AW, McCormick DK, Emmison N, Kraemer FB, Alberti KG, Yeaman SJ. Mechanism of anti-lipolytic action of acipimox in isolated rat adipocytes. Diabetologia 1996;39:45-53.

66. Clerk LH, Vincent MA, Jahn LA, Liu Z, Lindner JR, Barrett EJ. Obesity blunts insulin-mediated microvascular recruitment in human forearm muscle. Diabetes 2006;55:1436-1442.

67. Laakso M, Edelman SV, Brechtel G, Baron AD. Decreased effect of insulin to stimulate skeletal muscle blood flow in obese man. A novel mechanism for insulin resistance. J Clin Invest 1990;85:1844-1852.

68. Staiger K, Staiger H, Weigert C, Haas C, Haring HU, Kellerer M. Saturated, but not unsaturated, fatty acids induce apoptosis of human coronary artery endothelial cells via nuclear factor-kappaB activation. Diabetes 2006;55:3121-3126.

69. Itani SI, Ruderman NB, Schmieder F, Boden G. Lipid-induced insulin resistance in human muscle is associated with changes in diacylglycerol, protein kinase C, and IkappaB-alpha. Diabetes 2002;51:2005-2011.

70. Silver AE, Beske SD, Christou DD, Donato AJ, Moreau KL, Eskurza I, Gates PE, Seals DR. Overweight and obese humans demonstrate increased vascular endothelial NAD(P)H oxidase-p47(phox) expression and evidence of endothelial oxidative stress. Circulation 2007;115:627-637.

71. Naruse K, Rask-Madsen C, Takahara N, Ha SW, Suzuma K, Way KJ, Jacobs JR, Clermont AC, Ueki K, Ohshiro Y, Zhang J, Goldfine AB, King GL. Activation of Vascular Protein Kinase C-{beta} Inhibits Akt-Dependent Endothelial Nitric Oxide Synthase Function in Obesity-Associated Insulin Resistance. Diabetes 2006;55:691-698.

Chapter 3

THE EFFECT OF ACUTE CHANGES IN PLASMA FATTY ACID CONCENTRATIONS ON RESTING MUSCLE MICROVASCULAR BLOOD VOLUME IN LEAN AND OBESE INDIVIDUALS AS A FUNCTION OF PHYSICAL ACTIVITY LEVELS

3.1 INTRODUCTION

With the obesity epidemic spreading rapidly, more and more people are at risk of compromising their health and reducing their quality of life (World Health Organisation 2006[1]). Chronic obesity leads to substantial increases in the risk of developing hypertension, vascular and coronary artery disease, atherosclerosis, insulin resistance and type II diabetes (World Health Organisation 2006[1]). Impairments in endothelial metabolism have a negative impact on (micro)vascular function and have been proposed to represent the earliest common abnormality in the development of the obesity-related pathologies (Jonk et al. 2007[2]; Meyers and Gokce 2007[3]; Hartge et al. 2007[4]; Cersosimo and Defronzo 2006[5]; Kim et al. 2006[6]). An important role of the endothelium in the microvasculature of skeletal muscle is to regulate the recruitment and blood perfusion of capillaries that surround the skeletal muscle fibres, such that perfusion matches fuel and oxygen demands (Segal 2005[7]). Most of the control of perfusion of skeletal muscle capillaries is at the level of the terminal arterioles (Segal 2005[7]). A reduced skeletal muscle perfusion has been observed in the fasted resting state in obese mice (Traupe et al. 2002[8]; Traupe et al. 2002[9]) and obese Zucker rats (Wallis et al. 2002[10]; Frisbee 2007[11]), and has been proposed to occur in humans with hypertension and the metabolic syndrome (Lind and Lithell 1993[12]). The impaired skeletal muscle perfusion in obesity has been suggested to be the result of (i) a decreased capillary density, also called rarefaction (Frisbee 2007[11]; Gavin et al. 2005[13]), and (ii) an increased basal vascular tone (Traupe et al. 2002[8]; Traupe et al. 2002[9]; Frisbee 2007[11]; Ribeiro et al. 2001[14]). The increased vascular tone is likely to be the result of an imbalance in the mechanisms that lead to

vasodilation and to vasoconstriction (Frisbee 2007[11]) and plays an important role in the development of hypertension.

Obesity is commonly associated with increased circulating levels of fatty acids (FA) and triglycerides (TG; Lewis et al. 2002[15]; Frayn 2002[16]). Hydrolysis of plasma TG by lipoprotein lipase in the muscle capillary bed may further increase the local FA concentration (Oram and Bornfeldt 2004[17]). A large body of recent literature suggests that acute and chronic exposure of the microvasculature to high plasma FA play a role both in impairing the mechanisms that determine fasted and insulin-mediated NO-dependent vasodilation and in activating several mechanisms leading to vasoconstriction (Figure 3.1; detailed overview is given in the Discussion section).

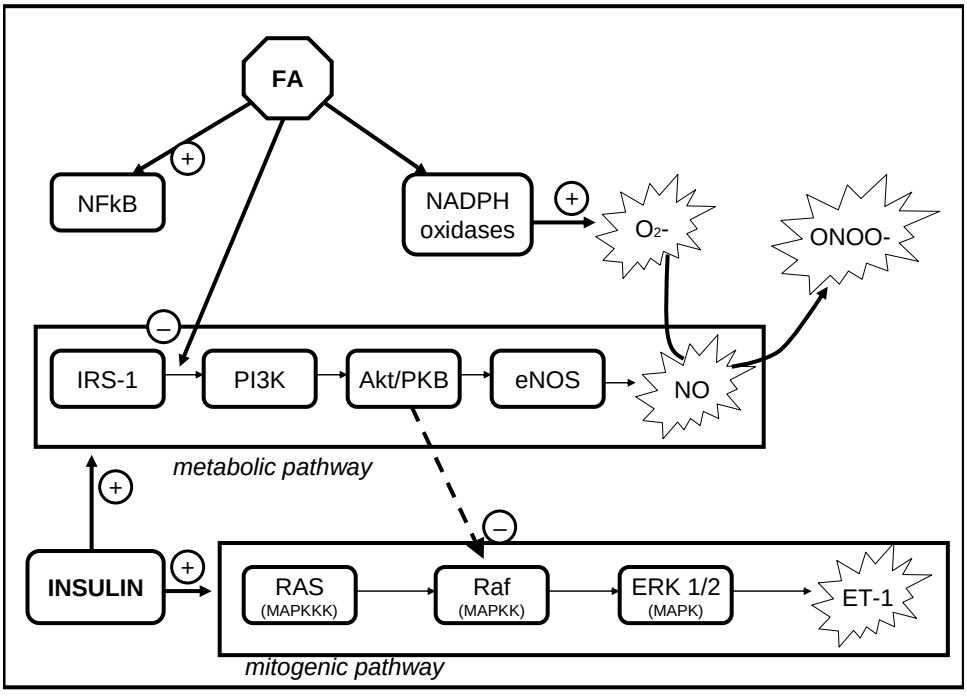

Figure 3.1 Schematic presentation of the main endothelial mechanisms by which a high concentration of plasma fatty acids (FA) reduce vasodilation and increase vasoconstriction of terminal arterioles leading to a net increase in vascular tone of the microvasculature and a potential underperfusion of skeletal muscle in the fasted resting state. Insulin activates two pathways in the microvascular endothelium. The metabolic pathway (traditionally called insulin-signalling pathway) leads to vasodilation via production of nitric oxide (NO) which then diffuses to the vascular smooth muscle layer of the terminal arterioles, while the mitogenic pathway leads to vasoconstriction via production of endothelin-1 (ET-1). Elevated levels of FA promote serine rather than tyrosine phosphorylation of IRS-1 thereby impairing downstream activation of Akt/PKB leading to reduced NO production and vasodilation as well as reduced inhibition of the mitogenic pathway leading to increased ET-1 production and vasoconstriction. FA will also activate endothelial NADPH oxidase leading to superoxide anion production (O_2^-), which reduces NO bioavailability and basal vasodilation by scavenging NO. This reaction generates peroxynitrite, which increases vasoconstriction via mechanisms specified in the first paragraph of the Discussion. NADPH oxidase activation and scavenging of endothelial NO also reduces the protective effect of NO on atherosclerosis and vascular damage, and is one of the pathways playing a role in the transition from obesity into the metabolic syndrome and cardiovascular disease. Elevated FA levels can activate the NFκB signalling pathway which, in addition to contributing to the mechanisms reducing vasodilation and increasing vasoconstriction, leads to increased expression of cellular adhesion molecules and leukocyte adhesion (vascular inflammation) and activates the mechanisms that lead to atherogenesis and endothelial apoptosis. Abbreviations: IRS-1 – insulin receptor substrate-1; PI3K – phosphotidylinositol 3-kinase; Akt/PKB – protein kinase B; eNOS – endothelial nitric oxide synthase; MAPK – mitogen activated protein kinase; MAPKK – MAPK kinase; MAPKKK – MAPKK kinase; ERK 1/2 – extracellular signal-regulated kinase 1/2; NFκB – nuclear factor κB; O_2^- – superoxide anion; $ONOO^-$ – peroxynitrite. Figure 3.1 is compiled with information taken from several references (Kim et al. 2005[18]; Eringa et al. 2004[19]; Brandes and Kreuzer 2005[20]; Bedard and Krause 2007[21]; Wagenmakers et al. 2006[22]; Silver et al. 2007[23]; Cardillo et al. 1999[24]; Cusi et al. 2000[25]; Jiang et al. 1999[26]; Federici et al. 2002[27]; Seger and Krebs 1995[28]).

Inactivity appears to play an important role in the mechanisms that lead to vasoconstriction, as it is a cause of rarefaction and of increases in endothelin-1 (ET-1; Frisbee 2007[11]; Thijssen et al. 2007[29]; Thijssen et al. 2008[30]). Exercise training, on the other hand reduces vascular tone in the fasted resting state via decreases in ET-1 (Thijssen et al. 2007[29]; Thijssen et al. 2008[30]), increases in endothelial nitric oxide synthase (eNOS) expression and protein content (McAllister and Laughlin 2006[31]) and increases in capillary density both in healthy lean subjects (Andersen and Henriksson 1977[32]; Shono et al. 2002[33]) and in obese subjects (Frisbee 2007[11]; Gavin et al. 2005[13]; Frisbee and Delp 2006[34]).

The aims of the present study were to (i) measure the blood volume present in the muscle microvasculature in the overnight fasted resting state and (ii) investigate whether acute changes in plasma FA concentration in lean and obese participants would change the microvascular blood volume (MBV). Total haemoglobin concentration (THC) of the biceps brachii muscle, an indirect measure of MBV, was monitored using near-infrared spectroscopy (NIRS). Niacin was used to reduce the plasma FA concentration (Carlson et al. 1968[35]; Wang et al. 2000[36]). Participants underwent two 3 h trials, namely, placebo and niacin trials, to test the hypothesis that lowering of the plasma FA levels with niacin would reduce the basal vascular tone, and thus would increase the THC in the muscle. Four participant groups were studied: (i) lean active, (ii) lean sedentary, (iii) obese active, and (iv) obese sedentary. The hypothesis was that the obese sedentary subjects, and potentially the lean sedentary subjects, would show an increased vascular tone in the fasted resting state and, therefore, would show an increase in THC upon lowering of the

circulating FA. We also hypothesized that regular exercise counteracts the negative impact of obesity on endothelial function and that, therefore, the active groups would have a higher capillary density leading to a higher basal THC, and would have little or no increase in THC upon lowering of plasma FA due to the lack of active vasoconstriction mechanisms.

Niacin ingestion is known to lead to an initial (3 hour) decrease in plasma FA and then to a subsequent increase (rebound) within a period of 5-6 h (Carlson et al. 1968[35]; Wang et al. 2000[36]). To monitor the size of the changes in plasma FA concentration and investigate the effect of the FA rebound on THC, we also performed a 6 hour study with blood samples taken to measure plasma FA. These studies were only performed in the two sedentary groups, as physical inactivity, by both decreasing capillarisation and promoting vasoconstriction, was regarded to be the main determinant of endothelial impairments leading to reduced skeletal muscle perfusion. The hypothesis to be tested in this second study was that the increase in plasma FA in the rebound phase after niacin ingestion would be large enough to increase net vasoconstriction in the lean sedentary group and would lead to a decrease in THC comparable to that of the obese sedentary group.

3.2 MATERIALS AND METHODS

3.2.1 Subjects

Thirty two healthy volunteers were recruited by word of mouth in the University of Birmingham. The volunteers were divided into four groups of eight participants, namely (i) lean active, (ii) lean sedentary, (iii) obese active, and (iv) obese sedentary. Their physical characteristics are displayed in Table 3.1. Volunteers met individually with the researcher to discuss the study, provide written informed consent, and complete preliminary measurements including a general health questionnaire, a physical activity questionnaire, measurements of height and weight, and determination of NIRS optimal probe positioning (see below). The research has been carried out in accordance with the Declaration of Helsinki (2000) of the World Medical Association and has been approved by the Ethics Committee of the School of Sport and Exercise Sciences at The University of Birmingham.

Table 3.1 Characteristics of the four participant groups

	Lean Active	**Lean Sedentary**	**Obese Active**	**Obese Sedentary**
Age (years)	20.4 *(±1.7)*	20.4 *(±2.3)*	21.6 *(±2.6)*	24.0 *(±5.1)*
Gender (m/f)	4/4	5/3	3/5	3/5
Skin thickness (mm)	2.4 *(±0.5)*	3.1 *(±0.5)*	8.1 *(±2.4)*	11.4 *(±2.8)*
Height (m)	1.72 *(± 0.10)*	1.73 *(± 0.11)*	1.72 *(± 0.10)*	1.70 *(± 0.12)*
Weight (kg)	64.7 *(± 0.13.3)*	65.6 *(± 8.7)*	86.3 *(± 25.7)*	102 *(± 25.2)*
BMI (kg/m^2)	21.5 *(±2.3)*	21.8 *(±1.6)*	28.5 *(±6.0)*	34.6 *(±3.5)*

Skin thickness was measured over the biceps brachii with skin fold callipers and represents an average of three measurements. Values given are the mean of 8 subjects with standard deviations given in brackets.

3.2.2 NIRS measurements

NIRS is a non-invasive optical technique based on the oxygen-dependent absorption changes of haemoglobin and myoglobin. While differentiation between oxygenated and deoxygenated states of the chromophores can be made, it is not possible to distinguish between haemoglobin and myoglobin as their absorption spectra overlap (van Beekvelt et al. 2001[37]). We used a continuous-wave NIR spectrometer (ISS OxyplexTS 95306, Champaign IL, USA), which measures the absorbance of the NIR light at wavelengths of 692 nm and 834 nm and uses calibrated software routines to calculate absolute concentrations from the measured NIR absorbance. Deoxygenated haemoglobin and myoglobin (Hb/Mb) absorbance was measured at wavelength 692 nm, while the sum of deoxygenated and oxygenated Hb/Mb was measured at wavelength 834 nm as they exhibit similar absorption coefficients at this higher wavelength (Wilson et al. 1989[38]). Since myoglobin concentrations were unlikely to change over the testing period, the sum of the absorbance signals at 834 nm was taken to reflect the relative change in THC (assuming a constant haematocrit; Kell et al. 2004[39]). We assumed that the changes in THC would reflect changes in capillary blood volume as NIRS measurements primarily reflect the microcirculation in skeletal muscle (Mancini et al. 1994[40]). NIRS measurements were carried out on the biceps brachii with a probe having an interoptode distance (ID) of 3-4.4 cm. This ID would allow a measurement depth of up to 2.2 cm based on the assumption that the measurement depth is half the ID (van Beekvelt et al. 2001[37]; Cui et al. 1991[41]; Homma et al. 1996[42]). The NIRS measurement unit was given at least a 2 h warm up time as this minimised signal drift in time and was calibrated before each trial. Data was sampled at 2000 Hz, displayed in real time, and stored on disk for off-line analysis.

3.2.3 Determination of optimal probe position

The optimum probe position for the individual was identified by systematically drawing five marks on the belly of the biceps brachii muscle of their dominant arm and making measurements with the NIRS probe for 2 min on each mark. The mark with the highest THC value was noted as the optimum probe position for the individual. The positioning marks were made with a black ballpoint pen and their placement was identified for each participant in the following way: (a) half distance between elbow (olcranon process) and shoulder (coracoid process) = mark 0; (b) circumference of arm at point 0 divided by 4; (c) value (0.25 of circumference) from point 0 across biceps towards inner arm = mark 1; (d) marks 2-5 are 1.5 cm from mark 1, as shown in Figure 3.2.

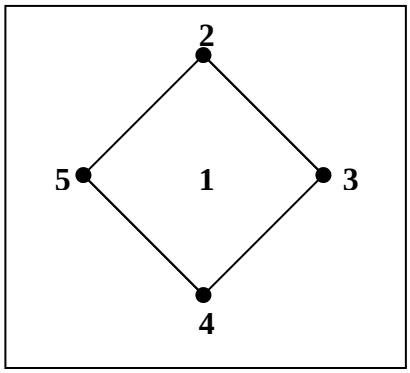

Figure 3.2 Position codes for determination of optimal NIRS probe position on the biceps brachii muscle of each participant. The positions were determined by (a) measuring half the distance between the elbow (olcranon process) and shoulder (coracoid process) = point 0; (b) measuring the circumference of the arm from point 0 and dividing it by 4; (c) the value (0.25 of circumference) from point 0 across biceps towards inner arm = mark 1; (d) marks 2-5 are 1.5 cm from mark 1. NIRS measurements were made for 2 min on each point and the point with the highest THC value was noted as the optimum probe position for the individual.

3.2.4 Niacin

Niacin (vitamin B3) is a nicotinic acid analogue which inhibits the release of FA from adipose tissue, thereby decreasing blood FA concentrations. This mechanism involves niacin binding to the HM74 receptor on the adipocyte (Tunaru et al. 2003[43]), leading to a suppression of intracellular cAMP levels which in turn decrease cAMP-dependent protein kinase activity. The result is a reduced association of hormone sensitive lipase and the lipid droplets within the adipocyte, thereby decreasing lipolysis and the subsequent release of FA into the blood stream (Christie et al. 1996[44]). As skeletal muscle does not express the HM74 receptor, this effect of niacin remains specific to adipose tissue (Tunaru et al. 2003[43]). A particular characteristic of niacin is its biphasic effect on plasma FA concentrations as after the low FA phase a rebound phase follows, elevating FA levels above basal concentrations. Pilot studies from our laboratory showed 500 mg of niacin to cause a decrease in FA commencing 10 min post capsule ingestion and reaching the lowest point at 60 min before beginning to rise again, surpassing baseline values 3 h post capsule ingestion, peaking at about 4 h and slowly returning towards baseline levels at about 5-6 h. For this reason, the initial study only measured 3 h post niacin ingestion to investigate the effects of low FA, while measurements lasting 6 h post ingestion were made later in two of the four groups to investigate both the low and high FA conditions created by the niacin ingestion. Side-effects of niacin ingestion include flushing, itching, nausea, gastrointestinal complaints, headaches, and skin rashes. In the present study, 30-50 min after capsule ingestion, 31 out of 32 participants showed flushing characterised by redness of the face, neck, and arms. Shortly after capsule

ingestion, 5 out of 32 participants reported a feeling of nausea which lasted approximately 15 min.

3.2.5 Experimental protocol 1

Participants visited the laboratory on two occasions arriving between 6 and 8 am in the overnight fasted state. The day before testing, participants were instructed to refrain from exercise and ingestion of caffeine, as well as to consume a low fat evening meal at 7 pm, followed by only low-fat snacks if they could not resist additional food intake. They were instructed to refrain from food and calorie intake from 10 pm, drinking only water until completion of the trial the following day. Visits were at least two days apart and were identical except for the contents of the capsules ingested. Two capsules were given together, each containing 250 mg of either niacin or placebo (microcrystalline cellulose) and administration was double-blinded.

Upon arrival at the laboratory, participants were asked to be seated and the NIRS probe was placed over the biceps brachii muscle in the previously identified optimum probe position. The probe was randomly assigned to the left or right arm of each participant and placed on the same arm for both visits. Once participants had the probe fastened with a Velcro strap on their arm, resting measurements were made for 10 min. Subjects were then asked to ingest two 250 mg capsules both containing either niacin or placebo. Following ingestion, volunteers remained in the resting state for a 3 h measurement period after which the probe was removed and the subjects could leave the laboratory.

3.2.6 Experimental protocol 2

The 16 volunteers from the sedentary lean and obese groups were asked to take part in two additional trials in which the measurement duration was increased to 6 h to include the FA rebound phase of niacin. Participants arrived at the laboratory between 6-8 am in the overnight fasted state. Upon arrival at the laboratory, they were asked to lie down on the bed while a flexible 20-gauge Teflon catheter (Quickcath, Becton Dickinson, Plymouth, United Kingdom) was inserted in the antecubital vein and fitted with a 3-way stopcock (PVB Medizintechnik, Kirchseean, Germany) to allow for repeated blood sampling. The NIRS probe was placed over the predetermined optimum position on the biceps brachii, and after a 10 min baseline measurement, a baseline blood sample was taken, and participants were asked to ingest two 250 mg capsules both containing either placebo or niacin, depending on the trial. The 6 h NIRS measurement then commenced. Blood samples were taken every 30 min during the 6 h and participants were asked to remain at rest for the length of the trial.

3.2.7 Blood samples

Blood samples (7 ml) were collected in EDTA-containing tubes and centrifuged at 1,000 g for 10 min at 4 °C. Aliquots of plasma were frozen immediately in liquid nitrogen and stored at -80 °C. Plasma FA concentrations were analyzed (NEFA-C; Wako Chemicals, Neuss, Germany), with a COBAS Mira Plus semiautomatic analyzer (ABX Diagnostics).

3.2.8 Calculations

van Beekvelt (2001)[37] proposed a calculation of the contribution of adipose tissue (+ skin) to the NIRS signal using the theoretical measurement depth and the recorded adipose (+ skin) thickness of the participants. As the theoretical measurement depth equals half the ID (van Beekvelt et al. 2001[37]; Cui et al. 1991[41]; Homma et al. 1996[42]) we should be able to measure a maximal depth of 2.2 cm (22 mm) with our 3-4.4 cm ID probe. The thickness of the skin and subcutaneous adipose tissue layer (skin thickness) for each participant group is shown in Table 3.1. Based on this, the contribution of subcutaneous adipose tissue (+ skin) in our four participant groups can be calculated by:

$$\frac{\text{Skin thickness (mm)}}{\text{½ maximal ID (mm)}} \times 100$$

3.2.9 Statistical Analysis

One-tailed independent samples t-tests were carried out between niacin and placebo plasma FA values for the lowest average FA point and the highest average FA point of the niacin trials to determine if there was a significant difference in FA concentrations between trials at the low and high FA points.

Two-tailed independent samples t-tests were carried out between baseline THC values of the four participant groups to investigate whether there are differences between groups that result either from a difference in capillary density and/or the net balance between vasodilation and vasoconstriction.

For protocol 1 (3 h resting measure), THC data from 0-3 h (low FA phase) was summarized to four time points (Matthews et al. 1990[45]), namely baseline, summary time

1, 2, and 3 as shown in Figure 3.2. A three way analysis of variance (ANOVA) for repeated measures was carried out on THC data for trial and time between the four participant groups which completed the 3 h resting measure to investigate whether there were changes in THC content over time and between trial conditions in the low FA phase (0-3 h) for the 4 participant groups.

For protocol 2 (6 h resting measure), THC data from 3-6 h (high FA phase) was summarised to three points, namely summary time 1, 2, and 3 as shown in Figure 3.3. A three way ANOVA for repeated measures was carried out on the THC data for trial and time between the two sedentary participant groups which completed the 6 h resting measure (protocol 2) to investigate whether there were significant changes in THC content over time and between trial conditions in the high FA phase (3-6 h).

If significance was found the Bonferroni post hoc test was applied.

All statistical tests were carried out using SPSS for windows version 16.0 software package (Chicago, IL, USA). All data are reported as means ± SD and statistical significance was set at $P < 0.05$.

3.3 RESULTS

In both protocols, there was no significant change in THC over time, and no difference in THC between trials. There were significant differences in baseline THC between lean and obese groups, but not between active or sedentary participants within the groups.

3.3.1 Plasma fatty acids

The blood samples taken in protocol 2 confirmed that the ingestion of 500 mg niacin led to an initial decrease in plasma FA concentrations of 48.4 % vs placebo followed by a rebound phase in which the plasma FA concentrations increased by 44.2 % vs placebo (Figure 3.3). The lowest FA value of the niacin trial was significantly different from FA at the same time point (60 min) of the placebo trial ($P = 0.004$), and this was also true for the highest FA value of the niacin trial (210 min; $P = 0.0085$).

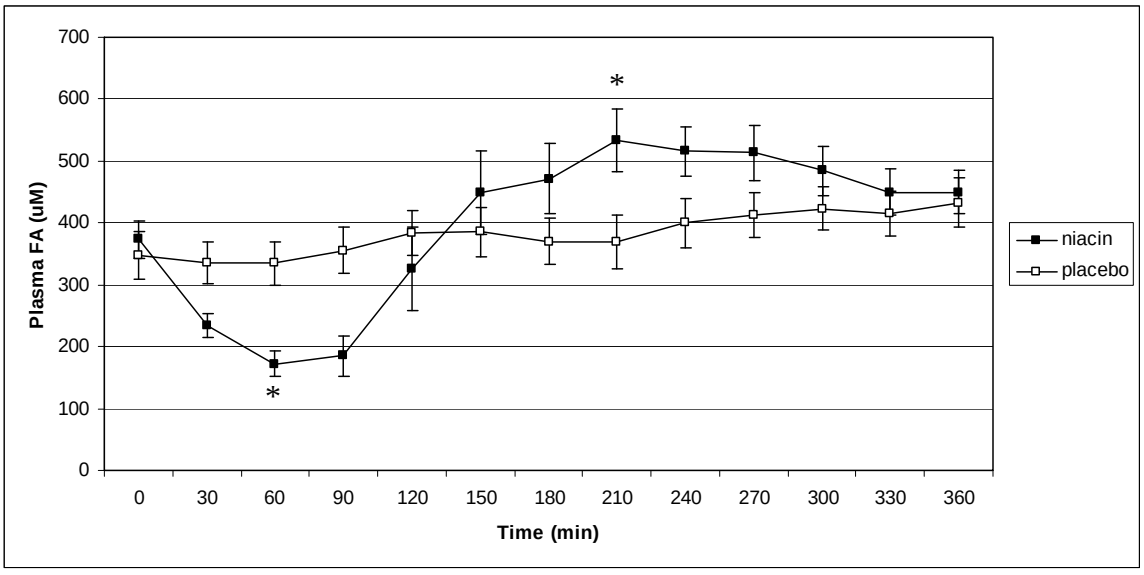

Figure 3.3 Plasma fatty acid (FA) data for niacin and placebo trials over 6 h. The niacin trial showed significantly lower FA levels at 60 min (FA = 172 ± 81 µM) compared to placebo (FA = 334 ± 132 µM) and significantly higher FA levels at 210 min (FA = 533 ± 190 µM) compared to placebo (FA = 370 ± 167 µM; * $P < 0.05$). Values given are the mean of 16 subjects (8 sedentary lean and 8 sedentary obese).

3.3.2 Protocol 1 (low FA condition only)

Analysis of baseline THC data showed that although active participants had greater THC values compared to their sedentary counterparts, these differences were not significant when assessed separately in the obese (P = 0.380) or lean (P = 0.502) subgroups. The active lean and obese groups had significantly different baseline THC (P = 0.005) as did the sedentary lean and obese groups (P = 0.001). Over the 3 h measurement period, no effect of trial on THC was found (P = 0.639), nor was there any change in THC over time (P = 0.122). The lack of change in THC over time was not affected by groups (P = 0.965). Data is shown in Figure 3.4 and Table 3.2.

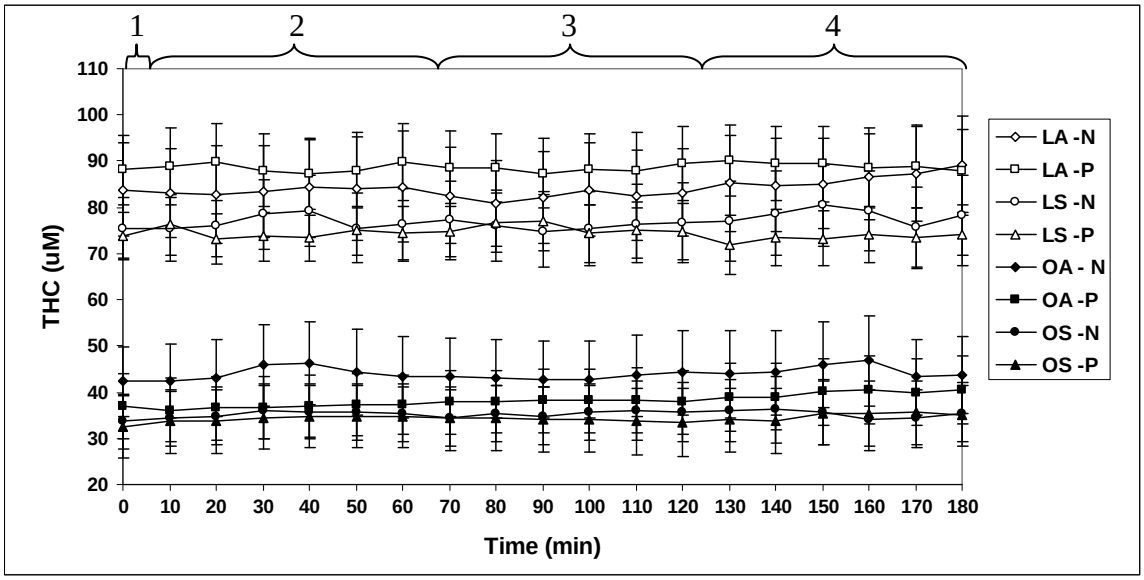

Figure 3.4 Mean total haemoglobin content (THC) for all 4 participant groups in placebo (P) and niacin (N) trials over 3 h. LA – lean active, LS – lean sedentary, OA – obese active, OS – obese sedentary. Numbers 1-4 reflect the summary time points used in analysis.

Table 3.2 Total haemoglobin content at baseline in niacin and placebo trials for all 4 participant groups.

	Lean Active	Lean Sedentary	Obese Active	Obese Sedentary

Baseline niacin (μM)	83.76 *(±28.60)*	75.41 *(±18.91)*	42.33 *(±21.20)*	33.68 *(±16.75)*
Baseline placebo (μM)	88.08 *(±21.50)*	73.84 *(±13.97)*	36.83 *(±19.91)*	32.49 *(±19.24)*

Values are given as the means ± SD of 8 subjects in each group.

3.3.3 Protocol 2 (low and high FA conditions)

Figure 3.5 shows the THC data for the 6 h resting measure. In the second half of the 6 h measurement period (reflecting the high FA phase), no significant effect of trial was found on THC (P = 0.364). There was, however, a significant effect of time on THC (P = 0.022) which was attributable to a significant difference between time point 1 and 2 (P = 0.019). THC was significantly different between lean and obese groups (P = 0.001).

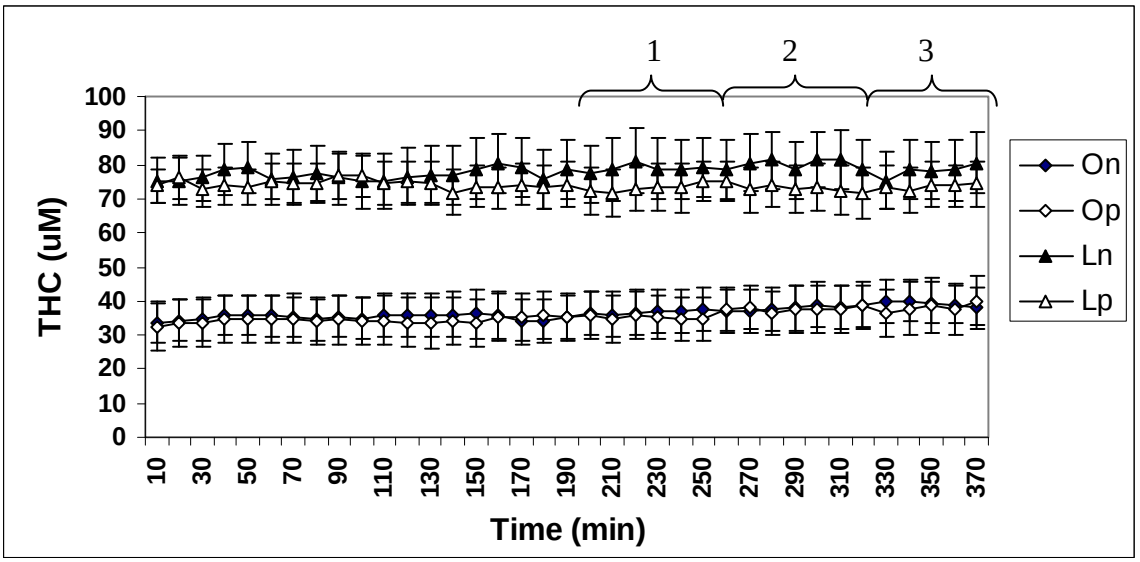

Figure 3.5 Total haemoglobin content (THC) in protocol 2 for niacin (n) and placebo (p) trials with obese (O) and lean (L) sedentary groups. Numbers 1-3 reflect the summary time points used in analysis.

3.4 DISCUSSION

A large body of recent literature suggests that the acute and chronic exposure of the microvasculature to high circulatory FA concentrations plays a key role in the mechanisms that lead to an imbalance between resting fasted vasodilation and vasoconstriction in the overweight and obese state. This provided the rationale to reduce plasma FA concentrations with niacin, a vitamin naturally occurring in our food. Acute exposure of the microvasculature to high circulation FA levels prevented insulin-induced capillary recruitment in healthy lean rats in vivo (Clerk et al. 2002[46]). High levels of FA also reduced insulin-induced IRS-1 tyrosine phosphorylation and downstream activation of protein kinase B (PKB/Akt) and eNOS in cultured endothelial cells (Kim et al. 2005[18]), while insulin-induced Akt- and eNOS-activation were blunted in the aorta of obese Zucker rats (Naruse et al. 2006[47]). In the fasted resting state FA-induced impairments in Akt-activation have been suggested to not only reduce basal nitric oxide (NO) production and vasodilation in obese subjects with and without the metabolic syndrome, but to also relieve the inhibition of the mitogenic insulin signalling pathway (Figure 3.1) and thus explain the high plasma levels of ET-1, which is a potent local vasoconstrictor produced by the endothelial cells (Eringa et al. 2004[19]; Thijssen et al. 2008[30]; Serne et al. 2006[48]). Secondly, high circulating levels of FA have been proposed to activate NADPH oxidase in the endothelium and vascular smooth muscle cells (VSMC) of the vascular wall and thus lead to excess production of superoxide anions (O_2^-; Brandes and Kreuzer 2005[20]; Bedard and Krause 2007[21]; Chinen et al. 2007[49]). Superoxide anions scavenge NO thereby reducing basal vasodilation, while peroxynitrite, the end product of this reaction, has been shown to increase vasoconstriction via a variety

mechanisms (Pacher et al. 2007[50]). Excess O_2^- production, by scavenging endothelial NO, has also been suggested to reduce the protective effect of NO on atherosclerosis and vascular damage (McAllister and Laughlin 2006[31]; Landmesser and Drexler 2007[51]). Thirdly, FA have been shown to activate the nuclear factor κB (NFκB) signaling network in cultured endothelial cells (Oram and Bornfeldt 2004[17]; Kim et al. 2005[18]; Artwohl et al. 2004[52]) and in obese Zucker rats (Chinen et al. 2007[49]). Activation of the NFκB pathway leads to reduced vasodilation as it decreases basal and insulin-stimulated Akt-activation (Figure 3.1; Chinen et al. 2007[49]) and, via accumulation of prostaglandin H_2 (PGH_2) resulting in thromboxane A_2 (ThA_2)/PGH_2 receptor activation also leads to vasoconstriction (Barnes and Karin 1997[53]; Yamamoto et al. 1995[54]). Activation of the NFκB pathway induces increased expression of cellular adhesion molecules and leukocyte adhesion (vascular inflammation) and activates the mechanisms that lead to atherogenesis and apoptosis (Wagenmakers et al. 2006[22]). Silver et al. (2007)[23] recently provided evidence that the above mechanisms not only operate in obese subjects with the metabolic syndrome and cardiovascular disease, but also in overweight and obese individuals without obvious pathology, by showing increased protein expression of ET-1, NADPH oxidase and NFκB, and evidence of protein nitrosylation by peroxynitrite in vascular endothelial cells harvested from these individuals.

Niacin was successfully used in this study to first decrease plasma FA concentrations with an average minimum value of only 49 ± 25 % of the overnight fasted baseline level and to then increase plasma FA concentrations in the rebound phase with an average maximum value of 153 ± 71 % of baseline. This observation is in line with previous

studies showing this biphasic response to niacin (Wang et al. 2000[36]). Despite this successful manipulation of plasma FA there were no significant differences in THC between the niacin and placebo trials in each group. No significant changes in THC over time were observed in any of the participant groups in protocol 1, but in protocol 2, time had a significant effect in the high FA phase. However, inspection of the mean THC data (56.03, 57.27, and 57.15 μM for time points 1-3, respectively) revealed a small statistically significant 1.24 μM difference in THC between points 1 and 2. Despite the statistical significance, this small difference is not regarded to be of physiological relevance and can be encompassed by the noise of the measurement signal.

This absence of a relevant significant change in THC over time during the niacin trials for all participant groups leads us to conclude that our hypothesis that decreases in plasma FA concentrations would improve the net balance between vasodilation and vasoconstriction in the microvasculature of the muscle of sedentary subjects, while increases in plasma FA would increase net vasoconstriction in both lean sedentary and obese sedentary subjects, was not confirmed. The results do show a significant difference in THC values between lean and obese groups in both protocols with higher values occurring in the lean.

The fact that the THC in the muscle microvasculature, which represents the volume of blood in the muscle microvasculature, was higher in lean individuals than in obese individuals seems to indicate that obese individuals either have an increased net vasoconstriction, a lower density of capillaries (rarefaction), or a combination of the two.

Regular exercise is known to lead to angiogenesis (formation of new capillaries leading to a higher muscle capillary density; Frisbee 2007[11]; Gavin et al. 2005[13]; Andersen and Henriksson 1977[32]; Shono et al. 2002[33]). In line with this, the active individuals in our study also had a higher THC than their sedentary counterparts, although the differences in THC between the two lean and the two obese groups were not significant due to the large individual variation in both of the groups.

Alternatively, the large adipose tissue thickness (ATT) over the biceps muscle of the obese participants may be affecting the observed NIRS absorption. The NIRS light photons pass through three tissues during measurement, namely the skin, the subcutaneous adipose tissue layer, and skeletal muscle tissue, and each one will contribute in varying degrees to the NIRS absorbance. Skin capillaries apparently make a very small contribution (<5 %) to the NIRS signal when the ID is greater than 20 mm (van Beekvelt et al. 2001[37]), as it was in our study. Furthermore, the absence of a visible increase in THC despite obvious flushing following niacin ingestion supports the notion that skin contribution to NIRS absorption is negligible. The NIRS absorbance due to adipose tissue (+ skin) in the four participant groups was estimated through a calculation proposed by van Beekvelt (2001)[37]. The contribution of adipose tissue (+ skin) was as high as 51.8 % of the NIRS absorbance in the obese sedentary, 36.8 % in the obese active, 14.1 % in the lean sedentary, and 10.9 % in the lean active. As there is evidence suggesting that the capillarisation of the adipose tissue is approximately one third lower than that of the most poorly perfused skeletal muscles in animals (Gersh and Still 1945[55]), it is possible that the lower THC content in the obese groups may in part originate from

the increased contribution of the subcutaneous adipose tissue layer to the NIRS absorbance signal rather than being solely the reflection of rarefaction in the skeletal muscle bed.

The calculation of tissue contribution to the NIRS signal also shows that over approximately half the NIRS absorbance should occur in skeletal muscle for both lean and obese groups. This implies that the lowering of plasma FA did not lead to a change in the balance between vasodilation and vasoconstriction of either the skeletal muscle or adipose tissue microvasculature in any of the groups studied. This is not in line with our observations of skin microvascular recruitment as clear flushing was seen shortly after niacin ingestion in 31 out of 32 participants, pointing at an increase in skin capillary perfusion. The lowering of FA with acipimox also showed increased skin microvascular perfusion (de Jongh et al. 2004[56]) when it was measured with capillaroscopy. Therefore, it would seem that a decrease in plasma FA has a different effect on skeletal muscle and subcutaneous adipose tissue microvascular perfusion as compared to skin.

However, in the obese group, the absence of an effect on THC by the lowering of FA can possibly be explained by the short duration of the low FA phase. Important causes of an imbalance between vasodilation and vasoconstriction in the obese are the increased gene expression and protein content of the enzyme NADPH oxidase and the transcription factor NFκB (Silver et al. 2007[23]). A reduction of the content of both of these proteins is quite likely to take more than 3 hours, which is the period with low FA concentrations. Furthermore, decreases in plasma FA concentrations do not necessarily lead to acute

decreases in the endothelial concentrations of the fatty acid metabolites (long-chain fatty acyl-CoA and diacylglycerol) that activate protein kinase C and increase serine phosphorylation of IRS-1 and thus reduce NO production and vasodilation in the resting fasted state (Naruse et al. 2006[47]; Serne et al. 2006[48]). The duration of the low FA phase in other words may have been too transient to correct the most important mechanisms that lead to net vasoconstriction in the obese and this may explain the absence of an acute change in THC levels in this study. To investigate whether more prolonged activation generates data in line with our hypotheses future studies should be carried out using prolonged use of niacin, a prolonged release form of niacin such as niaspan (Vogt et al. 2007[57]), or longer term acipimox (Bajaj et al. 2005[58]) to induce low plasma FA over periods lasting several days.

In conclusion, although it would be ideal if a vitamin like niacin could be used to acutely improve net balance between vasodilation and vasoconstriction our data support the conclusion that ingestion of a single bolus of niacin does not have this effect in a young obese group with a BMI of 31.6 ± 5.7. The likely reason is that the FA lowering effect is too transient to reverse induction of NADPH oxidase and NFκB gene expression and reduce serine phosphorylation of IRS-1. No effect on THC was seen in the microvasculature of both the muscle and subcutaneous adipose tissue in this study. Baseline THC measurements suggest that lean subjects have a higher muscle capillary density and/or an improved balance between vasodilation and vasoconstriction than obese subjects and that trained individuals in both groups have a higher capillary density than their inactive counterparts. The actual differences in microvascular blood volume

between lean and obese groups might be smaller than the difference in THC observed with NIRS due to the fact that, in the obese groups, a larger proportion of the NIRS absorbance resides in the thicker subcutaneous adipose tissue layer which is known to have a lower microvascular density than skeletal muscle (Gersh and Still 1945[55]).

3.5 REFERENCE LIST

1. World Health Organisation. Obesity and overweight. Fact Sheet No. 311, 2006.

2. Jonk AM, Houben AJ, de Jongh RT, Serne EH, Schaper NC, Stehouwer CD. Microvascular dysfunction in obesity: a potential mechanism in the pathogenesis of obesity-associated insulin resistance and hypertension. Physiology (Bethesda) 2007;22:252-260.

3. Meyers MR, Gokce N. Endothelial dysfunction in obesity: etiological role in atherosclerosis. Curr Opin Endocrinol Diabetes Obes 2007;14:365-369.

4. Hartge MM, Unger T, Kintscher U. The endothelium and vascular inflammation in diabetes. Diab Vasc Dis Res 2007;4:84-88.

5. Cersosimo E, Defronzo RA. Insulin resistance and endothelial dysfunction: the road map to cardiovascular diseases. Diabetes Metab Res Rev 2006;22:423-436.

6. Kim JA, Montagnani M, Koh KK, Quon MJ. Reciprocal relationships between insulin resistance and endothelial dysfunction: molecular and pathophysiological mechanisms. Circulation 2006;113:1888-1904.

7. Segal SS. Regulation of blood flow in the microcirculation. Microcirculation 2005;12:33-45.

8. Traupe T, D'Uscio LV, Muenter K, Morawietz H, Vetter W, Barton M. Effects of obesity on endothelium-dependent reactivity during acute nitric oxide synthase

inhibition: modulatory role of endothelin. Clin Sci (Lond) 2002;103 Suppl 48:13S-15S.

9. Traupe T, Lang M, Goettsch W, Munter K, Morawietz H, Vetter W, Barton M. Obesity increases prostanoid-mediated vasoconstriction and vascular thromboxane receptor gene expression. J Hypertens 2002;20:2239-2245.

10. Wallis MG, Wheatley CM, Rattigan S, Barrett EJ, Clark AD, Clark MG. Insulin-mediated hemodynamic changes are impaired in muscle of Zucker obese rats. Diabetes 2002;51:3492-3498.

11. Frisbee JC. Obesity, insulin resistance, and microvessel density. Microcirculation 2007;14:289-298.

12. Lind L, Lithell H. Decreased peripheral blood flow in the pathogenesis of the metabolic syndrome comprising hypertension, hyperlipidemia, and hyperinsulinemia. Am Heart J 1993;125:1494-1497.

13. Gavin TP, Stalling H.W., Zwetsloot KA, Westerkamp LM, Ryan NS, Moore RA, Pofahl WE, Hickner RC. Lower capillary density but no difference in VEGF expression in obese vs. lean young skeletal muscle in humans. J Appl Physiol 2005;98:315-321.

14. Ribeiro MM, Trombetta IC, Batalha LT, Rondon MU, Forjaz CL, Barretto AC, Villares SM, Negrao CE. Muscle sympathetic nerve activity and hemodynamic alterations in middle-aged obese women. Braz J Med Biol Res 2001;34:475-478.

15. Lewis GF, Carpentier A, Adeli K, Giacca A. Disordered fat storage and mobilization in the pathogenesis of insulin resistance and type 2 diabetes. Endocr Rev 2002;23:201-229.

16. Frayn KN. Adipose tissue as a buffer for daily lipid flux. Diabetologia 2002;45:1201-1210.

17. Oram JF, Bornfeldt KE. Direct effects of long-chain non-esterified fatty acids on vascular cells and their relevance to macrovascular complications of diabetes. Front Biosci 2004;9:1240-1253.

18. Kim F, Tysseling KA, Rice J, Pham M, Haji L, Gallis BM, Baas AS, Paramsothy P, Giachelli CM, Corson MA, Raines EW. Free fatty acid impairment of nitric oxide production in endothelial cells is mediated by IKKbeta. Arterioscler Thromb Vasc Biol 2005;25:989-994.

19. Eringa EC, Stehouwer CD, van Nieuw Amerongen GP, Ouwehand L, Westerhof N, Sipkema P. Vasoconstrictor effects of insulin in skeletal muscle arterioles are mediated by ERK1/2 activation in endothelium. Am J Physiol Heart Circ Physiol 2004;287:H2043-H2048.

20. Brandes RP, Kreuzer J. Vascular NADPH oxidases: molecular mechanisms of activation. Cardio Res 2005;65:16-27.

21. Bedard K, Krause KH. The NOX family of ROS-generating NADPH oxidases: physiology and pathophysiology. Physiol Rev 2007;87:245-313.

22. Wagenmakers AJ, van Riel NA, Frenneaux MP, Stewart PM. Integration of the metabolic and cardiovascular effects of exercise. Essays Biochem 2006;42:193-210.

23. Silver AE, Beske SD, Christou DD, Donato AJ, Moreau KL, Eskurza I, Gates PE, Seals DR. Overweight and obese humans demonstrate increased vascular endothelial NAD(P)H oxidase-p47(phox) expression and evidence of endothelial oxidative stress. Circulation 2007;115:627-637.

24. Cardillo C, Nambi SS, Kilcoyne CM, Choucair WK, Katz A, Quon MJ, Panza JA. Insulin stimulates both endothelin and nitric oxide activity in the human forearm. Circulation 1999;100:820-825.

25. Cusi K, Maezono K, Osman A, Pendergrass M, Patti ME, Pratipanawatr T, Defronzo RA, Kahn CR, Mandarino LJ. Insulin resistance differentially affects the PI 3-kinase- and MAP kinase-mediated signaling in human muscle. J Clin Invest 2000;105:311-320.

26. Jiang ZY, Lin YW, Clemont A, Feener EP, Hein KD, Igarashi M, Yamauchi T, White MF, King GL. Characterization of selective resistance to insulin signaling in the vasculature of obese Zucker (fa/fa) rats. J Clin Invest 1999;104:447-457.

27. Federici M, Menghini R, Mauriello A, Hribal ML, Ferrelli F, Lauro D, Sbraccia P, Spagnoli LG, Sesti G, Lauro R. Insulin-dependent activation of endothelial nitric oxide synthase is impaired by O-linked glycosylation modification of

signaling proteins in human coronary endothelial cells. Circulation 2002;106:466-472.

28. Seger R, Krebs EG. The MAPK signaling cascade. FASEB J 1995;9:726-735.

29. Thijssen DH, Ellenkamp R, Kooijman M, Pickkers P, Rongen GA, Hopman MT, Smits P. A causal role for endothelin-1 in the vascular adaptation to skeletal muscle deconditioning in spinal cord injury. Arterioscler Thormb Vasc Biol 2007;27:325-331.

30. Thijssen DH, Rongen GA, Smits P, Hopman MT. Physical (in)activity and endothelium-derived constricting factors: overlooked adaptations. J Physiol 2008;586:319-324.

31. McAllister RM, Laughlin MH. Vascular nitric oxide: effects of physical activity, importance for health. Essays Biochem 2006;42:119-131.

32. Andersen P, Henriksson J. Capillary supply of the quadriceps femoris muscle of man: adaptive response to exercise. J Physiol 1977;270:677-690.

33. Shono N, Urata H, Saltin B, Mizuno M, Harada T, Shindo M, Tanaka H. Effects of low intensity aerobic training on skeletal muscle capillary and blood lipoprotein profiles. J Atheroscler Thromb 2002;9:78-85.

34. Frisbee JC, Delp MD. Vascular function in the metabolic syndrome and the effects on skeletal muscle perfusion: lessons from the obese Zucker rat. Essays Biochem 2006;42:145-161.

35. Carlson LA, Oro L, Ostman J. Effect of a single dose of nicotinic acid on plasma lipids in patients with hyperlipoproteinemia. Acta Med Scand 1968;183:457-465.

36. Wang W, Basinger A, Neese RA, Christiansen M, Hellerstein MK. Effects of nicotinic acid on fatty acid kinetics, fuel selection, and pathways of glucose production in women. Am J Physiol Endocrinol Metab 2000;279:E50-E59.

37. van Beekvelt MC, Borghuis MS, van Engelen BG, Wevers RA, Colier WN. Adipose tissue thickness affects in vivo quantitative near-IR spectroscopy in human skeletal muscle. Clin Sci (Lond) 2001;101:21-28.

38. Wilson JR, Mancini DM, McCully K, Ferraro N, Lanoce V, Chance B. Noninvasive detection of skeletal muscle underperfusion with near-infrared spectroscopy in patients with heart failure. Circulation 1989;80:1668-1674.

39. Kell RT, Farag M, Bhambhani Y. Reliability of erector spinae oxygenation and blood volume responses using near-infrared spectroscopy in healthy males. Eur J Appl Physiol 2004;91:499-507.

40. Mancini DM, Bolinger L, Li H, Kendrick K, Chance B, Wilson JR. Validation of near-infrared spectroscopy in humans. J Appl Physiol 1994;77:2740-2747.

41. Cui W, Kumar C, Chance B. Experimental study of migration depth for the photons measured at sample surface. I. Time resolved spectroscopy and imaging. Proc SPIE Int Soc Opt Eng 1991;1431:180-191.

42. Homma S, Fukunaga T, Kagaya A. The influence of adipose tissue thickness on Near Infrared Spectoscopic signals in the measurement of human muscle. J Biomed Opt 1996;1:418-424.

43. Tunaru S, Kero J, Schaub A, Wufka C, Blaukat A, Pfeffer K, Offermanns S. PUMA-G and HM74 are receptors for nicotinic acid and mediate its anti-lipolytic effect. Nat Med 2003;9:352-355.

44. Christie AW, McCormick DK, Emmison N, Kraemer FB, Alberti KG, Yeaman SJ. Mechanism of anti-lipolytic action of acipimox in isolated rat adipocytes. Diabetologia 1996;39:45-53.

45. Matthews JN, Altman DG, Campbell MJ, Royston P. Analysis of serial measurements in medical research. BMJ 1990;300:230-235.

46. Clerk LH, Rattigan S, Clark MG. Lipid infusion impairs physiologic insulin-mediated capillary recruitment and muscle glucose uptake in vivo. Diabetes 2002;51:1138-1145.

47. Naruse K, Rask-Madsen C, Takahara N, Ha SW, Suzuma K, Way KJ, Jacobs JR, Clermont AC, Ueki K, Ohshiro Y, Zhang J, Goldfine AB, King GL. Activation of Vascular Protein Kinase C-{beta} Inhibits Akt-Dependent Endothelial Nitric Oxide Synthase Function in Obesity-Associated Insulin Resistance. Diabetes 2006;55:691-698.

48. Serne EH, de Jongh RT, Eringa EC, Ijzerman RG, de Boer MP, Stehouwer CD. Microvascular dysfunction: causative role in the association between

hypertension, insulin resistance and the metabolic syndrome? Essays Biochem 2006;42:163-176.

49. Chinen I, Shimabukuro M, Yamakawa K, Higa N, Matsuzaki T, Noguchi K, Ueda S, Sakanashi M, Takasu N. Vascular lipotoxicity: endothelial dysfunction via fatty-acid-induced reactive oxygen species overproduction in obese Zucker diabetic fatty rats. Endocrinology 2007;148:160-165.

50. Pacher P, Beckman JS, Liaudet L. Nitric oxide and peroxynitrite in health and disease. Physiol Rev 2007;87:315-424.

51. Landmesser U, Drexler H. Endothelial function and hypertension. Curr Opin Cardiol 2007;22:316-320.

52. Artwohl M, Roden M, Waldhausl W, Freudenthaler A, Baumgartner-Parzer SM. Free fatty acids trigger apoptosis and inhibit cell cycle progression in human vascular endothelial cells. FASEB J 2004;18:146-148.

53. Barnes PJ, Karin M. Nuclear factor-kappaB: a pivotal transcription factor in chronic inflammatory diseases. N Engl J Med 1997;336:1066-1071.

54. Yamamoto K, Arakawa T, Ueda N, Yamamoto S. Transcriptional roles of nuclear factor kappa B and nuclear factor-interleukin-6 in the tumor necrosis factor alpha-dependent induction of cyclooxygenase-2 in MC3T3-E1 cells. J Biol Chem 1995;270:31315-31320.

55. Gersh I, Still MA. Blood vessels in fat tissue. Relation to problems of gas exchange. J Exp Med 1945;81:219-232.

56. de Jongh RT, Serne EH, Ijzerman RG, de Vries G, Stehouwer CD. Impaired microvascular function in obesity: implications for obesity-associated microangiopathy, hypertension, and insulin resistance. Circulation 2004;109:2529-2535.

57. Vogt A, Kassner U, Hostalek U, Steinhagen-Thiessen E. Prolonged-release nicotinic acid for the management of dyslipidemia: an update including results from the NAUTILUS study. Vasc Health Risk Manag 2007;3:467-479.

58. Bajaj M, Suraamornkul S, Romanelli A, Cline GW, Mandarino LJ, Shulman GI, Defronzo RA. Effect of a Sustained Reduction in Plasma Free Fatty Acid Concentration on Intramuscular Long-Chain Fatty Acyl-CoAs and Insulin Action in Type 2 Diabetic Patients. Diabetes 2005;54:3148-3153.

Chapter 4

LIMITATIONS OF NEAR-INFRARED SPECTROSCOPY AS A METHOD TO MEASURE MUSCLE MICROVASCULAR BLOOD VOLUME IN OBESE INDIVIDUALS

4.1 INTRODUCTION

Obesity is associated with the development of a multitude of pathologies including type II diabetes and cardiovascular disease (CVD). Both chronic diseases greatly contribute to increased morbidity and mortality rates in obese populations (for references see Chapter 1). Endothelial dysfunction of the microvasculature in skeletal muscle is considered to be an early and central event in the mechanisms by which obesity leads to insulin resistance, type II diabetes and CVD (Bakker et al. 2009[1]; Orasanu and Plutzky 2009[2]; Jonk et al. 2007[3]; Meyers and Gokce 2007[4]; World Health Organisation 2006[5]; World Health Organisation 1999[6]). In the skeletal muscle microvasculature, the loss of endothelial function has been shown to lead to reductions in (a) the microvascular blood volume present in skeletal muscle (Rattigan et al. 2006[7]; Clerk et al. 2006[8]), (b) the blood perfusion rate of the microvascular bed (Clark 2008[9]), and (c) the capillary permeability surface area product (Gudbjornsdottir et al. 2003[10]; Gudbjornsdottir 2005[11]). The capillary permeability surface area product is a measure of a molecule's ability to be transported from the capillary lumen into the interstitial fluid surrounding the muscle fibres (when applied to muscle) and thus is a major determinant of transendothelial nutrient, oxygen and insulin transport (Gudbjornsdottir et al. 2003[10]). While capillary permeability depends on molecule size and endothelial transport characteristics, capillary surface area depends on capillary recruitment and filling, and thus on terminal arteriolar vasodilation. In addition to increasing the capillary surface area, vasodilation of the terminal arterioles is a major determinant of increases in microvascular blood volume (MBV) and microvascular flow velocity and thereby controls nutrient, insulin and oxygen

delivery to, and uptake by, skeletal muscle. Endothelial dysfunction will result in an imbalance between vasodilation and vasoconstriction, and will reduce increases in MBV (Clerk et al. 2006[8]) and permeability surface area product (Gudbjornsdottir et al. 2003[10]; Gudbjornsdottir 2005[11]) in response to glucose ingestion and insulin infusion. The NO-dependent vasodilation response to shear stress in feeding and resistance arteries is reduced by endothelial dysfunction in humans (Arcaro et al. 1999[12]; Brook et al. 2001[13]; Hamdy et al. 2003[14]; Meyers and Gokce 2007[4]) and in obese Zucker rats (Frisbee and Stepp 2001[15]; Frisbee 2004[16]). Thus, during exercise, endothelial dysfunction may prevent shear-stress induced dilation of feeding and resistance arteries leading to a reduced supply of blood to the muscle microvascular bed. Furthermore, net dilation of terminal arterioles by contraction-induced adenosine production and potassium release (Hudlicka 1985[17]; van Teefelen 2006[18]; Clifford and Hellsten 2004[19]) is likely to be counteracted by several vasoconstriction mechanisms (Serne et al. 2006[20]; Bakker et al. 2009[1]; Pacher et al. 2007[21]) and to result in reduced increases in MBV during exercise.

An imbalance between vasodilation and vasoconstriction will lead to net vasoconstriction and functional rarefaction (less blood in the muscle capillary bed as results of net vasoconstriction in the resting fasted state, after meal ingestion, and during exercise). A sedentary lifestyle and endothelial dysfunction also leads, via impaired NO synthesis, to reduced angiogenesis and a decrease in the total number of capillaries (rarefaction). MBV measures the sum of rarefaction and functional rarefaction and is thus an important indicator of endothelial function. An indirect measure of MBV can be obtained by near-infrared spectroscopy (NIRS). This simple, non-invasive technique involves placing a

NIR-light emitting probe on the skin above the desired sampling area. NIRS is based on the absorption of NIR-light (650-1000nm) by haemoglobin and deoxyhaemoglobin, and on the Beer-Lambert absorption law. The underlying principle is that the higher the total haemoglobin content (THC) in the sampling area, the more NIR-light is absorbed and not seen by the detectors. Light photons that travel though large vessels in muscle and skin, such as arteries and veins, are unlikely to be detected due to 100 % absorption by the high local haemoglobin concentration. Therefore, successful photon pathways in muscle will primarily proceed through minimal biological absorbers and in previous literature it has often been assumed that the NIR light absorption changes will mainly reflect changes in the haemoglobin content and oxygen saturation of the capillary network (Mancini et al. 1994[22]). It is, however, quite likely that the smaller arterioles and venules also contribute to the observed NIR light absorption changes. As NIRS equipment is relatively inexpensive and non-invasive, and the method uses simple assumptions and calculations, NIRS could in principle be the ideal method to measure changes in muscle MBV.

The light photons, however, have to travel through the skin and adipose tissue layer before entering the muscle and then have to pass through the adipose tissue and skin once more to return to the detector on the skin surface. As the subcutaneous adipose tissue layer can vary considerably between individuals it may very well present a limitation in the use of NIRS (van Beekvelt et al. 2001[23]). It is possible that with a thick adipose tissue layer, the amount of light able to reach the muscle layer is affected, as is the amount of light returning to the detector from the muscle. Thus in the obese population it remains uncertain as to whether NIRS can provide reliable information on skeletal

muscle MBV in vivo. Therefore, the aim of the present study was to investigate the effect of the thickness of the subcutaneous adipose tissue layer on the THC measured with NIRS at rest and during incremental arm cranking exercise. Exercise was chosen as means to increase MBV as it leads to much larger increases in MBV than meal ingestion or insulin infusion (Vincent et al. 2006[24]; Clark 2008[9]). Three groups of individuals with skin thicknesses of < 3 mm, 4-6 mm, and > 8 mm above the biceps brachii, named group I, II, and III, respectively, were tested. Two NIRS probes with different penetration depth properties, determined by the distance between light source and detector (termed 'interoptode distance') were used to help verify the extent of the confounding effect of adipose tissue. Probe A ('superficial') had interoptode distances of 2.0-3.5 cm and probe B ('deep') of 3.0-4.4 cm. Participants had a NIRS probe strapped to the biceps of their dominant arm for 10 min resting measures followed by an incremental arm cranking exercise till self-perceived exhaustion. Measurements were made during exercise as this is known to lead to substantial increases in muscle MBV (Vincent et al. 2006[24]), while only small MBV changes are assumed to occur in the subcutaneous adipose tissue. This protocol was repeated twice: once with each NIRS probe, in participants from each of the 3 skin thickness groups mentioned above.

We hypothesize that when the subcutaneous adipose tissue layer is very thin, both probe A and B will give comparable THC measures at rest and during exercise, and we expect this to be the case in group I. When the thickness is such that a significant part of the signal originates from the subcutaneous adipose tissue, then probe A will measure lower THC than probe B due to the adipose tissue contributing more to the NIRS signal and the

adipose tissue having a lower capillarisation (Gersh and Still 1945[25]). A thicker subcutaneous adipose tissue layer is also expected to reduce the increase in MBV during exercise. We expect this to be the case in group II and III. The extreme result could be that no light photons that have travelled through muscle tissue will be 'seen' by the NIRS detector in group III due to the large adipose tissue thickness. In that case both probe A and B will measure low THC concentrations as the NIRS signal will principally reflect the adipose tissue perfusion and no increase in THC will be detected during exercise as there are only minimal changes in subcutaneous adipose tissue perfusion during exercise.

4.2 MATERIALS AND METHODS

4.2.1 Subjects

Twenty four healthy volunteers were recruited by word of mouth in the University of Birmingham. The volunteers were required to have skin thicknesses covering the biceps muscle falling into one of the three following categories, 0-3 mm, 4-6 mm, and 8-14 mm, termed group I, II, and III, respectively. Their physical characteristics are displayed in Table 4.1. Volunteers met individually with the researcher to discuss the study, provide written, informed consent, and complete preliminary measurements including a general health questionnaire, measurements of height and weight, and determination of NIRS optimal probe positioning (see below). The research has been carried out in accordance with the Declaration of Helsinki (2000) of the World Medical Association and has been

approved by the Ethics Committee of the School of Sport and Exercise Sciences at The University of Birmingham, UK.

Table 4.1 Characteristics of the three participant groups

	Group I	**Group II**	**Group III**
Gender (m / f)	5 / 3	4 / 4	3 / 5
Age (yrs)	23.3 *(± 3.01)*	26.5 *(± 2.45)*	23.0 *(± 3.11)*
Skin thickness (cm)	0.22 *(± 0.05)*	0.51 *(± 0.06)*	1.25 *(± 0.22)*
Height (m)	1.76 *(± 0.09)*	1.75 *(± 0.09)*	1.71 *(± 0.09)*
Weight (kg)	68.8 *(± 9.56)*	72.7 *(± 12.5)*	98.0 *(±26.1)*
BMI (kg / m^2)	22.1 *(± 1.85)*	23.7 *(± 3.00)*	33.2 *(± 5.60)*

Skin thickness was measured over the biceps brachii with skin fold callipers and represents an average of three measurements. Values given are the mean of 8 participants ± standard deviations.

4.2.2 NIRS measurements

NIRS is a non-invasive optical technique based on the oxygen-dependent absorption changes of haemoglobin and myoglobin. While differentiation between oxygenated and deoxygenated states of the chromophores can be made, it is not possible to distinguish between haemoglobin and myoglobin as their absorption spectrums overlap (van Beekvelt et al. 2001[23]). We used a continuous-wave NIR spectrometer (ISS OxyplexTS 95306, Champaign IL, USA), which measures the absorbance of the NIRS light at wavelengths of 692 nm and 834 nm and uses calibrated software routines to calculate absolute concentrations from the measured NIR absorbance. Deoxygenated haemoglobin and myoglobin (Hb/Mb) absorbance was measured at wavelength 692 nm, while the sum of deoxygenated and oxygenated Hb/Mb was measured at wavelength 834 nm as they

exhibit similar absorption coefficients at this higher wavelength. (Wilson et al. 1989[26]). Since myoglobin concentrations were unlikely to change over the testing period, the sum of the absorbance signals at 834 nm was taken to reflect the relative change in total haemoglobin content or THC (assuming a constant haematocrit; Kell et al. 2004[27]). We assumed that the changes in THC would reflect changes in MBV as NIRS measurements primarily reflect the microcirculation in skeletal muscle (Mancini et al. 1994[22]). NIRS measurements were carried out on the biceps brachii with two probes of different interoptode distances (ID), namely 2.0-3.5 cm (probe A 'superficial) and 3.0-4.4 cm (probe B 'deep'). The NIRS unit was given at least a 2 h warm up time as this minimised signal drift in time and was calibrated before each trial. Data was sampled at 2000 Hz, displayed in real time, and stored on disk for off-line analysis.

4.2.3 Determination of optimal probe position

The optimum probe position for the individual was identified by systematically drawing five marks on the belly of the biceps brachii muscle of their dominant arm and making measurements with the NIRS probe for 2 min on each mark. The mark with the highest THC value was noted as the optimum probe position for the individual. The positioning marks were made with a black ball point pen and their placement was identified for each participant in the following way: (a) half distance between elbow (olcranon process) and shoulder (coracoid process) = mark 0; (b) circumference of arm at point 0 divided by 4; (c) value (0.25 of circumference) from point 0 across biceps towards inner arm = mark 1; (d) marks 2-5 are 1.5 cm from mark 1, as shown in Figure 4.1.

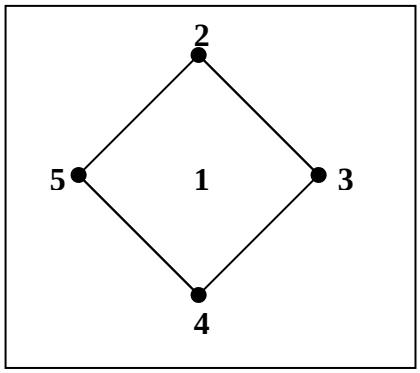

Figure 4.1 Position codes for determination of optimal NIRS probe position on the biceps brachii muscle of each participant. The positions were determined by (a) measuring half the distance between the elbow (olcranon process) and shoulder (coracoid process) = point 0; (b) measuring the circumference of the arm from point 0 and dividing it by 4; (c) the value (0.25 of circumference) from point 0 across biceps towards inner arm = mark 1; (d) marks 2-5 are 1.5 cm from mark 1. NIRS measurements were made for 2 min on each point and the point with the highest THC value was noted as the optimum probe position for the individual.

4.2.4 Protocol

Participants were required to come to the laboratory for two visits, each at least one hour apart and maximum one day apart. The two visits were identical apart from the NIRS probe, namely probe A or B. To which visit probe A and probe B were assigned was randomised. Participants were asked to refrain from exercising or ingesting a large meal less than an hour before testing.

Visit 1. Upon arrival to the laboratory participants were invited to sit in front of the arm crank machine and the assigned NIRS probe was fixed above the previously determined optimum position with a Velcro strap. After a 10 min rest measurement period, stage 1

of the exercise commenced. The participant was asked to start arm cranking at one revolution per beat, as sounded by a metronome set to 50 beats per minute, at 12.5 Watts for 5 min. At 15 sec before the end of stage 1, participants were asked to rate the perceived exertion of their arms, and of their body as a whole, using the Borg Scale of Perceived Exertion (1978), before progressing to exercise stage 2 at 25 Watts. Participants continued through the stages, reporting perceived whole body and arm exertion at the end of each stage, until they felt they could no longer continue. All stages lasted 5 min and progressed from 12.5 Watts through 25, 37.5, 50, 75, and up to 87.5 Watts (Figure 4.2). Once participants completed their last stage, they were required to sit at rest with their arm on their lap for another 10 min rest measurement. The probe was then removed and the first trial thus complete.

Visit 2. Participants were invited to sit in front of the arm crank machine while the other probe was placed over their previously selected optimum probe position mark. With their arm resting on their lap, 10 min rest measurements were taken before commencement of exercise through the stages up to the same stage the individual had completed in the first visit. A final 10 min rest measurement was made, after which the probe was removed and participants completed their testing.

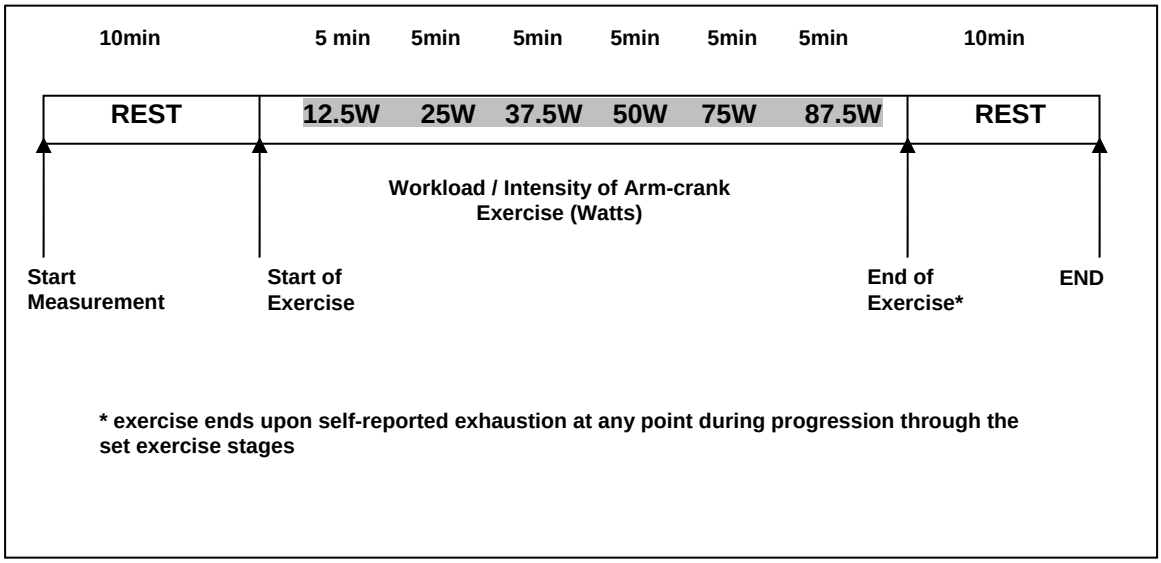

Figure 4.2 Testing protocol. The protocol begins with a 10 min resting measurement period. Arm cranking exercise commences at 12.5 W for 5 min and continues with work load increments every 5 min until self-perceived exhaustion. Another 10 min rest period follows.

4.2.5 Statistical Analysis

Two-tailed paired-sample t tests were carried out to locate differences observed between probes A and B at rest and during maximal exercise within each of the three groups for THC, percentage oxygen saturation ($\%O_2$), and oxygenated haemoglobin (HbO_2). Two-tailed paired-samples t tests were also used to identify differences between rest and maximal exercise for probes A and B in the three participant groups. Two-tailed independent-samples t tests were used to identify differences between groups for both probes at rest and maximal exercise THC, $\%O_2$, and HbO_2.

If significance was found the Bonferroni post hoc test was applied.

All statistical tests were carried out using SPSS for windows version 16.0 software package (Chicago, IL, USA). All data are reported as means ± SE and statistical significance was set at $P < 0.05$.

4.3 RESULTS

4.3.1 Total haemoglobin content

The principal finding was the distinct difference in THC measures between group I (ATT < 3 mm) and III (ATT > 8 mm) despite all participants exercising until exhaustion. In group II (4 mm < ATT < 6 mm), a difference was visible between the measurements made by probe A and B, while both probes tended to have similar readings within group I and group III. For all participants, there was a gradual increase in THC values as they progressed from rest through the exercise stages. Figure 4.3 shows the mean results of each group, with the first and last phases of each group reflecting resting measurements and the phases in between reflecting the incremental exercise stages. The number of exercise stages completed differed between participants thus in the last two exercise stages represented in Figure 4.3, the n numbers are less than 8 for all groups. In order to eliminate the variation in exercise stages completed, the data was viewed in terms of mean baseline resting THC value (termed 'rest') and mean THC value of the final exercise stage completed (termed 'max exercise') for all participants. The mean group values for rest and max exercise THC, as well as for the difference between these THC values (termed 'increase') are shown in Table 4.2.

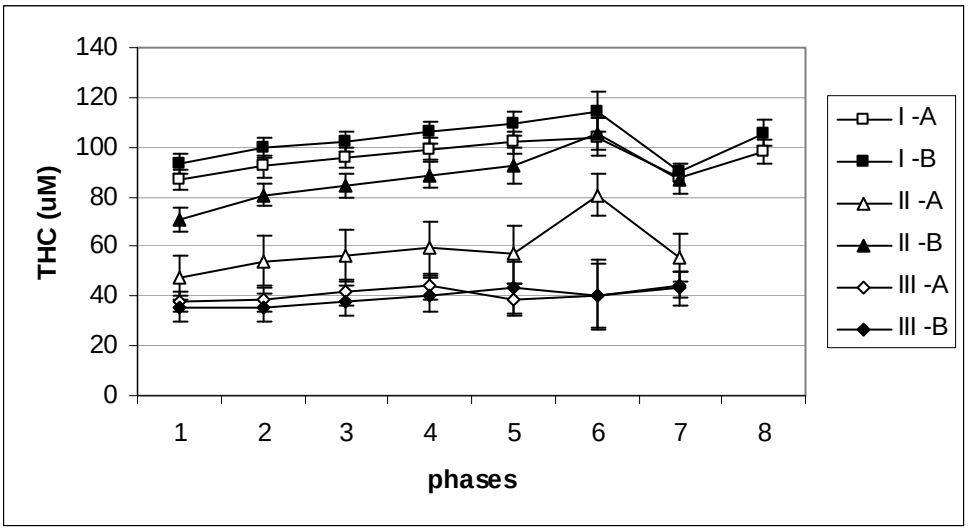

Figure 4.3 Total haemoglobin content (THC) values observed in groups I, II, and III during rest, incremental arm exercise, and followed by rest again. Values observed with probe A and B are given as means of 8 individuals. Due to individual differences in exercise increments achieved, n < 8 for the final 2 exercise increments in each group.

Table 4.2 Total haemoglobin content (THC) at rest and during the final increment of exercise (max exercise) for probes A and B in groups I, II, and III.

	Probe A	**Probe B**
Group I		
Rest	87 *(± 12)*	93 *(± 12)*
Max exercise	103 *(± 13)*	111 *(± 14)*
Increase	16 *(± 3)*	18 *(± 3)*
Group II		
Rest	47 *(± 25)*	71 *(± 13)*
Max exercise	62 *(± 31)*	94 *(± 18)*
Increase	14 *(± 10)*	23 *(± 9)*
Group III		
Rest	38 *(± 12)*	35 *(± 16)*

Max exercise	45 *(± 15)*	42 (*± 19)*
Increase	7 *(± 5)*	7 *(± 6)*

The increase shown is the change in THC from rest to maximal exercise. Data is expressed as mean ± standard deviations in micromolars (μM).

For group I, both probes gave the highest THC readings compared to groups II and III, and both rest and max exercise readings did not differ significantly between probes (P = 0.076 and P = 0.057, respectively). The THC increases from rest to max exercise for both probes were statistically significant (P = 0.001 for both probes) indicating a clear rise in MBV as participants progressed from rest through to maximal exercise for the measurement area underneath the probe.

For group III, THC values did not differ significantly between probes at rest and during max exercise (P = 0.541 and P = 0.698, respectively). THC was significantly lower in group III than in group I for both probes at rest and during max exercise (P = 0.001 for all comparisons) as can be seen in Table 4.2. The increase in THC from rest to max exercise for both probes did reach statistical significance (probe A P = 0.006, probe B P = 0.011) in group III, though the absolute increase in MBV was smaller than that seen in group I.

In group II a significant difference was seen between probes for THC measures at both rest and during max exercise (P = 0.014 and P = 0.005, respectively). Both probes showed significant increases in THC from rest to max exercise (probe A P = 0.006, and probe B P = 0.001), as was seen in group I and III. Comparison of the THC measures at

rest and max exercise of probe A between groups I and II, showed statistically significant lower values in group II (P = 0.003 and P = 0.006, respectively). However, the THC measures at max exercise of probe B between groups I and II were not significantly different (P = 0.052). Conversely, comparison of the THC measures at rest and max exercise of probe A between groups II and III, showed no significant differences (P = 0.359 and P = 0.186, respectively) while the THC measures at rest and max exercise with probe B were significantly different between groups II and III (P = 0.001 for both).

4.3.2 Haemoglobin oxygenation

In group I lower values for the HbO_2 concentration were seen during max exercise than at rest for both probes, but the difference was not significant for either probe. In groups II and III, however, higher values for the HbO_2 concentration were seen during max exercise than at rest. The difference was only significant for probe A in both groups (P = .049 and P = .019, respectively). HbO_2 concentration data are shown for all groups and probes in Figure 4.4 and Table 4.3.

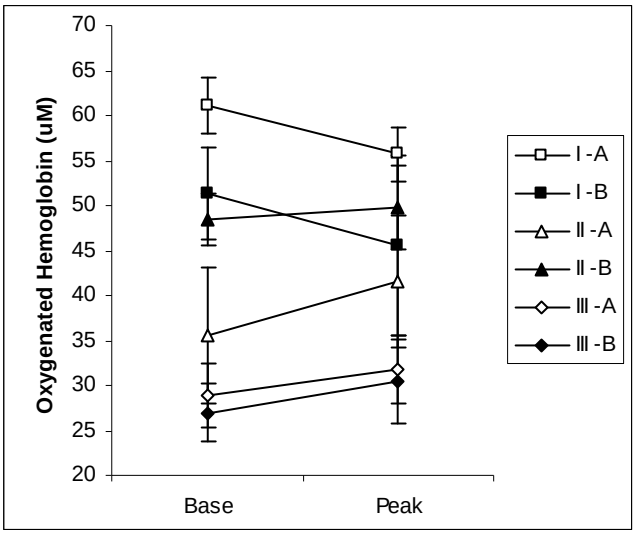

Figure 4.4 Oxygenated haemoglobin (HbO_2) concentrations are given as mean values for groups I, II, and III at rest and maximal exercise (mean HbO_2 value during the individual's maximal workload) for probes A and B.

Table 4.3 HbO_2 expressed as group averages at rest and the final stage of exercise completion (max exercise) from each individual for probes A and B in groups I, II, and III.

	Probe A	**Probe B**
Group I		
Rest	61.1 *(± 9)*	51.3 *(± 15)*
Max exercise	55.7 *(± 9)*	45.6 *(± 28)*
Increase	-5.4 *(± 10)*	-5.7 *(± 19)*
Group II		
Rest	35.5 *(± 21)*	48.4 *(± 8)*
Max exercise	41.6 *(± 21)*	49.8 *(± 13)*
Increase	6.1 *(± 7)*	1.4 *(± 12)*
Group III		
Rest	28.9 *(± 10)*	27.0 *(± 9)*
Max exercise	31.7 *(± 11)*	30.4 *(± 13)*
Increase	2.8 *(± 3)*	3.4 *(± 7)*

The increase shown is the change in HbO_2 concentration from rest to maximal exercise. Data is expressed as mean ± standard deviations in micromolars (μM)

4.3.3 Percentage oxygen saturation

The % O_2 saturation decreased significantly from rest to max exercise in group I for probe A ($P = 0.001$) and in group II for probe B ($P = 0.038$). No significant decrease was

seen in group III. % O_2 saturation data can be seen for all groups and probes in Figure 4.5 and Table 4.4.

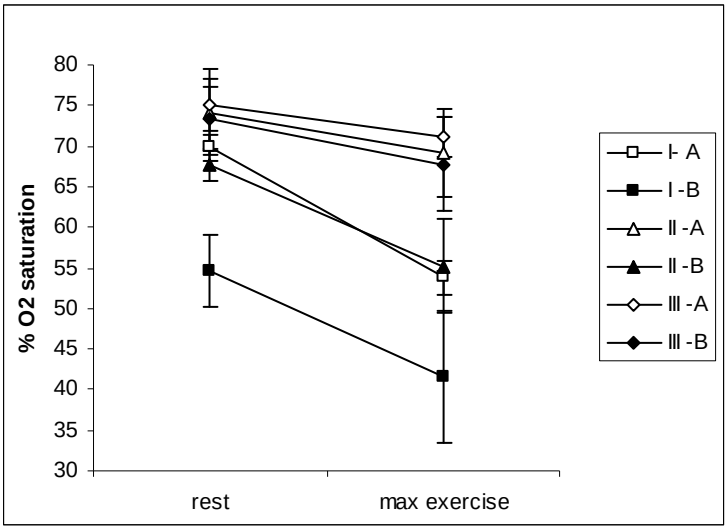

Figure 4.5 Percentage oxygen saturation (%O_2) mean values for groups I, II, and III at rest and maximal exercise (mean %O_2 value during the individual's maximal workload). Values are given for probe A and B.

Table 4.4 Percent oxygen saturation (%O_2) at rest and final stage of exercise completion (max exercise) from each individual for probes A and B in groups I, II, and III.

	Probe A	**Probe B**
Group I		
Rest	69.8 *(± 4)*	54.6 *(± 13)*
Max exercise	53.8 *(± 6)*	41.6 *(± 23)*
Increase	-16.0 *(± 8)*	-13.0 *(± 16)*
Group II		
Rest	74.1 *(± 15)*	67.8 *(± 6)*
Max exercise	69.1 *(± 15)*	55.2 *(± 17)*
Increase	-5.0 *(±6)*	-12.6 *(± 14)*
Group III		
Rest	75.1 *(± 9)*	73.3 *(± 11)*

Max exercise	71.1 *(± 7)*	67.7 *(±17)*
Increase	-4.0 *(± 5)*	-5.6 *(± 9)*

The increase shown is the change in $\%O_2$ from rest to maximal exercise. Data is expressed as mean ± standard deviations.

4.4 DISCUSSION

The present study demonstrates that NIRS may have major limitations if it is used to estimate MBV in skeletal muscle of obese individuals. The significantly lower resting THC values in the obese group suggest that most of the signal is originating from the adipose tissue which has a lower capillarisation than skeletal muscle (Gersh and Still 1945[25]). Furthermore, with increasing exercise intensity MBV and thus THC is expected to increase while HbO_2 concentration and especially $\%O_2$ saturation are expected to decrease. In the obese group (III) THC showed the smallest increase over the exercise period even though all groups achieved maximal exercise according to the ratings of perceived exertion (Borg scale 1978; Table 4.5). Similarly, HbO_2 concentration was very low for group III in comparison to groups I and II, and actually increased from rest to maximal exercise, with the increase from probe A reaching statistical significance. The $\%O_2$ saturation showed the smallest decrease from rest to max exercise in the obese group as compared to groups I and II, and the decrease was not significant for either probe. Taken together these results suggest that despite the increase in the ID (probe B), and the resultant increase in the penetration depth of NIR-light, the skeletal muscle made only a minor contribution to the absorbance of NIR light in the obese group.

Table 4.5 Borg ratings for arms and whole body

	Borg ratings		Exercise duration
Group	**-arms-**	**-body-**	**(min)**
I	17.7 *(± 1.3)*	15.4 *(± 2.9)*	23:48 *(± 3.5)*
II	17.5 *(± 1.3)*	13.9 *(± 1.2)*	20:36 *(± 3.2)*
III	17.7 *(± 2.0)*	15.9 *(± 3.2)*	18:48 *(± 4.4)*

Values are expressed as group means ± standard deviations and represent the final stage of exercise as well as mean exercise duration per group (n = 8).

It has been suggested that the measurement depth of the NIRS is equal to half the ID. Initially this was based on in vitro experiments. For example, Cui et al. (1991)[28] found this to be true using intralipid emulsions as a phantom medium. Later, Homma et al. (1996)[29] tested this theory in the human leg with ATT ranging from 4-10 mm and IDs of 20, 30, and 40 mm to find that the NIRS light penetrated at least deep enough to reach half the ID on all their tested combinations of ID and ATT. However, in the present study, participants in group III had a mean adipose tissue thickness of 12.5 mm (± 0.22) and despite probe B having an ID of 44 mm our data indicates that the skeletal muscle made only a minor contribution to the absorbance of NIR light.

A simple calculation of the theoretical skeletal muscle tissue contribution to the returning NIRS signal (not taking into account the different light-scattering properties of fat and muscle; van Beekvelt et al. 2001[23]) would suggest a 47.5 % contribution with probe B for group III (Figure 4.6; Table 4.6). The fact that we were unable to observe a substantial

increase in MBV from the skeletal muscle despite nearly half the signal theoretically originating from the muscle appears inconsistent with the calculations of the theoretical measurement depth. This can potentially be explained by the scattering and absorption properties of the adipose tissue layer. Rather than the adipose tissue layer simply adding to the penetration depth the photons need to travel in order to reach the muscle, the adipose tissue appears to scatter the photons thereby increasing their path length within the adipose tissue and thus reducing their penetration depth (Matsushita 1998[30]). Thus although the moderate ATT of our group II could be overcome by increasing the ID, the thickness of the adipose tissue layer in the obese group may have caused photon scattering and thus increased the adipose tissue path length to such an extent as to significantly reduce penetration depth and skeletal muscle contribution to the NIRS measurement.

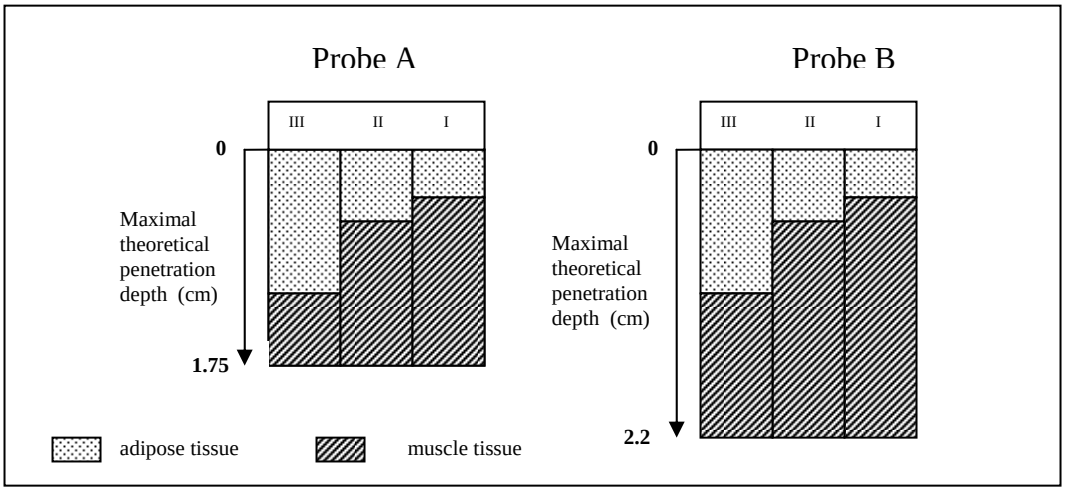

Figure 4.6 Theoretical contribution of adipose tissue (dots) and muscle tissue (lines) to the NIRS signal for probe A and B in groups I, II, and III. The maximal theoretical penetration depth is calculated as half the interoptode distance (ID). Probe A has a maximal ID of 3.5 cm, reflecting a theoretical penetration depth of 1.75 cm while probe B has a maximal ID of 4.4 cm, reflecting a theoretical penetration depth of 2.2 cm.

Table 4.6 Relative contributions of adipose and muscle tissue to the NIRS signal for probes A and B.

	Probe A				Probe B			
	Adipose		Muscle		Adipose		Muscle	
Group	**%**	**mm**	**%**	**mm**	**%**	**mm**	**%**	**mm**
I	12.6	2.2	87.4	15.3	10.0	2.2	90.0	19.8
II	29.1	5.1	70.8	12.4	23.0	5.1	76.8	16.9
III	71.4	12.5	28.0	5.0	56.8	12.5	47.5	9.5

Values are expressed as percentage and millimetre contributions and are based on the theoretical calculation of measurement depth equalling half the interoptode distance (ID). Probe A has a maximal ID of 35 mm, reflecting a theoretical penetration depth of 17.5 mm while probe B has a maximal ID of 44 mm, reflecting a theoretical penetration depth of 22 mm.

It is not possible to underpin the above conclusion with hard evidence as part of the reason for the lower resting THC value in group III may also be the result of a lower capillary density and net vasoconstriction in the muscle of obese individuals (Gavin et al. 2005[31]; Frisbee 2007[32]). Furthermore, the reduced increase in MBV during exercise may in part originate from a reduced net vasodilation of the terminal arterioles and therefore a reduced increase in MBV in the muscle during exercise (Arcaro et al. 1999[12]; Brook et al. 2001[13]; Hamdy et al. 2003[14]; Meyers and Gokce 2007[4]). However, the differences observed between groups I and III are large, and together with the theoretical estimates of the adipose tissue contribution to absorbance of the NIRS photons, lead to the conclusion that NIRS cannot be used to generate reliable estimates of MBV and oxygen saturation in obese subjects.

In conclusion, the data in the present study suggest that NIRS does not produce reliable information on the MBV in skeletal muscle even when a probe with an ID of 44 mm is used in obese participants with an ATT of 12.5 mm ± 0.22. This appears to be due to the fact that the detected signal primarily originates from the adipose tissue layer and differences in the microvasculature of adipose tissue and muscle will confound the adaptation of the muscle to the obese state. Thus for the obese population contrast enhanced ultrasound (Vincent et al. 2006[24]) seems to be required for the measurement of muscle MBV and for the detection of capillary recruitment defects in response to meal-induced increases in insulin concentration and exercise.

4.5 REFERENCE LIST

1. Bakker W, Eringa EC, Sipkema P, van H, V. Endothelial dysfunction and diabetes: roles of hyperglycemia, impaired insulin signaling and obesity. Cell Tissue Res 2009;335:165-189.

2. Orasanu G, Plutzky J. The pathologic continuum of diabetic vascular disease. J Am Coll Cardiol 2009;53:S35-S42.

3. Jonk AM, Houben AJ, de Jongh RT, Serne EH, Schaper NC, Stehouwer CD. Microvascular dysfunction in obesity: a potential mechanism in the pathogenesis of obesity-associated insulin resistance and hypertension. Physiology (Bethesda) 2007;22:252-260.

4. Meyers MR, Gokce N. Endothelial dysfunction in obesity: etiological role in atherosclerosis. Curr Opin Endocrinol Diabetes Obes 2007;14:365-369.

5. World Health Organisation. Diabetes. fact sheet 312 ed. 2006.

6. World Health Organisation. Definition, diagnosis and classification of diabetes mellitus and its complications. 1999:1-65.

7. Rattigan S, Bradley EA, Richards SM, Clark MG. Muscle metabolism and control of capillary blood flow: insulin and exercise. Essays Biochem 2006;42:133-144.

8. Clerk LH, Vincent MA, Jahn LA, Liu Z, Lindner JR, Barrett EJ. Obesity blunts insulin-mediated microvascular recruitment in human forearm muscle. Diabetes 2006;55:1436-1442.

9. Clark MG. Impaired microvascular perfusion: a consequence of vascular dysfunction and a potential cause of insulin resistance in muscle. Am J Physiol Endocrinol Metab 2008;295:E732-E750.

10. Gudbjornsdottir S, Sjostrand M, Strindberg L, Wahren J, Lonnroth P. Direct measurements of the permeability surface area for insulin and glucose in human skeletal muscle. J Clin Endocrinol Metab 2003;88:4559-4564.

11. Gudbjornsdottir S. Decreased Muscle Capillary Permeability Surface Area in Type 2 Diabetic Subjects. J Clin Endocrinol Metab 2005;90:1078-1082.

12. Arcaro G, Zamboni M, Rossi L, Turcato E, Covi G, Armellini F, Bosello O, Lechi A. Body fat distribution predicts the degree of endothelial dysfunction in uncomplicated obesity. Int J Obes Relat Metab Disord 1999;23:936-942.

13. Brook RD, Bard RL, Rubenfire M, Ridker PM, Rajagopalan S. Usefulness of visceral obesity (waist/hip ratio) in predicting vascular endothelial function in healthy overweight adults. Am J Cardiol 2001;88:1264-1269.

14. Hamdy O, Ledbury S, Mullooly C, Jarema C, Porter S, Ovalle K, Moussa A, Caselli A, Caballero AE, Economides PA, Veves A, Horton ES. Lifestyle modification improves endothelial function in obese subjects with the insulin resistance syndrome. Diabetes Care 2003;26:2119-2125.

15. Frisbee JC, Stepp DW. Impaired NO-dependent dilation of skeletal muscle arterioles in hypertensive diabetic obese Zucker rats. Am J Physiol Heart Circ Physiol 2001;281:H1304-H1311.

16. Frisbee JC. Enhanced arteriolar alpha-adrenergic constriction impairs dilator responses and skeletal muscle perfusion in obese Zucker rats. J Appl Physiol 2004;97:764-772.

17. Hudlicka O. Regulation of muscle blood flow. Clin Physiol 1985;5:201-229.

18. van Teeffelen. Rapid dilation of arterioles with single contraction of hamster skeletal muscle. 290 ed. 2006:H119-H127.

19. Clifford PS, Hellsten Y. Vasodilatory mechanisms in contracting skeletal muscle. J Appl Physiol 2004;97:393-403.

20. Serne EH, de Jongh RT, Eringa EC, Ijzerman RG, de Boer MP, Stehouwer CD. Microvascular dysfunction: causative role in the association between hypertension, insulin resistance and the metabolic syndrome? Essays Biochem 2006;42:163-176.

21. Pacher P, Beckman JS, Liaudet L. Nitric oxide and peroxynitrite in health and disease. Physiol Rev 2007;87:315-424.

22. Mancini DM, Bolinger L, Li H, Kendrick K, Chance B, Wilson JR. Validation of near-infrared spectroscopy in humans. J Appl Physiol 1994;77:2740-2747.

23. van Beekvelt MC, Borghuis MS, van Engelen BG, Wevers RA, Colier WN. Adipose tissue thickness affects in vivo quantitative near-IR spectroscopy in human skeletal muscle. Clin Sci (Lond) 2001;101:21-28.

24. Vincent MA, Clerk LH, Lindner JR, Price WJ, Jahn LA, Leong-Poi H, Barrett EJ. Mixed meal and light exercise each recruit muscle capillaries in healthy humans. Am J Physiol Endocrinol Metab 2006;290:E1191-E1197.

25. Gersh I, Still MA. Blood vessels in fat tissue. Relation to problems of gas exchange. J Exp Med 1945;81:219-232.

26. Wilson JR, Mancini DM, McCully K, Ferraro N, Lanoce V, Chance B. Noninvasive detection of skeletal muscle underperfusion with near-infrared spectroscopy in patients with heart failure. Circulation 1989;80:1668-1674.

27. Kell RT, Farag M, Bhambhani Y. Reliability of erector spinae oxygenation and blood volume responses using near-infrared spectroscopy in healthy males. Eur J Appl Physiol 2004;91:499-507.

28. Cui W, Kumar C, Chance B. Experimental study of migration depth for the photons measured at sample surface. I. Time resolved spectroscopy and imaging. Proc SPIE Int Soc Opt Eng 1991;1431:180-191.

29. Homma S, Fukunaga T, Kagaya A. The influence of adipose tissue thickness on Near Infrared Spectoscopic signals in the measurement of human muscle. J Biomed Opt 1996;1:418-424.

30. Matsushita K. Influence of adipose tissue on muscle oxygenation measurements with NIRS instrument. Proceedings of SPIE: The international society for optical engineers 1998;159-165.

31. Gavin TP, Stalling H.W., Zwetsloot KA, Westerkamp LM, Ryan NS, Moore RA, Pofahl WE, Hickner RC. Lower capillary density but no difference in VEGF expression in obese vs. lean young skeletal muscle in humans. J Appl Physiol 2005;98:315-321.

32. Frisbee JC. Obesity, insulin resistance, and microvessel density. Microcirculation 2007;14:289-298.

Chapter 5

METHOD DEVELOPMENT OF CONTRAST ENHANCED ULTRASOUND FOR THE MEASUREMENT OF SKELETAL MUSCLE MICROVASCULAR BLOOD VOLUME AND FLOW IN THE HUMAN FOREARM

The results of the experiment investigating the influence of adipose tissue thickness on NIRS measurements of skeletal muscle total haemoglobin content in chapter 4 led to the conclusion that NIRS was not a suitable tool to make such measurements in the muscle of obese individuals. We thus moved on to use a direct method to measure microvascular blood volume and blood flow, namely contrast enhanced ultrasound (CEU). This method was not in use in our laboratory and publications from groups using CEU lacked detailed descriptions and explanations of the procedures involved in preparation, testing, and analysis. Therefore this chapter describes in detail the effects of various preparation, testing, and analysis procedures on the data obtained with CEU, concluding with a description of the ideal CEU protocol for research in skeletal muscle perfusion of the human forearm.

5.1 The theory of contrast enhanced ultrasound

The contrast enhanced ultrasound method involves the infusion of microspheres which serve as a contrast-enhancing agent by acting as reflectors of the ultrasound beam. The microspheres remain entirely within the vascular space and have a similar size and rheology to red-blood cells. As they have a high echogenicity and, therefore, increase the contrast between blood and the surrounding tissues, they are an excellent tracer to measure the main perfusion variables (blood volume and blood flow velocity). The microspheres are administered as a constant infusion into the venous circulation and can be visualised by ultrasound in the tissue of interest. The videointensity of the image that is obtained with ultrasound is proportional to the concentration of the microspheres within the volume of tissue being imaged (microvascular blood volume) and is dependent on the frequency of the ultrasound beam. A single pulse of high-energy ultrasound is subsequently administered to simultaneously destroy all the microspheres within the ultrasound beam. Following this destruction, the rate of microsphere replenishment is measured and will reflect the blood flow velocity, while the plateau level of microspheres reached after the destruction again will reflect blood volume. As the larger vessels will fill more quickly, a background subtraction of the average videointensity generated within 1 second after the high-energy pulse is applied. This will eliminate the larger vessels from the analysis. Although it is not exactly known which size vessels are included in this analysis, it is generally assumed that they are terminal arterioles, capillaries (major contribution), and first and second degree venules. In this way, the CEU technique is expected to provide information on microvascular blood volume (MBV)

and microvascular blood flow velocity (MFV), while the product of the two gives microvascular blood flow (MBF).

5.2 Aim of the chapter

The main reason to develop the CEU technique in our laboratory is our interest in impaired endothelial function in obesity and its potential negative impact on skeletal muscle perfusion in the period following meal ingestion and during exercise. The primary aim of this chapter is to establish optimal conditions for maximal reproducibility and sensitivity of the CEU technique in human beings. In chapter 6 the optimal method will be subsequently used to investigate whether an oral glucose tolerance test in healthy trained men will lead to a detectable increase in skeletal muscle MBV, MFV and blood flow (product of MBV and MFV).

5.3 Protocol 1: CEU with Luminity and a multiple microsphere destruction protocol

The first protocol that we tested to make CEU measurements of MBV and MFV was the protocol used by Vincent et al. 2006[1]. As the paper contains very little detail of the CEU method used, Dr. George Balanos of our School went to the laboratory in Virginia to see the procedure and subsequent analysis. The preparation, testing, and analysis procedures used by Vincent et al. 2006[1] are described below.

5.3.1 Preparation procedures

Brand of microbubble

As Luminity was used in Vincent et al. 2006[1] (product name in the USA is 'Definity') we too ordered Luminity microspheres and their characteristics are shown in Table 5.3.

Dilution of microspheres

We followed the recommendation by the manufacturer and diluted one vial of Luminity in 50 ml of 0.9 % isotonic saline.

Ultrasound machine

The ultrasound machine requires certain presets to perform CEU imaging protocols. In most situations, the machine will also dictate the acquisition and analysis program that can be used as well as the probe that can be used. In our experiments we used the Philips Sonos 5500, the same as used in Vincent et al. 2006[1], with the cardiac transducer (S3).

Ultrasound imaging protocol

There are essentially two different imaging protocols which can be used to capture an imaging sequence for calculation of MBV and MFV. One protocol involves a sequence of microsphere destructions, using a high energy ultrasound pulse, with increasing time intervals to monitor the microsphere replenishment. The other protocol involves a single destruction followed by one complete replenishment curve

until plateau. The laboratory in Virginia uses the multiple microsphere destruction protocol and that is the method we initially adopted.

Multiple microsphere destruction protocol. The protocol involves simultaneously imaging and destroying all microspheres within the ultrasound beam by using a high-energy ultrasound pulse. In this protocol the ECG waveform was used to trigger the image capture and microsphere destruction at specific pulse intervals. Three images were captured at each of the following pulse intervals: 1, 2, 3, 4, 5, 8, 12, 15, and 20. In this way, the increasing length of time between the simultaneous image captures and destructions allowed for greater microsphere replenishment and eventually plateau formation in the higher pulse intervals. The data was then collated in relative time to create a single replenishment curve occurring over 20 heartbeats. The length of time required to complete this protocol was dependent on the individual heart rate and was approximately 5 minutes.

5.3.2 Experimental protocol in human volunteers

Measurement set up

The participants arrived in the morning after fasting overnight. Participants were asked to lie down on a bed and their dominant arm was rested on a pillow in a natural and relaxed position so as to be able to maintain this position without movement for the entire acquisition period. The ultrasound probe was positioned manually over the forearm flexor muscles and held in the desired place by a clamp attached to a flexible arm and fixed onto a heavy metal base. The probe position was drawn on the participant's arm so that CEU measurements at later time points during the testing were made in a close to similar position for reasons of comparison. A single lead

ECG was used to generate the pulse intervals required during the CEU protocol to trigger microsphere destruction and image capture.

Administration of microspheres

The administration of the microspheres required several steps including activation, dilution, handling once activated, infusion, and timing of acquisition commencement. The activation of Luminity microspheres involved vigorous shaking for 40 seconds in a mechanical shaking device (VIALMIX®) provided by the company. The activated microspheres were transferred to a syringe containing 50 ml saline and were then ready for infusion. Once activated, the microspheres need to be maintained in suspension to ensure a constant infusion concentration. This was achieved by gentle manual rotation of the infusion pump containing the syringe. The Luminity microspheres were infused at a rate of 1.6 ml/min, as recommended by the suppliers, and a steady state (constant plateau level of the videointensity) was reached in the vasculature in 3 min. The multiple destruction imaging protocol explained above was activated 3 min after the start of the constant intravenous infusion.

Data acquisition protocol

On the ultrasound machine, the programmed autobeat sequence was located by selection of ‘tools’ => ‘contrast agent’ => ‘physio’ => ‘autobeat sequence’. Once the 3 min of infusion was complete the ‘acquire’ command was selected. The ultrasound then commenced with the autobeat sequence and went through the programmed pulse intervals (1, 1, 1, 2, 2, 2, 3, 3, 3, etc) explained above. Once the sequence was completed the data were automatically saved and the acquisition stopped.

Care was taken to avoid accidentally touching or changing any controls which alter the intensity of the ultrasound image during measurement and between measurements in the same participant. Changes in MBV in response to a physiological signal (e.g. glucose ingestion or exercise) are based on relative changes of the intensity of the ultrasound image. Thus changing any of the settings that influence the echo-intensity will invalidate comparisons between CEU measurements. These settings include compression, gain (including the sliding time gain compensation and lateral gain controls) and frequency.

5.3.4 Analysis procedure and data quality check using QLAB

The CEU data acquired was originally analysed with the QLAB software from Philips (version 5.0), which was designed for cardiac CEU work. The data was imported into QLAB, images for analysis were selected and a region of interest was drawn as a contour of the flexor muscles. Imaging sequences with artifacts or movement were edited, an automatic background subtraction and curve fit was then applied, and MBV and MFV data automatically generated. It soon became clear, however, that the automatic background subtraction did not work properly in the QLAB software. When a background subtraction is applied in QLAB, for some reason, the ± 1.5 decibels (dB) difference between the first image and the last image of the sequence is lost as the first image is given an unexplained echo mean of 1 dB, while the subsequent images remain in echo means similar to the values before the background subtraction was applied (Figure 5.1). We were unable to make sense of this and Philips was unable to explain to us how their QLAB program calculated the background subtraction for the sequence or to provide us with a solution for this problem. For this reason, we simply used QLAB to define the images for analysis,

create regions of interest and check images for movement. The data was then exported from QLAB for manual completion of the analysis.

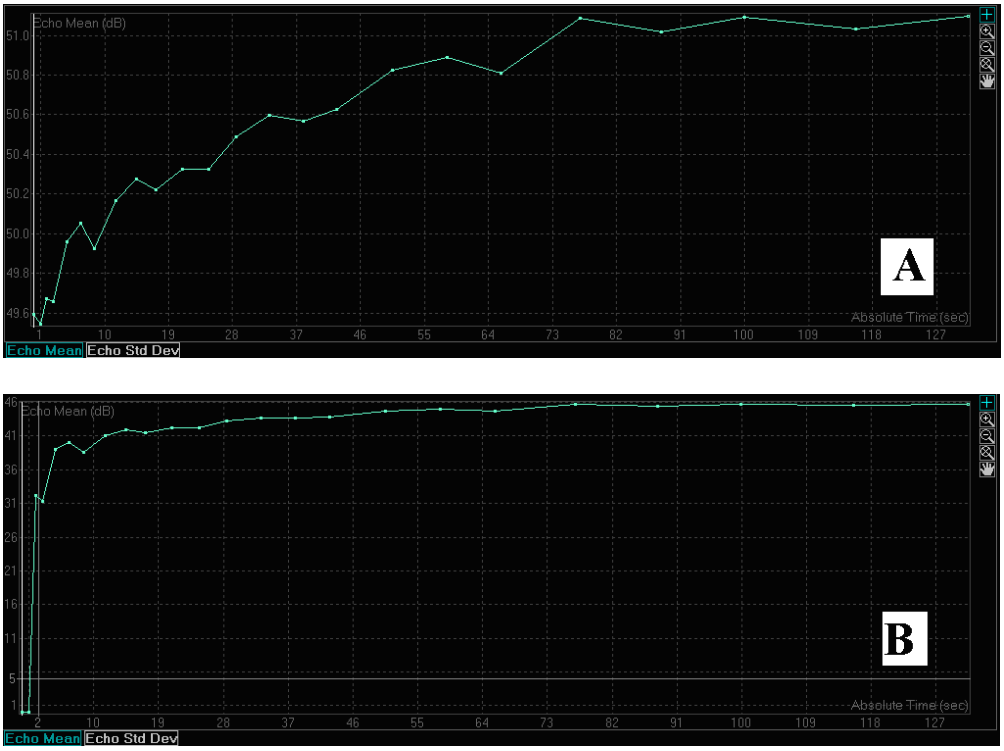

Figure 5.1 Background subtraction using QLAB. Depicting the data before (A) and after (B) background subtraction of first image in sequence. Graph presented in absolute time for easier visualization.

5.3.5 In house analysis procedure

Exporting data form QLAB to Microsoft Excel

In QLAB, brackets were used to define the start and end of the sequence, any erroneous slides (movement or other artifacts) were eliminated, the sequence was selected to be graphed in relative time on the x-axis and, without any background subtraction or fitting to a curve, the data was exported by saving it as a Microsoft Excel file. In Excel the data was converted from decibels to acoustic intensity (AI)

and the average of three images taken at the end of the first pulse interval was used as the background value, and was thus subtracted from the rest of the data. The data was converted from dB to AI because the latter has a linear relationship with increasing blood volume thus any increase in blood volume is reflected by an equally proportional increase in AI, where as this relationship is not simple and linear with dB.

Curve fitting

Once having been converted to AI and undergone background subtraction, the data were inserted into SigmaPlot where the following exponential function was applied to the curve: **f=a*(1-exp(-b*(x-1)))**, where **f** is the videointensity, **a** is plateau videointensity representing MBV, **b** is rate constant reflecting the rate of rise of videointensity representing MFV, and **x** is the pulsing interval. This resulted in the generation of MBV and MFV values.

Creating an optimal region of interest

As previous studies in rats and man did not explain how to select the region of interest (ROI) we performed a series of analyses to define the ROI that gave the most reproducible result. Originally we created detailed ROIs of the contour of the muscle on the ultrasound image in line with practice at the University of Virginia (Figure 5.2). However, a small change in the ROI gave a rather large change in the measured MBV and MFV (Table 5.1). This was thought to possibly be due to variation in the presence of larger vessels in close proximity to the muscle, and we therefore rejected this method.

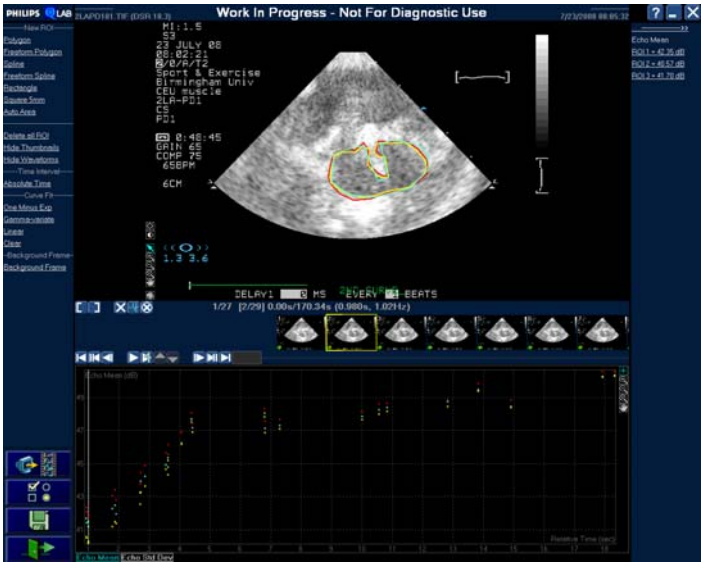

Figure 5.2 Three slightly different contours ROIs. The sequences are plotted below to show increasing videointensity created by the microspheres over relative time.

Table 5.1 Microvascular blood volume and flow velocity values for contours ROIs

	MBV (AI)	**% difference from ROI 1**	**MFV** (1/sec)	**% difference from ROI 1**
ROI 1	121790.6	/	0.074277	/
ROI 2	133099.0	9.29	0.060595	18.42
ROI 3	128755.9	5.72	0.062154	16.32

Data presented in acoustic intensity (AI) obtained from SigmaPlot after analysis with QLAB and Excel as described in section 5.5 for the three variations in contours ROI. The percentage difference from ROI 1 is presented for both MBV and MFV values.

In the subsequent analysis we created ROIs that had a more general shape, were slightly smaller than the muscle on the image, and would fit within the contour. In this way we expected to exclude a variable contribution of larger vessels surrounding the contours of the muscle. I refer to these as 'medium' ROIs and these are shown in Figure 5.3. The variations in the MBV and MFV of these medium ROIs were also large. In addition, a substantial proportion of the medium size ROIs did not give an

acceptable exponential curve fit in Sigmaplot and thus no MBV and MFV values could be attained.

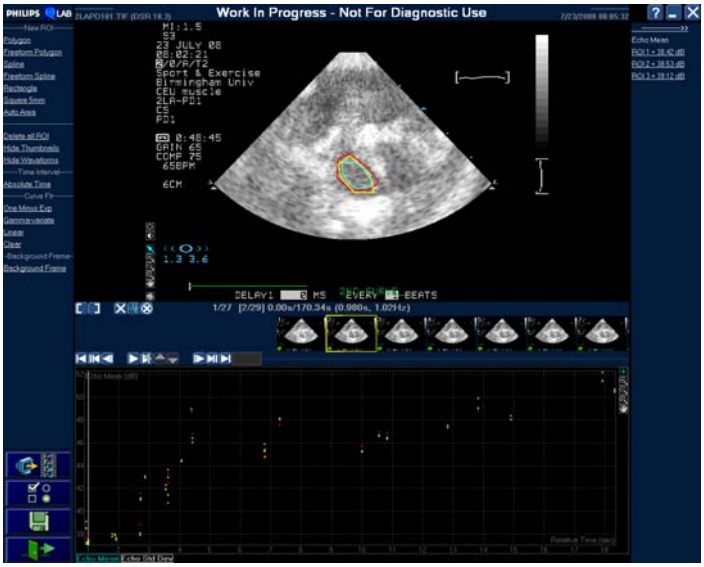

Figure 5.3 Medium ROIs, all of which did not converge in SigmaPlot and thus no A and B values could be attained. The sequences are plotted below to show increasing videointensity created by the microspheres over relative time.

We thus attempted to use very small ROIs, as routinely done in cardiac CEU. These were created to fit clearly within a central aspect of the muscle which showed little or no artifact influence, as discerned by continuously running through the sequence of images to ensure the ROI was placed as accurately as possible in such a desired position (Figure 5.4). However, once again, there were problems with the curve fitting in SigmaPlot so only MBV and MFV values for ROI 3 were obtained. Therefore the use of 'small' ROIs was also rejected.

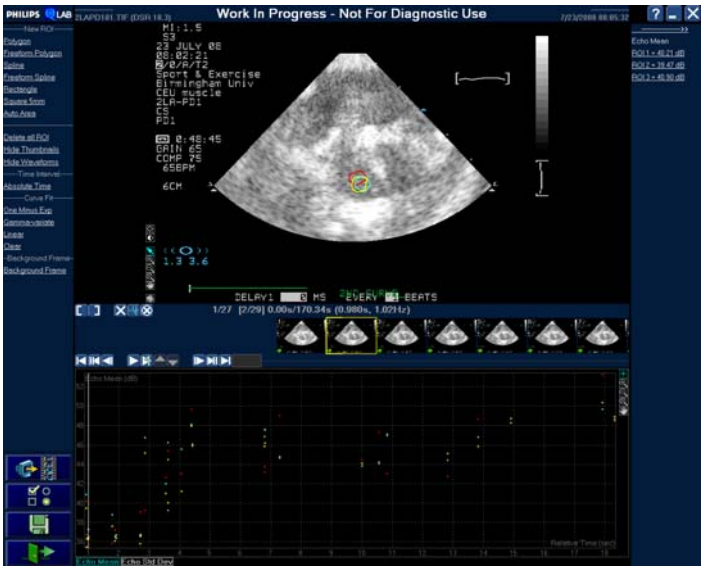

Figure 5.4 Small ROIs. Only one of the 3 small ROIs gave data that could be converged by SigmaPlot to give MBV and MFV values. These were distinctly different from those given by the full and contour ROIs. The sequences are plotted below to show increasing videointensity created by the microspheres over relative time.

Furthermore, it can be seen in the plotted graph for the three small ROIs (Figure 5.3), that there is much more variation in the videointensity over time than with the contours and medium ROIs. This is likely explained by the larger ROIs being able to 'average out' regional variations in videointensity (potentially the consequence of smaller variation in larger vessel contribution or other echogenic structures), and provide a more homogenous, and therefore reproducible and accurate, representation of the muscle microvascular blood volume.

We next attempted the use of an entire image ROI, which will be referred to as 'full ROI'. Full ROIs are used by the laboratory of Dr. Stephen Rattigan in rat muscle CEU (Figure 5.5). Although this would also include non-muscle tissue surrounding the muscle, the background subtraction done to eliminate the contribution of large

vessels, according to Dr. Rattigan, would also eliminate the contribution of non-muscle tissues as their perfusion would not be changing. In order to confirm this, ROIs were created in the tissue outside and surrounding skeletal muscle in the video image. The resultant QLAB analysis indicated that there was no replenishment of the microsphere videointensity in the surrounding tissues after high-energy pulse destruction.

SigmaPlot analysis produced MBV and MFV values for the three full ROIs, and the variability in these values between the three full ROIs was smaller as compared to the contours, medium and small ROIs (Table 5.2). Furthermore, in the plotted graph for the three full ROIs (Figure 5.5), there is clearly less variation in the videointensity over time as compared to the small and medium ROIs, and even the contours ROIs. For this reason, and because the full ROIs are much easier to create, we chose to use the full image ROI.

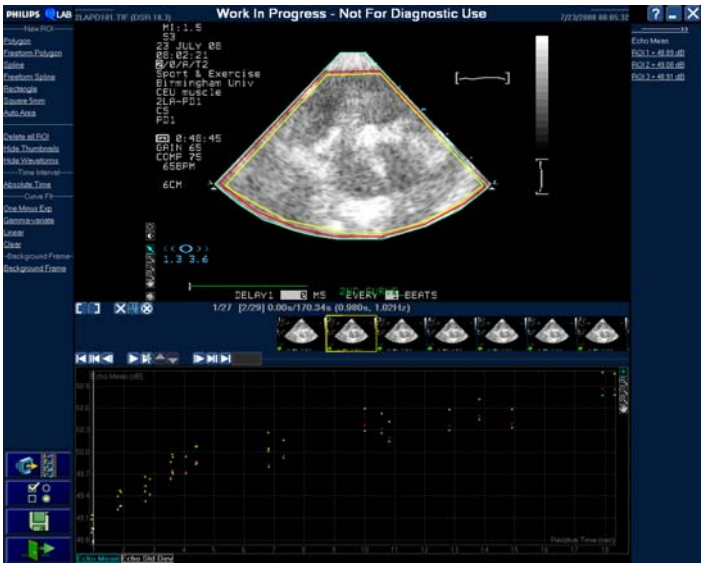

Figure 5.5 Three slightly different full image ROIs, plotted below to show increasing microsphere intensity over relative time.

Table 5.2 Microvascular blood volume and flow velocity values for full ROIs

	MBV (AI)	**% difference from ROI 1**	**MFV** (1/sec)	**% difference from ROI 1**
ROI 1	41864.78	/	0.157826	/
ROI 2	44601.81	6.54	0.158246	0.27
ROI 3	39207.20	6.35	0.162030	2.66

Data presented in acoustic intensity (AI) obtained via SigmaPlot after analysis with QLAB and Excel as described in section 5.5 for the three variations in full ROI. The percentage difference from ROI 1 is presented for both MBV and MFV values.

5.3.6 Conclusions on CEU with Luminity and multiple microsphere destruction protocol

The alterations made in the analysis procedure as described above gave us confidence in our ability to accurately and consistently analyse CEU data in single sequences using the multiple microsphere destruction protocol. However, when we used this procedure for repeated measurements before and during oral glucose tolerance tests (see Chapter 6) it became clear that there were other sources of variation in physiological experiments lasting longer than 1 hour and consisting of several CEU measurement time points.

One source of variation came from the removal and replacement of the ultrasound probe on the participant's arm between CEU measurements within the experimental protocol. This likely disrupted the acquisition of consistent and comparable CEU data because, although the probe was being placed as accurately as possible on the same place over the forearm flexor muscles, it was difficult to be very accurate with the flexible arm which held the probe and we had no means to control the angle at which the probe was placed at each measurement time point. A change in probe angle meant

a different section of the muscle was imaged and thus comparisons between CEU data with slightly different muscle sections were not very meaningful.

A second source of variation was that many subjects were not able to prevent arm movement, or muscle contraction and movement, during the ± 5 min acquisition time for the multiple microsphere destruction protocol. The arm movements which occurred during testing resulted in several imaging sequences having to be discarded in the analysis process when movement of the muscle within the image was identified and/or led to poor curve fits, thereby resulting in incomplete data.

For these reasons we decided to further optimize the positioning and stability of the arm and the positioning and stability of the probe, while reducing the acquisition time of one sequence by using a single microsphere destruction protocol.

5.4 Protocol 2: CEU with SonoVue and single microsphere destruction protocol

5.4.1 Preparation procedures

Brand of microsphere

As Luminity microspheres were withdrawn from the European market in August 2008 and legal restrictions prevented us from purchasing them in the USA, where production continued, we were forced to switch to SonoVue®. It is heavily used in cardiac CEU imaging and gave promising results in a few pilot studies in the human forearm (data not shown). The characteristics of SonoVue microspheres are shown in Table 5.3.

Table 5.3 Comparison of the characteristics of commercially available microspheres.

	Luminity® perflutren	**SonoVue**® sulphur hexafluoride
Supply company	Bristol Myers Squibb	Bracco
Storage requirements	Before activation: refrigerator (2-8°C) After activation: do not store above 30°C	Does not require any special storage conditions
Contents of microsphere kits	1.5 ml vial of Luminity® perflutren	1 vial containing 25 mg lyophilised powder in an atmosphere of sulphur hexafluoride, 1 pre-filled syringe of 5 ml sodium chloride (0.9 %), 1 Mini-Spike transfer system
Activation method	Vigorous shaking via shaking device VIALMIX®	Mix powder and solvent by hand shaking
Concentration of microsphere gas per ml	1ml of Luminity contains approximately 150 μL of perflutren gas	1ml contains 8 μL of sulphur hexafluoride gas
Mean diameter range of microspheres	1.1-2.5 μm	2.5 μm
Active shelf-life	12 hours; but it can be re-activated up to 48 hours after initial activation and used up to 12 hours after the second activation	Sonovue should be used within 6 hours of preparation; If sonovue is not used immediately after reconstitution, the dispersion needs to be shaken again before being drawn up into a syringe
Stability in suspension	Increased stability of microspheres due to high molecular weight of perflutren gas thus stable in suspension for 12 hours	Chemical and physical stability has been shown for up to 6 hours
Infusion concentration safety limit	1 vial (1.6 ml) per person per study	4 vials per person per study
Recommended dilution	1 vial in 50 ml isotonic saline	When mixed each vial results in 5 ml solution which requires no further dilution
Recommended infusion rate for skeletal muscle use	1.6 ml/min or 96 ml/h	1ml /min
Support for use	Mechanical shaking device VIALMIX® for microsphere activation; no support for maintaining suspension once activated - infusion pump is rotated manually	All microspheres supplied with activation kit and infusion kit (Vueject kit); mixing infusion device (Vueject pump) is available for maintaining bubbles in suspension once activated

All information obtained directly from the respective supply companies.

Ultrasound imaging protocol

After consultation with Dr. Stephen Rattigan we set up an alternative imaging protocol measuring replenishment after a single microsphere destruction. This protocol has been repeatedly used in his laboratory in experiments in rats. In this protocol we record replenishment as a continuous sequence of images taken at every

heartbeat for 20 beats after the destruction pulse. A low ultrasound intensity (mechanical index) was used to capture the images so as not to destroy the microspheres during replenishment. This protocol took approximately 20 seconds to complete and we ran 8 of these sequences at a frequency of 1 sequence per 40 sec for each measurement time. The average MBV and MFV of the 8 sequences was used to obtain an accurate value of MBV and MFV at each time point. The key benefit of using this protocol was the short duration, which reduced the risk of participant movement during imaging and also allowed repeated measurements for each time point to strengthen the reliability of data comparisons made between time points.

5.4.2 Experiment protocol in human volunteers

In the testing procedures, there are three differences compared to protocol 1. These differences lie in the positioning of the arm and the probe, the infusion protocol of the microspheres, and the data acquisition sequence and mode of analysis.

Stable and reproducible positioning of arm and probe

During the first series of tests with Luminity we discovered that it is of vital importance to avoid movement of the arm and contractions of the skeletal muscles when acquiring the ultrasound imaging sequence, as movement will reduce the quality and reliability of the data.

To ensure a stable position of the probe under a fixed angle we created a holder for the ultrasound probe. The holder consists of two detachable parts: one part contains a mold in which the probe fits securely, and this fits precisely into the second part which is fixed to the arm (Figure 5.6). This second part of the holder is fixed in place

by double sided medical tape to help avoid movement during testing. This allowed us to detach the probe between ultrasound measurements if necessary, while being able to accurately reposition the probe in both placement and angle for subsequent measures within the same testing visit. In this way, we were able to measure the same tissue section over the different measurements, allowing for comparisons of MBV and MFV between time points. To our knowledge, such a holder to improve probe position reproducibility between measurements has not been used in any of the previous studies using CEU in man (Vincent et al. 2006[1], Clerk et al. 2006[2], Keske et al. 2009[3]; Liu et al. 2009[4]).

To ensure a comfortable and relatively immobile positioning of the patient's arm, with ideal exposure of the measurement area, we used a vacuum support cushion (RBF products limited, Essex, UK). When the vacuum is created by use of a foot pump, the cushion will form a cast of the participant's arm, thereby supporting their arm in this comfortable position and limiting the potential for arm movement.

Figure 5.6 Stable measurement set up with vacuum support cushion and ultrasound probe holder

Administration of microspheres

The administration of SonoVue microspheres involves several steps, namely, activation and transfer to a single syringe, set up of syringe in mechanical mixing infusion pump, infusion rate selection, and timing of acquisition commencement.

SonoVue comes in powder form and is activated by mixing with 5 ml of 0.9 % saline solution. The vial containing the lyophilized powder, the pre-filled syringe containing the saline, and the Mini Spike transfer system to connect the vial to the syringe, are all provided in each SonoVue microsphere kit. The saline is emptied from the syringe into the vial via the transfer system and to activate the microspheres the vial is shaken vigorously by hand for 20 sec until a white milky liquid is seen. In line with the supplier recommendation we used 4 vials per person per testing visit. This implies that the content of 4 activated vials was transferred via the Mini Spike system to a single 20 ml syringe also provided in the infusion kit (Vueject kit). The Vueject kit also contained an infusion line and cannula, both of which should be used as other cannuli and infusion lines may bind or damage the microspheres during infusion. In our hands, the use of standard lines and cannulae substantially reduced the echo signal and did not lead to replenishment curves with a good exponential fit (data not shown). The activated microspheres in the 20 ml syringe were kept in suspension by use of a mechanical mixing infusion pump (Vueject pump, Bracco, UK).

In order to achieve a steady state of microspheres in the circulation before commencement of acquisition, we found that a priming of 2 ml/min for 1 min followed by 1 ml/min for another 1 min was sufficient in creating a steady state. The

principle of a priming dose is that the sum of the decline in microsphere enrichment from the priming dose and the rise in microspheres from the continuous infusion will equal the eventual plateau microsphere enrichment (Wolfe and Chinkes 2004[5]). In this way, after 2 min of infusion, steady state was achieved and acquisition could begin. The infusion rate during acquisition was then maintained at 1 ml/min as this was found to be sufficient to produce optimal ultrasound images during the single microsphere destruction protocol.

Data acquisition protocol

Once the 2 min infusion was complete 'acquire' was selected on the ultrasound machine, the timer was started, and immediately 'impulse' was selected in the 'tools' menu. A flash appeared with the high-energy ultrasound pulse and 20 heart beats from the impulse were counted before 'acquire' was selected again to stop acquisition and save the data. This sequence took approximately 20 sec, depending on the participant's heart rate. When the timer approached 40 sec 'acquire' was selected and at 40 sec 'impulse' was selected. Once again, 20 heart beats were counted before stopping the acquisition as described above. A total of 8 sequences were collected at 40 sec intervals for the time point before the infusion was stopped.

5.4.3 Detailed analysis procedure

The analysis of the ultrasound data involved three basic steps: (1) the conversion of the microsphere intensity on the image sequences to numerical data via QLAB, (2) the background subtraction to provide data reflecting microvascular perfusion in Microsoft Excel, and (3) fitting the data to an exponential curve to obtain MBV and MFV in SigmaPlot.

5.4.3.1 QLAB

We used the Philips QLAB version 5.0 for the initial step in the analysis of our CEU data. This initial step required several procedures, as discussed below.

Importing images on to QLAB

The ultrasound sequences were transferred from the ultrasound disk to the computer and the first sequence to be analysed was opened via the QLAB program.

Selecting the optimal region of interest

As explained in section 5.3.5, the full image ROI was found to be ideal, and was thus applied to the analysis here.

Using same ROI for all subsequent measurements

In order to make accurate comparisons between sequences it is best to use the exact same full image ROI for all sequences. This was done via a standard 'copy and paste' procedure of the desired ROI into other sequences. First, an ROI (shape did not matter) was inserted in all the sequences that required copying of the desired ROI into. In the standard procedure the 'square 5mm' ROI was selected for this purpose and placed at random in each of the relevant sequences. The 'square 5 mm' ROI was used for two reasons: firstly, since it could be selected in one click and secondly, because this ROI was much smaller than the full image ROI and could, therefore, be easily recognised as the initial ROI used for copying purposes only.

Once the desired ROI was created in the first sequence, and the square 5 mm ROIs were placed in all the other sequences that needed to be analysed, the subsequent steps were followed to copy and paste the desired ROI into the other sequences.

1. 'My Computer' => 'C drive (C:\)' => 'program files' => 'Philips' => 'QLAB' => 'persistent data'. In 'persistent data' the folder with the folders of the sequences for analysis was identified and opened.

2. Inside, the folders of all the sequences which have ROIs drawn were found. The sequence with the desired full ROI to be copied was identified.

3. The folder of that sequence was opened and by right clicking over the 'parameters.xml' file a little menu appeared in which 'copy' was selected.

4. Selecting the 'back' button we then opened the next sequence folder and, by right clicking within it, selected to 'paste'. The computer asked if we wanted to replace the existing 'parameters.xml' file and provided the sizes of the files for comparison. Indeed we wanted to replace the little 'parameters.xml' (for the square 5mm ROI) with the larger one which was our desired full image ROI. We clicked 'yes' and moved on to paste it in the next sequence.

5. When the desired ROI was pasted in the folders of all the sequences needing to be analysed, we returned to QLAB. Each sequence in which the desired ROI was pasted needed to be opened and the new ROI activated by *left* clicking slowly twice on the ROI, being careful not to move it or alter its shape. This caused QLAB to reset its calculations using the pasted ROI instead of the square 5 mm ROI with which it had previously run its calculations. *Right* clicking twice resulted in a flash on the screen as though it was resetting itself with the new calculations for the new ROI but it was

not! To activate the new ROI, we had to *left* click slowly twice, being careful not to move the ROI.

Checking sequence images

Once the ROI was in place, each sequence was checked image by image for any movement or artifact within the sequence. In the rare occurrence that affected slides were found and these greatly altered the final A and B values, the slide could be discarded if occurring near the end of the sequence or the entire sequence could be discarded and the average A and B values for that time point obtained from 7 as opposed to 8 sequences.

Exporting the echomean of each sequence from QLAB to Microsoft Excel

We simply used the brackets to define the true start and end of the sequence, eliminated any erroneous slides if applicable, ensured the sequence was graphed in relative time for multiple destruction protocol and absolute time for single destruction protocol on the x-axis and, without any background subtraction or fitting to a curve, exported the data by saving it as a Microsoft Excel file.

5.4.3.2 Analysing the Excel file

Upon opening of the Excel file, the data for the ROI was presented in three columns, namely (i) Absolute Time (sec), (ii) Echomean (dB), and (iii) Echomean Std Dev (dB). The first two columns were copied and pasted into a separate Excel sheet and in this new sheet the steps detailed below were carried out. Figure 5.7 shows the final layout of the Excel sheet in a format that can be used for SigmaPlot analysis.

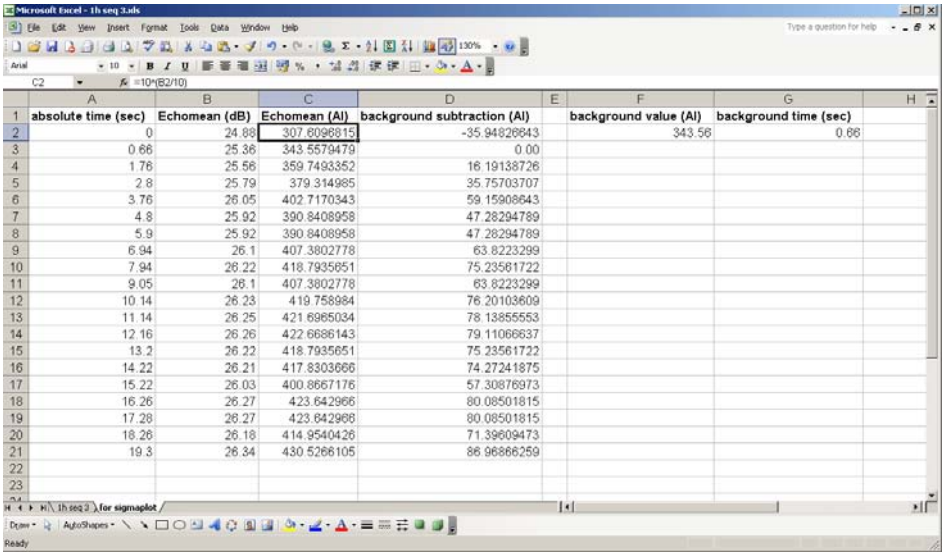

	A	B	C	D	E	F	G	H
1	absolute time (sec)	Echomean (dB)	Echomean (AI)	background subtraction (AI)		background value (AI)	background time (sec)	
2	0	24.88	307.6096815	-35.94826843		343.56	0.66	
3	0.66	25.36	343.5579479	0.00				
4	1.76	25.56	359.7493352	16.19138726				
5	2.8	25.79	379.314985	35.75703707				
6	3.76	26.05	402.7170343	59.15908643				
7	4.8	25.92	390.8408958	47.28294789				
8	5.9	25.92	390.8408958	47.28294789				
9	6.94	26.1	407.3802778	63.8223299				
10	7.94	26.22	418.7935651	75.23561722				
11	9.05	26.1	407.3802778	63.8223299				
12	10.14	26.23	419.758984	76.20103609				
13	11.14	26.25	421.6965034	78.13855553				
14	12.16	26.26	422.6686143	79.11066637				
15	13.2	26.22	418.7935651	75.23561722				
16	14.22	26.21	417.8303666	74.27241875				
17	15.22	26.03	400.8667176	57.30876973				
18	16.26	26.27	423.642966	80.08501815				
19	17.28	26.27	423.642966	80.08501815				
20	18.26	26.18	414.9540426	71.39609473				
21	19.3	26.34	430.5266105	86.96866259				
22								
23								

Figure 5.7 Microsoft Excel sheet final layout of data ready for SigmaPlot analysis. Data shown for single destruction protocol.

Converting the echomean units from decibels to acoustic intensity

As QLAB 5.0 only provided the videointensity values of the data in decibels (dB), which has a non-linear relation to MBV, the data needed to be converted to acoustic intensity (AI) as this has a linear relationship which means increasing MBV values are linearly represented by increasing AI values, thereby allowing for relative analysis. To convert the videointensity from dB to AI, a new column (column C) was created adjacent to that of echomean in dB (column B) and the function [=10^(B2/10)] was applied, with 'B2' being the cell which has the echomean in dB for that time point. Then the 'C2' cell which contained the dB to AI conversion function and all the empty cells beneath it were selected. The commands 'edit' => 'fill' => 'down' were used to automatically apply the function to the rest of the time points and the result was a column of echomean in AI (column C).

Background subtraction

The background value was selected as the echomean in AI for the image taken closest to 1 sec after microsphere destruction. In the example shown in Figure 5.7, the image taken at 0.66 sec was selected as the background image. Two new columns were created (column F and G) to display the background value and time selected for that sequence particular sequence. Column D was created for the values in which the background value was subtracted from the AI data in column C. The absolute time and echomean in AI with background subtraction (column A and D starting from and including row 3) were used in SigmaPlot to fit an exponential curve to the data for the calculation of MBV and MFV, as described below.

5.4.3.3 SigmaPlot

Importing data into SigmaPlot

To import data into SigmaPlot columns A and D (starting from and including row 3) were copied from the Excel spreadsheet and pasted into the SigmaPlot spreadsheet as columns 1 and 2.

Fitting a curve to the data

Before proceeding to fit the curve, the cells which contain the relevant data were selected. This was done quickly by clicking on the little box icon as shown circled in Figure 5.8. Alternatively this was achieved by clicking on 'edit' => 'select all'. If this was not done, the data was not graphed correctly, though the numeric results were the same. The steps below were subsequently carried out:

1. 'Statistics' => 'regression wizard' => 'exponential rise to max'
2. In the equation category 'single, 2 parameter' equation name was selected

3. To incorporate the background subtraction, the equation was modified by clicking the ‘edit code’ tab and then the ‘add as…’ tab and providing the new equation name (“background subtraction”) in the box that appeared. The equation was then adjusted by adding the subtraction of the background time in sec from ‘x’. In our example, the background image was taken at time 0.66 sec, thus the equation was adjusted from f=a*(1-exp(-b*x)) to f=a*(1-exp(-b*(x-0.66))). We then clicked ‘ok’ to save the equation. In the future this equation appeared under the ‘user-defined’ equation category and had to be modified in this way for every individual sequence by incorporating the precise background value time for that sequence.

4. Once the sequence was modified, the ‘next’ commands were used to continue through the steps of the regression wizard during which the columns for the data and the outputs were selected. The ‘first empty’ columns for the outputs were always selected.

Sigmaplot output

In the ‘parameters’ column of the data page, the first value given was the A value or MBV, and the second value was the B value or MFV. Both were calculated from the data after curve fitting (Figure 5.8). The graph produced by SigmaPlot displaying the curve fit of the data to the exponential rise to max equation is shown in Figure 5.9.

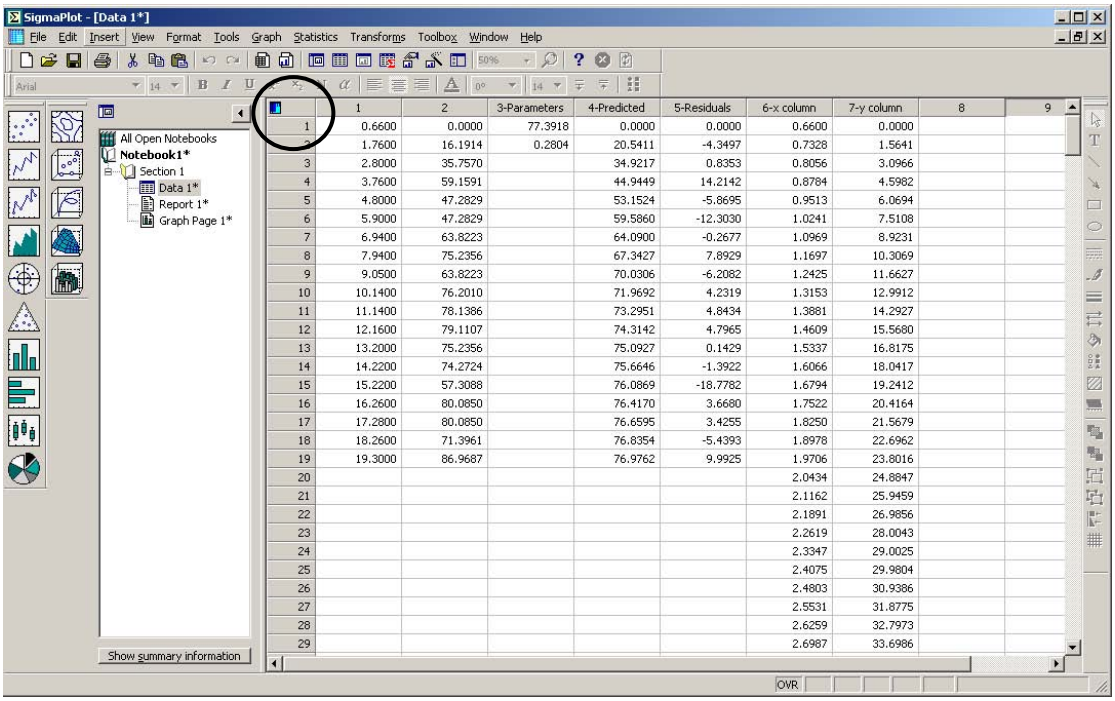

	1	2	3-Parameters	4-Predicted	5-Residuals	6-x column	7-y column	8	9
1	0.6600	0.0000	77.3918	0.0000	0.0000	0.6600	0.0000		
2	1.7600	16.1914	0.2804	20.5411	-4.3497	0.7328	1.5641		
3	2.8000	35.7570		34.9217	0.8353	0.8056	3.0966		
4	3.7600	59.1591		44.9449	14.2142	0.8784	4.5982		
5	4.8000	47.2829		53.1524	-5.8695	0.9513	6.0694		
6	5.9000	47.2829		59.5860	-12.3030	1.0241	7.5108		
7	6.9400	63.8223		64.0900	-0.2677	1.0969	8.9231		
8	7.9400	75.2356		67.3427	7.8929	1.1697	10.3069		
9	9.0500	63.8223		70.0306	-6.2082	1.2425	11.6627		
10	10.1400	76.2010		71.9692	4.2319	1.3153	12.9912		
11	11.1400	78.1386		73.2951	4.8434	1.3881	14.2927		
12	12.1600	79.1107		74.3142	4.7965	1.4609	15.5680		
13	13.2000	75.2356		75.0927	0.1429	1.5337	16.8175		
14	14.2200	74.2724		75.6646	-1.3922	1.6066	18.0417		
15	15.2200	57.3088		76.0869	-18.7782	1.6794	19.2412		
16	16.2600	80.0850		76.4170	3.6680	1.7522	20.4164		
17	17.2800	80.0850		76.6595	3.4255	1.8250	21.5679		
18	18.2600	71.3961		76.8354	-5.4393	1.8978	22.6962		
19	19.3000	86.9687		76.9762	9.9925	1.9706	23.8016		
20						2.0434	24.8847		
21						2.1162	25.9459		
22						2.1891	26.9856		
23						2.2619	28.0043		
24						2.3347	29.0025		
25						2.4075	29.9804		
26						2.4803	30.9386		
27						2.5531	31.8775		
28						2.6259	32.7973		
29						2.6987	33.6986		

Figure 5.8 SigmaPlot output spreadsheet.

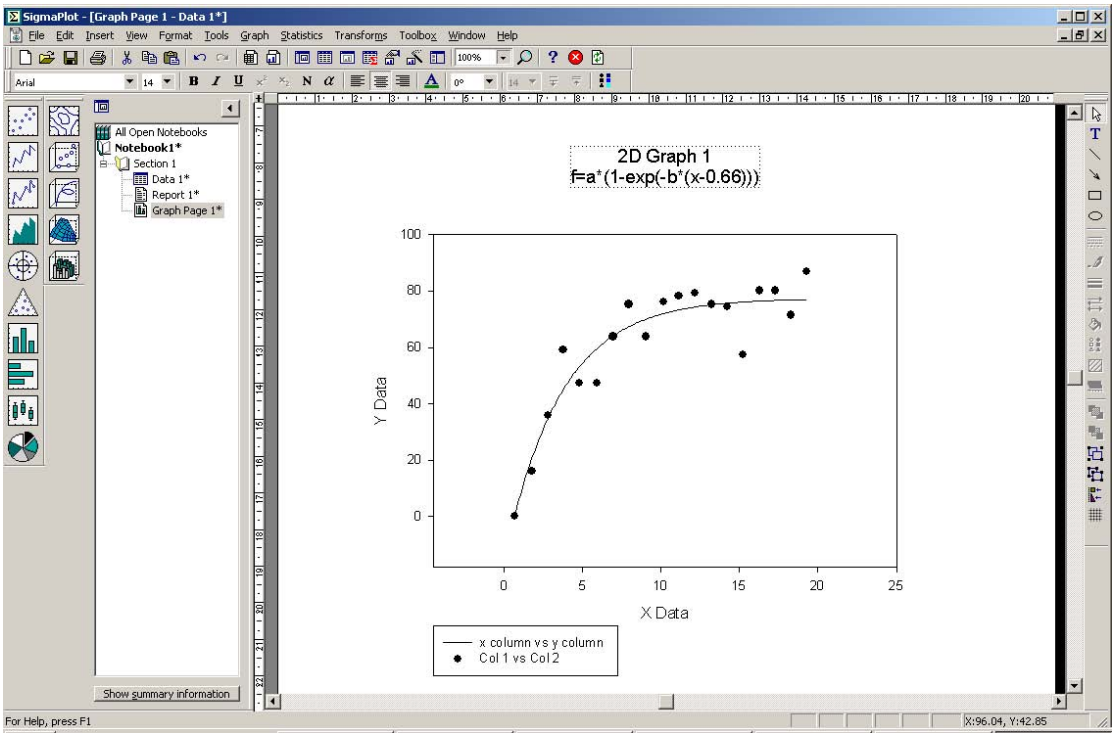

Figure 5.9 Graph produced by SigmaPlot representing the curve fit of the data for the equation f=a*(1-exp(-b*(x-0.66))).

5.4.3.4 Conclusions on CEU with SonoVue and single microsphere destruction protocol

Two key alterations were made to the testing procedure, namely the stable measurement set up with the probe holder and vacuum cushion and the single destruction protocol. These alterations greatly reduced the chances of arm and muscle movement and increased the accuracy of probe placement and angle between time points if the probe was temporarily removed. This allowed for the collection of MBV and MFV data which was comparable between time points.

Furthermore, the use of the single destruction protocol reduced the chance of arm and muscle movement during sequence acquisition due to its short duration. This also permitted the collection of 6-8 sequences per measurement time point. By collecting several sequences per time point, outliers potentially caused by involuntary movement could be discarded and the data for the particular time point simply averaged from less sequences. This is a major difference with the multiple microsphere destruction protocol in which movement often meant that the data at that particular time point were lost. By using the average of multiple sequences, a more accurate value of MBV and MFV for a given time point was obtained, thus increasing the reliability of the statistical comparison between time points. For MBV, the intra-individual coefficient of variation (CV) of our first subject at baseline and 1 h post glucose ingestion was 17.8 % and 23.7 %, respectively, and this assured us the method was effective and promoted us to continue with other subjects.

These alterations made to the testing procedure, namely the single destruction protocol and the stable measurement set up, provided us with reproducible and

meaningful data during pilot testing. This gave us confidence in our ability to measure a change in MBV over repeated time intervals. We thus used this method to measure MBV in response to an OGTT in lean trained healthy individuals, as detailed in Chapter 6.

5.5 REFERENCE LIST

1. Vincent MA, Clerk LH, Lindner JR, Price WJ, Jahn LA, Leong-Poi H, Barrett EJ. Mixed meal and light exercise each recruit muscle capillaries in healthy humans. Am J Physiol Endocrinol Metab 2006;290:E1191-E1197.

2. Clerk LH, Vincent MA, Jahn LA, Liu Z, Lindner JR, Barrett EJ. Obesity blunts insulin-mediated microvascular recruitment in human forearm muscle. Diabetes 2006;55:1436-1442.

3. Keske MA, Clerk LH, Price WJ, Jahn LA, Barrett EJ. Obesity Blunts Microvascular Recruitment in Human Forearm Muscle Following a Mixed Meal. Diabetes Care 2009.

4. Liu Z, Liu J, Jahn LA, Fowler DE, Barrett E. Infusing lipid raises plasma FFA and induces insulin resistance in muscle microvasculature. x ed. 2009:x.

5. Wolfe RR, Chinkes DL. Calculations of substrate kinetics: single-pool model. Isotope tracers in metabolic research: Principles and practice of kinetics analysis. 2 ed. Hoboken, New Jersey: Wiley Blackwell, 2004:21-50.

Chapter 6

MICROVASCULAR BLOOD VOLUME INCREASES IN RESPONSE TO AN OGTT IN FOREARM SKELETAL MUSCLE OF LEAN TRAINED HUMANS

6.1 INTRODUCTION

The world is facing an obesity epidemic accompanied by a dramatic increase in obesity-related pathologies (World Health Organisation 2006[1]). Particularly striking is the increase in type II diabetes and cardiovascular disease (CVD; World Health Organisation 2006[2]; Gonzalez and Selwyn 2003[3]). An important contributor to the pathogenesis of obesity is impaired glycemic control after meal ingestion. Skeletal muscle is the largest site for glucose disposal (Ferrannini et al. 1985[4]; Defronzo et al. 1985[5]; Nuutila et al. 1994[6]) and the meal-induced increase in circulating insulin promotes glucose clearance by (i) activating signalling pathways in the vascular endothelium which induce vasodilation and microvascular perfusion under normal conditions (Liu et al. 2009[7]), and (ii) activating insulin signalling in skeletal muscle leading to GLUT4 translocation from the microsomal stores to the plasma membrane (Chang et al. 2004[8]; Thong et al. 2005[9]; Wojtaszewski and Richter 2006[10]). The obese population, however, show impaired vasodilation and skeletal muscle perfusion in response to insulin infusion (Clerk et al. 2006[11]; de jongh et al. 2004[12]) and to meal-induced increases in insulin (Keske et al. 2009[13]). Consequently, glucose and insulin delivery to the muscle and subsequent glucose uptake is impaired, resulting in prolonged glucose excursions after meal ingestion (Krentz et al. 2009[14]). Elevated glucose levels exacerbate the endothelial dysfunction (Brownlee 2005[15]), and over time chronic hyperglycemia will develop. These sustained elevations in plasma glucose play a significant role in promoting vascular dysfunction and further devastate glycemic control (Krentz et al. 2009[14]).

It is therefore important to develop interventions for improving the vascular response to insulin after meal ingestion in individuals with non-complicated obesity so as to halt the developing vascular dysfunction, restore glycemic control, and avoid the progression to type II diabetes and CVD (Krentz et al. 2009[14]). A principal outcome measure of such interventions would be a greater increase in skeletal muscle microvascular blood volume (MBV) in response to physiological (nutrient-stimulated) increases in insulin. A larger MBV by definition leads to an increased capillary permeability surface area product and a faster rate of glucose uptake by skeletal muscle (Gudbjornsdottir et al. 2003[16]). In addition, improved endothelial function as a result of successful intervention may lead to increases in microvascular flow velocity (MFV) and microvascular blood flow (MBF), the product of MBV and MFV. In order to be able to evaluate the effect of obesity and the effectiveness of interventions in future studies, in the present study we aim to test the reliability of the CEU method developed in chapter 5 to measure skeletal muscle MBV and MFV responses during an oral glucose tolerance test (OGTT) in healthy lean trained individuals.

Contrast enhanced ultrasound (CEU) is emerging as the preferred method for the measurement of human skeletal muscle MBV and MFV (Vincent et al. 2006[17]; Clerk et al. 2006[11]; Porter 2009[18]; Womack et al. 2009[19]; Keske et al. 2009[13]). CEU involves the infusion of microspheres (contrast agent the size of red blood cells) which can be visualised by ultrasound in the tissue of interest. The videointensity of the image obtained is proportional to the concentration of microspheres within the volume of tissue being imaged. A single pulse of high-energy ultrasound is administered to

simultaneously destroy all the microspheres within the ultrasound beam. Subsequently, the rate of microsphere replenishment is measured and will reflect MFV while the plateau level of microspheres reached after destruction will reflect MBV. As the larger vessels will fill more quickly, a background subtraction of the average videointensity generated within 1 second after the high-energy pulse is applied. This will eliminate the larger vessels from the analysis. Although it is not exactly known which size vessels are included in this analysis, it is generally assumed that they are terminal arterioles, capillaries (major contribution), and first and second degree venules. In this way, the CEU technique is able to provide measures of MBV and MFV, and the product of these variables: MBF.

In the present study, we used CEU to measure MBV and MFV in 10 lean, healthy participants before and 1 h into an oral glucose tolerance test (OGTT). An OGTT was used as it induces a greater insulin response than a mixed meal (Vincent et al. 2006[17]; Keske et al. 2009[13]) and is simple and less invasive than a hyperinsulinaemic euglycemic clamp. Therefore, an OGTT is more practical for the repeated measurement of MBV responses to insulin when evaluating the effectiveness of interventions aimed at improving this response in obese individuals.

The primary aim of the study was to obtain an accurate estimate of baseline MBV and to assess the effectiveness of the CEU technique in measuring an increase in MBV in response to an OGTT in lean, healthy, trained individuals. The assumed underlying mechanism is that the increased plasma insulin levels in response to an OGTT would

induce vasodilation of the terminal arterioles, subsequently increasing MBV (Barrett et al. 2009[20]). This would increase the capillary permeability surface area product and therefore allow for insulin stimulated glucose clearance into the muscle fibres (Gudbjornsdottir et al. 2003[16]; Barrett et al. 2009[20]). In addition, increases in insulin during the OGTT may also lead to increases in MBV by inducing vasodilation and increasing blood flow velocity higher up the arterial tree (Barrett et al. 2009[20]; Clark et al. 2003[21]). These will be investigated by measurements of brachial artery diameter and flow using Doppler Ultrasound.

Increases in glucose and insulin concentrations during the OGTT are expected to lead to rapid increases in glucose oxidation and suppression of fat oxidation (Sidossis and Wolfe 1996[22]; Sidossis et al. 1996[23]), and therefore to a rapid switch between fat and carbohydrate (CHO) as main fuels in the transition from the early morning fasted state to the glucose fed state. Such a rapid switch has been termed 'metabolic flexibility' (Storlien et al. 2004[24]) and we hypothesise that metabolic flexibility is dependent on adequate increases in MBV. Failure to increase MBV in obese subjects during meal ingestion (Keske et al. 2009[13]) and during a hyperinsulinemic euglycemic clamp (Clerk et al. 2006[11]) reduced glucose uptake in skeletal muscle. Gudbjornsdottir et al. (2005)[25] also observed a reduced increase in capillary permeability surface area product and reduced muscle glucose uptake in obese individuals, entirely in line with the impaired metabolic flexibility observed in obese individuals (Storlien et al. 2004[24]; Corpeleijn et al. 2008[26]).

Furthermore, the elevated insulin concentration will promote diet-induced thermogenesis (DIT) in healthy lean individuals measured both at whole body level (Lowell and Bachman 2003[27]; de Jonge and Bray 1997[28]; Tappy 1996[29]) and in skeletal muscle (Petersen et al. 2005[30]). DIT has several components. In the insulin sensitive skeletal muscle, the increased activation of mitochondrial oxidation, and the increase in glycogen and protein synthesis after meal ingestion greatly contribute to DIT (Petersen et al. 2005[30]; Wagenmakers 2005[31]). Here, we hypothesise that the increase in DIT is dependent on an adequate increase in MBV and that this is the mechanism behind the lower DIT at whole body level that has previously been observed in obese individuals (de Jonge and Bray 1997[28]; Tappy 1996[29]). As previously proposed by Wagenmakers (2005)[31], failure of insulin to increase MBV might also explain the substantial reduction in the increase in muscle ATP turnover observed in the insulin resistant offspring of parents with type II diabetes in comparison to lean controls during a hyperinsulinemic euglucemic clamp (Petersen et al. 2005[30]).

In conclusion, we hypothesised that in lean trained insulin sensitive subjects the OGTT would induce an increase in plasma insulin, followed by an increase in MBV and blood flow in feeding arteries. This would be attended by a rapid transition from fat to carbohydrate as the primary fuel, and a substantial increase in DIT. Originally we planned to make a comparison between the effect of an OGTT in the lean trained group and in an obese group, but as the development of the CEU method took much more time than expected we have not been able to investigate the other leg of the hypothesis: that in obese subjects the OGTT will not increase MBV and the blood flow in feeding arteries

and that, therefore, in the obese the transition from fat to carbohydrate as the primary fuel will be delayed (metabolic inflexibility; Storlien et al. 2004[24]; Corpeleijn et al. 2008[26]) and the increase in DIT will be smaller (de Jonge and Bray 1997[28]).

6.2 MATERIALS AND METHODS

6.2.1 Subjects

Ten lean, trained, healthy male volunteers were recruited by word of mouth in the University of Birmingham. Volunteers met individually with the researcher to discuss the study, provide written informed consent, and complete preliminary measurements including a general health questionnaire, a physical activity questionnaire, measurements of height and weight, blood pressure, cardiac echocardiograph, and a blood sample for fasting glucose concentrations. Participant characteristics are displayed in Table 6.1. The research was carried out in accordance with the Declaration of Helsinki (2000) of the World Medical Association and was approved by the Birmingham East, North and Solihull Research Ethics Committee.

Table 6.1. Mean participant characteristics

Age (yrs)	28 *(± 3.2)*
Height (m)	1.78 *(± 0.04)*
Weight (kg)	76.2 *(± 6.31)*
BMI (kg/m^2)	24.1 *(± 1.4)*
Fasting glucose (mmol/L)	4.65 *(± 0.32)*

Fasting insulin (μlU/ml)	7.81 *(± 2.29)*
Blood pressure – systolic	122 *(± 7.9)*
- diastolic	69 *(± 5.2)*

Values are expressed as means ± standard deviations.

6.2.2 CEU measurements

Four vials of SonoVue microspheres (Bracco, Amsterdam, the Netherlands) were activated according to the company guidelines and their content was combined in a single 20 ml syringe. This was placed in the Vueject mixing infusion pump (Bracco, Amsterdam, the Netherlands) which maintained the microspheres in suspension by gentle rotation during the entire protocol. The participant's arm was rested on a vacuum support cushion (RBF products limited, Essex, UK) which created a cast of the arm, thereby supporting it in a comfortable position and limiting the potential for arm movement during data acquisition. A specially made ultrasound probe holder was fixed over the forearm flexor muscles of the participant to ensure stable positioning of the probe at a fixed location and angle between measurements. The microspheres were infused at 2 ml/min for 1 min followed by 1 ml/min to create a plateau microsphere plasma enrichment before data acquisition as confirmed in pilot studies (data not shown). A single high energy ultrasound pulse was used to destroy the microspheres and the subsequent reperfusion data was recorded for 20 pulse intervals in a period of approximately 20 seconds. Measurements were made with the Philips Sonos 5500 and the cardiac transducer (S3). Eight such sequences were recorded per measurement time point and analysed via QLAB, Microsoft Excel, and SigmaPlot to generate MBV and

MFV data, of which the average of the 8 sequences was used to determine accurate MBV and MFV values for each time point. A detailed description of the CEU protocol can be found in chapter 5.

6.2.3 Doppler Ultrasound

Brachial artery blood flow measurements were performed using Doppler ultrasound. An ultrasound system (Philips, Sonos 5500) with a linear transducer (3-11 MHz) was used to acquire an image of the brachial artery in the longitudinal plane approximately 5 cm proximal to the antecubital fold. Colour Doppler mode was used to identify the flow within the vessel and then pulse wave spectral traces were obtained in order to measure the velocity of the flow. Subsequently, two-dimensional imaging of the brachial artery was performed. Images were triggered to the R wave of the cardiac cycle, and the brachial artery diameter was measured using online video callipers. Blood flow was calculated using the following equation:

$$Q = v \cdot \pi \left(\frac{d}{2}\right)^2$$

where Q is brachial artery blood flow, v is mean brachial artery blood flow velocity, and d is brachial artery diameter.

6.2.4 Indirect Calorimetry

Overnight fasted resting metabolic rate and diet induced thermogenesis were measured by indirect calorimetry. This method makes indirect estimates of the heat produced by the combined metabolic processes going on in the human body. Indirect calorimetry or respirometry measures the respiratory exchange of O_2 (consumption) and CO_2

(production). O_2-consumption can be used to calculate metabolic rate as, in the aerobic oxidation processes that cover the metabolic needs, the amount of heat produced is proportional to the quantity of oxygen consumed. To translate the amount of oxygen consumed to equivalent heat production, the relative amounts of carbon and hydrogen oxidized must be known. In practice this is done via simultaneous measurements of CO_2-production and the use of equations of the chemical reactions that describe the combustion reactions involved in the oxidation of glucose, fatty acids, and protein.

The ventilated hood method is an open-circuit indirect calorimetry method. The ventilated hood, constructed of transparent plastic material, covers the head and upper part of the participant's body. Air is drawn into the hood through a designated inlet by a pump. The pump creates a below atmospheric pressure throughout the calorimeter and eliminates leakage of expired air to the atmosphere. Expired air is continuously analyzed by a highly sensitive and accurate breath analysis system (Oxycon Pro, Jaeger, Germany). Data is sampled every 10 sec, displayed in real time, and stored on disk for off-line analysis.

6.2.5 Experimental Protocol

The day before visit I. The day before visit I participants were instructed to limit physical activity to light exercise of short duration. They were asked to abstain from intake of alcohol and caffeine until after completion of testing the following day. Subjects ate their regular breakfast and lunch. For dinner, they were provided with a standard evening meal (50% carbohydrate, 35% fat, half of which was saturated, and 15

% protein) that they were to consume at 7 pm, and a standard evening drink and snack that they were to consume at 10 pm (choice of glass of semi-skimmed milk or fruit juice, and a cereal bar, or a piece for fruit: apple or banana or orange). After 10 pm the participants were instructed to drink only water and restrict physical activity to an absolute minimum until completion of the study the following day.

Visit I. The next morning, subjects remained fasted and drank only water. Participants were requested to avoid exercise as much as possible and travel to the Wellcome Trust Clinical Research Facility (WT CRF) in the Queen Elizabeth Hospital by car or taxi, arriving at 8:30 am in the fasted state.

After 15 min rest on a bed in semi-recumbent position a flexible 20-gauge Teflon catheter (Quickcath, Becton Dickinson, Plymouth, United Kingdom) was inserted in the antecubital vein of the non-dominant arm and fitted with two 3-way tap (PVB Medizintechnik, Kirchseean, Germany) to allow for repeated blood sampling and microsphere infusion. After a further 15 min rest (at 9 am) a ventilated hood was placed over the participant's head for baseline measures of energy expenditure 30 min prior to drink ingestion. Energy expenditure data was acquired every 2 seconds. Data from the final 10 min of this 30 min period was averaged to obtain a baseline value for energy expenditure and RER. Fifteen minutes into the energy expenditure measurements, a Doppler ultrasound measure was taken, followed by a baseline blood sample and CEU. The ventilated hood was then momentarily removed as participants ingested the OGTT drink (75 g glucose dissolved in 300 ml water). They were asked to consume this within

2 min. Upon ingestion of the drink the ventilated hood was placed once again over the participant's head and a 2 h measurement period commenced. The hood was removed for a 5 min break after 1 h of measurement, to allow participants to stand up and stretch their legs, or go to the toilet if necessary. Every time acquisition recommenced after a break from the hood, the subsequent 5 min of data were discarded to allow for the participant to settle again into a resting state. The indirect calorimetry data was analysed in 5 min averages and the missing values (when hood was removed) were interpolated to obtain a complete data set of 5 min averages for the entire 2 h OGTT. Energy expenditure data acquired over the first 55 min after glucose ingestion was averaged to create a 1^{st} h energy expenditure value, and from 60 min to 115 min to create a 2^{nd} h energy expenditure value. Data from the last 5 min of the OGTT was averaged to create a 2 h energy expenditure value. During the 2 h measurement period, Doppler ultrasound measurements were taken at t = 25, 55, 85, and 115 min. Blood samples were taken at t = 15, 30, 45, 60, 90, and 120 min, while a second CEU measurement occurred at 60 min, after the blood sample. Following the final blood sample, the ventilated hood and intravenous catheter were removed and participants were given lunch before they went home.

6.2.6 Blood Samples

Recruitment visit blood samples (5 ml) were immediately analysed for fasting plasma glucose concentration (YSI 2300 STAT Plus Analyser, Ohio, USA). Visit I blood samples (5 ml) were collected in heparin-containing tubes and centrifuged at 1000 rpm for 10 min at 4 °C. Aliquots of plasma were frozen immediately in liquid nitrogen and

stored at -80 °C. Plasma was analysed for glucose (Glucose HK, Horiba ABX, Monpellier, France) with the COBAS Mira Plus semiautomatic analyzer (ABX diagnostics) and insulin (EIA-2935, DRG Instruments, Marburg, Germany).

6.2.7 Statistical Analysis

The coefficient of variation (CV) for MBV was calculated by

$$C.V. = \frac{s}{\bar{x}} * 100$$

Where s is the standard deviation and $\bar{x}$ is the mean. The intra-subject CV for MBV was calculated by determining the CV for the 8 sequences for each of the 10 subjects and then averaging the CVs, while the inter-subject CV for MBV was calculated using the group mean and standard deviation value of the 10 subjects.

Paired samples t-tests were conducted to compare baseline and 1 hour measures for microvascular blood volume, flow velocity and blood flow, and for brachial artery diameter, flow velocity, and blood flow. Paired samples t-tests were also conducted to compare baseline and plateau value of carbohydrate oxidation, fat oxidation, and RER.

A repeated measures ANOVA was conducted to identify significant changes in energy expenditure, plasma glucose and insulin concentrations over the time course of the OGTT.

To assess the magnitude of the intervention (OGTT) effect, the effect size was calculated using the eta squared statistic (η^2) as it defines the proportion of variance associated with the main effect. This was calculated by:

$$\eta^2 = \frac{t^2}{t^2 + df}$$

Where *t* is the *t* value, and *df* is the degrees of freedom.

If significance was found the Bonferroni post hoc test was applied.

All statistical tests were carried out using SPSS for windows version 16.0 software package (Chicago, IL, USA). All data are reported as means ± SD and statistical significance was set at $P < 0.05$.

6.3 RESULTS

6.3.1 CEU data

The intra-subject CV for MBV was 38.0 videointensity (VI) units ± 20.4 and 23.4 VI units ± 8.2 at baseline and 1 h post glucose ingestion, respectively, while the inter-subject CV for MBV was 45.2 and 39.1 VI units for baseline and 1 h post glucose ingestion, respectively. There was a statistically significant increase in MBV from baseline to 1 hour post OGTT ingestion (42.7 VI units ± 19.3 and 56.7 VI units ± 22.2, respectively, $P = 0.015$), and the eta squared statistic (0.50) indicated a large effect size (Figure 6.1). There was no statistically significant increase in MFV from baseline to 1 hour post

OGTT ingestion (0.22 1/sec ± 0.07 and 0.24 1/sec ± 0.06, respectively, $P = 0.509$; Figure 6.2). Microvascular blood flow (MBF) showed a statistically significant increase from baseline to 1 hour post OGTT ingestion (9.1 VI/sec ± 4.5 and 13.2 VI/sec ± 4.6, respectively, $P = 0.005$), and the eta squared statistic (0.61) indicated a large effect size (Figure 6.3).

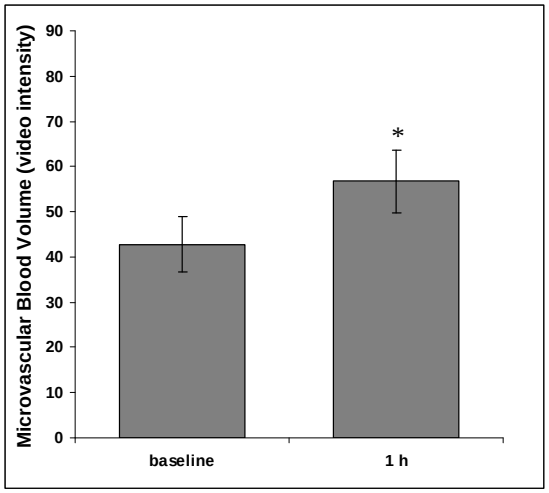

Figure 6.1 Microvascular blood volume at baseline and 1 h post-glucose ingestion. n = 10, * $P = 0.015$ from baseline.

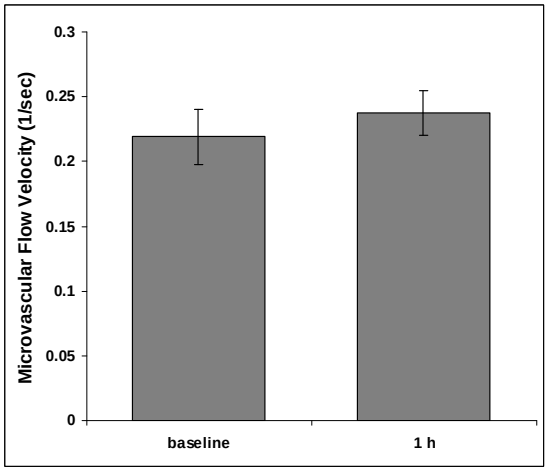

Figure 6.2 Microvascular flow velocity (1/sec) at baseline and 1 h post-glucose ingestion (n = 10).

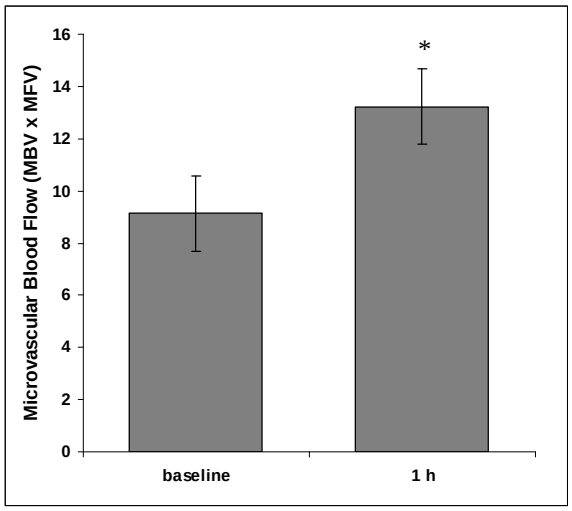

Figure 6.3 Microvascular blood flow at baseline and 1 h post-glucose ingestion (n = 10). * P = 0.005 from baseline.

6.3.2 Brachial artery data

Brachial artery diameter increased significantly from baseline to 1 hour post-OGTT ingestion (4.47 mm ± 0.40 vs 4.60 mm ± 0.30, P = 0.041). The eta squared statistic (0.39) indicates a large effect size. Brachial artery velocity and flow did not show a significant change from baseline to 1 hour post-OGTT ingestion. Figure 6.4 depicts the brachial artery diameter, flow velocity, and blood flow data.

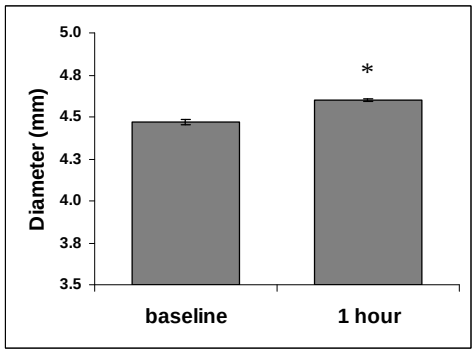

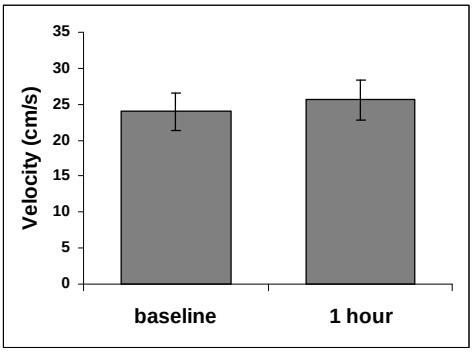

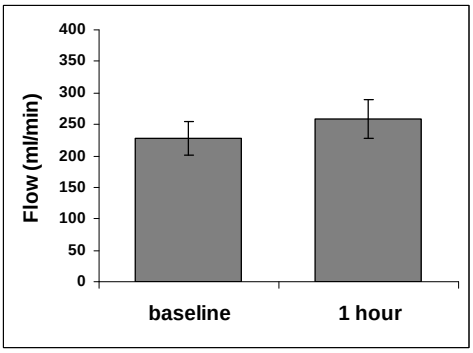

Figure 6.4 Brachial artery diameter, flow velocity, and blood flow changes from baseline to 1 h post-glucose ingestion. Data expressed as means ± standard error (n = 10). * P = 0.041 from baseline.

6.3.3 Blood data

Plasma glucose concentrations increased significantly from baseline to peak (4.31 mM ± 0.68 and 8.82 mM ±1.28, respectively; P = 0.001) in response to the OGTT. Peak glucose concentrations were seen at 42 min ±13 post glucose ingestion. Plasma glucose concentration at 2 hours post glucose ingestion was 5.34 mM ± 1.47, and was not significantly different from baseline (P = 0.065). Insulin concentrations increased significantly from baseline to peak (7.81 μU/ml ± 2.29 and 71.1.5 μU/ml ± 20.2, respectively; P = 0.001) in response to the OGTT. Peak insulin concentrations were seen at 47 min ± 22 post-glucose ingestion. Plasma insulin concentration at 2 hours post

glucose ingestion was 20.22 μU/ml ± 9.20, and was significantly different from baseline (P = 0.008). Figure 6.5 shows the plasma glucose and insulin concentration at baseline, peak values, and 2 hours post glucose ingestion.

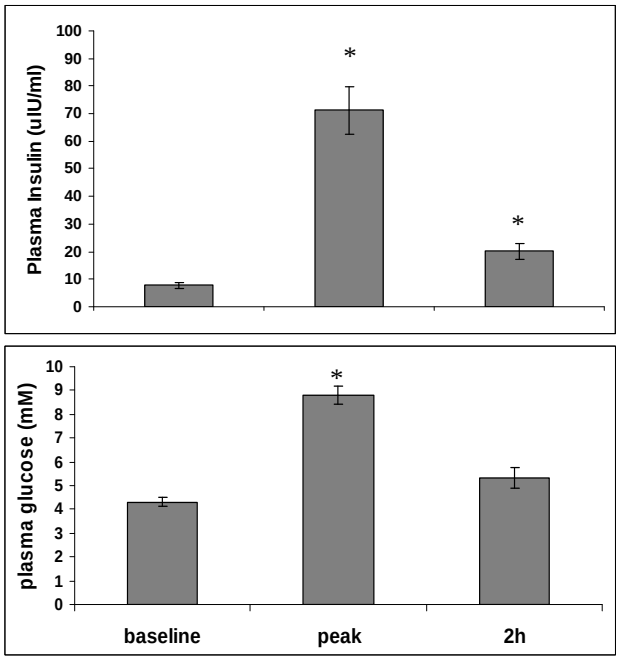

Figure 6.5 Plasma insulin (n = 10) and glucose (n = 10) concentration at baseline, pre-glucose ingestion, and peak and 2 hour values post-glucose ingestion. Values are expressed as mean ± standard error. * P < .01 from baseline.

6.3.4 Energy expenditure, rate of fuel switch, and DIT

In response to the OGTT, there was a statistically significant increase in CHO oxidation from baseline to plateau (81.2 mg/min ± 34.4 and 175.8 mg/min ± 23.7, respectively, P = 0.001), and the eta squared statistic (0.97) indicated a large effect size. A statistically significant decrease in fat oxidation from baseline to plateau (54.4 mg/min ± 22.9 and

23.5 mg/min ± 17.4, respectively, $P = 0.001$) was seen in response to the OGTT. The eta squared statistic (0.88) indicates a large effect size. Figure 6.6 shows the change in fat and CHO oxidation over time. The respiratory exchange ratio (RER) showed a statistically significant increase from baseline to plateau (0.82 ± 0.06 and 0.94 ± 0.07, respectively, $P = 0.001$). The eta squared statistic (0.93) indicates a large effect size (Figure 6.7). Table 6.2 shows the CHO oxidation, fat oxidation, and RER values for baseline, the time at which the baseline values started to change (time of slope start), the rate of change (slope), the time at which a plateau is reached (time of plateau) and the plateau value.

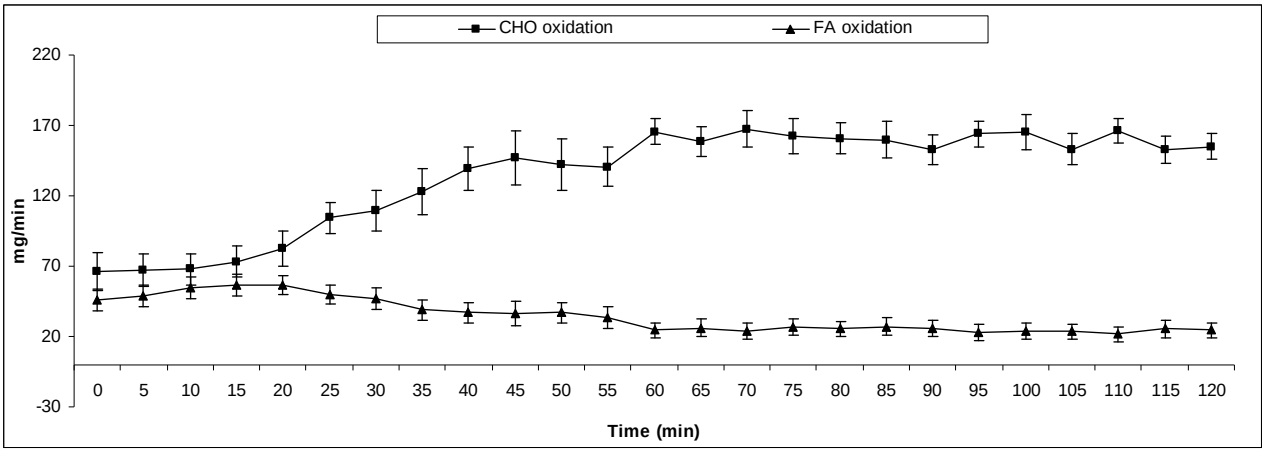

Figure 6.6 Fatty acid and carbohydrate oxidation over 2 h OGTT (n = 10)

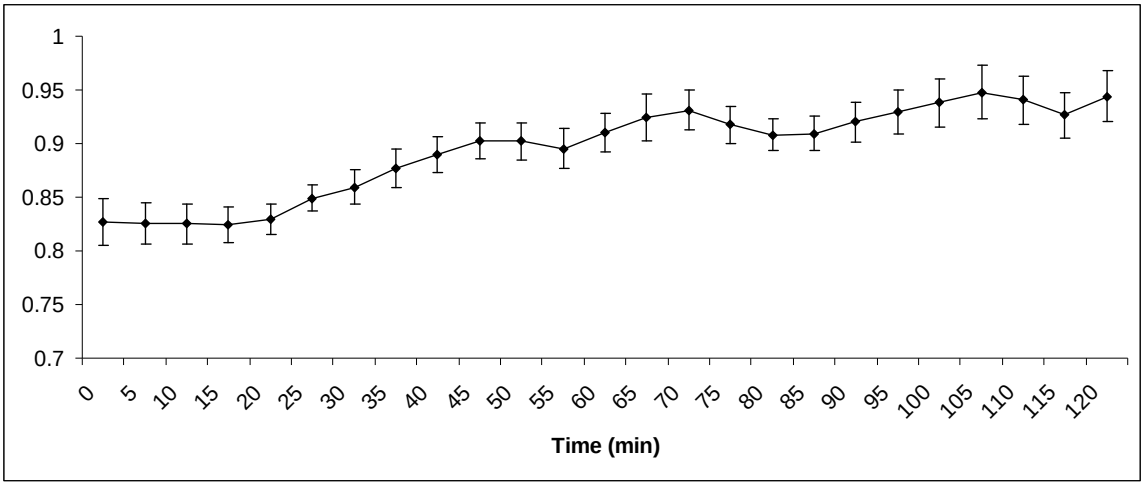

Figure 6.7 Respiratory exchange ratio over 2 h OGTT (n = 10)

Table 6.2. Kinetic analysis of time courses for CHO oxidation (n = 9), fat oxidation (n = 9), and respiratory exchange ratio (RER; n = 10).

	Baseline	**Time of slope start** (min)	**Slope**	**Time of plateau** (min)	**Plateau**
CHO oxidation	81.2 *(± 34.4)* mg/min	15 *(± 8.0)*	4.7 *(± 1.7)* mg/min	44 *(± 11.7)*	175.8 * *(± 23.7)* mg/min
Fat oxidation	54.4 *(± 22.9)* mg/min	21 *(± 15.2)*	8.8 *(± 14.4)* mg/min	59 *(± 26.2)*	23.5* *(± 17.4)* mg/min
RER	0.82 *(± 0.06)*	23 *(± 8.19)*	0.004 *(± 0.0023)*	59 *(± 26.4)*	0.94* *(± 0.07)*

Data given as mean values ± standard deviations. * $P < 0.05$ from baseline.

Energy expenditure over the 2 h OGTT is shown in Figure 6.8. The data were divided into four values for analysis, namely the baseline value, followed by the average energy expenditure value of the first hour post-OGTT ingestion and of the average of the second hour post-OGTT ingestion, concluding with the 2 h energy expenditure value (Table 6.3).

The baseline value was obtained by averaging the last 10 min of the 30 min resting period, at which data was acquired every 2 sec, while the 2 h value was an average of the last 5 min of the 2 h measuring period post glucose ingestion. A repeated measures ANOVA revealed 1st h average, 2nd h average, and 2h value to be significantly different from baseline (P = 0.001, P = 0.008, and P = 0.027, respectively) while not significantly different from each other (P = 1.000).

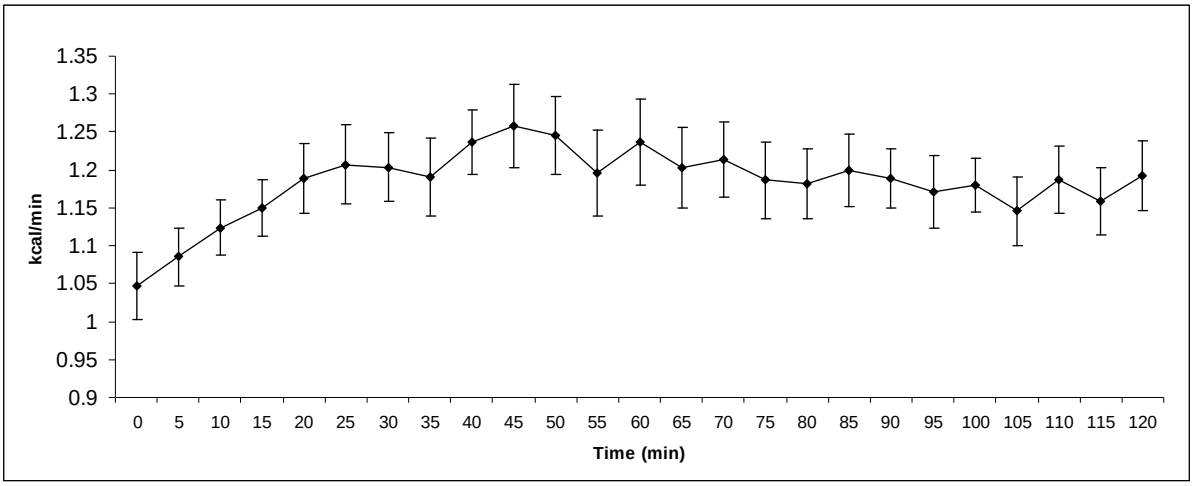

Figure 6.8 Energy expenditure over 2 h OGTT

Table 6.3 Energy expenditure (kcal/min)

Baseline	1st h average	2nd h average	2h value
1.047 *(± 0.14)*	1.194* *(± 0.14)*	1.183* *(± 0.14)*	1.192* *(± 1.15)*

Data expressed as means ± standard deviations (n = 10). * P < 0.05 from baseline

6.4 DISCUSSION

The principal finding of the study is that MBV, measured by CEU, increased significantly in response to an OGTT in lean, trained, healthy individuals. This was in line with our hypothesis, and to our knowledge this is the first time an increase in MBV has been measured in response to an OGTT. A significant increase in brachial artery diameter from baseline to 1 hour post-glucose ingestion was also observed again as hypothesised. However, no significant change was seen in brachial artery blood flow velocity or blood flow. This may be due to the OGTT not inducing a sufficient increase in plasma insulin to cause a measureable effect in the macrocirculation.

The rapid rises in blood glucose and insulin concentration to moderate peak values corresponded with the hypothesis. Peak glucose concentration occurred at 42 min ± 13 and peak insulin concentration at 47 min ± 22. Glucose levels subsequently began to decrease such that at 2 hours post glucose ingestion plasma glucose was no longer significantly different from baseline, while 2 hour plasma insulin had fallen but was still significantly elevated above baseline.

The increase in plasma insulin may have induced the increase in MBV in several ways. Firstly, insulin has been found to stimulate NO production in terminal arterials, thereby inducing vasodilation and an increase in blood delivery to the capillary network (Barrett et al. 2009[20]). Secondly, insulin has also been shown to induce NO production higher up the arterial tree (Barrett et al. 2009[20]) and thereby dilate the larger arteries, as seen by the increase in brachial artery diameter in the present study. This would allow for an increase in blood delivery to the microcirculation and may therefore contribute to the

increase in MBV. Thirdly, the increase in blood delivery to the skeletal muscle and its microcirculation due to insulin-induced NO production and subsequent vasodilation may increase shear stress, which in healthy arteries would induce further vasodilation (Arcaro et al. 1999[32]; Pacher et al. 2007[33]), thereby potentially contributing to the increase in MBV.

We observed a rapid significant increase in carbohydrate oxidation and a significant decrease in fat oxidation, as well as a rapid significant increase in RER. This corresponded with the hypothesis that lean trained individuals would have a high metabolic flexibility with a rapid switch from primarily fat oxidation in the fasted state to primarily carbohydrate oxidation after glucose ingestion (Storlien et al. 2004[24]). A rapid significant increase in energy expenditure in response to the OGTT was also observed and this too was in line with the hypothesis that the OGTT would increase MBV and DIT in parallel.

In conclusion, to our knowledge this is the first study in humans in vivo to use CEU during an OGTT and show an increase in MBV. This is an important observation as an OGTT is much simpler to conduct than a hyperinsulinaemic euglycemic clamp. To fully appreciate the impact of adequate increases in MBV during the OGTT on metabolic flexibility (rate at which fat and carbohydrate oxidation switch after glucose ingestion) and on increases in DIT, future studies should investigate the effect of an OGTT in obese individuals. Only then we will be able to investigate the major hypothesis of this study: that reduced increases in MBV will reduce DIT and metabolic flexibility and will delay

the kinetics of the metabolic transitions that occur in the 2 h period following glucose ingestion. In addition, the modifications of the CEU method that we developed in chapter 5 will allow measurement of changes in MBV and MBF at a high significance level with a high statistical power in 10 individuals. Therefore, the modified CEU method should be able to evaluate the effect of exercise interventions and pharmacological therapies in obese and insulin resistant individuals.

6.5 REFERENCE LIST

1. World Health Organisation. Obesity and overweight. Fact Sheet No 311 ed. 2006.

2. World Health Organisation. Diabetes. fact sheet 312 ed. 2006.

3. Gonzalez MA, Selwyn AP. Endothelial function, inflammation, and prognosis in cardiovascular disease. Am J Med 2003;115 Suppl 8A:99S-106S.

4. Ferrannini E, Bjorkman O, Reichard GA, Jr., Pilo A, Olsson M, Wahren J, Defronzo RA. The disposal of an oral glucose load in healthy subjects. A quantitative study. Diabetes 1985;34:580-588.

5. Defronzo RA, Gunnarsson R, Bjorkman O, Olsson M, Wahren J. Effects of insulin on peripheral and splanchnic glucose metabolism in noninsulin-dependent (type II) diabetes mellitus. J Clin Invest 1985;76:149-155.

6. Nuutila P, Knuuti MJ, Heinonen OJ, Ruotsalainen U, Teras M, Bergman J, Solin O, Yki-Jarvinen H, Voipio-Pulkki LM, Wegelius U, . Different alterations in the insulin-stimulated glucose uptake in the athlete's heart and skeletal muscle. J Clin Invest 1994;93:2267-2274.

7. Liu Z, Liu J, Jahn LA, Fowler DE, Barrett E. Infusing lipid raises plasma FFA and induces insulin resistance in muscle microvasculature. x ed. 2009:x.

8. Chang L, Chiang S.H., Saltiel AR. Insulin signaling and the regulation of glucose transport. 10 ed. 2004:65-71.

9. Thong FSL, Dugani CB, Klip A. Turning signals on and off: GLUT4 traffic in the insulin-signaling highway. 20 ed. 2005:271-284.

10. Wojtaszewski JF, Richter EA. Effects of acute exercise and training on insulin action and sensitivity: focus on molecular mechanisms in muscle. Essays Biochem 2006;42:31-46.

11. Clerk LH, Vincent MA, Jahn LA, Liu Z, Lindner JR, Barrett EJ. Obesity blunts insulin-mediated microvascular recruitment in human forearm muscle. Diabetes 2006;55:1436-1442.

12. de Jongh RT, Serne EH, Ijzerman RG, de Vries G, Stehouwer CD. Impaired microvascular function in obesity: implications for obesity-associated microangiopathy, hypertension, and insulin resistance. Circulation 2004;109:2529-2535.

13. Keske MA, Clerk LH, Price WJ, Jahn LA, Barrett EJ. Obesity Blunts Microvascular Recruitment in Human Forearm Muscle Following a Mixed Meal. Diabetes Care 2009.

14. Krentz AJ, Clough G, Byrne CD. Vascular Disease in the Metabolic Syndrome: Do We Need to Target the Microcirculation to Treat Large Vessel Disease? J Vasc Res 2009;46:515-526.

15. Brownlee M. The pathobiology of diabetic complications: a unifying mechanism. Diabetes 2005;54:1615-1625.

16. Gudbjornsdottir S, Sjostrand M, Strindberg L, Wahren J, Lonnroth P. Direct measurements of the permeability surface area for insulin and glucose in human skeletal muscle. J Clin Endocrinol Metab 2003;88:4559-4564.

17. Vincent MA, Clerk LH, Lindner JR, Price WJ, Jahn LA, Leong-Poi H, Barrett EJ. Mixed meal and light exercise each recruit muscle capillaries in healthy humans. Am J Physiol Endocrinol Metab 2006;290:E1191-E1197.

18. Porter TR. Capillary blood flow abnormalities in the skeletal muscle and microvascular complications in diabetes lessons that cannot be learned from larger vessels. J Am Coll Cardiol 2009;53:2184-2185.

19. Womack L, Peters D, Barrett EJ, Kaul S, Price W, Lindner JR. Abnormal skeletal muscle capillary recruitment during exercise in patients with type 2 diabetes mellitus and microvascular complications. J Am Coll Cardiol 2009;53:2175-2183.

20. Barrett EJ, Eggleston EM, Inyard AC, Wang H, Li G, Chai W, Liu Z. The vascular actions of insulin control its delivery to muscle and regulate the rate-limiting step in skeletal muscle insulin action. Diabetologia 2009;52:752-764.

21. Clark MG, Wallis MG, Barrett EJ, Vincent MA, Richards SM, Clerk LH, Rattigan S. Blood flow and muscle metabolism: a focus on insulin action. Am J Physiol Endocrinol Metab 2003;284:E241-E258.

22. Sidossis LS, Wolfe RR. Glucose and insulin-induced inhibition of fatty acid oxidation: the glucose-fatty acid cycle reversed. 270 ed. 1996:E733-E738.

23. Sidossis LS, Stuart CA, Shulman GI, Lopaschuck GD, Wolfe RR. Glucose plus insulin regulate fat oxidation by controlling the rate of fatty acid entry into the mitochondria. 98 ed. 1996:2244-2250.

24. Storlien L, Oakes ND, Kelley DE. Metabolic flexibility. Proc Nutr Soc 2004;63:363-368.

25. Gudbjornsdottir S. Decreased Muscle Capillary Permeability Surface Area in Type 2 Diabetic Subjects. J Clin Endocrinol Metab 2005;90:1078-1082.

26. Corpeleijn E., Mensink M, Kooi M.E, Roekaerts P.M.H.J, Saris WH, Blaak EE. Impaired skeletal muscle substrate oxidation in glucose-tolerant men improves after weight loss. 16 ed. 2008:1025-1032.

27. Lowell BB, Bachman ES. Beta-Adrenergic receptors, diet-induced thermogenesis, and obesity. J Biol Chem 2003;278:29385-29388.

28. de Jonge L, Bray GA. The thermic effect of food and obesity: a critical review. 5(6):622-31 ed. 1997:622-631.

29. Tappy L. Thermic effect of food and sympathetic nervous system activity in humans. Reprod Nutr Dev 1996;36:391-397.

30. Petersen KF, Dufour S, Shulman GI. Decreased insulin-stimulated ATP synthesis and phosphate transport in muscle of insulin-resistant offspring of type 2 diabetic parents. PLoS Med 2005;2:e233.

31. Wagenmakers AJ. Insulin resistance in the offspring of parents with type 2 diabetes. PLoS Med 2005;2:e289.

32. Arcaro G, Zamboni M, Rossi L, Turcato E, Covi G, Armellini F, Bosello O, Lechi A. Body fat distribution predicts the degree of endothelial dysfunction in uncomplicated obesity. Int J Obes Relat Metab Disord 1999;23:936-942.

33. Pacher P, Beckman JS, Liaudet L. Nitric oxide and peroxynitrite in health and disease. Physiol Rev 2007;87:315-424.

Chapter 7

GENERAL DISCUSSION

7.1 Overview

There has been a dramatic global rise in obesity over the last thirty years (World Health Organisation 2006[1]) with concomitant increases in obesity-related pathology, in particular type II diabetes (World Health Organisation 2006[2]) and cardiovascular disease (CVD; Department of Health 2008[3]). The enormous cost of obesity-related pathology to the quality of life of individuals and to national economies warrants urgent action to tackle obesity and its progression into type II diabetes and CVD. The loss of glycemic control is a key player in the development of obesity-related pathology (**chapter 1**). Skeletal muscle and its microvasculature are particularly important in the maintenance of glucose homeostasis as skeletal muscle is the largest site of glucose disposal (Ferrannini et al. 1985[4]; DeFronzo et al. 1985[5]; Nuutila et al. 1994[6]) and is reliant on its microvasculature for delivery of glucose for clearance after meal ingestion (Orasanu and Plutzky 2009[7]). Obese individuals display a reduced capillary recruitment response to insulin (Clerk et al. 2006[8]; de Jongh et al. 2004[9]; Keske et al. 2009[10]), as compared to their lean counterparts, which results in increased and prolonged glucose excursions after a meal, jeopardizing vascular health and glycemic control. Obese individuals also display impaired NO-dependent vasodilation in response to increased flow in feeding and resistance arteries (Brook et al. 2001[11]; Hamdy et al. 2003[12]; Meyers and Gokce 2007[13]; Arcaro et al. 1999[14]), thus it is also possible that obese individuals may have a reduced microvascular perfusion response to exercise. This would limit the delivery of oxygen and fuels and thus reduce exercise tolerance and the capacity to burn calories, as well as encourage the adoption of a sedentary lifestyle. Plasma fatty acids (FA), elevated in obesity, have been shown to play a key role in impairing microvascular function (**chapter 1**), and

may be a target for improving the microvascular perfusion of the obese. However, the extent of their contribution in impairing skeletal muscle perfusion at rest and during exercise is not fully understood. Therefore, the aims of this thesis were (i) determine the effect of FA on muscle microvascular blood volume at rest and during exercise, (ii) investigate whether near-infrared spectroscopy can be used to measure skeletal muscle microvascular blood volume in the obese, (iii) develop the contrast enhanced ultrasound (CEU) method in our laboratory for measuring skeletal muscle microvascular blood volume and blood flow of the human forearm, and (iv) use CEU to measure microvascular blood volume and blood flow changes in response to an OGTT in lean trained individuals with the scope of using this method in the obese to assess the effectiveness of interventions aimed at improving microvascular perfusion and glycemic control.

7.2 The effect of acute changes in FA concentrations on skeletal muscle perfusion in response to exercise and during the resting fasted state

The prominent role of FA in inducing endothelial dysfunction and insulin resistance, and the impaired perfusion response to insulin in obese individuals (**chapter 1**), suggests the potential for FA to impair the skeletal muscle perfusion response to exercise in the obese as endothelial dysfunction impairs NO-mediated vasodilation and this vasodilation mechanism plays a role in exercise-induced perfusion. In **chapter 2** we investigated whether an acute decrease in plasma FA concentration would increase the MBV response to an acute exercise bout in obese individuals. As endothelial dysfunction involves the loss of vasodilatory mechanisms and the

increased activation of pathways inducing vasoconstriction, the ability of elevated FA levels to impair endothelial function suggests the presence of increased vasoconstriction. In **chapter 3** we investigated whether an acute decrease in plasma FA would increase the skeletal muscle MBV of obese individuals in the resting fasted state.

We measured microvascular blood volume as it is a major determinant of capillary permeability surface area product and glucose uptake (Gudbjornsdottir 2005[15]). Near-infrared spectroscopy (NIRS) was used in both chapters to measure changes in total haemoglobin content (THC) which was considered to represent changes in blood volume in the measured compartment. Niacin was used to acutely reduce plasma FA concentration. Our results showed no significant differences in the exercise-induced increase in THC between control and low FA conditions in obese individuals (**chapter 2**). There were also no significant differences in resting THC levels between control and low FA conditions (**chapter 3**). We concluded that the results could potentially be explained by the short duration of the time window with a low FA concentration created by niacin. We and others (Wang et al. 2000[16]; Carlson et al. 1968[17]) found plasma FA concentration reached its lowest point 1 h post niacin ingestion, but at 90 min FA concentrations started to increase again and baseline FA levels were reached approximately 2 h post niacin ingestion. It is possible that the mechanisms involved in inducing endothelial dysfunction and insulin resistance require a longer exposure to reduced plasma FA concentrations before they are reversed. For example, before alterations in gene expression lead to measurable changes in protein content of NADPH oxidase and NFκB, and to measurable effects on the balance between vasoconstriction and vasodilation (Silver et al. 2007[18]), longer

periods of low FA concentration than those induced by niacin might well be required. Furthermore, it is possible that acute changes in plasma FA concentrations may not necessarily lead to acute decreases in endothelial concentrations of fatty acid metabolites that activate protein kinase C and increase serine phosphorylation of IRS-1 and thus reduce NO production and vasodilation in the resting fasted state (Serne et al. 2006[19]; Naruse et al. 2006[20]). The absence of a statistically significant difference between lean and obese participants in the exercise-induced THC increase did not confirm the hypothesis that obese individuals would have an impaired blood flow response to exercise (**chapter 2**). This is potentially due to the inability of NIRS to measure haemoglobin concentration in the muscle microvasculature when a thick subcutaneous adipose tissue layer is present and absorbs all the NIR light (van Beekvelt et al. 2001[21]). We concluded that the large difference in resting THC between trained lean and obese individuals (**chapter 3**) was at least partially the result of the inability of NIRS to successfully penetrate into the skeletal muscle of the obese, rather than the presence of rarefaction or impaired microvascular dilation in trained obese individuals. These results warranted a more detailed investigation of the effect of the thickness of the adipose tissue layer on the ability of NIRS to measure changes in THC in the skeletal muscle microvasculature.

7.3 Evaluating the ability of NIRS to measure exercise induced increases in MBV in obese individuals

The subcutaneous adipose tissue layer can vary greatly between individuals. A large adipose tissue thickness will likely affect the THC measurements as the NIR light has

to travel through it before reaching the muscle (van Beekvelt et al. 2001[21]). Nevertheless, it has been suggested that the measurement depth of the NIRS is equal to half the interoptode distance (ID; Cui et al. 1991[22]; Homma et al. 1996[23]), and thus increasing the ID would allow for photons to pass the thick adipose tissue layer and penetrate into skeletal muscle. A calculation of the theoretical skeletal muscle tissue contribution to the returning NIRS signal would suggest an approximate 50 % muscle contribution for the obese participants (**chapter 2 and 3**). However, the results from **chapters 2 and 3** suggested that the large ID was not sufficient to avoid a major contribution of the thick subcutaneous adipose tissue layer of the obese participants to the NIRS absorption. **In chapter 4** we investigated the effect of subcutaneous adipose tissue thickness (ATT) on NIRS measurements at rest and during incremental exercise. During exercise, THC in the skeletal muscle microvasculature is expected to increase, while haemoglobin oxygenation and especially oxygen saturation are expected to decrease. The results showed a small increase in THC during exercise in the obese participants, as compared to lean controls. Haemoglobin oxygenation actually increased, while the decrease in oxygen saturation did not reach statistical significance (**chapter 4**). The fact that we were unable to observe a substantial increase in THC from the skeletal muscle despite nearly half the signal theoretically originating from the muscle appears inconsistent with the calculations of the theoretical measurement depth. This can potentially be explained by the scattering and absorption properties of the adipose tissue layer. Rather than the adipose tissue layer simply adding to the penetration distance that the photons need to travel in order to reach the muscle, we concluded that adipose tissue might scatter the photons thereby increasing their path length within the adipose tissue and reducing their penetration depth (Matsushita 1998[24]). Therefore, although moderate ATT could be

overcome by increasing the ID (**chapter 4**), the large ATT in the obese participants may have caused photon scattering and increased the adipose tissue path length to such an extent as to significantly reduce penetration depth and skeletal muscle contribution to the NIRS measurement. As a result, despite a large ID, skeletal muscle microvascular data could not be obtained with NIRS in obese participants. We concluded that in order to measure the skeletal muscle microvasculature in obese individuals, the contrast enhanced ultrasound (CEU) method would be required.

7.4 Developing the CEU method to measure skeletal muscle microvascular blood volume in human forearm

Most of the publications result from 2 laboratories using CEU to measure skeletal muscle microvascular blood volume in rats and humans (Rattigan et al. 2005[25]; Vincent et al. 2006[26]), and the published methodological descriptions are very succinct and lacking in detail. In **chapter 5** we set out to determine the optimal CEU procedure to measure skeletal muscle MBV of the human forearm. The primary objective was to establish if the CEU technique could detect increases in skeletal muscle MBV in lean healthy individuals in response to an oral glucose tolerance test (OGTT). The secondary objective was to compare the microvascular blood volume and blood flow response to an OGTT between trained lean and obese individuals, to establish the extent of impaired perfusion in the obese. The third objective was to eventually (in future studies) implement interventions aimed at improving the skeletal muscle perfusion in the patient groups and use CEU to measure the effect of the interventions.

Traditionally CEU measurements have been made without arm fixation and using a multiple microsphere destruction protocol. However, our endeavour to determine the optimal CEU protocol for measurement of MBV and MFV in the human forearm revealed that it is of vital importance that there is no movement of the arm or muscles during measurement as it will invalidate the data and the shape of the replenishment curve, as well as the resultant estimates of MBV and MFV. We concluded that it is essential to create a stable and reproducible measurement set up. This was achieved by the use of a vacuum support cushion to stabilise the arm, and fixing a specially made holder to the forearm into which the ultrasound probe could be inserted in a fixed position. This holder also allowed removal of the probe between measurements while ensuring the maintenance of accurate placement and angle when the probe was returned. In addition to the stable measurement set up, the use of a single microsphere destruction protocol, as advised by Dr. Stephen Rattigan, reduced the chances of arm movement during measurement as sequences only took approximately 20 sec as opposed to nearly 5 min with the multiple microsphere destruction protocol. Furthermore, the single microsphere destruction protocol also allowed repeated measures at baseline and during the OGTT thus improving the quality of the data. The analysis procedure for the CEU data has never been clearly specified in any of the human studies published so far and we concluded that for the most consistent and accurate analyses it was essential to use the full image ROI and export the data from QLAB to Microsoft Excel and subsequently to SigmaPlot for specific steps in the analysis procedure.

7.5 Using CEU to measure the microvascular response to an OGTT

In healthy individuals, an OGTT induces an increase in plasma insulin concentration (Matsuda and DeFronzo 1999[27]) which increases skeletal muscle MBV and capillary permeability surface area product (Gudbjornsdottir et al. 2003[28]; Gudbjornsdottir 2005[15]), thereby increasing the delivery of glucose to the muscle fibre for clearance. In **chapter 6** we investigated whether the optimised CEU protocol developed in **chapter 5** was able to detect the increase in MBV in response to an OGTT in lean trained individuals. The results showed a significant increase in MBV in response to the OGTT, which corresponded with the increases in glucose oxidation and energy expenditure in the form of diet-induced thermogenesis (DIT). It is assumed that elevated circulating levels of insulin stimulate the dilation of terminal arterioles in vivo and thus increase skeletal muscle capillary perfusion (Clerk 2006[8]), and this was supported by our increase in MBV. In turn, increased microvascular perfusion increases the delivery of insulin and glucose to the muscle fibres, thereby promoting glucose clearance (Muniyappa et al. 2007[29]). Elevated insulin levels will promote DIT in healthy lean individuals at a whole body level (Lowell and Bachman 2003[30]; de Jonge and Bray 1997[31]; Tappy 1996[32]) and in skeletal muscle (Petersen et al. 2005[33]). DIT has several components. In the insulin sensitive skeletal muscle, the increased activation of mitochondrial oxidation, and the increase in glycogen and protein synthesis after meal ingestion greatly contribute to DIT (Petersen et al. 2005[33]; Wagenmakers 2005[34]). We hypothesised that the increase in DIT was dependent on an adequate increase in MBV. Indeed, we saw a significant increase in energy expenditure in response to the OGTT. Increased plasma insulin concentration and glucose uptake into the muscle fibre induces an increase in carbohydrate oxidation and a concomitant decrease in fat oxidation, and the rate of this switch in fuels reflects the metabolic flexibility of the individual (Storlien et al. 2004[35]; Galgani et al.

2008[36]). Our data was in line with this as carbohydrate oxidation increased significantly while fat oxidation decreased significantly.

We therefore concluded that the use of CEU with an OGTT created measureable increases in MBV which corresponded with changes in plasma insulin and glucose, as well as fat oxidation, carbohydrate oxidation, and energy expenditure responses to an OGTT, and that this technique was therefore suited to test the main hypothesis mentioned above.

7.6 Future Research

The CEU technique is emerging as an effective tool to measure MBV, MFV and MBF of the skeletal muscle microvasculature, as reflected by changes in MBV, in humans. Due to problems with setting up the method the time constraints meant we were not able to measure obese subjects. Therefore future studies should use CEU to measure MBV in response to OGTT in obese individuals, and test the hypotheses that an OGTT will not induce measureable changes in MBV and that, therefore, in the obese the transition from fat to carbohydrate as the primary fuel will be delayed (metabolic inflexibility; Storlien et al. 2004[35]; Corpeleijn et al. 2008[37]) and the increase in DIT will be smaller (de Jonge and Bray 1997[31]). Improved glucose clearance after meal ingestion is of vital importance in limiting glucose excursions and the vascular damage hyperglycemia can induce (**chapter 1**). As a larger MBV by definition leads to an increased capillary permeability surface area product and a faster rate of glucose uptake by skeletal muscle (Gudbjornsdottir et al. 2003[28]), future studies should

investigate the effect of interventions aimed at improving the MBV response after meal ingestion so as to improve glucose disposal.

To test hypothesis that increased insulin production by the pancreas would overcome the impairment in MBV response to meal ingestion we propose that one potential intervention would be the addition of amino acids to the glucose load to create a modified OGTT as the combined ingestion of amino acids and glucose has been shown to induce a greater insulin response than glucose alone (Manders et al. 2005[38]). The greater insulin response may overcome the insulin resistance of the muscle fibre and microvasculature, thereby allowing for optimal glucose disposal. Other interventions aimed at improving glycemic control involve an acute exercise bout and exercise training, as both are known to improve glucose tolerance (Wojtaszewski and Richter 2006[39]), and their effectiveness could be assessed with the use of CEU and the MBV response to an OGTT pre- and post-intervention.

As NIRS was found to be unable to measure the skeletal muscle microvasculature in the presence of a thick subcutaneous adipose tissue layer we do not have an answer to the important question whether limitations in skeletal muscle perfusion limit exercise capacity in the obese, thereby promoting the adoption of a sedentary lifestyle. In future experiments, CEU should therefore be used to determine if there is a reduced perfusion response to exercise in obese individuals as compared to lean controls. Such a reduction in perfusion would limit exercise capacity and therefore could be an important target for interventions to help obese individuals increase their energy expenditure to control and reduce their excessive adiposity. CEU could thus be used to assess the effectiveness of interventions at improving the perfusion response to

exercise so the most effective strategies can be implemented to help increase the exercise tolerance of the obese population.

We have developed the CEU technique in such a way that it can now generate reliable MBV data in response to an OGTT in lean trained individuals and can likely be used in group comparisons and for the evaluation of interventions in the obese. However, there are also alternative methods to measure endothelial function that could be important complimentary methods for use in future research to measure group differences and intervention effects. The venous occlusion plethysmographic methods has been successfully used to assess the muscle microvascular exchange capacity, expressed as the capillary filtration coefficient (K_f), non-invasively measures the rate of fluid exchange from blood to muscle across the entire microvascular bed (Clough et al. 2009[40]; Bates 2003[41]; Gamble 2002[42]). Venous occlusion plethysmography is a well-validated technique which provides a measure of K_f through the use of small-step or cumulative increases in venous occlusion pressure and the subsequent changes in limb volume (Clough et al. 2009[40]; Gamble et al. 1993[43]; Gamble 2002[42]). Furthermore, it does not affect the function of the vasculature being assessed (Clough et al. 2009[40]). Thus the use of plethysmography measuring K_f appears to be a favourable method to assess microvascular function (Anim-Nyame et al. 2003[44]), and future studies may wish to explore the use of plethysmography to assess improvements in microvascular function in conjunction with glucose disposal in response to interventions aimed at improving glycemic control. The venous occlusion plethysmography method has already been used to measure differences in microvascular function between trained and sedentary individuals, as well as the effect of training and of electrical stimulation on

microvascular function (Brown et al. 2001[45]; Charles et al. 2006[46]). Brown et al. (2001)[45] found that endurance trained athletes showed a greater capacity for fluid filtration compared to sedentary and resistance trained athletes, and that a 4-week electrical stimulation programme in sedentary individuals significantly increased the fluid filtration capacity. Charles et al. (2006)[46] found K_f nearly doubled in elderly individuals after 14 weeks of endurance exercise training. Recently the plethysmography method also has been used to assess microvascular function after statin treatment (Clough et al. 2009[40]).

Statins are an important class of drugs extensively used in obesity and the metabolic syndrome to lower plasma lipids. Although there are numerous drugs available for treating the variety of dysfunctions capable of inducing pathology in obese and diabetic patients, drugs may not be the solution to improving microvascular perfusion. An improvement in macrovascular function after 6 months of statin therapy was documented, however, despite reduced dislipidemia, no improvement in microvascular function was observed (Clough et al. 2009[40]). The improved lipid parameters and macrovascular function documented by Clough et al. (2009)[40] reflect a reduced risk of pathology, in particular macrovascular disease (Clough et al. 2009[40]). However, glycemic control is largely reliant on microvascular function, and the loss of glucose homeostasis is a key contributor to the pathogenesis of type II diabetes and its vascular complications, as well as CVD (Brownlee 2005[47]). Therefore, it is of vital importance to implement interventions at improving microvascular function and glycemic control even in conjunction with statin therapy.

Two tools are now available for the investigation of microvascular function in humans, namely CEU and venous occlusion plethysmography. Future studies will need to investigate the microvascular function of obese individuals to define the suspected impairments and determine the effectiveness of interventions aimed at improving the microvascular response to exercise and meal ingestion so as to improve exercise tolerance and glycemic control and thereby halt the development of obesity-related pathology.

7.7 REFERENCE LIST

1. World Health Organisation. Obesity and overweight. Fact Sheet No. 311, 2006.

2. World Health Organisation. Diabetes. Fact sheet No. 312, 2006.

3. Department of Health. Coronary heart disease. 2008.

4. Ferrannini E, Bjorkman O, Reichard GA, Jr., Pilo A, Olsson M, Wahren J, Defronzo RA. The disposal of an oral glucose load in healthy subjects. A quantitative study. Diabetes 1985;34:580-588.

5. Defronzo RA, Gunnarsson R, Bjorkman O, Olsson M, Wahren J. Effects of insulin on peripheral and splanchnic glucose metabolism in noninsulin-dependent (type II) diabetes mellitus. J Clin Invest 1985;76:149-155.

6. Nuutila P, Knuuti MJ, Heinonen OJ, Ruotsalainen U, Teras M, Bergman J, Solin O, Yki-Jarvinen H, Voipio-Pulkki LM, Wegelius U, . Different alterations in the insulin-stimulated glucose uptake in the athlete's heart and skeletal muscle. J Clin Invest 1994;93:2267-2274.

7. Orasanu G, Plutzky J. The pathologic continuum of diabetic vascular disease. J Am Coll Cardiol 2009;53:S35-S42.

8. Clerk LH, Vincent MA, Jahn LA, Liu Z, Lindner JR, Barrett EJ. Obesity blunts insulin-mediated microvascular recruitment in human forearm muscle. Diabetes 2006;55:1436-1442.

9. de Jongh RT, Serne EH, Ijzerman RG, de Vries G, Stehouwer CD. Impaired microvascular function in obesity: implications for obesity-associated

microangiopathy, hypertension, and insulin resistance. Circulation 2004;109:2529-2535.

10. Keske MA, Clerk LH, Price WJ, Jahn LA, Barrett EJ. Obesity Blunts Microvascular Recruitment in Human Forearm Muscle Following a Mixed Meal. Diabetes Care 2009.

11. Brook RD, Bard RL, Rubenfire M, Ridker PM, Rajagopalan S. Usefulness of visceral obesity (waist/hip ratio) in predicting vascular endothelial function in healthy overweight adults. Am J Cardiol 2001;88:1264-1269.

12. Hamdy O, Ledbury S, Mullooly C, Jarema C, Porter S, Ovalle K, Moussa A, Caselli A, Caballero AE, Economides PA, Veves A, Horton ES. Lifestyle modification improves endothelial function in obese subjects with the insulin resistance syndrome. Diabetes Care 2003;26:2119-2125.

13. Meyers MR, Gokce N. Endothelial dysfunction in obesity: etiological role in atherosclerosis. Curr Opin Endocrinol Diabetes Obes 2007;14:365-369.

14. Arcaro G, Zamboni M, Rossi L, Turcato E, Covi G, Armellini F, Bosello O, Lechi A. Body fat distribution predicts the degree of endothelial dysfunction in uncomplicated obesity. Int J Obes Relat Metab Disord 1999;23:936-942.

15. Gudbjornsdottir S. Decreased Muscle Capillary Permeability Surface Area in Type 2 Diabetic Subjects. J Clin Endocrinol Metab 2005;90:1078-1082.

16. Wang W, Basinger A, Neese RA, Christiansen M, Hellerstein MK. Effects of nicotinic acid on fatty acid kinetics, fuel selection, and pathways of glucose production in women. Am J Physiol Endocrinol Metab 2000;279:E50-E59.

17. Carlson LA, Oro L, Ostman J. Effect of a single dose of nicotinic acid on plasma lipids in patients with hyperlipoproteinemia. Acta Med Scand 1968;183:457-465.

18. Silver AE, Beske SD, Christou DD, Donato AJ, Moreau KL, Eskurza I, Gates PE, Seals DR. Overweight and obese humans demonstrate increased vascular endothelial NAD(P)H oxidase-p47(phox) expression and evidence of endothelial oxidative stress. Circulation 2007;115:627-637.

19. Serne EH, de Jongh RT, Eringa EC, Ijzerman RG, de Boer MP, Stehouwer CD. Microvascular dysfunction: causative role in the association between hypertension, insulin resistance and the metabolic syndrome? Essays Biochem 2006;42:163-176.

20. Naruse K, Rask-Madsen C, Takahara N, Ha SW, Suzuma K, Way KJ, Jacobs JR, Clermont AC, Ueki K, Ohshiro Y, Zhang J, Goldfine AB, King GL. Activation of Vascular Protein Kinase C-{beta} Inhibits Akt-Dependent Endothelial Nitric Oxide Synthase Function in Obesity-Associated Insulin Resistance. Diabetes 2006;55:691-698.

21. van Beekvelt MC, Borghuis MS, van Engelen BG, Wevers RA, Colier WN. Adipose tissue thickness affects in vivo quantitative near-IR spectroscopy in human skeletal muscle. Clin Sci (Lond) 2001;101:21-28.

22. Cui W, Kumar C, Chance B. Experimental study of migration depth for the photons measured at sample surface. I. Time resolved spectroscopy and imaging. Proc SPIE Int Soc Opt Eng 1991;1431:180-191.

23. Homma S, Fukunaga T, Kagaya A. The influence of adipose tissue thickness on Near Infrared Spectoscopic signals in the measurement of human muscle. J Biomed Opt 1996;1:418-424.

24. Matsushita K. Influence of adipose tissue on muscle oxygenation measurements with NIRS instrument. Proceedings of SPIE: The international society for optical engineers 1998;159-165.

25. Rattigan S, Wheatley C, Richards SM, Barrett EJ, Clark MG. Exercise and insulin-mediated capillary recruitment in muscle. Exerc Sport Sci Rev 2005;33:43-48.

26. Vincent MA, Clerk LH, Lindner JR, Price WJ, Jahn LA, Leong-Poi H, Barrett EJ. Mixed meal and light exercise each recruit muscle capillaries in healthy humans. Am J Physiol Endocrinol Metab 2006;290:E1191-E1197.

27. Matsuda M, Defronzo RA. Insulin sensitivity indices obtained from oral glucose tolerance testing: comparison with the euglycemic insulin clamp. Diabetes Care 1999;22:1462-1470.

28. Gudbjornsdottir S, Sjostrand M, Strindberg L, Wahren J, Lonnroth P. Direct measurements of the permeability surface area for insulin and glucose in human skeletal muscle. J Clin Endocrinol Metab 2003;88:4559-4564.

29. Muniyappa R, Montagnani M, Koh KK, Quon MJ. Cardiovascular actions of insulin. Endocr Rev 2007;28:463-491.

30. Lowell BB, Bachman ES. Beta-Adrenergic receptors, diet-induced thermogenesis, and obesity. J Biol Chem 2003;278:29385-29388.

31. de Jonge L, Bray GA. The thermic effect of food and obesity: a critical review. 5(6):622-31 ed. 1997:622-631.

32. Tappy L. Thermic effect of food and sympathetic nervous system activity in humans. Reprod Nutr Dev 1996;36:391-397.

33. Petersen KF, Dufour S, Shulman GI. Decreased insulin-stimulated ATP synthesis and phosphate transport in muscle of insulin-resistant offspring of type 2 diabetic parents. PLoS Med 2005;2:e233.

34. Wagenmakers AJ. Insulin resistance in the offspring of parents with type 2 diabetes. PLoS Med 2005;2:e289.

35. Storlien L, Oakes ND, Kelley DE. Metabolic flexibility. Proc Nutr Soc 2004;63:363-368.

36. Galgani JE, Moro C, Ravussin E. Metabolic flexibility and insulin resistance. Am J Physiol Endocrinol Metab 2008;295:E1009-E1017.

37. Corpeleijn E., Mensink M, Kooi M.E, Roekaerts P.M.H.J, Saris WH, Blaak EE. Impaired skeletal muscle substrate oxidation in glucose-tolerant men improves after weight loss. 16 ed. 2008:1025-1032.

38. Manders RJ, Wagenmakers AJ, Koopman R, Zorenc AH, Menheere PP, Schaper NC, Saris WH, van Loon LJ. Co-ingestion of a protein hydrolysate and amino acid mixture with carbohydrate improves plasma glucose disposal in patients with type 2 diabetes. Am J Clin Nutr 2005;82:76-83.

39. Wojtaszewski JF, Richter EA. Effects of acute exercise and training on insulin action and sensitivity: focus on molecular mechanisms in muscle. Essays Biochem 2006;42:31-46.

40. Clough GF, Turzyniecka M, Walter L, Krentz AJ, Wild SH, Chipperfield AJ, Gamble J, Byrne CD. Muscle microvascular dysfunction in central obesity is related to muscle insulin insensitivity but is not reversed by high-dose statin treatment. Diabetes 2009;58:1185-1191.

41. Bates DO. Pre-eclampsia and the microcirculation: a novel explanation. Clin Sci (Lond) 2003;104:413-414.

42. Gamble J. Realisation of a technique for the non-invasive, clinical assessment of microvascular parameters in man; the KM factor. Eur Surg Res 2002;34:114-123.

43. Gamble J, Gartside IB, Christ F. A reassessment of mercury in silastic strain gauge plethysmography for microvascular permeability assessment in man. J Physiol 1993;464:407-422.

44. Anim-Nyame N, Gamble J, Sooranna SR, Johnson MR, Sullivan MH, Steer PJ. Evidence of impaired microvascular function in pre-eclampsia: a non-invasive study. Clin Sci (Lond) 2003;104:405-412.

45. Brown MD, Jeal S, Bryant J, Gamble J. Modifications of microvascular filtration capacity in human limbs by training and electrical stimulation. 173 ed. 2001:359-368.

46. Charles M, Charifi N, Verney J, Pichot V, Feasson L, Costes F, Denis C. Effect of endurance training on muscle microvascular filtration capacity and vascular bed morphometry in the elderly. 187 ed. 2006:399-406.

47. Brownlee M. The pathobiology of diabetic complications: a unifying mechanism. Diabetes 2005;54:1615-1625.